Analysis of singularities and Matter in 6-dimensional F-theory

Rinto Kuramochi

Department of Particle and Nuclear Physics,
School of High Energy Accelerator Science,
The Graduate University for Advanced Studies, SOKENDAI

1-1 Oho, Tsukuba, Ibaraki, 305-0801, Japan

Abstract

In this thesis, we consider F-theory compactifications, especially, we focus on an F-theory on an elliptically fibred Calabi-Yau threefold over a Hirzebruch surface. In six- or lower-dimensional F-theories, if a fibre type has the condition that an exceptional curve splits into two irreducible ones, we can distinguish the singular fibre types into two types depending on whether the split exceptional curve can split globally or not: "split" and "non-split". It is known that split models correspond to the ADE gauge symmetry implied by Kodaira's classification. On the other hand, in non-split models, the two split exceptional curves are identified by monodromy. Since this caused a projection by a diagram automorphism, the expected gauge symmetry in the non-split models is reduced to the non-simply-laced one.

In the six-dimensional F-theory, when a model has the A_5, D_6 or E_7 codimension-one singularity, the model has half-hypermultiplets as massless charged matter fields and interesting structures of singularities. These gauge symmetries correspond to particular quaternionic Kähler symmetric spaces and are related to the Freudenthal-Tits magic square. The C_3 gauge symmetry is the only non-simply-laced one among them. In the first half of this thesis, as a final magical example, we investigate an F-theory on an elliptic fibration over a Hirzebruch surface with the non-split I_6 fibre, in which the unbroken gauge symmetry is C_3. We then find a significant qualitative difference between the F-theory models of the split types with half-hypermultiplets and the non-split one. Next, we consider the puzzles of non-local matter generation near the codimension-two singularities where the codimension-one singularity is enhanced to D_6. In terms of the anomaly cancellation condition and the resolution of the singularities, we state the puzzles.

These puzzles are not unique to the non-split I_6 model; other non-split models also have them. In the last half of this thesis, toward understanding these puzzles related to non-local matter generation, for all models where the fibre type is distinguished into the split and the non-split fibre type, we investigate the relationship between the split and the non-split models, respectively. We then show that the split/non-split transition, except for a special class of models, can be regarded as a conifold transition. This is related to the conifold singularities remaining after the blow-ups of the codimension-one singularity at the codimension-two singularities where the codimension-one singularity is enhanced to D_{2k+2} ($k \geq 1$) or E_7. This clarifies that "local deformed conifolds" appear where matter fields exist without any special parameter tuning in non-split models. And this also shows that the puzzle in resolution analysis is due to conifold singularities becoming deformed. These are non-local in terms of the base space and thus imply non-local matter generation. We also examine how previous proposals for non-local matter generation can be implemented in our resolution analysis.

Contents

Chapter 1

Introduction

Superstring theory is a leading candidate for a unified theory involving quantum gravity. Thus, there have been many attempts to construct phenomenological models from superstring theory. For example, Models beyond the Standard Model such as the Grand Unified Theory (GUT) have been constructed: the intersecting D-brane model, the models based on the Calabi-Yau compactification of the Heterotic superstring theory, etc. Also, models of early cosmology such as inflationary models have been constructed: the KKLT model [2, 3], etc. However, models based on the isotropic Calabi-Yau compactification of Heterotic superstring theory have a difficulty in that the experimental results cannot be explained for weak coupling since Newton's constant and the GUT coupling constant are related to each other [4]. One way to solve this difficulty is to consider warped compactification, and a brane picture is useful for this setup. In addition, D-branes are also useful when considering moduli stabilization and are often used in cosmological model building. Therefore, it is interesting to construct a model with a brane picture.

It is known that a theory on a D-brane in Type IIB superstring theory has $U(1)$ gauge symmetry derived from the fundamental string. In addition, if we consider symmetry enhancement by stacking N D-branes, the $(S)U(N)$ non-abelian gauge theory and its bifundamental representation appear [5]. However, if we consider only D-branes (and orientifold planes) and fundamental strings, the spinor representation which includes all of the matter fields of the Standard Model in one generation does not appear[1]. In order to realize the spinor representation, it is necessary to have a mechanism in which the exceptional gauge symmetry (i.e., E_6, E_7 and E_8) breaks into the $SO(n)$ gauge symmetry. Such a mechanism with a brane picture can be realized in F-theory and its dual superstring theory[2].

---

[1]There is another problem with the intersecting D-brane model. The SU(5) GUT can naturally explain the assignment of hypercharges to quarks and leptons. However, The $SU(5)$ GUT model based on the intersecting D-brane model prohibits up-type Yukawa coupling [6]. On the other hand, in F-theory, this problem does not arise when we consider that the exceptional gauge symmetry breaks into $SU(5)_{GUT}$ [7].

[2]After the LHC experiments, global F-theory GUTs have attracted great interest (see e.g. [8–40]).

Before going into the discussion of the F-theory, we describe the properties of a vacuum for Type IIB superstring theory. We consider that the axio-dilaton field τ, and thus the string coupling constant $g_s = e^\phi$, is allowed to vary. In this case, this means that there are 7-branes; and then, the configuration of the axio-dilaton field depends only on the coordinates of a complex n-dimensional compact subspace B_n of the ten-dimensional space-time:

$$\tau(B_n) = C_0(B_n) + ie^{-\phi(B_n)} \tag{1.0.1}$$

where C_0 is the Ramond-Ramond (R-R) scalar field and ϕ is the dilaton field. More specifically, in the case of $B_1 = \mathbb{P}^1$, if we consider the case where there is a D-brane at $z = 0$ (z is an affine coordinate of $\mathbb{P}^1$), the axio-dilaton field near $z = 0$ is

$$\tau(z) \sim \frac{1}{2\pi i} \log(z), \tag{1.0.2}$$

not constant, since a 7-brane is a magnetic charge for $\tau(B_n)$ and the BPS condition requires that $\tau(B_n)$ be a holomorphic function. Thus, the configuration of τ varies and nontrivial monodromy occurs around the point where the value of τ diverges and there is a D7-brane.

This monodromy and the $SL(2, \mathbb{Z})$ transformation allows 7-branes with not only R-R charges p but also Neveu-Schwarz-Neveu-Schwarz (NS-NS) charges q to appear. Note that, since Type IIB superstring theory has the self $SL(2, \mathbb{Z})$ duality [51], all monodromies made by $[p, q]$7-branes can be identified under the $SL(2, \mathbb{Z})$ S-duality transformation:

$$\tau \rightarrow \frac{a\tau + b}{c\tau + d}, \quad \begin{pmatrix} a & b \\ c & d \end{pmatrix} \in SL(2, \mathbb{Z}). \tag{1.0.3}$$

Therefore, when a general 7-brane exists alone, we can consider the 7-brane is identified with the $D([1, 0])$7-brane. Similarly, even if multiple 7-branes lie on top of each other, each 7-brane is similar to this case after deforming each 7-brane to exist alone. However, when stacking 7-branes at a point, of course, it may be possible to stack 7-branes with different charges (p, q). This causes the non-locality among the 7-branes and gives rise to open-string-like trivalent objects: string junctions. F-theory is an attempt to give a geometric interpretation to this vacuum of Type IIB superstring theory.

F-theory is a geometrical framework of non-perturbative compactifications of Type IIB superstring theory with general 7-branes, proposed by Vafa in 1996 [52][3]. There is a duality between F-theory and Type IIB superstring:

F/elliptically fibred Y_{n+1} over $B_n \simeq$ IIB/ B_n with 7-branes,

On the other hand, for papers on local F-theory GUTs, which is an analysis based on the quantum field theory, decoupling the closed string contribution, see e.g. [41–50].

[3]There are many good reviews for F-theory [53–58].

where $n \in \mathbb{N}$ and Y_{n+1} is a complex n-dimensional total manifold and we denote a duality as $\simeq$. In F-theory, the configuration of the axio-dilaton field (1.0.1) in Type IIB superstring theory is described by the complex structure modulus of the torus in an elliptic fibration over the base space B_n. Then, the $SL(2, \mathbb{Z})$ S-duality transformation (1.0.3) is identical to the modular transformation of a torus in F-theory. The non-perturbative aspects of F-theory arise from nontrivial monodromies among 7-branes in Type IIB superstring theory.

F-theory has a duality with M-theory as well [52, 59]:

$$(10 - 2n)\text{-dim. F/elliptically fibred } Y_{n+1}$$
$$\simeq (9 - 2n)\text{-dim. M/elliptically fibred } Y_{n+1}|_{V \to 0}$$

where $V := \mathrm{Vol}(\mathbb{E}_\tau)$ and $\mathbb{E}_\tau$ is an elliptic curve. $V \to 0$ on the M-theory side corresponds to the fact that a Kähler modulus does not arise from the extra two dimensions $\mathbb{E}_\tau$ in F-theory. This means that the extra two dimensions in F-theory are *virtual*, in contrast to M-theory, where all eleven dimensions, including the extra one dimension, are physical space-time. Since Y_{n+1} is only composed of physical space on the M-theory side, the first Chern class c_1 of Y_{n+1} has to vanish in order to preserve supersymmetry. This implies that Y_{n+1} is a Calabi-Yau manifold [60, 61]. For example, in the case of flat eight dimensions, Y_2 and the base space B_1 are the elliptically fibred $K3$ and $\mathbb{P}^1$, respectively.

Let us discuss F-theory more specifically. An elliptic fibration over the base space B_n with section is described by the Weierstrass equation

$$y^2 = x^3 + f(B_n)x + g(B_n), \tag{1.0.4}$$

where f and g are sections of certain line bundles over the base space B_n. A cycle of an elliptic curve $\mathbb{E}_\tau$ over the discriminant locus

$$\Delta(B_n) := 4f(B_n)^3 + 27g(B_n)^2 = 0 \tag{1.0.5}$$

vanishes and the fibre becomes a singular fibre. In particular, We consider the case for an elliptic fibre to be singular and a total space Y_{n+1} not to be. We can confirm that this case corresponds to the case that a 7-brane exists alone and that the discriminant locus gives the position of a 7-brane on the Type IIB superstring theory side. In addition, a vanishing cycle gives information about the charge (p, q).

We consider the case for not only an elliptic fibre but also an elliptic surface to be singular. This case corresponds to multiple 7-branes stacked on the dual IIB superstring theory side; and then, we can consider the non-abelian gauge symmetries arising from there. Such singularities of an elliptic surface are classified by Kodaira, which is called the Kodaira classification [62]. Kodaira's classification is based on the intersection diagrams of exceptional curves $\mathbb{P}^1$ that arise after the blow-ups (Table 3.2). We can confirm that these intersection diagrams correspond exactly to the Dynkin diagrams of the expected

gauge symmetries[4]. Therefore, a type of (non-abelian) gauge symmetry corresponds to a singular fibre type of the elliptic surface in F-theory. In particular, E_6, E_7 and E_8 gauge symmetries are realized when the Kodaira fibre types are IV^*, III^* and II^*, respectively. This is one of the virtues of F-theory.

It was shown that the Kodaira singular fibre types are labeled by the conjugate class of the $SL(2, \mathbb{Z})$ monodromy around the singular fibres [63–65]. Therefore, through the monodromy, we can see a correspondence between F-theory and Type IIB superstring theory. As the result, it is known that the exceptional non-abelian gauge symmetries and the spinor representations have been explained by using string junctions in the dual Type IIB superstring theory [63–83][5].

In this thesis, we consider matter generation in F-theory. For this purpose, we focus on six-dimensional F-theories. We introduce the Heterotic/F-theory duality, which is useful in discussing matter generation. If the properties are particularly good ("stable degeneration limit"), this duality is [52, 87–89]

$$\text{F/ } K3 \text{ fibred over } B_{n-1} \simeq E_8 \times E_8 \text{ Het./elliptically fibred over } B_{n-1}.$$

In particular, in the six-dimensional ($n = 2$) case, we are to consider a Calabi-Yau three-fold which is an elliptic fibration over a Hirzebruch surface $\mathbb{F}_n$. In this case, we can classify their singular fibres by Tate's algorithm [90, 91]. However, unfortunately, a dictionary connecting F-theory and Heterotic superstring theory for the generation of matter fields has not yet been fully established. In this thesis, we focus on an F-theory on an elliptic fibration over a Hirzebruch surface $\mathbb{F}_n$.

In order to understand six- or lower-dimensional F-theories, we need to consider the cases beyond the Kodaira classification. When considering an elliptically fibred Calabi-Yau threefold, there are not only "codimension-one"[6] singularities but also "codimension-two" ones[7]. The "codimension-one" singularity is a codimension-two locus in the total elliptically fibred Calabi-Yau threefold, where an elliptic fibre becomes a singular fibre. In other words, a "codimension-one" locus, which is the projection of this codimension-two locus onto the base space, is the discriminant locus (1.0.5). On the Type IIB superstring theory side, a non-abelian gauge symmetry is realized on this "codimension-one" locus,

---

[4]In this thesis, we use "the singularity is G" in F-theory since there is an almost one-to-one correspondence between a Kodaira singular fibre type and a Dynkin diagram of a simply-laced gauge theory G (except for $G = SU(2)$ and $SU(3)$). In the following chapters, these scare quotes are omitted.

[5]It was shown that a string junction is necessary to understand the spectrum of BPS states in the gauge theory on the brane from the standpoint of superstring theory [79, 80, 84]. The string junctions are also useful for describing chiral matter [85] and the non-simply laced gauge symmetries [86].

[6]We use the scare quotes to emphasize that the codimension is not counted in the total space but in the base space of the elliptic fibration. In the following chapters, these scare quotes are omitted.

[7]When considering an elliptically fibred Calabi-Yau threefold, there are also "codimension-three" singularities. The "codimension-three" singularities are involved in the Yukawa couplings in the four-dimensional theory [41, 42, 44, 92].

where stacks of 7-branes reside on top of each other. If this "codimension-one" singularity is resolved, we can yield a collection of exceptional curves aligned along the "codimension-one" locus, thus we can discuss the singular fibre type beyond the Kodaira classification over the "codimension-one" locus.

In six- or lower-dimensional F-theories, if a fibre type has the condition that an exceptional curve splits into two irreducible ones, then depending on whether the exceptional curve can split globally or not, the fibre types can be distinguished into two types: "split" and "non-split" [90]. In split models, each intersection diagram of exceptional curves that arises after the resolution corresponds to the ADE Dynkin diagram implied by Kodaira's classification at a point on the "codimension-one" locus. On the other hand, in non-split models, the two split exceptional curves are identified by monodromy that is different from ones made by 7-branes. Therefore, each ADE gauge symmetry in the split models is reduced to the non-simply-laced one (i.e., B_n, C_n, F_4 and G_2) by being subject to a projection by a diagram automorphism. The fibre type I_n ($n = 3, 4, \cdots$), I_n^* ($n = 0, 1, \cdots$), IV or IV^* can involve such identification of exceptional curves (Table 5.1 and 6.1).

The "codimension-two" singularity is associated with the "codimension-two" locus on the base space, on which "codimension-one" singularities intersect each other and their singularities are enhanced. On the Type IIB superstring theory side, this "codimension-two" locus corresponds to the intersection of stacks of 7-branes, where the expected gauge symmetry is enhanced. Therefore, the "codimension-two" singularity is involved in matter generation. In particular, in a split model, if a "codimension-two" singularity is resolved, we can yield an intersection diagram of exceptional curves that is different from one on a "codimension-one" locus and explains the enhancement of the gauge symmetry[8].

In this thesis, we first review the basics and the dualities of F-theory. As we have seen so far, in F-theory, singularities are essential for geometrically realizing various aspects of string theory[9]. Thus, we review the relationship between the information of both the matter representations and the gauge symmetries and the singularities of geometry.

Next, we consider an F-theory on an elliptic fibration over a Hirzebruch surface $\mathbb{F}_n$. In the six-dimensional F-theory, the matter fields are the hypermultiplets. However, if a model has the split I_6, I_2^* or III^* "codimension-one" singularity corresponding to the A_5, D_6 or E_7 gauge symmetry, respectively, half-hypermultiplets and interesting structures of singularity appear in the model [87, 88, 90, 93, 97]. In addition, the gauge enhancements in which the half-hypermultiplets arise in these models are associated with the applications to GUT model building in F-theory. In this thesis, we review this discussion using

---

[8]In some split models, we can yield new two-cycles by small resolutions of the conifold singularities at a "D_{2k+2} ($k \geq 1$)" or "E_7" point [93–95]. In the M-theory dual, an $M2$-brane wrapped around one of these two-cycles generates the localized matter multiplets [96].

[9]In particular, it is important that the phenomenological model building based on F-theory by analyzing geometric singularities can be done without decoupling the closed string contribution.

the A_5 case as an example [93][10]. Also, these gauge symmetries correspond to particular quaternionic Kähler symmetric spaces and are related to the Freudenthal-Tits magic square. The C_3 gauge symmetry is the only non-simply-laced one among them. As a final magical example, we investigate the non-split I_6 "codimension-one" singularity, in which the unbroken gauge symmetry is C_3 [99]. We then find the puzzles of non-local matter generation in the base space near the "codimension-two" singularities where the "codimension-one" singularity is enhanced to D_6 [99].

These puzzles are not unique to the non-split I_6 model but are ones that other non-split models also have [1, 90, 95, 100–104]. Finally, toward understanding these puzzles, we investigate the relationship between the split and the non-split models in all models where there is a distinction between split and non-split fibre types [95]. We also discuss the correspondence between our resolution analysis and previous proposals [1] for non-local matter generation [95].

This thesis is organized as follows: In Chapter 2, we introduce the $[p, q]$7-branes and their monodromies for the construction of F-theory. We also classify the monodromies made by 7-branes at a point and the 7-brane configurations. In Chapter 3, we give an overview of F-theory. We first discuss some mathematical facts for the F-theory construction and find that a discriminant locus of a Weierstrass equation corresponds to a position of 7-branes at a point. Next, we consider "codimension-one" singularities. We see what kind of gauge symmetry is realized for a 7-brane configuration from the standpoint of the Kodaira classification which is the classification of the singular fibres of the elliptic surface. Finally, we briefly explain the F-/M-theory duality. In Chapter 4, we summarize the Heterotic/F-theory duality. We also find the anomaly cancellation condition. In addition, we see that the analysis on the Heterotic superstring theory side satisfies this condition. In the last section, we discuss whether this condition is also satisfied on the F-theory side; and then, we find that matter fields arise at "codimension-two" singularities when we consider ADE (split type) "codimension-one" singularities. In Chapter 5, we perform the analysis by resolution for the six-dimensional F-theory models, in which half-hypermultiplets arise. In particular, we consider the case of the gauge symmetries: A_5 and C_3, in other words, I_6^s and I_6^{ns} "codimension-one" singularities in the six-dimensional F-theory. We also show the non-split models have some puzzles regarding the non-local matter generation. This chapter is based on our paper [99]. In Chapter 6, we consider all models which have non-split fibre in six-dimensional F-theory, toward understanding these puzzles. From the standpoint of resolution analysis, we investigate the relationship between a split and the corresponding non-split model for all cases in which a non-split model exists, focusing on a conifold singularity. We also examine the correspondence between our resolution analysis and the previous proposal [1] for the non-local matter generation in the non-split models. This chapter is based on our paper [95].

---

[10]The case of D_6 and E_7 is discussed in [98].

Chapter 2

7-brane Solution of Type IIB Superstring theory

In this chapter, we consider the 7-brane solution of Type IIB superstring theory for constructing F-theory [52]. We first construct the 7-brane solution and introduce the monodromy made by a 7-brane. Next, we introduce $[p, q]$7-branes as general 7-branes and string junctions due to the $SL(2, \mathbb{Z})$ transformation. This string junction [81] is an open-string-like trivalent object and is needed to realize an exceptional gauge symmetry or a spinor representation [63–70, 79, 80, 82, 84]. We then classify the configurations of 7-branes by the classification of the monodromies created by the 7-branes. Finally, we discuss the configuration of 7-branes and the expected gauge symmetries by analyzing the monodromies in Type IIB superstring theory [63–65].

2.1 Construction of 7-brane solution

The bosonic content of Type IIB superstring theory consists of C_p ($p = 0, 2, 4$), which is the R-R p-form field, $g_{\mu\nu}$, B_2 and ϕ, which are the metric, the NS-NS 2-form field and the dilaton field, respectively. By combining C_0 and ϕ, we can define a complex massless scalar field called the axio-dilaton field

$$\tau = C_0 + ie^{-\phi}. \tag{2.1.1}$$

Note that the string coupling constant $g_s = e^\phi$. In this section, we find the classical solution for which the axio-dilaton field τ depends only on the coordinates of the complex projective line $\mathbb{P}^1 : z = x_8 + ix_9$. This is called the 7-brane solution[1]. A 7-brane is an object that extends to one dimension in time and seven dimensions in space. When we consider compactification to $(1+7)$-dimensions, it extends in the flat $(1+7)$-dimensional direction. It is also a complex codimension-one object in the compact space of Type

---

[1]The 7-brane solution is a $\frac{1}{2}$ BPS solution and conserves 16 supercharges.

IIB superstring theory. Since the 7-brane carries the magnetic charge of the axio-dilaton field τ^2, the vacuum expectation value of $\tau(z)$ can vary when the 7-brane exists as a background field.

The action of a ten-dimensional $\mathcal{N} = (2, 0)$ supergravity theory, which is the low-energy effective theory of Type IIB superstring theory, is

$$\frac{1}{2\pi} S_{\text{IIB,string}} = \int d^{10}x e^{-2\phi}\sqrt{-g}\left(R + 4g_{\mu\nu}\partial^\mu\phi\partial^\nu\phi\right) - \frac{1}{2}\int e^{-2\phi}H_3 \wedge *H_3$$

$$-\frac{1}{4}\sum_{p=0}^{4}\int F_{2p+1} \wedge *F_{2p+1} - \frac{1}{2}\int C_4 \wedge H_3 \wedge F_3$$

$$+\text{(fermionic term)} \qquad (2.1.2)$$

in the string frame, where μ, $\nu = 0, 1, \ldots, 9$ and the string length is normalized to $l_s = 2\pi\sqrt{\alpha'} \equiv 1$. The field strengths are, respectively,

$$\begin{aligned}
H_3 &= dB_2, \\
F_1 &= dC_0, \\
F_3 &= dC_2 - C_0 dB_2, \\
F_5 &= dC_4 - \frac{1}{2}C_2 \wedge dB_2 + \frac{1}{2}B_2 \wedge dC_2, \\
F_9 &= *F_1, \\
F_7 &= -*F_3,
\end{aligned} \qquad (2.1.3)$$

where C_p $(p = 0, 2, 4)$ is the R-R p-form field and B_2 is the NS-NS 2-form field. However, it is necessary to impose the duality relation:

$$F_5 = *F_5 \qquad (2.1.4)$$

at the level equation of motion for this action.

Since the transformation from a string frame, which is convenient for world sheet theory, to an Einstein frame, which is convenient for gravity theory, can be performed by

$$g_{\mu\nu} \rightarrow e^{\frac{\phi}{2}}g_{\mu\nu}, \qquad (2.1.5)$$

the action in the Einstein frame is by

$$\frac{1}{2\pi} S_{\text{IIB,Einstein}} = \int d^{10}x\sqrt{-g}\left(R - \frac{\partial_\mu\tau\partial^\mu\bar{\tau}}{2(\text{Im}\,\tau)^2} - \frac{1}{2}\frac{|G_3|^2}{\text{Im}\,\tau} - \frac{1}{4}|F_5|^2\right)$$

---

[2]In general, the electric charge and the magnetic charge of a $(p + 1)$-form field in the supergravity approximation of string theory are interpreted as being carried by a p-brane and a $(7 - p)$-brane, respectively [105]. For example, it is known that the R-R scalar field C_0 is 0-form and is carried by a $D7$-brane.

$$+\frac{1}{4i}\int \frac{1}{\operatorname{Im}\tau}C_4 + G_3 \wedge \bar{G}_3 + \text{(fermionic term)}, \qquad (2.1.6)$$

where

$$G_3 \;=\; dC_2 - \tau dB_2, \qquad (2.1.7)$$

$$|F_p|^2 \;=\; \frac{1}{p!}F_{\mu_1\ldots\mu_p}F^{\mu_1\ldots\mu_p}. \qquad (2.1.8)$$

This action is invariant under the $SL(2,\mathbb{Z})$ transformation ($SL(2,\mathbb{Z})$ duality):

$$
\begin{aligned}
M &= \begin{pmatrix} a & b \\ c & d \end{pmatrix} \in SL(2,\mathbb{Z}), \\
\tau &\to \frac{a\tau + b}{c\tau + d}, \\
\begin{pmatrix} C_2 \\ B_2 \end{pmatrix} &\to M \begin{pmatrix} C_2 \\ B_2 \end{pmatrix}, \\
C_4 &\to C_4, \\
g_{\mu\nu} &\to g_{\mu\nu},
\end{aligned}
\qquad (2.1.9)
$$

where

$$\tau \in \mathbf{H}/SL(2,\mathbb{Z})$$

since the axio-dilaton field τ is $Im\ \tau > 0$. In particular, considering the S ($\in SL(2,\mathbb{Z})$) transformation, the transformation of the axio-dilaton field: τ is

$$M = S := \begin{pmatrix} 0 & -1 \\ 1 & 0 \end{pmatrix}, \quad \tau \;\to\; -\frac{1}{\tau} \qquad (2.1.10)$$

and thus the S transformation is a transformation that swaps strongly coupled and weakly coupled regions.

The $D7$-brane is an object carrying the electric charge of the R-R 8-form field C_8 and the magnetic charge of the R-R scalar field C_0. If there is a $D7$-brane in $\mathbb{R}^{1,7}$ ($\subset \mathbb{R}^{1,9} \simeq \mathbb{R}^{1,7} \times \mathbb{C}$) and at $z = z_i \in \mathbb{C}$ exists, since a $D7$-brane has R-R charge 1, the Bianchi identity for F_9 holds

$$\oint_{z_i} *F_9 = \oint_{z_i} dC_0 = 1, \qquad (2.1.11)$$

where $\oint_{z_i}$ denotes the circumferential integral around z_i.

Next, we find the 7-brane solution. Assume that all fields depend only on $z = x_8 + ix_9$:

$$\tau \;=\; \tau(z, \bar{z}). \qquad (2.1.12)$$

If we impose the condition

$$B_2 \quad = \quad C_2 = C_4 = \text{(fermionic term)} = 0, \tag{2.1.13}$$

$$ds^2 \quad = \quad -dt^2 + e^{\varphi(z,\bar{z})}dzd\bar{z} + \left(dx^i\right)^2 \quad (i = 1, \ldots, 7), \tag{2.1.14}$$

Eq. (2.1.6) becomes

$$\frac{1}{2\pi}S_{\text{IIB,Einstein}} = \int d^{10}x\sqrt{-g}\left(R - \frac{\partial_\mu\tau\partial^\mu\bar{\tau}}{2(\text{Im}\,\tau)^2}\right). \tag{2.1.15}$$

From Eq. (2.1.15), the equation of motion for $\bar{\tau}$ is

$$\partial_z\partial_{\bar{z}}\tau \quad = \quad \frac{2}{\tau - \bar{\tau}}\partial_z\tau\partial_{\bar{z}}\tau. \tag{2.1.16}$$

Also, the 89 and ii components of the Einstein equation are

$$0 \quad = \quad \partial_z\tau\partial_z\bar{\tau} - \partial_{\bar{z}}\tau\partial_{\bar{z}}\bar{\tau}, \tag{2.1.17}$$

$$\partial_z\partial_{\bar{z}}\varphi \quad = \quad \frac{1}{(\tau - \bar{\tau})^2}(\partial_z\tau\partial_{\bar{z}}\bar{\tau} + \partial_{\bar{z}}\tau\partial_z\bar{\tau}), \tag{2.1.18}$$

respectively. The 88 and 99 components of the Einstein equation are identities. We choose

$$\partial_{\bar{z}}\tau \quad = \quad 0 \tag{2.1.19}$$

as the solution for Eq. (2.1.16) and Eq. (2.1.17). Thus, the axio-dilaton field τ is the holomorphic function of z ($\in \mathbb{C}$):

$$\tau(z,\bar{z}) = \tau(z). \tag{2.1.20}$$

From the $SL(2,\mathbb{Z})$ symmetry of Type IIB superstring theory (2.1.9), $\tau(z)$ is a one-to-one map from $\mathbb{C}$ to the $SL(2,\mathbb{Z})$ fundamental region ($\mathbb{H}/SL(2,\mathbb{Z})$). For example, if the axio-dilaton field τ is a single-valued function, from Eq. (2.1.20), the value of τ is uniquely determined at each point in the complex plane: $z_j \in \mathbb{C}$ and there is no monodromy. We consider the Bianchi identity (2.1.11) and if the axio-dilaton field τ is a multi-valued function to allow for monodromy which can be identified by $SL(2,\mathbb{Z})$ transformations, then

$$\tau(z) \quad = \quad \frac{1}{2\pi i}\log(z - z_i) + \text{(terms regular at } z_i). \tag{2.1.21}$$

Thus, τ varies over the compact space of Type IIB superstring theory. In this case, there is a $D7$-brane at $z = z_i$ and

$$\tau(z \to z_i) \quad \to \quad i\infty \tag{2.1.22}$$

is obtained. This corresponds to the limit of the weakly coupled region where the contribution of the dilaton field ϕ is larger. Also, from Eq. (2.1.21), we obtain

$$\tau(z) = \frac{N}{2\pi i} \log(z - z_i) + \text{(terms regular at } z_i) \tag{2.1.23}$$

when N $D7$-branes exist at $z = z_i$. The z-dependence of $\tau(z)$ means that the 7-brane introduces a branch cut since the *log* is a multi-valued function.

We explain the monodromy. Considering $\tau(z)$ to orbit around the 7-brane, the operation $(z - z_i) \to e^{2\pi i}(z - z_i)$ results in the modification:

$$\tau \quad \to \quad \tau + 1, \tag{2.1.24}$$

since $\tau(z)$ has a *log*-like term. This is thought to be because the R-R scalar field C_0 picks up the R-R charge of a $D7$-brane as it orbits around the $D7$-brane. And this is called having a monodromy. This monodromy comes from the fact that τ is a multi-valued function, as allowed by the $SL(2, \mathbb{Z})$ symmetry. Then, M defined in Eq. (2.1.9) is called a monodromy matrix. This monodromy (matrix) by a $D7$-brane is represented by

$$M = \begin{pmatrix} 1 & 1 \\ 0 & 1 \end{pmatrix} =: T. \tag{2.1.25}$$

Moreover, from the $SL(2, \mathbb{Z})$ symmetry of Type IIB superstring theory, we assume that all monodromies that are $SL(2, \mathbb{Z})$-conjugate with the T transformation are allowed. This is discussed in Section 2.3 and 2.6.

In the discussion up to this point, we considered the solution for the case of one $D7$-brane. In the next section, we will find the 7-brane solution when there are multiple 7-branes.

2.2   2D metric in $\mathbb{P}^1$

In this section, we derive a metric for the compact space of Type IIB superstring theory $\mathbb{P}^1$ for considering the elliptically fibred $K3$ compactification of F-theory. The metric is obtained as a solution of the Einstein equation (2.1.18) when the conditions are imposed [106]. In this section, we obtain this metric by noting that its supersymmetry is conserved [107]. We obtain the concrete equation for the metric when we make the same assumptions as in the previous section.

As in the previous section, we assume that the metric is

$$ds^2 = -dt^2 + \left(dx^i\right)^2 + e^{\varphi(z,\bar{z})} dz d\bar{z} \quad (i = 1, \ldots, 7). \tag{2.2.1}$$

Furthermore, we assume that the axio-dilaton field of Type IIB superstring theory: τ is a holomorphic function:

$$\tau = \tau(z) \tag{2.2.2}$$

from Eq. (2.1.19) and The values of all other supergravity fields are set to zero. Then, the supersymmetric transformations of gravitino ψ_μ and dilatino λ are [108, 109]:

$$\delta\psi_\mu = \frac{1}{\kappa}\left(\partial_\mu - \frac{1}{4}\omega_{\mu\alpha\beta}\gamma^{\alpha\beta} - \frac{i}{2}Q_\mu\right)\epsilon, \tag{2.2.3}$$

$$\delta\lambda = \frac{i}{\kappa}P_\mu\gamma^\mu\epsilon^*, \tag{2.2.4}$$

where κ is a constant, $\omega_{\mu\alpha\beta}$ is the spin connection, and ϵ is the killing spinor. Also, P_μ and Q_μ are $SU(1,1)$-invariant connections, given by

$$P_\mu = -\frac{\partial_\mu\tau}{\tau - \bar\tau}, \tag{2.2.5}$$

$$Q_\mu = -\frac{i}{2}\frac{\partial_\mu(\tau + \bar\tau)}{\tau - \bar\tau}. \tag{2.2.6}$$

z and $\bar z$ are

$$z = x^8 + ix^9, \quad \bar z = x^8 - ix^9, \tag{2.2.7}$$

using the space-time coordinates: x^8 and x^9. Also, the two-dimensional γ matrices are

$$\gamma^8 = \sigma_1, \quad \gamma^9 = \sigma_2, \tag{2.2.8}$$

and then

$$\gamma^z = \sigma_1 + i\sigma_2, \quad \gamma^{\bar z} = \sigma_1 - i\sigma_2. \tag{2.2.9}$$

We consider Eq. (2.2.4). Note that the axio-dilaton field τ is a holomorphic function,

$$P_{\bar z} = 0. \tag{2.2.10}$$

Therefore, since

$$\delta\lambda = \frac{i}{\kappa}P_z\gamma^z\epsilon^*$$

$$\propto \begin{pmatrix} 0 & \# \\ 0 & 0 \end{pmatrix}\epsilon^* \quad (\# \in \mathbb{C}), \tag{2.2.11}$$

where $\tilde\epsilon$ is an arbitrary complex number and

$$\epsilon^* = \begin{pmatrix} \tilde\epsilon^* \\ 0 \end{pmatrix}, \tag{2.2.12}$$

then Eq. (2.2.4) becomes

$$\delta\lambda = 0. \tag{2.2.13}$$

Next, we consider Eq. (2.2.3). From the assumption of the metric (2.2.1) the nontrivial spin connection components are only

$$\omega_{z89} = \frac{i}{2}\partial_z\varphi = -\omega_{z98}, \tag{2.2.14}$$

$$\omega_{\bar{z}89} = -\frac{i}{2}\partial_{\bar{z}}\varphi = -\omega_{\bar{z}98}. \tag{2.2.15}$$

Also, since the axio-dilaton field τ is a holomorphic function,

$$Q_z = -\frac{i}{2}\frac{\partial_z\tau}{\tau - \bar{\tau}} = -\frac{i}{2}\frac{\partial_z(\tau - \bar{\tau})}{\tau - \bar{\tau}}, \tag{2.2.16}$$

$$Q_{\bar{z}} = -\frac{i}{2}\frac{\partial_{\bar{z}}\bar{\tau}}{\tau - \bar{\tau}} = +\frac{i}{2}\frac{\partial_{\bar{z}}(\tau - \bar{\tau})}{\tau - \bar{\tau}}. \tag{2.2.17}$$

Since

$$\epsilon = \begin{pmatrix} \tilde{\epsilon} \\ 0 \end{pmatrix} \tag{2.2.18}$$

from Eq. (2.2.12), Eq. (2.2.3) is

$$\left(\partial_z - \frac{1}{4}\omega_{z\alpha\beta}\gamma^{\alpha\beta} - \frac{i}{2}Q_z\right)\epsilon = \begin{pmatrix} \partial_z\tilde{\epsilon} + \frac{1}{4}\partial_z(\varphi - \log(\tau - \bar{\tau}))\cdot\tilde{\epsilon} \\ 0 \end{pmatrix}, \tag{2.2.19}$$

$$\left(\partial_{\bar{z}} - \frac{1}{4}\omega_{\bar{z}\alpha\beta}\gamma^{\alpha\beta} - \frac{i}{2}Q_{\bar{z}}\right)\epsilon = \begin{pmatrix} \partial_{\bar{z}}\tilde{\epsilon} - \frac{1}{4}\partial_{\bar{z}}(\varphi - \log(\tau - \bar{\tau}))\cdot\tilde{\epsilon} \\ 0 \end{pmatrix}. \tag{2.2.20}$$

For supersymmetry (SUSY) to be conserved,

$$\delta\psi_\mu = 0 \tag{2.2.21}$$

must hold, and thus φ must be

$$\varphi(z, \bar{z}) = \log\frac{\tau - \bar{\tau}}{2i} + F(z) + \bar{F}(\bar{z}), \tag{2.2.22}$$

where $F(z)$ is an arbitrary holomorphic function. The component of the killing spinor $\tilde{\epsilon}$ is

$$\tilde{\epsilon} = e^{\frac{1}{4}(F - \bar{F})} \times \text{ const. }, \tag{2.2.23}$$

and half of SUSY is conserved.

Since the metric has the $SL(2, \mathbb{Z})$ invariance of Type IIB superstring theory, we further restrict the holomorphic function $F(z)$ to be

$$F(z) = 2\log\eta(\tau(z)) + f(z), \tag{2.2.24}$$

where $\eta(\tau)$ is Dedekind's η-function defined by

$$\eta(\tau) = q^{\frac{1}{24}} \prod_{n=1}^{\infty} (1 - q^n) , \quad q = e^{2\pi i \tau}. \tag{2.2.25}$$

The first term is the term needed to conserve $SL(2, \mathbb{Z})$ invariance and $f(z)$ is the function needed to keep the metric from going to zero at the location of 7-branes. Since the axio-dilaton field τ is given by Eq. (2.1.21), then

$$\tau \sim \frac{1}{2\pi i} \log(z - z_i) \tag{2.2.26}$$

when there is a 7-brane at $z = z_i$. Then, since $\tau \to i\infty$ ($\text{Im}\,\tau \to \infty$), it corresponds to the limit of $q \to 0$. In this limit,

$$\frac{\tau(z) - \bar{\tau}(\bar{z})}{2i} \eta^2(\tau(z)) \bar{\eta}^2(\bar{\tau}(\bar{z})) \quad \to \quad \frac{\tau(z) - \bar{\tau}(\bar{z})}{2i} (z - z_i)^{\frac{1}{12}} (\bar{z} - \bar{z}_i)^{\frac{1}{12}}, \tag{2.2.27}$$

and thus,

$$f(z) \sim -\frac{1}{12} \log(z - z_i). \tag{2.2.28}$$

From the above, if there are N 7-branes, the metric of $\mathbb{P}^1$ is

$$\begin{aligned} ds^2_{\mathbb{P}^1} &= e^{\varphi(z,\bar{z})} dz d\bar{z} \\ &= \frac{\tau(z) - \bar{\tau}(\bar{z})}{2i} \eta^2(\tau(z)) \bar{\eta}^2(\bar{\tau}(\bar{z})) \prod_{i=1}^{N} (z - z_i)^{-\frac{1}{12}} (\bar{z} - \bar{z}_i)^{-\frac{1}{12}} dz d\bar{z}. \end{aligned} \tag{2.2.29}$$

We obtain the 7-brane solution when there are some 7-branes.

Finally, we investigate the metric structure of the z-plane at infinity. Since $\tau(z) \to const.$ when $|z| \to \infty$, we have

$$e^{\varphi} \quad \to \quad |z^{-\frac{N}{12}}|^2 \times const. \tag{2.2.30}$$

Thus, if we ignore the constant-doubling contribution, the metric is

$$ds^2_{\mathbb{P}^1} \quad \to \quad |z^{-\frac{N}{12}} dz|^2. \tag{2.2.31}$$

If we consider a coordinate transformation that rewrites this into the flat metric

$$ds^2_{\mathbb{P}^1} = |dw|^2, \tag{2.2.32}$$

we obtain

$$w = z^{1-\frac{N}{12}}. \tag{2.2.33}$$

Thus, for the transformation $z \to e^{2\pi i} z$,

$$w \quad \to \quad e^{2\pi i(1-\frac{N}{12})} w. \tag{2.2.34}$$

From the above, there is a missing angle of $2\pi \frac{N}{12}$ at infinity in the z-plane. Therefore, the condition for the z-plane to be compact ($\mathbb{P}^1$) (i.e., smooth at infinity) is when only $N = 24$, in other words, when there are only 24 7-branes as background fields. This corresponds to the fact that we consider F-theory on elliptically fibred $K3$, which will be discussed later.

2.3 (p,q)-string and $[p,q]$7-brane

In Type IIB superstring theory, there is not only the D7-brane that can be introduced as a background field. We briefly explain this. There are not only R-R 2-form field C_2 but also NS-NS 2-form field B_2 in Type IIB supergravity theory. These two types of fields are converted by

$$\begin{pmatrix} C_2 \\ B_2 \end{pmatrix} \rightarrow M \begin{pmatrix} C_2 \\ B_2 \end{pmatrix}, \quad M \in SL(2,\mathbb{Z}) \tag{2.3.1}$$

and mixed with each other under the $SL(2,\mathbb{Z})$ transformation of Type IIB superstring theory. Thus, the open string in Type IIB superstring theory has two charges, NS-NS charge q and R-R charge p. An open string with NS-NS charge q and R-R charge p is called a (p,q)-string, which can have an endpoint at $[p,q]$-brane. For example, the fundamental string (F-string) of Type IIB string theory is a $(1,0)$-string and the D-brane is a $[1,0]$-brane. Also, The $D1$-brane (D-string) is a $(0,1)$-string and the NS-brane is a $[0,1]$-brane. In other words, a (p,q)-string is a bounded state of p F-strings and q D-strings. From the above, Therefore, not only the $D7$-brane but also the $[p,q]$7-brane can be introduced as a background field in the Type IIB superstring theory.

Next, we consider the monodromy of a $[p,q]$7-brane. The gauge field on the world volume of the 7-brane is coupled to the NS-NS 2-form field B_2 and the R-R 2-form field C_2 at the endpoints of the (p,q)-string and is the source of each charge. In other words, there exists a coupling [110] such that

$$\int dx^8 (q\ \ p) \begin{pmatrix} C_2 \\ B_2 \end{pmatrix} \wedge *F, \tag{2.3.2}$$

where F is the field strength of the 2-form field and $*$ is the Hodge operator in eight-dimensional space-time. Since the integrand in Eq. (2.3.2) must be unique in eight dimensions, it must be $SL(2,\mathbb{Z})$ invariant. Thus, the integrand in Eq. (2.3.2) must be invariant to the transformation by Eq. (2.3.1). Therefore,

$$(q\ \ p) M \begin{pmatrix} C_2 \\ B_2 \end{pmatrix} = (q\ \ p) \begin{pmatrix} C_2 \\ B_2 \end{pmatrix}, \quad M \in SL(2,\mathbb{Z}) \tag{2.3.3}$$

holds. And then,

$$(q\ \ p) M_{p,q} = (q\ \ p) \tag{2.3.4}$$

should hold when the monodromy matrix of [p,q]7-brane is then denoted by $M_{p,q}$. This equation (2.3.4) is uniquely determined under the equivalence relation $(nq\ \ np) \sim (q\ \ p)$ $(n \in \mathbb{N})$. Conversely, for open strings whose charge is not (p,q), the integrand in Eq. (2.3.2) is not invariant under the monodromy $M_{p,q}$. Therefore, (p,q)-strings can be only attached to a $[p,q]$-brane with monodromy $M_{p,q}$.

We obtain a specific equation for the monodromy $M_{p,q}$. Here, the monodromy

$$M_{1,0} = T := \begin{pmatrix} 1 & 1 \\ 0 & 1 \end{pmatrix} \tag{2.3.5}$$

discussed in Section 2.1 is the monodromy when there is a $D7$-brane. In this case, equality

$$(0 \ \ 1)M_{1,0} \ \ = \ \ (0 \ \ 1) \tag{2.3.6}$$

holds. In general, under a suitable $SL(2, \mathbb{Z})$ transformation, one can transform a fundamental string into any (p, q)-string, using any integer $\#$, as

$$(0 \ \ 1)K_{p,q} = (0 \ \ 1) \begin{pmatrix} \# & \# \\ q & p \end{pmatrix} = (q \ \ p), \quad K_{p,q} \in SL(2, \mathbb{Z}). \tag{2.3.7}$$

Since the only difference between the $[p, q]7$-brane and the $D7$-brane is the $SL(2, \mathbb{Z})$ transformation

$$K_{p,q} \ \ := \ \ \begin{pmatrix} \# & \# \\ q & p \end{pmatrix}, \tag{2.3.8}$$

we obtain

$$(0 \ \ 1)M_{1,0}K_{p,q} = (q \ \ p)K_{p,q}^{-1}M_{1,0}K_{p,q} \ \ = \ \ (q \ \ p) \tag{2.3.9}$$

if Eq. (2.3.6) is multiplied by the K from the right. Thus, since (p, q)-string can only have endpoints in $[p, q]$-brane, Eq. (2.3.4) holds and the monodromy $M_{p,q}$ is

$$M_{p,q} \ \ = \ \ K_{p,q}^{-1}M_{1,0}K_{p,q} = \begin{pmatrix} 1 + pq & p^2 \\ -q^2 & 1 - pq \end{pmatrix}. \tag{2.3.10}$$

In this chapter, monodromy is considered to arise when a branch cut made by a 7-brane is crossed. From Eq. (2.3.10) and the $SL(2, \mathbb{Z})$ duality of Type IIB superstring theory, all 7-branes are equivalent under the $SL(2, \mathbb{Z})$ transformation, so a 7-brane looks like a $D7$-brane locally when it exists alone. However, when two or more 7-branes exist, they cannot all be considered $D7$-branes simultaneously by $SL(2, \mathbb{Z})$ transformation if their (p, q)-charges are different:

$$K_{p,q}M_{p,q}K_{p,q}^{-1} \ \ = \ \ M_{1,0}, \tag{2.3.11}$$

$$K_{p,q}M_{p',q'}K_{p,q}^{-1} \ \ \neq \ \ M_{1,0}, \tag{2.3.12}$$

where $p \neq p'$ and $q \neq q'$. Therefore, such an argument becomes important when there are two or more 7-branes.

2.4 String junction: Hanany-Witten effect

In this section, we introduce an open string called a string junction that has a branch and at least three endpoints.

The fundamental string ($(1,0)$-string) can have endpoints on a $D1$-brane ($(0,1)$-string). In terms of preserving the (p,q)-charge at the endpoints, this requires a $(1,1)$-string ($(1,-1)$-string) if we consider the D1-brane to be a (D-)string. This is the string junction introduced by Schwartz [81] (see Fig. 2.1 on the right). In general, the string junction is the charge conservation

$$\sum_{1}^{3}(p_i, q_i) = (0,0) \tag{2.4.1}$$

at each intersection of three open strings and is an object with an arbitrary number of intersections.

In Type IIB superstring theory, the string junction plays the same role as an open string. This is illustrated in the following. We consider the change in (r,s)-charge when the $(r \neq p, s \neq q)$-string moves counterclockwise around a $[p,q]$7-brane and crosses a branch cut made by the $[p,q]$7-brane. It is known that the tension of the (r,s)-string [111] is given by

$$T_{r,s} \quad = \quad \frac{1}{\sqrt{\mathrm{Im}\tau}}|r + s\tau|. \tag{2.4.2}$$

Also, from Eq. (2.2.29), the metric of $\mathbb{P}^1$ is given by

$$ds^2_{\mathbb{P}^1} \quad = \quad \frac{\tau(z) - \bar{\tau}(\bar{z})}{2i}\eta^2(\tau(z))\bar{\eta}^2(\bar{\tau}(\bar{z}))\prod_{i=1}^{N}(z - z_i)^{-\frac{1}{12}}(\bar{z} - \bar{z}_i)^{-\frac{1}{12}}dzd\bar{z} \tag{2.4.3}$$

when we consider eight-dimensional Type IIB superstring theory (or F-theory) [106]. From the discussion in Section 2.2, the metric is invariant under the transformation by monodromy ($SL(2,\mathbb{Z})$ transformation). The local mass of the (r,s)-string is given by

$$m_{r,s} \quad := \quad \int_C T_{r,s} \, ds_{\mathbb{P}^1}, \tag{2.4.4}$$

where C is the path of the open string. Since we consider that monodromy is caused by crossing a branch cut, for Eq. (2.4.4) to be invariant under the monodromy transformation of τ:

$$\tau \to M_{p,q}\tau, \tag{2.4.5}$$

it must transform as

$$(s \quad r) \to (s \quad r)M_{p,q}^{-1} \tag{2.4.6}$$
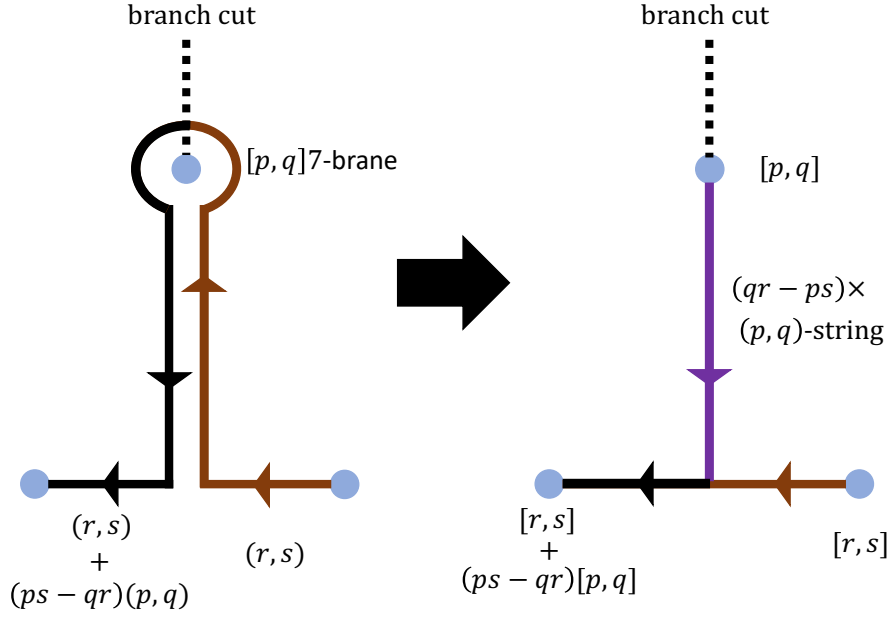
Figure 2.1: Hanany-Witten effect: (r, s)-string and string junction

when crossing the branch cut made of the $[p, q]$7-brane. Therefore, the change in (r, s)-charge is

$$
(s \quad r) \quad \rightarrow \quad (s \quad r) \begin{pmatrix} 1 - pq & -p^2 \\ q^2 & 1 + pq \end{pmatrix}
$$

$$
= \quad (s \quad r) + (qr - ps)(q \quad p) \tag{2.4.7}
$$

when moving counterclockwise around the $[p, q]$7-brane and crossing the branch cut made of the $[p, q]$7-brane. Since the change in (r, s)-charge is proportional to (p, q)-charge, we can consider (p, q)-strings that can have endpoints at a $[p, q]$7-brane by matching the path to and from $[p, q]$7-brane. Thus, we obtain a picture of a string junction where an (r, s)-string and $(qr - ps)$ (p, q)-strings join at an inter, (Fig. 2.1). In other words, moving the (r, s)-string downward across the $[p, q]$7-brane in Fig. 2.1 draws $(qr - ps)$ (p, q)-strings from the $[p, q]$7-brane to conserve the charge (the Hanany-Witten effect [112]). This means that a string junction is created. In Type IIB superstring theory with a 7-brane background field, a string junction naturally appears when considering open strings.

This can be explained by exchanging monodromy matrices [63–65]. Note that since the overall monodromy is invariant for exchanges of matrices, which do not change the number of 7-branes, they are all considered to be equivalent 7-brane configurations. Also, the reordering of the 7-brane in a 7-brane configuration corresponds to the replacement of each branch cut. In this case, we assume that the $[r, s]$7-brane crosses the branch cut made by the $[p, q]$7-brane in a counterclockwise direction. Let $M_{p,q}$ be the monodromy

matrix of the $[p, q]$7-brane and $M_{r,s}$ be the monodromy matrix of the $[r, s]$7-brane, then

$$M_{p,q}M_{r,s}M_{r,s} = (M_{p,q}M_{r,s}M_{p,q}^{-1})M_{p,q}M_{r,s} = M_{r+(qr-ps)p,s+(qr-ps)q}M_{p,q}M_{r,s}. \quad (2.4.8)$$

This is consistent with the mechanism for generating string junctions described in the previous paragraph when the open string connecting the two $[r, s]$7-branes on the right crosses the $[p, q]$7-brane branch cut in a counterclockwise direction. Thus, in the **ABC** description, the reordering of the 7-brane in a 7-brane configuration corresponds to the exchange of monodromy matrices; the change in (r, s)-charge can be explained by the exchange of monodromy matrices as given by Eq. (2.4.8).

2.5 Classification of monodromy and 7-brane configuration

2.5.1 Classification of monodromy

In this section, we classify the monodromy in the case where multiple 7-branes exist simultaneously and consider what there are configurations of the 7-branes. Here, from the discussion in the previous section, we consider all $SL(2, \mathbb{Z})$-conjugate monodromies to be identical; Thus, the following monodromy M and M' are identical:

$$M' = K^{-1}MK \sim M, \quad K \in SL(2, \mathbb{Z}). \quad (2.5.1)$$

In Type IIB superstring theory, the value of the axio-dilaton field τ on a 7-brane does not change depending on the monodromy created by the 7-brane. We will consider classifying fixed points by monodromy transformations ($SL(2, \mathbb{Z})$ transformations) using $\text{Tr } M$ invariant under Eq. (2.5.1). In this section, we denote

$$M = \begin{pmatrix} a & b \\ c & d \end{pmatrix}, \quad \det M = 1, \quad M \in SL(2, \mathbb{Z}), \quad (2.5.2)$$

$$T = \begin{pmatrix} 1 & 1 \\ 0 & 1 \end{pmatrix}, \quad S = \begin{pmatrix} 0 & -1 \\ 1 & 0 \end{pmatrix} \quad T, S \in SL(2, \mathbb{Z}). \quad (2.5.3)$$

Since a fixed point is an equivalence τ under the $SL(2, \mathbb{Z})$ transformation, we obtain

$$M\tau' := \frac{a\tau' + b}{c\tau' + d} = \tau', \quad (2.5.4)$$

where τ' is the fixed point. Solving Eq. (2.5.4) yields

$$\tau' = \frac{1}{2c}\{(a - d) \pm \sqrt{(\text{Tr } M)^2 - 4}\}. \quad (2.5.5)$$

We divide this into three cases:

$$
\begin{aligned}
|\operatorname{Tr} M| = 2 &\quad : \quad \text{Parabolic}, \\
|\operatorname{Tr} M| < 2 &\quad : \quad \text{Elliptic}, \\
|\operatorname{Tr} M| > 2 &\quad : \quad \text{Hyperbolic}.
\end{aligned}
\tag{2.5.6}
$$

Here, we use the Caylay=Hamilton formula

$$
M^2 - (\operatorname{Tr} M)M + \hat{\mathbf{1}} = \hat{\mathbf{0}}
\tag{2.5.7}
$$

to obtain the specific monodromy equation.

(1) $|\operatorname{Tr} M| = 2$: The case of Parabolic

From Eq. (2.5.5), τ' is a rational number. Since rational numbers can always be transformed by $SL(2, \mathbb{Z})$ transformation to the infinity point $i\infty$ in the fundamental region, this corresponds correctly when there is a $D7$-brane. To realize $\tau' \to i\infty$, we need $c = 0$; then, $a = d = \pm 1$ (double-sign corresponds) from $\det M = 1$. Therefore, The conjugate class of monodromies that satisfies Eq. (2.5.7) are

$$
T^n = \begin{pmatrix} 1 & N \\ 0 & 1 \end{pmatrix},
\tag{2.5.8}
$$

$$
-T^n = \begin{pmatrix} -1 & -N \\ 0 & -1 \end{pmatrix}
\tag{2.5.9}
$$

for $\operatorname{Tr} M = 2$ and $\operatorname{Tr} M = -2$, respectively. Here, $N \in \mathbb{Z}$. Since this monodromy transforms $\tau \to \tau + N$, the behavior of $\tau(z)$ when z is sufficiently large, is

$$
\tau(z) \sim \frac{N}{2\pi i} \log(z).
\tag{2.5.10}
$$

However, when 7-branes overlap at $z = 0$, if $N < 0$, then $\tau \to -i\infty$. In this case, in Type IIB superstring theory, the vacuum expectation value of the dilaton field ϕ is imaginary. Also, in F-theory, there is no corresponding bundle, the elliptic curve. Therefore, for $N < 0$, the 7-branes cannot be collected at a point.

(2) $|\operatorname{Tr} M| < 2$: The case of Elliptic

From Eq. (2.5.5), τ' is an imaginary number and corresponds to a point on the upper half-plane $\mathbb{H}$. Such a point can always be transformed by $SL(2, \mathbb{Z})$ transformation to a point in the fundamental region (except at infinity point $i\infty$). Therefore, in this case, it cannot be constructed from one $D7$-brane and multiple 7-branes are needed. Eq. (2.5.5) is

$$
\tau' = \frac{1}{c}(a \pm i)
\tag{2.5.11}
$$
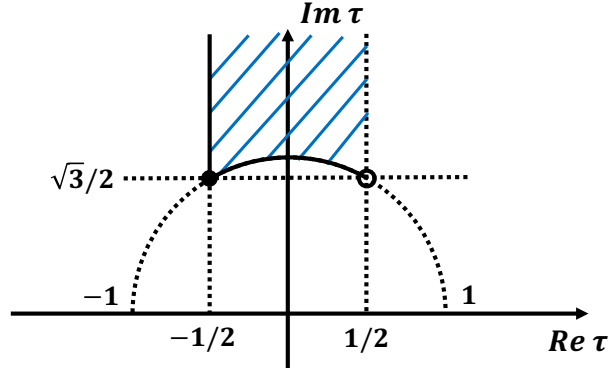
Figure 2.2: The "usual" fundamental region of τ.

when $\operatorname{Tr} M = 0$. Therefore, when τ' is a point in the "usual" fundamental region (Fig 2.2),

$$\operatorname{Im} \tau' \geq \frac{\sqrt{3}}{2}, \quad -\frac{1}{2} \leq \operatorname{Re} \tau' < \frac{1}{2} \tag{2.5.12}$$

must at least be satisfied, and considering also $\det M = 1$, this solution is satisfied by $d = -a = 0$ and $b = -c = \mp 1$ (double-sign corresponds). Therefore, The conjugate class of monodromies that satisfies Eq. (2.5.7) are

$$S = \begin{pmatrix} 0 & -1 \\ 1 & 0 \end{pmatrix}, \quad -S = \begin{pmatrix} 0 & 1 \\ -1 & 0 \end{pmatrix} \tag{2.5.13}$$

and the fixed point is $\tau' = i$. Then, Eq. (2.5.5) is

$$\tau' = \frac{1}{2c}(2a - 1 \pm i\sqrt{3}), \tag{2.5.14}$$

$$\tau' = \frac{1}{2c}(2a + 1 \pm i\sqrt{3}) \tag{2.5.15}$$

when $\operatorname{Tr} M = 1$ and $\operatorname{Tr} M = -1$, respectively. Thus, when τ' is a point in the "usual" fundamental region, this solution is satisfied by $c = 1$, $a = 0$ or $c = -1$, $a = 1$ when $\operatorname{Tr} M = 1$ and by $c = 1$, $a = -1$ or $c = -1$, $a = 0$ when $\operatorname{Tr} M = -1$. Furthermore, considering also the value of $\operatorname{Tr} M$ and $\det M = 1$, when $\operatorname{Tr} M = 1$, the conjugate class of monodromies that satisfies Eq. (2.5.7) are

$$-T^{-1}S = -U = \begin{pmatrix} 1 & 1 \\ -1 & 0 \end{pmatrix}, \quad ST = U^2 = \begin{pmatrix} 0 & -1 \\ 1 & 1 \end{pmatrix}, \tag{2.5.16}$$

where $U := T^{-1}S$. Also, when $\operatorname{Tr} M = -1$, we obtain

$$T^{-1}S = U = \begin{pmatrix} -1 & -1 \\ 1 & 0 \end{pmatrix}, \quad -ST = -U^2 = \begin{pmatrix} 0 & 1 \\ -1 & -1 \end{pmatrix}. \tag{2.5.17}$$

In these cases, the fixed point is $\tau' = e^{\frac{2\pi i}{3}}$[3].

(3) $|\operatorname{Tr} M| > 2$: The case of Hyperbolic

From Eq. (2.5.5), τ' is an irrational number. Since an irrational number cannot be transformed to a point in the "usual" fundamental domain by an $SL(2, \mathbb{Z})$ transformation, In this case, there is no corresponding bundle, the elliptic curve, in F-theory. Therefore, when the monodromies made by 7-brane configurations satisfy $|\operatorname{Tr} M| > 2$, the 7-branes cannot be collected at a point.

From the above, the condition of monodromy that allows the 7-branes to be collected at a point is

$$|\operatorname{Tr} M| \leq 2. \tag{2.5.21}$$

However, when $|\operatorname{Tr} M| = 2$, we need $N \geq 0$ in Eq. (2.5.8) and Eq. (2.5.9).

2.5.2 Monodromy and 7-brane configuration

In this section, we explain the monodromy when multiple 7-branes can be collected at a point. First, we consider how many 7-branes are collected at a point to make these monodromies when Eq. (2.5.21) is satisfied. Note that all $SL(2, \mathbb{Z})$-conjugate monodromies are considered to be identical since we consider that all configurations obtained by the $SL(2, \mathbb{Z})$-conjugate transformation of the overall configuration of the 7-branes are equivalent:

$$M' = K^{-1}MK \sim M, \quad K \in SL(2, \mathbb{Z}), \tag{2.5.22}$$

especially, in the case that there is a 7-brane alone,

$$M_{p,q} = K^{-1}M_{1,0}K \sim M_{1,0} = T. \tag{2.5.23}$$

---

[3]This depends on how the fundamental region is chosen. For example, instead of Eq. (2.5.12), if we choose

$$\operatorname{Im} \tau' \geq \frac{\sqrt{3}}{2}, \quad -\frac{1}{2} < \operatorname{Re} \tau' \leq \frac{1}{2}, \tag{2.5.18}$$

the fixed point is $\tau' = e^{\frac{\pi i}{3}}$. In this case, when $\operatorname{Tr} M = 1$, the conjugate class of monodromies that satisfies Eq. (2.5.7) are

$$-ST^{-1} = \begin{pmatrix} 0 & 1 \\ -1 & 1 \end{pmatrix}, \quad TS = \begin{pmatrix} 1 & -1 \\ 1 & 0 \end{pmatrix}. \tag{2.5.19}$$

Also, when $\operatorname{Tr} M = -1$, we obtain

$$ST^{-1} = \begin{pmatrix} 0 & -1 \\ 1 & -1 \end{pmatrix}, \quad -TS = \begin{pmatrix} -1 & 1 \\ -1 & 0 \end{pmatrix}. \tag{2.5.20}$$

Also, since the overall monodromy is invariant for exchanges of matrices, which do not change the number of 7-branes, we consider them all to be equivalent 7-brane configurations. In order to classify the lowest number of 7-branes collected at a point for each monodromy, we consider the abelianization of the $SL(2, \mathbb{Z})$ group:

$$\text{The abelianization of } SL(2, \mathbb{Z}) \text{ is the cyclic group } \boldsymbol{Z}_{12}. \tag{2.5.24}$$

Since the $SL(2, \mathbb{Z})$ group is constructed by S and $U := T^{-1}S$ and also $U^3 = S^2 = -\hat{\boldsymbol{1}}$, we find that the representative elements of the $\boldsymbol{Z}_{12}$ group are

$$\{\hat{\boldsymbol{1}}, -SU^2, -U, -S, -U^2, US, -\hat{\boldsymbol{1}}, SU^2, U, S, U^2, -US\}, \tag{2.5.25}$$

where $-SU^2$ is the generator of the $\boldsymbol{Z}_{12}$ group. Rewriting this using S and T, we obtain

$$\{\hat{\boldsymbol{1}}, T, -T^{-1}S, -S, -ST, -T^{-1}, -\hat{\boldsymbol{1}}, -T, T^{-1}S, S, ST, T^{-1}\}. \tag{2.5.26}$$

For simplicity, we will denote each representative component by

$$\{\boldsymbol{0}, \boldsymbol{1}, \boldsymbol{2}, \boldsymbol{3}, \boldsymbol{4}, \boldsymbol{5}, \boldsymbol{6}, \boldsymbol{7}, \boldsymbol{8}, \boldsymbol{9}, \boldsymbol{10}, \boldsymbol{11}\} \tag{2.5.27}$$

when each component is represented by the N-th power of the generator. We define a homomorphism:

$$\mu : \ M \in SL(2, \mathbb{Z}) \to MG_c \in G/G_c, \tag{2.5.28}$$

where $G_c := [SL(2, \mathbb{Z})]_c$ is the commutator subgroup of the $G := SL(2, \mathbb{Z})$. Also, using Eq. (2.5.28), we denote

$$\mu(M) = S^n U^m G_c \tag{2.5.29}$$

when M is generated from n S's and m U's. Since $M_{p,q}$ is the monodromy of a $[p, q]7$-brane,

$$\mu(M_{p,q}) = \boldsymbol{1}. \tag{2.5.30}$$

This can be shown from $\mu(M_{1,0}) = T = -SU^2 = \boldsymbol{1}$ and the fact that $M_{p,q}$ is $SL(2, \mathbb{Z})$-conjugate with $M_{1,0}$ (Eq. (2.3.10)). Thus, given the monodromy made by N 7-branes,

$$\mu(M_1 M_2 \cdots M_N) = \boldsymbol{N} \pmod{12}, \quad M_i = M_{p_i, q_i}. \tag{2.5.31}$$

From the above, when the monodromy made by a configuration of the 7-branes gives $\mu(M) = \boldsymbol{N}$, at least N (mod 12) 7-branes are needed. Also, when twelve 7-branes are collected at a point, the monodromy (matrix) is trivial (unit matrix $\hat{\boldsymbol{1}}$).

Next, we consider which $[p, q]7$-branes are collected at a point to make these monodromies when Eq. (2.5.21) is satisfied. In this thesis, $D7 (= [1, 0]7)$-brane is denoted as

A-brane, $[1, 1]$7-brane as **B**-brane, $[1, -1]$7-brane as **C**-brane and $NS7(= [0, 1]7)$-brane as **N**-brane. Then, the notation

$$\mathbf{A} = M_{1,0} = \begin{pmatrix} 1 & 1 \\ 0 & 1 \end{pmatrix} = T,$$

$$\mathbf{N} = M_{0,1} = -\begin{pmatrix} 1 & 0 \\ -1 & 1 \end{pmatrix} = STS,$$

$$\mathbf{B} = M_{1,1} = -\begin{pmatrix} 2 & 1 \\ -1 & 0 \end{pmatrix} = T^{-2}S, \tag{2.5.32}$$

$$\mathbf{C} = M_{1,-1} = -\begin{pmatrix} 0 & 1 \\ -1 & 2 \end{pmatrix} = ST^{-2}$$

is used for each 7-brane monodromy. We also assume that branch cuts extend upward from each 7-brane. If l **A**-branes, m **B**-branes, and n **C**-branes are ordered from left to right, the configuration is denoted as $\mathbf{A}^l\mathbf{B}^m\mathbf{C}^n$ ($l, m, n \geq 0$, $lmn \neq 0$). If we consider moving counterclockwise around the $[p, q]$7-branes, the monodromy is

$$\mathbf{A}^l\mathbf{B}^m\mathbf{C}^n : \quad M_{1,0}^l M_{1,1}^m M_{1,-1}^n \tag{2.5.33}$$

when the monodromy (matrix) of each 7-brane is multiplied by the order in which the branch cuts are crossed. Such an argument using **A**-brane, **B**-brane and **C**-brane is called **ABC** description [63–65].

(i) The case of $\mathrm{Tr}\, M = 2$

The independent monodromy is given by

$$T^N = \begin{pmatrix} 1 & N \\ 0 & 1 \end{pmatrix}, \quad N \in \mathbb{Z} \tag{2.5.34}$$

from Eq. (2.5.8) for $N > 0$. Thus, from

$$\mu(T^N) = \mathbf{N}, \tag{2.5.35}$$

the configuration of the 7-branes, in this case, is

$$\mathbf{A}^N. \tag{2.5.36}$$

The gauge symmetry of the theory on the brane when N $D7$-branes are collected at a point is $A_{N-1} = SU(N)$ ($N \geq 2$). This corresponds to A_{N-1} ($N \geq 2$) in the Kodaira classification [62, 113, 114] used in the next chapter.

For $N = 0$, since the unit matrix is

$$\mu(\hat{\mathbf{1}}) = \mathbf{0} = \mathbf{12}, \tag{2.5.37}$$

at least twelve 7-branes are needed. Therefore, since

$$M_{1,0}^8 M_{1,1} M_{1,-1} M_{1,1} M_{1,-1} = \hat{\mathbf{1}}, \tag{2.5.38}$$

the configuration of the 7-branes, in this case, is

$$\boldsymbol{A}^8 \boldsymbol{B} \boldsymbol{C} \boldsymbol{B} \boldsymbol{C}. \tag{2.5.39}$$

(ii) The case of $\operatorname{Tr} M = 1$

Since the independent monodromy is given by

$$\mu(-T^{-1}S) \;\; = \;\; \mathbf{2}, \tag{2.5.40}$$

$$\mu(ST) \;\; = \;\; \mathbf{10}, \tag{2.5.41}$$

from Eq. (2.5.16), at least two and ten 7-branes are needed, respectively. Thus, from

$$M_{1,0} M_{1,1} \;\; = \;\; -T^{-1}S, \tag{2.5.42}$$

$$M_{1,0}^6 M_{1,1} M_{1,-1} M_{1,1} M_{1,0} \;\; = \;\; ST, \tag{2.5.43}$$

the configurations of the 7-branes, in these cases, are

$$\boldsymbol{A} \boldsymbol{B}, \tag{2.5.44}$$

$$\boldsymbol{A}^6 \boldsymbol{B} \boldsymbol{C} \boldsymbol{B} \boldsymbol{A}, \tag{2.5.45}$$

respectively. To make the degrees of freedom of the group easier to understand, an $SL(2, \mathbb{Z})$-conjugate transformation of Eq. (2.5.45) yields

$$M_{1,0}^7 M_{1,1} M_{1,-1} M_{1,1} = TS, \tag{2.5.46}$$

$$\boldsymbol{A}^7 \boldsymbol{B} \boldsymbol{C} \boldsymbol{B}. \tag{2.5.47}$$

We consider the gauge symmetry at these configurations of the 7-branes: for $\boldsymbol{A} \boldsymbol{B}$, There are no open strings connecting them and the gauge symmetry enhancement does not occur. And, for $\boldsymbol{A}^6 \boldsymbol{B} \boldsymbol{C} \boldsymbol{B} \boldsymbol{A}$, the gauge symmetry is E_8. In the Kodaira classification, these correspond to H_0 and E_8, respectively.

(iii) The case of $\operatorname{Tr} M = 0$

Since the independent monodromy is given by

$$\mu(-S) = \mathbf{3}, \tag{2.5.48}$$

$$\mu(S) = \mathbf{9}, \tag{2.5.49}$$

from Eq. (2.5.13), at least three and nine 7-branes are needed, respectively. Thus, from

$$M_{1,0}^2 M_{1,1} = -S, \tag{2.5.50}$$

$$M_{1,0}^6 M_{1,1} M_{1,-1} M_{1,1} = S, \tag{2.5.51}$$

the configurations of the 7-branes, in these cases, are

$$\boldsymbol{A}^2 \boldsymbol{B}, \tag{2.5.52}$$

$$\boldsymbol{A}^6 \boldsymbol{B} \boldsymbol{C} \boldsymbol{B}, \tag{2.5.53}$$

respectively. We consider the gauge symmetry at these configurations of the 7-branes: for $\boldsymbol{A}^2 \boldsymbol{B}$, there are two 7-branes of the same type, so the gauge symmetry is $SU(2)$. And, for $\boldsymbol{A}^6 \boldsymbol{B} \boldsymbol{C} \boldsymbol{B}$, the gauge symmetry is E_7. In the Kodaira classification, these correspond to H_1 and E_7, respectively.

(iv) The case of $\operatorname{Tr} M = -1$

Since the independent monodromy is given by

$$\mu(-ST) = \mathbf{4}, \tag{2.5.54}$$

$$\mu(T^{-1}S) = \mathbf{8}, \tag{2.5.55}$$

from Eq. (2.5.17), at least four and eight 7-branes are needed, respectively. Thus, from

$$M_{1,0}^2 M_{1,1} M_{1,0} = -ST, \tag{2.5.56}$$

$$M_{1,0}^5 M_{1,1} M_{1,-1} M_{1,1} = T^{-1}S, \tag{2.5.57}$$

the configurations of the 7-branes, in these cases, are

$$\boldsymbol{A}^2 \boldsymbol{B} \boldsymbol{A}, \tag{2.5.58}$$

$$\boldsymbol{A}^5 \boldsymbol{BCB}, \tag{2.5.59}$$

respectively. To make the degrees of freedom of the group easier to understand, an $SL(2,\mathbb{Z})$-conjugate transformation of Eq. (2.5.45) yields

$$M_{1,0}^3 M_{1,1} M_{1,0} = -TS, \tag{2.5.60}$$

$$\boldsymbol{A}^3 \boldsymbol{B}. \tag{2.5.61}$$

We consider the gauge symmetry at these configurations of the 7-branes: for $\boldsymbol{A}^3 \boldsymbol{B}$, there are three 7-branes of the same type, so the gauge symmetry is $SU(3)$. And, for $\boldsymbol{A}^5 \boldsymbol{BCB}$, the gauge symmetry is E_6. In the Kodaira classification, these correspond to H_2 and E_6, respectively.

(v) The case of $\operatorname{Tr} M = -2$

The independent monodromy is given by

$$-T^N = \begin{pmatrix} -1 & -N \\ 0 & -1 \end{pmatrix} = -\hat{\mathbf{1}} M_{1,0}^N \tag{2.5.62}$$

from Eq. (2.5.9) for $N > 0$. Therefore, we can add additional N $\boldsymbol{A}(D)$-branes to the configuration of the 7-branes with the monodromy $-\hat{\mathbf{1}}$ and collect them at a point. Since

$$\mu(-\hat{\mathbf{1}}) = \mathbf{6}, \tag{2.5.63}$$

at least six 7-branes are needed. Here,

$$M_{1,0}^4 M_{1,-1} M_{1,1} = -\hat{\mathbf{1}}, \tag{2.5.64}$$

then,

$$\boldsymbol{A}^4 \boldsymbol{BC}. \tag{2.5.65}$$

From the above, by adding N $D7$-branes to this configuration of the 7-brane at a point, we obtain a series with $N \geq 0$. When N $D7$-branes can overlap at a point, this series is

$$\boldsymbol{A}^{N+4} \boldsymbol{BC}, \quad N \geq 0. \tag{2.5.66}$$

The corresponding gauge symmetry is $D_{N+4} = SO(2N+8)$ ($N \geq 0$). In the Kodaira classification, this corresponds to D_{N+4} ($N \geq 0$).

Table 2.1: Classification of 7-brane configuration. Note that the configuration of the 7-branes is up to $\mathbf{A}^8\mathbf{BCBC}$ and $N \geq 1$. Here, H_i are brane types in the Kodaira classification discussed in the next chapter.

Gauge symmetry	7-brane configuration	Monodromy	Tr M	Foxed point
A_{N-1}	$\mathbf{A}^N$	T^N	2	$i\infty$
(H_0)	$\boldsymbol{AB}$	$-T^{-1}S$	1	$e^{\frac{2\pi i}{3}}$
A_1 (H_1)	$\boldsymbol{A^2B}$	$-S$	0	i
A_2 (H_2)	$\boldsymbol{A^3B}$	$-TS$	-1	$e^{\frac{\pi i}{3}}$
D_4	$\mathbf{A}^4\mathbf{BC}$	$-\hat{\mathbf{1}}$	-2	$arb.$
D_{N+4}	$\mathbf{A}^{N+4}\mathbf{BC}$	$-T^N$	-2	$i\infty$
E_8	$\boldsymbol{A^7BCB}$	TS	1	$e^{\frac{\pi i}{3}}$
E_7	$\boldsymbol{A^6BCB}$	S	0	i
E_6	$\boldsymbol{A^5BCB}$	$T^{-1}S$	-1	$e^{\frac{2\pi i}{3}}$
$-$	$\boldsymbol{A^8BCBC}$	$\hat{\mathbf{1}}$	2	$-$

2.6   Classification of 7-brane configuration

In this section, we summarize the conclusions of this chapter. Summarizing the configurations of the 7-branes that can collect 7-branes at a point and the monodromy made by 7-brane configurations, we obtain the following Table 2.1. Table 2.1 shows the configurations of 7-branes in a form that is easy to understand the group structure (simple roots). In this chapter, we briefly consider the open strings connecting each 7-brane and give a conclusion about the gauge symmetry of the theory on the 7-brane at each configuration.

To briefly illustrate the relationship between gauge symmetries and the configurations of the 7-branes, we consider the $D_4 = SO(8)$ case as the most simple example with string junctions. In this case, the configuration of the 7-branes is

$$\mathbf{AAAABC}. \tag{2.6.1}$$

Since $SU(4)$ gauge symmetry appears from the four $\mathbf{A}$-branes, we consider dividing $\mathbf{AAAABC}$ into four $\mathbf{A}$-branes and a pair of $\mathbf{B}$- and $\mathbf{C}$-brane. In other words, the $SO(8)$ gauge symmetry is decomposed into $SU(4) \times U(1)$, which gives

$$\mathbf{28} = \mathbf{15} + \mathbf{6} + \bar{\mathbf{6}} + \mathbf{1}. \tag{2.6.2}$$

Here, "$\mathbf{15}$" corresponds to the three Cartans of $SU(4)$ and the open string directly connecting the four $\mathbf{A}$-branes. Also, "$\mathbf{1}$" corresponds to the one remaining Cartan of $SO(8)$. The "$\mathbf{6} + \bar{\mathbf{6}}$" corresponds to string junctions with two intersections and four endpoints and connecting two $\mathbf{A}$-branes, a $\mathbf{B}$-brane and a $\mathbf{C}$-brane due to the orientation of the strings and the number of choices of the two $\mathbf{A}$-branes ($_4C_2 = 6$). The string junctions

are generated by the Hanany-Witten effect when considering open strings that lead from one **A**-brane to another **A**-brane after passing counterclockwise around the **B**-brane and the **C**-brane. To specify the corresponding simple roots, labeled

$$\mathbf{A}_1\mathbf{A}_2\mathbf{A}_3\mathbf{A}_4\mathbf{B}_5\mathbf{C}_6 \tag{2.6.3}$$

and denoting the 7-brane at its endpoint by the lower-case alphabet corresponding to each (p, q)-charge, the open strings corresponding to the simple roots of $SO(8)$ are

$$
\begin{aligned}
\mathbf{a}_1 - \mathbf{a}_2, \\
\mathbf{a}_2 - \mathbf{a}_3, \\
\mathbf{a}_3 - \mathbf{a}_4, \\
\mathbf{a}_3 + \mathbf{a}_4 - \mathbf{b}_5 - \mathbf{c}_6.
\end{aligned} \tag{2.6.4}
$$

As the above, string junctions are needed to realize symmetries other than $SU(N)$ gauge symmetries, e.g., exceptional-type symmetries, as symmetries of theories on branes[4].

---

[4]There are more detailed analyses in [63–65].

Chapter 3

Overview of F-theory

In this chapter, we consider the basics of F-theory [52, 87, 88]. F-theory describes geometrically the set-up of Type IIB superstring theory discussed in the previous chapter. We construct F-theory by identifying the axio-dilaton field in Type IIB superstring theory with the complex structure modulus of a torus as extra *virtual* two dimensions. Therefore, The compact spaces in F-theory need to be the manifolds with elliptic fibres. The elliptically fibred Calabi-Yau n-fold with section is described by the Weierstrass equation and its complex structure modulus τ is obtained via the modular J-function. We can confirm that the positions of 7-branes correspond to the discriminant loci, over which a fibre becomes the singular fibre, and the charges (p, q) of 7-branes can be read by the monodromies around the discriminant loci [85, 115, 116]. Next, we consider the classification of the singular fibre, called Kodaira's classification [62, 113, 114]. We then see the correspondence between the set-up of Type IIB superstring theory and F-theory via monodromies. Finally, we discuss the duality between F-theory and M-theory [52, 59, 111]. We then show that the F-theory compact space must be the elliptically fibred Calabi-Yau n-fold for conserving its supersymmetry.

3.1   Elliptic fibration and Weierstrass equation

F-theory is a geometrical framework of nonperturbative compactifications of Type IIB superstring theory with $[p, q]$7-branes. In F-theory, the axio-dilaton field $\tau := C_0 + ie^{-\phi}$, which depends only on the coordinates of the compact space of Type IIB superstring theory discussed in the previous section, is identified as a complex structure $\tau := \tau_1 + i\tau_2$ of an elliptic curve $\mathbb{E}_\tau$ (a two-dimensional torus T^2). In this case, we consider τ varies over the compact space of Type IIB superstring theory. The axio-dilaton field $\tau := C_0 + ie^{-\phi}$ is transformed as

$$\tau \to \frac{a\tau + b}{c\tau + d}, \quad \begin{pmatrix} a & b \\ c & d \end{pmatrix} \in SL(2, \mathbb{Z}) \tag{3.1.1}$$

under the $(P)SL(2, \mathbb{Z})$ duality in Type IIB superstring theory. The $(P)SL(2, \mathbb{Z})$ invariance is identical to the modular invariance, which is an invariance of the complex structure of an elliptic curve $\mathbb{E}_\tau$ with respect to $(P)SL(2, \mathbb{Z})$ transformations. Note that a compact space of F-theory is described by an elliptic fibration Y_{n+1}. In the previous section, we showed that the number of 7-branes must be 24. In the $n = 1$ case, the elliptically fibred Calabi-Yau twofold with 24 singularities is called an elliptically fibred $K3$ surface. In this section, we discuss the eight-dimensional F-theory, which is F-theory on the elliptically fibred $K3$ [52].

An elliptic curve $\mathbb{E}_\tau$ is a nonsingular[1] cubic algebraic curve in $\mathbb{P}^2$, denoted by

$$Y^2 Z + a_1 XYZ + a_3 Y Z^2 \;=\; X^3 + a_2 X^2 Z + a_4 X Z^2 + a_6 Z^3 \tag{3.1.2}$$

where $[X : Y : Z] \in \mathbb{P}^2$ in homogeneous coordinates and $a_i \in K$ (K is a coefficient field). Here, $\mathbb{P}^2$ is a projective plane with the identification of the coordinates given by

$$(X, Y, Z) \sim \lambda (X, Y, Z). \tag{3.1.3}$$

Topologically, an elliptic curve $\mathbb{E}_\tau$ is a nonsingular projective algebraic curve of genus-one. In inhomogeneous coordinates $x = \frac{X}{Z}$, $y = \frac{Y}{Z}$ and $Z \neq 0$, Eq. (3.1.2) is

$$P \;=\; -(y^2 + a_1 xy + a_3 y) + x^3 + a_2 x^2 + a_4 x + a_6 = 0 \tag{3.1.4}$$

called "Tate form". In particular, if the characteristic of K is different from 2 and 3 (or with section), then the curve can be described as the Weierstrass equation (or Weierstrass form):

$$y^2 \;=\; x^3 - g_2 x - g_3 \tag{3.1.5}$$

or

$$y^2 \;=\; x^3 + fx + g, \tag{3.1.6}$$

where f, $g \in K^2$. In this section, we only consider $K = \mathbb{C}$; thus, the characteristic of K has a section. Since the complex structure modulus τ of the elliptic curve $\mathbb{E}_\tau$ is given by

$$\tau = \frac{\oint_\beta \omega}{\oint_\alpha \omega}, \quad \omega = \frac{dx}{y}, \tag{3.1.11}$$

---

[1]Nonsingular means that there are no curves with nodes or cusps.

[2]An elliptic curve $\mathbb{E}_\tau$ is described as a hypersurface in the weighted projective space $W\mathbb{C}P^2(2, 3, 1)$, which is a generalized projective space with the identification of the coordinates given by

$$(X, Y, Z) \sim (\lambda^2 X, \lambda^3 Y, \lambda Z), \tag{3.1.7}$$

where $[X : Y : Z]$ are homogeneous coordinates of $W\mathbb{C}P^2(2, 3, 1)$ and $\lambda \in \mathbb{C}^* = \mathbb{C} - \{0\}$. We define the Weierstrass form (or Weierstrass equation) as

$$P_{\mathrm{W}} = Y^2 - X^3 - fXZ^4 - gZ^6 = 0, \tag{3.1.8}$$

where f, $g \in K$. In particular, when we choose the inhomogeneous coordinates as

$$x = \frac{X}{Z^2}, \quad y = \frac{Y}{Z^3}; \tag{3.1.9}$$

where α, β are the one-cycles of the elliptic curve $\mathbb{E}_\tau$ and ω is the holomorphic one-form on the elliptic curve $\mathbb{E}_\tau$. Thus, we can compute the complex structure modulus of the elliptic curve $\mathbb{E}_\tau$ from the Weierstrass equation. The complex structure modulus τ of the elliptic curve $\mathbb{E}_\tau$ is known to be determined from the coefficients of the Weierstrass equation: f and g, due to the relation between the (modular) J-function and the Weierstrass equation

$$J(\tau) \;\; = \;\; \frac{4f^3}{4f^3 + 27g^2}. \tag{3.1.12}$$

Mathematically, the (modular) J-function is defined by

$$J(\tau) \;\; := \;\; \frac{(\vartheta_2(\tau)^8 + \vartheta_3(\tau)^8 + \vartheta_4(\tau)^8)^3}{54\vartheta_2(\tau)^8\vartheta_3(\tau)^8\vartheta_4(\tau)^8}. \tag{3.1.13}$$

where the definition of the ϑ-constants are

$$\vartheta_2(\tau) := \vartheta_2(0;\tau) = 2q^{\frac{1}{8}} \prod_{m=1}^{\infty}(1-q^m)(1+q^m)^2,$$

$$\vartheta_3(\tau) := \vartheta_3(0;\tau) = \prod_{m=1}^{\infty}(1-q^m)(1+q^{m-\frac{1}{2}})^2, \tag{3.1.14}$$

$$\vartheta_4(\tau) := \vartheta_4(0;\tau) = \prod_{m=1}^{\infty}(1-q^m)(1-q^{m-\frac{1}{2}})^2.$$

The (modular) J-function is a one-to-one map from the fundamental region $(\mathbb{H}/(P)SL(2,\mathbb{Z}))$ of τ to $\mathbb{C}$ and is a $(P)SL(2,\mathbb{Z})$ (modular) invariant function. Also, the denominator of the right-hand side of Eq. (3.1.12) is called the discriminant and is denoted by

$$\Delta \;\; := \;\; 4f^3 + 27g^2. \tag{3.1.15}$$

In F-theory, we consider the elliptic fibration Y_{n+1} as the compact spaces since the complex structure τ of an elliptic curve $\mathbb{E}_\tau$ depends only on the coordinates of the compact space of Type IIB superstring theory. The elliptic fibration Y_{n+1} is defined as

$$\begin{aligned} \pi: \quad \mathbb{E}_\tau &\to \quad Y_{n+1} \\ &\downarrow \\ &\quad B_n, \end{aligned} \tag{3.1.16}$$

then, the Weierstrass equation is expressed as

$$y^2 = x^3 + fx + g. \tag{3.1.10}$$

where B_n is a complex n-dimensional base space. From Eq. (3.1.6) and Eq. (3.1.12), the elliptic fibration Y_{n+1} is described as

$$P_{Y_{n+1}} = = y^2 + x^3 + f(B_n)x + g(B_n) = 0, \tag{3.1.17}$$

$$J(\tau(B_n)) = \frac{4f(B_n)^3}{4f(B_n)^3 + 27g(B_n)^2}, \tag{3.1.18}$$

where we abbreviate the coordinates of B_n as B_n. Note that a fibre, which is elliptic curve $\mathbb{E}_\tau$, can become the singular fibre at the discriminant loci:

$$\Delta(B_n) := 4f(B_n)^3 + 27g(B_n)^2 = 0, \tag{3.1.19}$$

as discussed later. In this section, we focus on the $n = 1$ case where Y_2 is an elliptically fibred $K3$ surface and B_1 is $\mathbb{P}^1$.

We focus on an elliptically fibred $K3$ (elliptic surface) or a fibre product of two rational elliptic surfaces with section. From Eq. (3.1.17), It is represented by

$$P_z = -y^2 + x^3 + f(z)x + g(z) = 0, \tag{3.1.20}$$

where $z \in \mathbb{C}$ is the coordinate on the affine patch of the base space $\mathbb{P}^1$, and $f(z)$ and $g(z)$ are holomorphic functions of z. The complex structure modulus $\tau(z)$ is a holomorphic function of z, $\mathrm{Im}\,\tau > 0$ and is a one-to-one map from $\mathbb{C}$ to the fundamental region $(\mathbb{H}/(P)SL(2,\mathbb{Z})))$ of τ due to the $(P)SL(2,\mathbb{Z})$ transformation. From Eq. (3.1.18) and Eq. (3.1.19),

$$J(\tau(z)) = \frac{4f(z)^3}{4f(z)^3 + 27g(z)^2}, \tag{3.1.21}$$

$$\Delta(z) := 4f(z)^3 + 27g(z)^2. \tag{3.1.22}$$

In F-theory, the complex structure modulus $\tau(z)$ is given as an inverse function of the J-function from Eq. (3.1.21):

$$\tau(z) = J^{-1}(z). \tag{3.1.23}$$

This naturally satisfies the requirement for the axio-dilaton field $\tau := C_0 + ie^{-\phi}$ in Type IIB superstring theory discussed in the previous section. When we consider a compact space as an elliptically fibred $K3$, the coefficient functions $f(z)$ and $g(z)$ are 8th- and 12th-degree polynomials in z, respectively; and then the discriminant: $\Delta(z)$ is a 24th-degree polynomial in z. Also, when we consider a compact space as a fibre product of two rational elliptic surfaces, the coefficient functions $f(z)$ and $g(z)$ are 4th- and 6th-degree polynomials in z, respectively; and then the discriminant: $\Delta(z)$ is a 12th-degree polynomial in z. These correspond to the fact that a dual IIB superstring theory has 24 7-branes since the degree of $\Delta(z)$ is equal to the number of 7-branes as discussed below.

First, we show that a position of a 7-brane is given by a locus of the pole of the J-function. We consider the condition that an elliptic surface or an elliptic fibre is singular.

If the elliptic surface is singular, then the elliptic fibre is singular; thus, the x and y derivative of P_z in Eq. (3.1.20) is zero. Therefore, we obtain

$$
\begin{aligned}
3x^2 + f(z) &= 0, \\
y &= 0.
\end{aligned}
\tag{3.1.24}
$$

Substituting Eq. (3.1.24) into Eq. (3.1.20), we obtain the condition that an elliptic surface or an elliptic fibre becomes singular:

$$
4f(z)^3 + 27g(z)^2 \quad =: \quad \Delta(z) = 0.
\tag{3.1.25}
$$

$\Delta(z) = 0$ is a divisor. In particular, we consider the condition for an elliptic fibre to be singular and an elliptic surface not to be, in other words, the z derivative of P_z in Eq. (3.1.20) is not zero and ord(f) =ord(g) = 0, ord(Δ) = 1:

$$
f'(z)x + g'(z) \neq 0.
\tag{3.1.26}
$$

The condition corresponds to the condition for the Kodaira I_1 singular fibre discussed in the next section. In this case, if Eq. (3.1.25) is satisfied for $z = z_i$, then the condition is $\Delta(z) \sim (z - z_i)$ and $J(\tau) = \frac{4f^3}{\Delta} \sim (z - z_i)^{-1}$. In the limit $z \to z_i$,

$$
J(\tau) \quad \sim \quad (z - z_i)^{-1} \sim e^{-2\pi i \tau} \to \quad \infty,
\tag{3.1.27}
$$

since $J(\tau) \to \left(\frac{1}{12}\right)^3 e^{-2\pi i \tau}$ in the limit $\tau \to i\infty$ ($q := e^{2\pi i \tau} \to 0$), mathmatically. Therefore, we obtain

$$
\tau(z \sim z_i) \quad \sim \quad \frac{1}{2\pi i} \log(z - z_i) \quad \to \quad i\infty.
\tag{3.1.28}
$$

This corresponds to Eq. (2.1.21) and Eq. (2.1.22) discussed for a (D)7-brane. From the above, the position of a 7-brane corresponds to the point where the discriminant locus, in other words, the point where the elliptic fibre is the Kodaira I_1 singular fibre. Moreover, from the $(P)SL(2, \mathbb{Z})$ symmetry of the complex structure modulus τ, all $(P)SL(2, \mathbb{Z})$-conjugate monodromies are considered to be identical to $T \in (P)SL(2, \mathbb{Z})$. Thus, from a geometric point of view, since a 7-brane is locus: $\Delta(z) = 0$, they do not differ from each other; and then, a [p, q]7-brane, which is introduced in Section 2.3, is locally a D7-brane.

Also, If the z derivative of P_z in Eq. (3.1.20) is zero:

$$
f'(z)x + g'(z) \neq 0,
\tag{3.1.29}
$$

we obtain the two cases: ord(f) ≥ 1, ord(g) ≥ 2, ord(Δ) ≥ 3 and ord(f) =ord(g) = 0, ord(Δ) ≥ 2. These cases correspond to the non-abelian gauge symmetries. In particular, the latter case corresponds to that N D7-branes exist from the discussion in the next section. This can be explained by the following facts. When N (≥ 2) D7-branes exist at $z = z_i$,

$$
\tau(z) \quad \sim \quad \frac{N}{2\pi i} \log(z - z_i)
\tag{3.1.30}
$$

from Eq. (2.1.23). In this case, we obtain

$$\Delta(z) \sim (z - z_i)^N \tag{3.1.31}$$

in the limit $z \to z_i$. These show that the degree of $\Delta(z)$ is equal to the number of 7-branes. A more detailed discussion will follow in the next section.

Next, we show that we can obtain the monodromy that occurs when $\tau(z)$ moves around a singularity, by investigating the value of the J-function [85]. Also, we can obtain (p, q)-charges of 7-branes from the monodromies as in the previous chapter. The properties of the J-function are as follows: the J-function is a one-to-one map from the fundamental region of τ to $\mathbb{C}$ and is a $(P)SL(2, \mathbb{Z})$ (modular) invariant function. It is also a one-to-one map from $\mathrm{Re}\,\tau < 0$ in the fundamental region of τ to the upper half-plane $\mathbb{H}$ and a one-to-many map from the upper half-plane $\mathbb{H}$ to $\mathbb{C}$, with boundary correspondence:

$$
\begin{aligned}
J(\tau = e^{\frac{2\pi i}{3}}) &= 0, \\
J(\tau = i) &= 1, \\
J(\tau \to i\infty) &\to \infty.
\end{aligned}
\tag{3.1.32}
$$

We consider the change in the value of the J-function when the complex structure modulus τ is changed in the upper half-plane $\mathbb{H}$ by the $(P)SL(2, \mathbb{Z})$ transformation. Since τ is a multivalued function, depending on what $(P)SL(2, \mathbb{Z})$ (monodromy) transformations are performed on τ, the value of the J-function returns to its original value along what path in the image space $\mathbb{C}$. This is shown concretely in

$$
\begin{aligned}
T &: \ \tau \to \tau + 1 & \Rightarrow & \quad \text{Crossing } (1, \infty) \text{ and } (\infty, 0) \text{ in order,} \\
S &: \ \tau \to -\frac{1}{\tau} & \Rightarrow & \quad \text{Crossing } (1, \infty) \text{ and } (0, 1) \text{ in order.}
\end{aligned}
\tag{3.1.33}
$$

Here, (a, b) denote the line segments on the real axis of the image space $\mathbb{C}$ of the J-function. We can measure the monodromies from Eq. (3.1.33). This is summarized in Table 3.1. Here $1_{+(-)}$ represents a clockwise (counterclockwise) rotation around 1 in the image space $\mathbb{C}$ of the J-function, and $0_{+(-)}$ represents a clockwise (counterclockwise) rotation around 0 in the image space $\mathbb{C}$ of the J-function. Also, longer paths can be described by a combination of these.

There is another way how we can measure the monodromies, using a "dessin d'enfant" [115, 116]. A "dessin d'enfant" is a topological graph (on the Riemann sphere $S^2 \sim \mathbb{P}^1$) [117–119]. In general, a "dessin d'enfant" is characterized by a complex-valued meromorphic function $F(z)$[3], whose values of the branch points are either 0, 1 or ∞. These values are called "critical values", and the inverse images of these values are called the "critical points". Such a complex-valued meromorphic function $F(z)$ To draw a "dessin" on the z-plane, we first mark the inverse images of 0 and 1, namely $F^{-1}(0)$ and $F^{-1}(1)$, respectively. We then draw lines along the inverse image of the line segment $[0, 1]$. This graph

---

[3]$F(z)$ is referred to as a "Belyi function".

Table 3.1: Value of J function & monodromy

Value of J function and monodromy	
0_+1_+	T
1_+	S
1_-	S^{-1}
0_+	TS^{-1}
0_-	ST^{-1}

is a "dessin d'enfant". Finally, we add inverse images of ∞ and lines along the inverse image of $[-\infty, 0]$ and $[1, \infty]$ to the "dessin d'enfant". Due to these additional lines, we can draw a triangulation on the z-plane ($z \in \mathbb{P}^1$).

We introduce how the "dessin" can be drawn on $\mathbb{P}^1$ in F-theory. $J(\tau(z))$ of the left-hand side of Eq. (3.1.21) is the modular J-function. And the complex structure modulus $\tau(z)$ of an elliptic fibre over $z \in \mathbb{P}^1$ is determined by solving Eq. (3.1.21). Assuming that $f(z)$ and $g(z)$ are polynomials in z^4, the right-hand side of Eq. (3.1.21) is a complex-valued meromorphic function of z. Thus, using Eq. (3.1.21), we can draw a "dessin d'enfant" and additional inverse images associated with ∞ on $\mathbb{P}^1$. We first mark points of the zero loci of $f(z)$, $g(z)$ and discriminant $\Delta(z)$ on the z-plane. From Eq. (3.1.21) and (3.1.32), we find that the zero loci of $f(z)$ and $g(z)$ correspond to the critical points in a "dessin": 0 and 1, respectively. The discriminant loci $\Delta(z) = 0$ also corresponds to ∞. They define codimension-one objects on $\mathbb{P}^1$[15]. We next draw lines at the inverse images of $-\infty < J(\tau(z)) < 0$, $0 < J(\tau(z)) < 1$ and $1 < J(\tau(z)) < \infty$, which correspond to the line segment $[-\infty, 0]$, $[0, 1]$ and $[1, \infty]$, respectively. These are called a T-wall, an S-wall and a T'-wall, denoted by a green line $\mathbf{G}$, a blue line $\mathbf{B}$ and a dashed green line $\mathbf{dG}$, respectively [115, 116]. In this way, we can triangulate regions of the "dessin" on $\mathbb{P}^1$.

By utilizing this "dessin", it is quite easy to read the monodromies made by 7-brane. The reasons why this set-up allows for such are as follows. From the right-hand side of Eq. (3.1.21), we can find that the ramification index of the $J = 0$ ($f = 0$) and $J = 1$ ($g = 0$) critical points are always three and two, respectively. On the other hand, a modular J-function $J(\tau)$ behaves $J(\tau) \sim O((\tau - e^{\frac{2\pi i}{3}})^3)$ near $\tau \sim e^{\frac{2\pi i}{3}}$ and $J(\tau) \sim 1 + O((\tau - i)^2)$ near $\tau \sim i$. In other words, there are always three and two fundamental regions of τ around the $f = 0$ locus and the $g = 0$ locus on $\mathbb{P}^1$, respectively. Therefore, Eq. (3.1.21) induces a local homeomorphism between the z-plane and the upper-half plane $\mathbb{H}$ (which is associated with the base $\mathbb{P}^1$ and $\tau(z)$, respectively). In other words, the "dessin" can

---

[4] We consider only the case if the elliptic fibration is an elliptically fibred $K3$ or a rational elliptic surface in this section.

[5] The zero loci of $f(z)$ and $g(z)$ are called "elliptic point planes" [115, 116].
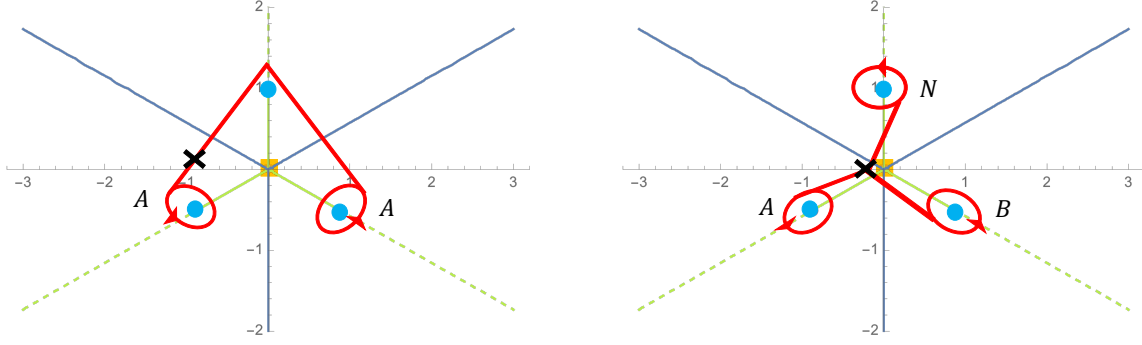
Figure 3.1: Example: Kodaira singular fibre of type III

provide a chart on the base $\mathbb{P}^1$ that exactly points to the corresponding position on the upper half-plane $\mathbb{H}$.

We explain how to read the monodromies using the "dessin". In order to read a monodromy along a given counterclockwise path around a 7-brane, we first list the walls that the path crosses in sequence. When the path crosses two walls, we multiply particular $SL(2, \mathbb{Z})$ matrices according to the following rules from left to right in the order in which the walls are crossed if the base point of the path is in a cell region with $\mathrm{Im} J > 0$:

$$
\begin{aligned}
\to \mathbf{dG} \to \mathbf{G} \to &= T, \\
\to \mathbf{G} \to \mathbf{dG} \to &= T^{-1}, \\
\to \mathbf{dG} \to \mathbf{B} \to = \ \to \mathbf{B} \to \mathbf{dG} \to \ &= \ S, \\
\to \ \mathbf{B} \ \to \mathbf{G} \to &= ST, \\
\to \ \mathbf{G} \ \to \mathbf{B} \to &= T^{-1}S.
\end{aligned} \tag{3.1.34}
$$

Also, if the base point of the path is in a cell region with $\mathrm{Im} J < 0$[6], the rule is

$$
\begin{aligned}
\to \mathbf{dG} \to \mathbf{G} \to &= T^{-1}, \\
\to \mathbf{G} \to \mathbf{dG} \to &= T, \\
\to \mathbf{dG} \to \mathbf{B} \to = \ \to \mathbf{B} \to \mathbf{dG} \to \ &= \ S, \\
\to \ \mathbf{B} \ \to \mathbf{G} \to &= ST^{-1}, \\
\to \ \mathbf{G} \ \to \mathbf{B} \to &= TS.
\end{aligned} \tag{3.1.35}
$$

We show the example in Fig. 3.1. For more detail on this method, see [115] and concrete examples can be found in [116].

We summarize this section. In the eight-dimensional F-theory, there is a duality:

---

[6]Whether a given cell region is one with $\mathrm{Im} J > 0$ or with $\mathrm{Im} J < 0$ can be easily distinguished as follows: We consider a small loop path that starts from any point in the given cell region and goes around a D-brane counterclockwise. If the path crosses as $\to \mathbf{dG} \to \mathbf{G} \to$, the cell region is a cell region with $\mathrm{Im} J > 0$. On the other hand, if it crosses $\to \mathbf{G} \to \mathbf{dG} \to$, the cell region is one with $\mathrm{Im} J < 0$.
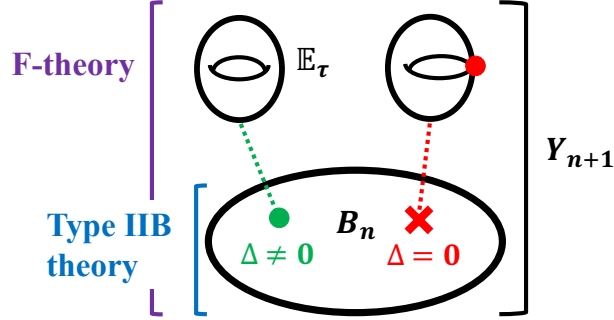
Figure 3.2: The duality between F-theory and Type IIB superstring field theory.

$$
\begin{aligned}
\text{F-theory on } \mathbb{R}^{1,7} \quad &\times \quad \text{elliptically fibred } K3 \\
&\simeq \quad \text{Type IIB theory on } \mathbb{R}^{1,7} \times \mathbb{P}^1 \text{ with 7-brane.} \quad (3.1.36)
\end{aligned}
$$

More generally, there is a duality (Fig. 3.2):

$$
\begin{aligned}
\text{F-theory on } \mathbb{R}^{1,9-2n} \quad &\times \quad \text{elliptically fibred Calabi-Yau } (n+1)\text{-fold } Y_{n+1} \\
&\simeq \quad \text{Type IIB theory on } \mathbb{R}^{1,9-2n} \times B_n \text{ with 7-brane.} \quad (3.1.37)
\end{aligned}
$$

In these cases, there is the correspondence between the complex structure modulus $\tau(B_n) := \tau_1(B_n) + i\tau_2(B_n)$ of the elliptic curve $\mathbb{E}_\tau$ in F-theory and the axio-dilaton field $\tau(B_n) := C_0(B_n) + ie^{-\phi(B_n)}$ in Type IIB superstring theory:

$$
\tau(B_n) := \tau_1(B_n) + i\tau_2(B_n) \simeq \tau(B_n) := C_0(B_n) + ie^{-\phi(B_n)}, \quad (3.1.38)
$$

where B_n is the coordinates of the base space B_n.

3.2 Kodaira's Classification and 7-brane configurations

In this section, we summarize the results of the classification and the correspondence between the codimension-one singularities and gauge symmetries. The Kodaira's singular fibres are classified by Tate's algorithm. The classification is called Kodaira's classification [62, 113, 114] and is summarized in Table 3.2. The basis for the correspondence with each Kodaira singular fibre type and each gauge symmetry is that each intersection diagram of the exceptional curves that appear by the crepant resolution[7] (blow-ups) of

---

[7]In algebraic geometry, a crepant resolution is a resolution that does not change the canonical class of the manifold.

Table 3.2: Kodaira's classification and 7-brane configurations. The $\mathrm{ord}(f)$, $\mathrm{ord}(g)$ and $\mathrm{ord}(\Delta)$ denote the orders of zeros of f, g and the discriminant Δ of the Weierstrass equation and $n \geq 1$, $(n \in \mathbb{N})$. Here, $\mathrm{ord}(\Delta)$ corresponds to the number of 7-branes collected and the 7-brane configuration can be explained from the analysis of monodromy in Chapter 2. Note that when $\mathrm{ord}(f) \geq 4$ and $\mathrm{ord}(g) \geq 6$, the singularities are so bad that the triviality of the canonical bundles is broken in general.

Fibre type	$\mathrm{ord}(f)$	$\mathrm{ord}(g)$	$\mathrm{ord}(\Delta)$	Monodromy	7-brane config.	Brane type
smooth (I_0)	≥ 0	≥ 0	0	$-$	$-$	$-$
I_n	0	0	n	T^n	$\boldsymbol{A}^n$	A_{n-1}
II	≥ 1	1	2	$-T^{-1}S$	$\boldsymbol{AB}$	H_0
III	1	≥ 2	3	$-S$	$\boldsymbol{A}^2\boldsymbol{B}$	H_1
IV	≥ 2	2	4	$-TS$	$\boldsymbol{A}^3\boldsymbol{B}$	H_2
I_0^*	≥ 2	3	6	$-\hat{1}$	$\boldsymbol{A}^4\boldsymbol{BC}$	D_4
I_n^*	≥ 2	3	$6+n$	$-\hat{1} \times T^n$	$\boldsymbol{A}^{n+4}\boldsymbol{BC}$	D_{n+4}
I_n^*	2	≥ 3	$6+n$	$-\hat{1} \times T^n$	$\boldsymbol{A}^{n+4}\boldsymbol{BC}$	D_{n+4}
II^*	≥ 4	5	10	TS	$\boldsymbol{A}^7\boldsymbol{BCB}$	E_8
III^*	3	≥ 5	9	S	$\boldsymbol{A}^6\boldsymbol{BCB}$	E_7
IV^*	≥ 3	4	8	$T^{-1}S$	$\boldsymbol{A}^5\boldsymbol{BCB}$	E_6
non-minimal	4	6	12	$\hat{1}$	$\boldsymbol{A}^8\boldsymbol{BCBC}$	$-$

each singularity coincide with each Dynkin diagram. In addition, from the coincidence of the monodromy made by each 7-brane configuration at a point and the monodromy around the point where there are Kodaira's singular fibres, we obtain Table 3.2. Note that a gauge symmetry on the 7-branes is the same as one in Kodaira's classification. This corresponds to the fact that the degrees of freedom of the open strings coincide with the degrees of freedom of the roots of a gauge symmetry.

To briefly illustrate the fact that a Dynkin diagram coincides with an intersection diagram of the exceptional curves that appear by the crepant resolution of a codimension-one singularity, we consider the I_3 case as the most simple example. Note that the smooth manifold obtained after the crepant resolution of a singular one is also a Calabi-Yau manifold since a crepant resolution does not change the canonical class of the Calabi-Yau [54]. We start from the Weierstrass equation (3.1.20), where

$$
\begin{aligned}
f(z) &= f_0 + f_1 z + \cdots + f_4 z^4, \\
g(z) &= g_0 + g_1 z + \cdots + g_6 z^6,
\end{aligned}
\tag{3.2.1}
$$

f_i, $g_i \in \mathbb{C}$ and z is the coordinate on the affine patch of the base space $\mathbb{P}^1$. Then, the discriminant Δ of (3.1.20) is

$$
\begin{aligned}
\Delta(z) &= 4f(z)^3 + 27g(z)^2 \\
&= (4f_0^3 + 27g_0^2) + 6(2f_0^2 f_1 + 9g_0 g_1)z
\end{aligned}
$$

$$+3(4f_0^2 f_2 + 4f_0 f_1^2 + 18g_0 g_2 + 9g_1^2)z^2$$
$$+2(6f_0^2 f_3 + 12f_0 f_1 f_2 + 2f_1^3 + 27g_0 g_3 + 27g_1 g_2)z^3 + O(z^4). \qquad (3.2.2)$$

First, we obtain the local equation with the I_3 singular fibre from the Weierstrass equation (3.1.20). From Table 3.2, we set

$$
\begin{aligned}
f_0 &= -3a^2, \;\; g_0 = 2a^3 \\
g_1 &= -af_1 = 0, \\
g_2 &= -af_2 = 0, \\
g_3 &\neq -af_3, \\
f_4 &= g_4 = g_5 = g_6 = 0,
\end{aligned}
\qquad (3.2.3)
$$

where $a \in \mathbb{C} - \{0\}$; and then, if we choose $a = f_3 = g_3 = 1$, we obtain the local equation with the I_3 singular fibre at $z = 0$:

$$\Psi_{I_3}(x, y, z) \;\; := \;\; -y^2 + x^3 + (-3 + z^3)x + (2 + z^3) = 0, \qquad (3.2.4)$$
$$\Delta(z)_{I_3} \;\; = \;\; 216z^3 + O(z^6). \qquad (3.2.5)$$

In Eq. (3.2.4), there are the singularities at $(x, y, z) = (1, 0, 0)$. For simplicity, a variable transformation yields

$$\Phi_{I_3}(x, y, z) \;\; := \;\; -y^2 + x^3 + 3x^2 + z^3 x + 2z^3 = 0. \qquad (3.2.6)$$

In Eq. (3.2.6), there is the singularity at $(x, y, z) = (0, 0, 0)$.

Next, we consider the crepant resolution of a singularity [93, 98, 120] of the local equation (3.2.6) along $(x, y, z) = (0, 0, 0)$; and then, we obtain the exceptional curves $\mathcal{C}_i$'s and their intersection diagrams. Here, the exceptional curve $\mathcal{C}_i$ is the intersection of $\mathbb{P}^2$ in Eq. (3.2.7) and after the blow-up of the singularity of elliptic surface (for example, $\Phi_{z I_3}(x_1, y_1, z)$ in Eq. (3.2.8)); and then, the exceptional curves $\mathcal{C}_i$'s are $\mathbb{P}^1$'s. For the crepant resolution, we replace the point $(x, y, z) = (0, 0, 0)$ with a $\mathbb{P}^2$, by replacing $\mathbb{C}^3$ with

$$\hat{\mathbb{C}}^3 = \{((x, y, z) \times (\xi : \eta : \zeta)) \in \mathbb{C}^3 \times \mathbb{P}^2 | (x : y : z) = (\xi : \eta : \zeta)\}. \qquad (3.2.7)$$

We are blowing up the singularity in inhomogeneous coordinates defined by the three different affine patches of $\mathbb{P}^2$, for example, $(x : y : z) = (\xi : \eta : \zeta) = (x_1 : y_1 : 1) (1_z, z \neq 0)$. Thus, to replace $\mathbb{C}^3$ with $\hat{\mathbb{C}}^3$, we simply replace (x, y, z) with $(x_1 z, y_1 z, z)$ in the equation (3.2.6) in Chart 1_z. To not change the canonical class, the equation after the blow-ups is defined as follows:

$$z^{-2}\Phi_{I_3}(x_1 z, y_1 z, z) =: \Phi_{z I_3}(x_1, y_1, z) = 0. \qquad (3.2.8)$$

We then obtain

Chart 1_z

$$\Phi_{zI_3}(x_1, y_1, z) = -y_1^2 + x_1^3 z + 3x_1^2 + z^2 x + 2z,$$
$$\mathcal{C}_{p_1}^{\pm} \text{ in } 1_z : \ z = 0, \quad y_1 = \pm\sqrt{3}x_1, \tag{3.2.9}$$
$$\text{Singularities : None.}$$

Similarly, we need to check the other patches: 1_x $(x \neq 0)$ and 1_y $(y \neq 0)$, by the same procedure,

Chart 1_x

$$\Phi_{xI_3}(x, y_1, z_1) = -y_1^2 + x + 3 + z_1^3 x^2 + 2z_1^3 x,$$
$$\mathcal{C}_{p_1}^{\pm} \text{ in } 1_x : \ x = 0, \quad y_1 = \pm\sqrt{3}, \tag{3.2.10}$$
$$\text{Singularities : None,}$$

and

Chart 1_y

$$\Phi_{yI_3}(x_1, y, z_1) = -1 + x_1^3 y + 3x_1^2 + z_1^3 x_1 y^2 + 2z_1^3 y,$$
$$\mathcal{C}_{p_1}^{\pm} \text{ in } 1_y : \ y = 0, \quad x_1 = \pm 1/\sqrt{3}, \tag{3.2.11}$$
$$\text{Singularities : None.}$$

No singularities remain; thus the blowup is finished. We obtain $\mathcal{C}_{p_1}^{\pm}$ and an intersection diagram of the exceptional curves after the crepant resolution of the I_3 codimension-one singularity (Fig. 3.3); and then, we can check the fact that a Dynkin diagram coincides with the intersection diagram of the exceptional curves. In eight-dimensional F-theory, this result similarly holds for all singular fibre types in Kodaira's classification; thus the singularity types in Kodaira's classification exactly match the conjectured enhanced gauge symmetries, respectively.

3.3 M-/F-theory Duality

It was shown that there is a duality between F-theory and M-theory [52,59,111]. In this section, we briefly explain it.

It is known that the bosonic part of the action of the eleven-dimensional $\mathcal{N} = 1$ supergravity theory, which is the low-energy effective theory of M-theory, is given by

$$S = \frac{2\pi}{\ell_{11}^9} \left(\int_{\mathbb{R}^{1,10}} \sqrt{-g}R - \frac{1}{2} \int_{\mathbb{R}^{1,10}} dC_3 \wedge *dC_3 - \frac{1}{6} \int_{\mathbb{R}^{1,10}} C_3 \wedge G_4 \wedge G_4 \right)$$
$$+ \frac{2\pi}{\ell_{11}^3} \int_{\mathbb{R}^{1,10}} C_3 \wedge I_8 + \text{(fermionic term)}, \tag{3.3.1}$$

where ℓ_{11} is the Planck length in eleven dimensions, C_3 is the 3-form gauge potential, $G_4 := dC_3$ is the field strength and g_{MN} $(M, N = 0, 1, \cdots, 10)$ is the eleven-dimensional
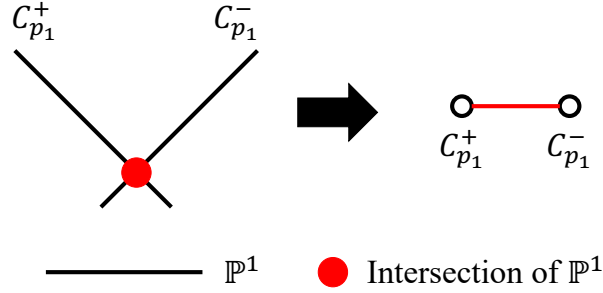
Figure 3.3: Example: intersection diagrams of the exceptional curves of a I_3 singular fibre.

metric. Also, I_8 is a topological higher curvature [121]:

$$I_8 = \frac{1}{(2\pi)^4} \left(-\frac{1}{768} \left(\text{tr} \, R^2 \right)^2 + \frac{1}{192} \, \text{tr} \, R^4 \right). \tag{3.3.2}$$

This action is invariant under the transformation $C_3 \rightarrow C_3 + d\Lambda_2$, where Λ_2 is an arbitrary 2-form. C_3 is electrically coupled to the $M2$-brane as

$$S_{\text{M2}} = \frac{2\pi}{\ell_{11}^3} \int_{\text{M2}} \sqrt{-g} + \frac{2\pi}{\ell_{11}^3} \int_{\text{M2}} C_3. \tag{3.3.3}$$

C_6, which is dual to C_3, is electrically coupled to the $M5$-brane. It is known that the M_2-brane solution is

$$ds_{M2}^2 = f_{M2}^{-2/3}(r)\eta_{\mu\nu}dx^\mu dx^\nu + f_{M2}^{1/3}(r)\delta_{ij}dx^i dx^j, \tag{3.3.4}$$

$$f_{M2}(r) = 1 + \frac{32\pi^2\ell_{11}^6 N_{M2}}{r^6}, \quad r^2 = \delta_{ij}x^i x^j, \tag{3.3.5}$$

where N_{M2} is the number of $M2$-branes $\mu, \nu = 0, 1, 2$ and $i, j = 3, \cdots, 10$. It is also known that the M_5-brane solution is

$$ds_{M5}^2 = f_{M5}^{-1/3}(r)\eta_{\mu\nu}dx^\mu dx^\nu + f_{M5}^{2/3}(r)\delta_{ij}dx^i dx^j, \tag{3.3.6}$$

$$f_{M5}(r) = 1 + \frac{\pi\ell_{11}^3 N_{M5}}{r^3}, \quad r^2 = \delta_{ij}x^i x^j, \tag{3.3.7}$$

where N_{M5} is the number of $M5$-branes $\mu, \nu = 0, \cdots, 5$ and $i, j = 6, \cdots, 10$.

We briefly explain a duality between M-theory on $\mathbb{R}^{1,8} \times T^2$ and Type IIB superstring theory on $\mathbb{R}^{1,8} \times S^1$ [111]. To distinguish cycles S_i^1, we label them as S_i^1 and denote the radius of S_i^1 as R_i. We consider

$$T^2 := S_a^1 \times S_b^1. \tag{3.3.8}$$

We denote R_a and R_b as the radii of S_a^1 and S_b^1, respectively. In this case, $g_{10\mu}$ ($\mu = 0, 1, \cdots, 9$) corresponds to the R-R field C_μ and g_{1010} to the dilaton field ϕ in Type IIA superstring theory. First, when $R_a \to 0$, there is a duality between M-theory on S_a^1 and the Type IIA superstring theory [122]. Next, there is T-duality between Type IIA superstring theory on $\mathbb{R}^{1,8} \times S_B^1$ and Type IIB superstring theory on $\mathbb{R}^{1,8} \times \tilde{S}_B^1$. There is a relation between the radii of S^1 of each other:

$$\tilde{R}_b = \frac{\ell_s^2}{R_b}, \tag{3.3.9}$$

where l_s is the string length and $\tilde{R}_B$ is the radius of $\tilde{S}_B^1$. In this case, $C_{\mu=9}$ corresponds to the R-R scalar field C_0 in Type IIB superstring theory. And their dilaton fields correspond to each other. The limit $R_B \to 0$ corresponds to the limit $\tilde{R}_B \to \infty$; thus, It is equivalent to the fact that we consider Type IIB superstring theory on $\mathbb{R}^{1,9}$. Therefore, if we consider $\mathbb{R}^{1,8} \times \tilde{S}_B^1 \big|_{\tilde{R}_B \to \infty} \to \mathbb{R}^{1,9}$, there is a duality:

$$\text{M-theory on } \mathbb{R}^{1,8} \times T^2 \left(:= S_A^1 \times S_B^1 \right) \big|_{R_A, R_B \to 0} \simeq \text{Type IIB theory on } \mathbb{R}^{1,9}. \tag{3.3.10}$$

In this thesis, we denote a duality as $\simeq$. In this case, there is a correspondence between the complex structure modulus $\tau := \tau_1 + i\tau_2$ of T^2 in M-theory and the axio-dilaton field $\tau := C_0 + ie^{-\phi}$ in Type IIB superstring theory:

$$\tau := \tau_1 + i\tau_2 \ \simeq \ \tau := C_0 + ie^{-\phi}. \tag{3.3.11}$$

Also, using the volume V of T^2 in the M-theory, the metric of Type IIB superstring theory in the Einstein frame can be written as

$$ds_{\text{IIB}}^2 = ds_{\mathbb{R}^{1,8}}^2 + \frac{\ell_s^4}{V} d\tilde{x}_9^2, \quad \tilde{x}_9 \sim \tilde{x}_9 + 1, \tag{3.3.12}$$

where $\tilde{x}_9 \sim \tilde{x}_9 + 1$ is a periodic boundary condition for $\tilde{S}_B^1$. Thus, in the limit $V \to 0$, the dual Type IIB superstring theory has ten-dimensional Poincare symmetry.

We discuss this duality in general. The elliptic fibration Y_{n+1} is defined as

$$\begin{array}{rcl} \pi : & \mathbb{E}_\tau \to & Y_{n+1} \\ & & \downarrow \\ & & B_n, \end{array} \tag{3.3.13}$$

where $\mathbb{E}_\tau$ and B_n are an elliptic curve and a complex n-dimensional base space, respectively. And then, we can regard Y_{n+1} as a holomorphic line bundle $\mathcal{L}$ over B_n with a choice of sections. If we consider $\mathbb{R}^{1,8-2n} \times B_n \times \tilde{S}_B^1 \big|_{\tilde{R}_B \to \infty} \to \mathbb{R}^{1,9-2n} \times B_n$, there is a duality in general:

$$\text{M-theory on } \mathbb{R}^{1,8-2n} \times Y_{n+1}|_{V \to 0} \simeq \text{Type IIB theory on } \mathbb{R}^{1,9-2n} \times B_n, \tag{3.3.14}$$

where $V := \mathrm{Vol}(\mathbb{E}_\tau)$ and $n \geq 1$. Then, using the volume V of the elliptic curve $\mathbb{E}_\tau$ on the M-theory side, we can write the metric of Type IIB superstring theory in Einstein frame as

$$ds^2 = ds^2_{\mathbb{R}^{1,8-2n}} + ds^2_{B_n} + \frac{\ell_s^4}{V} d\tilde{x}_9^2, \quad \tilde{x}_9 \sim \tilde{x}_9 + 1. \tag{3.3.15}$$

The first Chern class of Y_{n+1} is given by

$$c_1(Y_{n+1}) = c_1(B_n) - c_1(\mathcal{L}). \tag{3.3.16}$$

There is a relation

$$c_1(B_n) = c_1(\mathcal{L}) \tag{3.3.17}$$

from the Einstein equation and the discussion about supersymmetry [61]. Therefore, we obtain

$$c_1(Y_{n+1}) = 0. \tag{3.3.18}$$

This means that Y_{n+1} is a Calabi-Yau $(n+1)$-fold. In particular, in the $n=1$ case, Y_2 is the complex two-dimensional elliptically fibred Calabi-Yau, the elliptically fibred $K3$; and then, the base space B_1 is $\mathbb{P}^1$. In this case, half of SUSY is conserved in M-theory. This corresponds to the fact that we consider the 7-brane solution in Type IIB superstring theory discussed in the previous chapter.

When considering F-theory on elliptically fibred Calabi-Yau $(n+1)$-fold, there is a duality in general:

$$\begin{aligned} \text{F-theory on } \mathbb{R}^{1,9-2n} \quad &\times \quad \text{elliptically fibred Calabi-Yau } (n+1)\text{-fold } Y_{n+1} \\ &\simeq \quad \text{Type IIB theory on } \mathbb{R}^{1,9-2n} \times B_n \text{ with 7-brane} \end{aligned} \tag{3.3.19}$$

from the discussion in Section 3.1. In particular, if considering F-theory on elliptically fibred $K3$, the base $B_1 = \mathbb{P}^1$ ($n = 1$). In the eight-dimensional F-theory, there is a duality:

$$\begin{aligned} \text{F-theory on } \mathbb{R}^{1,7} \quad &\times \quad \text{elliptically fibred } K3 \\ &\simeq \quad \text{Type IIB theory on } \mathbb{R}^{1,7} \times \mathbb{P}^1 \text{ with 7-brane.} \end{aligned} \tag{3.3.20}$$

On the affine patch of the base space of the elliptically fibred $K3$: B_1 ($= \mathbb{P}^1$) with the coordinate $z = x_8 + ix_9$, there is the correspondence between the complex structure modulus $\tau(z) := \tau_1(z) + i\tau_2(z)$ of the elliptic curve $\mathbb{E}_\tau$ in F-theory and the axio-dilaton field $\tau(z) := C_0(z) + ie^{-\phi(z)}$ in Type IIB superstring theory:

$$\tau(z) := \tau_1(z) + i\tau_2(z) \simeq \tau(z) := C_0(z) + ie^{-\phi(z)}. \tag{3.3.21}$$

From the above, when considering the eight-dimensional F-theory, there is a duality between M-theory and F-theory:

$$
\begin{aligned}
\text{M-theory on } \mathbb{R}^{1,6} \quad &\times \quad \text{elliptically fibred } K3|_{V\to 0} \\
&\simeq \quad \text{F-theory on } \mathbb{R}^{1,7} \times \text{elliptically fibred } K3. \qquad (3.3.22)
\end{aligned}
$$

In this case, since the coordinate on the affine patch of the base space $\mathbb{P}^1$ on the M-theory side and the F-theory side are $z = x_7 + ix_8$ and $z = x_8 + ix_9$, respectively, the complex structure moduli $\tau(z) := \tau_1(z) + i\tau_2(z)$ of the elliptic curves $\mathbb{E}_\tau$ correspond to each other. Therefore, because we consider the limit $V := \mathrm{Vol}(\mathbb{E}_\tau) \to 0$ on the M-theory side, a dynamical modulus is not the volume (Kähler) modulus ($V := \mathrm{Vol}(\mathbb{E}_\tau)$) but the complex structure modulus $\tau(z)$ of the elliptic curve $\mathbb{E}_\tau$ on the F-theory side. This means that the extra two dimensions $\mathbb{E}_\tau$ in F-theory are *virtual*. More generally, the M-/F-theory duality is

$$
\begin{aligned}
\text{M-theory on } \mathbb{R}^{1,8-2n} &\times \text{elliptically fibred Calabi-Yau } (n+1)\text{-fold } Y_{n+1}|_{V\to 0} \\
&\simeq \text{F-theory on } \mathbb{R}^{1,9-2n} \times \text{elliptically fibred Calabi-Yau } (n+1)\text{-fold } Y_{n+1}; \quad (3.3.23)
\end{aligned}
$$

and then, the complex structure moduli of the elliptic curves $\mathbb{E}_\tau$ correspond to each other too.

Finally, we explain how the (p,q)-string in Type IIB superstring theory can be interpreted in dual M-theory. Considering the duality between M-theory and F-theory, if an $M2$-brane is wrapped around a cycle of an elliptic curve, there are two pieces of information: a line segment on the base space and a cycle around which it is wrapped. We explain what the information in this cycle corresponds to. When we consider F-theory on the elliptically fibred Calabi-Yau $(n+1)$-fold, there are some 7-brane at the points where the elliptic fibrations are singular (where the elliptic curve degenerates). On the other hand, in Type IIB superstring theory, the 7-brane is an object to which the endpoints of an open string are attached. Thus, at least a cycle of an elliptic curve (two-torus T^2) degenerates at the point where a 7-brane exists. This is called a vanishing cycle. The vanishing cycle is determined by the charge (p,q) of the $[p,q]$7-brane. Therefore, the line segment on the base space and the cycle $p\alpha + q\beta$ around which an $M2$-brane is wrapped in dual M-theory corresponds to the path and the charge (p,q) of the (p,q)-string in Type IIB superstring theory, respectively (Fig. 3.4). Here, α and β are two cycles of an elliptic curve $\mathbb{E}_\tau$.
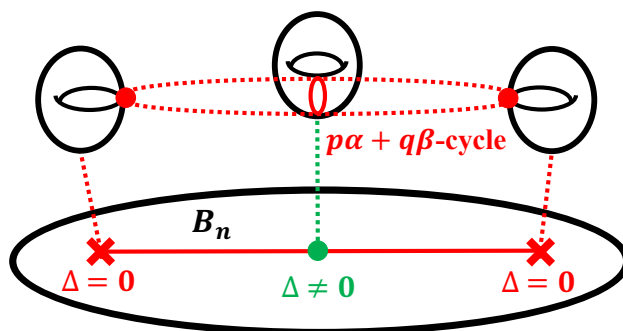
Figure 3.4: The line segment on the base space and the cycle $p\alpha + q\beta$ in dual M-theory.

Chapter 4

Heterotic/F-theory Duality

In this chapter, we discuss the duality between F-theory and Heterotic superstring theory [52, 53, 87–89, 123, 124]. In particular, for considering mater generation in F-theory, we focus on an F-theory on an elliptically fibred Calabi-Yau threefold over $\mathbb{F}_n$ in the stable degeneration limit, which is dual to an $E_8 \times E_8$ Heterotic superstring theory on elliptically fibred $K3$ with instanton numbers $(12 + n, 12 - n)$ in each E_8 [87, 88, 90]. We then introduce the anomaly cancellation condition [90, 125] and see that the matter contents in the dual Heterotic superstring theory satisfy this condition [90]. In addition, on the F-theory side, from the Weierstrass equation, if the charged matter fields are localized at all codimension-two singularities, the number of the matter fields in a model with ADE codimension-one singularity is consistent with this condition [90]. This is one of the reasons why the massless charged matter fields are localized at all codimension-two singularities in a model with ADE codimension-one singularity.

4.1 Heterotic/F-theory duality in eight dimensions

The Heterotic/F-theory duality in eight dimensions [52, 53, 87, 123, 124] (see [54, 126] for a review) is

$$\text{Heterotic superstring theory on } \mathbb{R}^{1,7} \times T^2$$
$$\simeq \text{F-theory on } \mathbb{R}^{1,7} \times \text{elliptically fibred } K3. \tag{4.1.1}$$

One of the pieces of evidence suggesting the duality (4.1.1) is that their moduli spaces:

$$SO(2, 18; \mathbb{Z}) \setminus SO(2, 18) / SO(2) \times SO(18) \tag{4.1.2}$$

coincide with each other[1]. In particular, in the cases of the perturbative $E_8 \times E_8$ Heterotic superstring theory, the duality (4.1.1) can be understood concretely in the weakly coupling

---

[1]A gauge symmetry can be realized only if the root lattice of its gauge algebra can be embedded into the unimodular lattice $\Gamma^{2,18}$ [127].

limit, which is realized by $V \to \infty$ (V is the volume of T^2). The volume modulus V on the Heterotic superstring theory side corresponds to a complex structure modulus τ of the elliptic curve $\mathbb{E}_\tau$ on the F-theory side. On the F-theory side, we consider the compact space $K3$ as a fibre product of two rational elliptic surfaces dP_9 in the cases of the $E_8 \times E_8$ limit, which is called the "stable degeneration limit" [87–89]. In the stable degeneration limit, we can match the non-abelian gauge symmetries arising from the configurations of the Wilson lines in the perturbative $E_8 \times E_8$ Heterotic superstring theory to the ones arising from Kodaira singular fibre over points on the F-theory base space $\mathbb{P}^1$, respectively.

In lower dimensions, the dualities are briefly understood by considering compact spaces with eight-dimensional cases fibred over the common base spaces B_n in both of these theories, respectively [52, 87, 88]:

$$\text{Heterotic theory on } \mathbb{R}^{1,7-2n} \times \text{elliptically fibred over } B_n$$
$$\simeq \text{F-theory on } \mathbb{R}^{1,7-2n} \times \text{elliptically fibred over } \tilde{B}_{n+1}, \qquad (4.1.3)$$

where $n \in \mathbb{N}$ and $\tilde{B}_{n+1}$ is constructed as a $\mathbb{P}^1$ bundle over B_n. In other words,

$$\text{Heterotic theory on } \mathbb{R}^{1,7-2n} \times \text{elliptically fibred Calabi-Yau } (n+1)\text{-fold } Y_{n+1}$$
$$\simeq \text{F-theory on } \mathbb{R}^{1,7-2n} \times K3\text{-fibred Calabi-Yau } (n+2)\text{-fold } \tilde{Y}_{n+2}, \quad (4.1.4)$$

where both the elliptically fibred Calabi-Yau $(n+1)$-fold Y_{n+1} and $(n+2)$-fold $\tilde{Y}_{n+2}$ have section. This argument is also true for the eight-dimensional case when regarded as the common base space B_0 is a point and $\tilde{B}_1 = \mathbb{P}^1$ is the unique $\mathbb{P}^1$ bundle over the point.

4.2 Heterotic/F-theory duality in six dimensions

In six dimensions, there is a unique common base space $B_1 = \mathbb{P}^1$ in Eq. (4.1.3). Thus, the Heterotic/F-theory duality with the smooth dual geometries in six dimensions is [87, 88]

$$\text{Heterotic theory on } \mathbb{R}^{1,5} \times \text{ elliptically fibred over } \mathbb{P}^1 \text{ (elliptically fibred } K3)$$
$$\simeq \text{ F-theory on } \mathbb{R}^{1,5} \times \text{elliptically fibred over } \mathbb{F}_n, \quad (4.2.1)$$

where $\mathbb{F}_n$ is a Hirzebruch surface, which will be defined later, and both the elliptically fibred Calabi-Yau twofold Y_2 and threefold $\tilde{Y}_3$ have section. In this thesis, we only consider the Heterotic/F-theory duality with the smooth dual geometries in which no small instantons arise[2]. As the case in eight dimensions, on the F-theory side, codimension-one singularities (corresponding to the positions of 7-branes in Type IIB superstring theory),

---

[2]The Heterotic/F-theory duality can be extended by incorporating non-perturbative effects in Heterotic superstring theory. In this case, for example, $\tilde{B}_2 = \mathbb{P}^2$, as the base space in F-theory, can be realized [88, 128]. The base spaces $\tilde{B}_2$ in F-theory can be classified in terms of the divisor structure [97].

which are codimension-one loci in the base space $\mathbb{F}_n$ (codimension-two in the total space $\tilde{Y}_3$) where elliptic fibres become the singular fibres, correspond to the expected ADE gauge symmetries implied by Kodaira's classification [90, 91, 93, 98, 120]. In addition, in six or lower dimensions, this can include non-simply-laced gauge symmetries when monodromies exist. Also, there are intersections of the codimension-one loci in the base space $\mathbb{F}_n$. These codimension-two loci where the codimension-one singularities and the expected gauge symmetries are enhanced correspond to intersections of 7-branes in Type IIB superstring theory. Thus, the codimension-two loci are involved in matter generation and are called codimension-two singularities.

In the stable degeneration limit, especially, the dual Heterotic theory is the $E_8 \times E_8$ Heterotic theory on elliptically fibred $K3$ with instanton numbers $(12+n, 12-n)$ in each E_8 [87, 88]. Here, n in instanton numbers on the Heterotic theory side is equal to n of $\mathbb{F}_n$ on the F-theory side. In this thesis, we focus only on this case henceforth.

The Hirzebruch surface $\mathbb{F}_n$ is a $\mathbb{P}^1$ bundle over $\mathbb{P}^1$, characterized by an integer n. This n is the number of "twists" of a $\mathbb{P}^1$ bundle over a $\mathbb{P}^1$ and $(0 \leq) n \leq 12$ in the mathematical framework of minimal surfaces (where there are no curves of self-intersection -1) [129]. We define the elliptic fibred Calabi-Yau threefold over the Hirzebruch surface $\mathbb{F}_n$ described by Weierstrass form (3.1.17) as follows: the Hirzebruch surface $\mathbb{F}_n$ is defined as a toric variety with the following two toric charges:

$$
\begin{array}{c|cccc}
 & u' & v' & u & v \\
\hline
Q^{(\lambda)} & 1 & 1 & n & 0 \\
Q^{(\mu)} & 0 & 0 & 1 & 1
\end{array}
\tag{4.2.2}
$$

Here, $(u' : v')$ and $(u : v)$ are the homogeneous coordinates of the base $\mathbb{P}^1$ of the fibre $\mathbb{P}^1$, respectively, This means that the Hirzebruch surface $\mathbb{F}_n$ is defined as

$$
F_n = \left\{ \mathbb{C}^4 - \hat{\mathbf{0}} \right\} / \sim,
\tag{4.2.3}
$$

where "$\sim$" contains the two identifications:

$$
\begin{aligned}
(u', v', u, v) &\sim (\lambda u', \lambda v', \lambda^n u, v), &\tag{4.2.4} \\
(u', v', u, v) &\sim (u', v', \mu u, \mu v), &\tag{4.2.5}
\end{aligned}
$$

where $\lambda, \mu \in \mathbb{C}$ and $(12 \geq) n \in \mathbb{Z}$. When $n = 0$, the $\mathbb{P}^1$ fibration is trivial: $\mathbb{P}^1 \times \mathbb{P}^1$. We introduce the affine coordinates as

$$
w = \frac{u'}{v'}, \quad z = \frac{u}{v};
\tag{4.2.6}
$$

and then, the Weierstrass form is given by

$$
y^2 = x^3 + f(z, w) x + g(z, w),
\tag{4.2.7}
$$

where

$$f(z, w) := \sum_{i=0}^{I} z^i f_{8+n(4-i)}(w),$$

$$g(z, w) := \sum_{j=0}^{J} z^j g_{12+n(6-j)}(w),$$

(4.2.8)

where I and J are the largest integer that satisfies $I \leq 8$, $8 + n(4 - I) \geq 0$ and $J \leq 12$, $12 + n(6 - J) \geq 0$, respectively. In this chapter, all subscripts denote the degree of the polynomial in w. The correlation between the degree of $f_{8+n(4-i)}$ ($g_{12+n(6-j)}$) and the power of z in f (g) is determined by the charges $Q^{(\lambda)}$ and $Q^{(\mu)}$ in Eq. (4.2.2) from the condition for conserving supersymmetry [54]. The charges $Q^{(\lambda)}$ and $Q^{(\mu)}$ of x and y are assigned as follows:

	x	y
$Q^{(\lambda)}$	$2n + 4$	$3n + 6$
$Q^{(\mu)}$	4	6

(4.2.9)

In this case, the discriminant locus (3.1.19) is given by

$$
\begin{aligned}
\Delta(z, w) &= 4f^3(z, w) + 27g^2(z, w) \\
&= \left(4f_{4n+8}^3(w) + 27g_{6n+12}^2(w)\right) \\
&\quad + 6\left(2f_{4n+8}^2(w) f_{3n+8}(w) + 9g_{6n+12}(w) g_{5n+12}(w)\right) z \\
&\quad + 3\left(4f_{4n+8}^2(w) f_{2n+8}(w) + 4f_{4n+8}(w) f_{3n+8}^2(w)\right. \\
&\qquad \left. + 18g_{6n+12}(w) g_{4n+12}(w) + 9g_{5n+12}^2(w)\right) z^2 \\
&\quad + 2\left(6f_{4n+8}^2(w) f_{n+8}(w) + 12f_{4n+8}(w) f_{3n+8}(w) f_{2n+8}(w) + 2f_{3n+8}^3(w)\right. \\
&\qquad \left. + 27g_{6n+12}(w) g_{3n+12}(w) + 27g_{5n+12}(w) g_{4n+12}(w)\right) z^3 \\
&\quad + \cdots \cdots \\
&\quad + \left(4f_{-4n+8}^3(w) + 27g_{-6n+12}^2\right) z^{24}.
\end{aligned}
$$

(4.2.10)

The coefficients of z^4 and z^6 in Eq. (4.2.8): $f_4(w)$ and $g_6(w)$ correspond to the moduli of the elliptically fibred $K3$ on the Heterotic theory side [88]. Thus, w can be regarded as the inhomogeneous coordinates of the common base $\mathbb{P}^1$ on the Heterotic theory side. In the limit where the size of the common basis $\mathbb{P}^1$ is sufficiently large, at $w = const.$, the result is expected to be the same as in the eight-dimensional case. Also, w is expected to be the parameter describing to gauge symmetry enhancement.

In the stable degeneration limit, on the F-theory side, the gauge symmetries are localized at two points: $z_1 = 0, \infty$. $f_{8+n(4-i)}$ ($i < 4$) and $g_{12+n(6-j)}$ ($j < 6$) control the moduli of one E_8 with the instanton number $12 + n$ near $z = 0$; and then, when all $f_{8+n(4-i)}$ ($i > 4$) and $g_{12+n(6-j)}$ ($j > 6$) are set to zero, g_{12+n} corresponds to $12 + n$ small instantons. On the other hand, $f_{8+n(4-i)}$ ($i > 4$) and $g_{12+n(6-j)}$ ($j > 6$) control the moduli

of another E_8 with the instanton number $12 - n$ near $z \sim \infty$; and then, when all $f_{8+n(4-i)}$ $(i < 4)$ and $g_{12+n(6-j)}$ $(j < 6)$ are set to zero, g_{12-n} corresponds to $12 - n$ small instantons.

On the Heterotic theory side, an E_8 with the instanton number $12 + n$ has a $(30n + 112)$-dimensional hypermultiplet moduli space. On the other hand, on the F-theory side, we count the degree of freedom of $f_{8+n(4-i)}$ $(i < 4)$ and $g_{12+n(6-j)}$ $(j < 6)$ in Eq. (4.2.8); and then, we find $31n + 114$. Note that there are the $n + 2$ reparameterizations: $z \to az + P_n(w)$ $(a \in \mathbb{C})$. Thus, we obtain the dimension of the moduli space on the F-theory side:

$$(31n + 114) - (n + 2) = 30n + 112. \tag{4.2.11}$$

In this way, we can confirm that the dimensions of the hypermultiplet moduli spaces on the F-theory and the Heterotic theory sides coincide. The case that E_8 is broken: $E_8 \to H$ is discussed in the next sections.

4.3 Anomaly cancellation conditions in six-dimensional F-theory

The gravitational anomaly cancellation condition in six-dimensional supergravity (as summarized in [130–132]) is given by

$$\tilde{n}_H - n_V = 273 - 29n_T, \tag{4.3.1}$$

where $\tilde{n}_H$, n_V and n_T are the numbers of hypermultiplets, vector multiplets and tensor multiplets, respectively. Note that $\tilde{n}_H$ contains 20 hypermultiplets from the gravity multiplet, then,

$$\tilde{n}_H = n_H + 20 := n_{charged} + n_0 + 20, \tag{4.3.2}$$

where $n_{charged}$ and n_0 are the numbers of the charged and the neutral hypermultiplets. When we consider the elliptically fibred Calabi-Yau threefold over the Hirzebruch surface $\mathbb{F}_n$ on the F-theory side, the number of tensor multiplet, which comes from the gravity multiplet, is

$$n_T = h^{1,1}(\mathbb{F}_n) - 1 = 1. \tag{4.3.3}$$

Thus, we obtain $n_H - n_V = 224$. For each E_8 with instanton numbers $(12 + n, 12 - n)$, the anomaly cancellation conditions [90, 125] are

$$\begin{aligned} n_H - n_V &= -30n + 112 \ (E_8 \text{ with } 12 - n \text{ instantons}) \tag{4.3.4} \\ &= 30n + 112 \ (E_8 \text{ with } 12 + n \text{ instantons}). \tag{4.3.5} \end{aligned}$$

In this way, the numbers of the hypermultiplets of E_8's must be preserved, even in the case that E_8 is broken: $E_8 \to H$.

In this section, we focus on the Heterotic string theory side, especially, E_8 with the instanton number $12 + n$. We introduce the gauge invariant three-form for anomaly cancellation:

$$\omega_3 = dB_2 + \omega_{3L} - \omega_{3Y}, \tag{4.3.6}$$

where ω_{3L} and ω_{3Y} are Chern-Simons three-forms of the spin connection (L: Lorents) and the gauge field (Y: Yang-Mills), respectively. Since this three-form (4.3.6) must be well-defined globally, The integral of the exterior derivative of the three-form $d\omega_3$ over $K3$ needs to be zero:

$$\frac{1}{16\pi^2} \int_{K3} \left(Tr_{fund.} R^2 - \frac{1}{30} Tr_{adj.} F^2 \right) = 0, \tag{4.3.7}$$

where we denote traces as $Tr_{rep.}$ in the "$representation$", for example, $fund.$ and $adj.$ are the fundamental and adjoint representations, respectively. The term of a gravitational contribution $Tr_{fund.} R^2$ corresponds to half of the Pontryagin number (or the number of singularities) and gives 24 for an elliptically fibred $K3$. On the other hand, the term of a gauge field contribution $Tr_{adj.} F^2 / c_2(E_8)$ gives the instanton number. Here, $c_2(E_8) = 30$ is the dual Coxeter number of E_8. Therefore, there is the configuration of the gauge fields in the $K3$ with 24 instantons.

We consider gauge symmetry enhancement in the case of the following maximal subgroup G:

$$E_8 \subset G \times H, \tag{4.3.8}$$

where G and H are the unbroken and broken gauge symmetries, respectively[3]. Also, irreducible representations $\mathbf{R_i}$ of G and $\mathbf{S_i}$ of H come from

$$\mathbf{Adj}(E_8) = \mathbf{248} = \sum_i (\mathbf{R_i}, \mathbf{S_i}). \tag{4.3.9}$$

An enhanced gauge symmetry G corresponds to embedding all $12 + n$ instantons in H. In this case, we obtain the charged and neutral hypermultiplets and the number of the vector multiplets is

$$n_V = \dim G. \tag{4.3.10}$$

First, we consider the numbers of the neutral hypermultiplets n_0. The number of neutral hypermultiplets in G is given by the dimension of the moduli subspace of G:

$$n_0 = \dim \mathcal{M}(G) = c_2(H)(12 + n) - \dim H, \tag{4.3.11}$$

---

[3]H is simple and the commutant of G.

where $c_2(H)$ is the dual Coxeter number of H and $\dim H$ is equal to the dimension of the adjoint representation of H.

Next, we consider the numbers of the (massless) charged hypermultiplets $n_{charged}$. From an index theorem, we obtain

$$
\begin{aligned}
N_i &= \frac{1}{16\pi^2} \int_{K3} \left(Tr_{S_i}(F^H)^2 - \frac{1}{24} \dim(S_i) \, Tr_{fund.} R^2 \right) \\
&= \frac{1}{16\pi^2} \int_{K3} r_i \, Tr_{adj.}(F^H)^2 - \dim(S_i) \\
&= \text{index}(S_i)(12+n) - \dim(S_i) \\
&= 30 r_i (12+n) - \dim(S_i),
\end{aligned}
\tag{4.3.12}
$$

where N_i is the number of R_i and r_i is

$$
r_i = \frac{Tr_{S_i}(F^H)^2}{Tr_{adj.}(F^H)^2}
\tag{4.3.13}
$$

listed in Table 4.1 for all the simple groups. Thus, we obtain the numbers of the charged massless matter fields for G:

$$
n_{charged} = \sum_i N_i \times \dim \mathbf{R_i}.
\tag{4.3.14}
$$

The above calculations are summarized in Table 4.2. Note how the instantons are assigned, if H consists of the direct product of the two groups: the unbroken D_6, A_5 and C_3 gauge symmetries. In these cases, we consider the case where $12+n$ instantons are distributed among $(8+n-r, 4+r)$ in (A_1, A_1), (A_2, A_1) and (G_2, A_1). We can check that all cases in Table 4.2 satisfy the anomaly cancellation condition (4.3.5). "Relaxing" the restrictions on embedding instantons in H' ($\supset H$) corresponds to breaking G to G' ($\subset G$) by the Higgs mechanism, giving an expectation value to some charged hypermultiplets of G. In the next section, we will discuss this mechanism on the F-theory side.

4.4 Gauge Enhancement and matter in 6D F-theory

In this section, we only consider $i \leq 4$, $j \leq 6$ and near $z = 0$ so that we focus on an E_8 with the instanton number $12+n$ in heterotic dual, in line with the previous section. Toward constructing a dictionary connecting F-theory and Heterotic superstring theory for matter multiplet, we discuss the "Relaxing" mechanism in F-theory.

We can confirm that the number of neutral hypermultiplets of each G in Heterotic theory *completely* matches the dimension of the moduli spaces of compactification with

Table 4.1: Group theoretic coefficients r_i and dim $\mathbf{R_i}$. Note that $r_{adj.} = 1$. The second row of each group without E_8 is the adjoint representation, respectively. For the Dynkin label of $\mathbf{R_i}$, the same notation is used as for [133].

unbroken sym. G	Dynkin label of $\mathbf{R_i}$	dim $\mathbf{R_i}$	r_i
A_{N-1}	$(1,0,\ldots,0)$	N	$1/2N$
	$(1,0,\ldots,0,1)$	N^2-1	1
	$(0,1,0\ldots,0)$	$N(N-1)/2$	$(N-2)/2N$
	$(2,0,\ldots,0)$	$N(N+1)/2$	$(N+2)/2N$
	$(0,0,1,0,\ldots,0)$	$N(N-1)(N-2)/6$	$(N-2)(N-3)/4N$
	$(3,0,\ldots,0)$	$N(N+1)(N+2)/6$	$(N-2)(N-3)/4N$
B_N	$(1,0,\ldots,0)$	$2N+1$	$1/(2N-1)$
	$(0,1,0\ldots,0)$	$N(2N+1)$	1
	$(0,\ldots,0,1)$	2^N	$2^{N-3}/(2N-1)$
C_N	$(1,0,\ldots,0)$	$2N$	$1/2(N+1)$
	$(2,0,\ldots,0)$	$N(2N+1)$	1
	$(0,1,0\ldots,0)$	$(N-1)(2N+1)$	$(N-1)/(N+1)$
	$(0,0,1,0,\ldots,0)$	$2N(N-2)(2N+1)/3$	$(N-1)(2N-3)/2(N+1)$
D_N	$(1,0,\ldots,0)$	$2N$	$1/2(N-1)$
	$(0,1,0\ldots,0)$	$N(2N-1)$	1
	$(0,\ldots,0,1)$	2^{N-1}	$2^{N-4}/2(N-1)$
E_6	$(1,0,0,0,0,0)$	27	$1/4$
	$(0,0,0,0,0,1)$	78	1
E_7	$(0,0,0,0,0,1,0)$	56	$1/3$
	$(1,0,0,0,0,0,0)$	133	1
E_8	$(0,0,0,0,0,0,1,0)$	248	1
F_4	$(0,0,0,1)$	26	$1/3$
	$(1,0,0,0)$	52	1
G_2	$(0,1)$	7	$1/4$
	$(1,0)$	14	1

each "G"[4] singularity in F-theory. In this section, we assume that the matter fields locally exist at the loci where the polynomials $f_{8+n(4-i)}$ and $g_{12+n(6-j)}$ (4.2.8) are zero. We also assume that the matter representation is determined by which singularity the Kodaira singular fibre is enhanced on this locus. In addition, if the singularity enhancement $G \to G'$ at this codimension-two singularity is characterized by

$$\frac{G'}{G \times U(1)},\qquad(4.4.1)$$

we assume that the hypermultiplet appears as a matter multiplet at this codimension-

---

[4]In this and the next chapter, quotation marks are restored as appropriate to avoid confusion.

Table 4.2: Matter contents on the dual Heterotic side. Note that $\mathbf{X}\frac{1}{2}$ means a half-hypermultiplet.

unbroken sym.	Charged matter contents	n_0	n_V
E_7	$(n+8)\mathbf{56}\frac{1}{2}$	$2n+21$	133
E_6	$(n+6)\mathbf{27}$	$3n+28$	78
F_4	$(n+5)\mathbf{26}$	$4n+34$	52
B_5	$(n+4)\,\mathbf{32}\frac{1}{2}+(n+7)\mathbf{11}$	$3n+26$	55
D_5	$(n+4)\mathbf{16}+(n+6)\mathbf{10}$	$4n+33$	45
B_4	$(n+5)\mathbf{9}+(n+4)\mathbf{16}$	$5n+39$	36
D_4	$(n+4)\,(\mathbf{8}_c+\mathbf{8}_s+\mathbf{8}_v)$	$6n+44$	28
B_3	$(n+3)\mathbf{7}+(2n+8)\mathbf{8}$	$7n+48$	21
G_2	$(3n+10)\mathbf{7}$	$9n+56$	14
A_4	$(3n+16)\mathbf{5}+(2+n)\mathbf{10}$	$5n+36$	24
A_3	$(n+2)\mathbf{6}+(4n+16)\mathbf{4}$	$8n+51$	15
$C_2=B_2$	$(n+1)\mathbf{5}+(4n+16)\mathbf{4}$	$9n+53$	10
$A_1\times A_1$	$n(\mathbf{2},\mathbf{2})+(4n+16)[(\mathbf{1},\mathbf{2})+(\mathbf{2},\mathbf{1})]$	$10n+54$	6
A_2	$(6n+18)\mathbf{3}$	$12n+66$	8
A_1	$(6n+16)\mathbf{2}$	$18n+83$	3
D_6	$r\mathbf{32}\frac{1}{2}+(4+n-r)\,\mathbf{32'}\frac{1}{2}+(n+8)\mathbf{12}$	$2n+18$	66
A_5	$r\mathbf{20}\frac{1}{2}+(16+r+2n)\mathbf{6}+(2+n-r)\mathbf{15}$	$3n-r+21$	35
C_3	$(32+4n+3r)\,\mathbf{6}\frac{1}{2}+(n+1-r)\mathbf{14}+r\mathbf{14'}\frac{1}{2}$	$4n+23-2r$	21

two singularity. This is because the representation that appears in this gauge symmetry enhancement is a real or complex representation. Also, if the singularity enhancement is characterized by

$$\frac{G'}{G\times A_1(\cong C_1)},\qquad(4.4.2)$$

we assume that the *half*-hypermultiplet appears as a matter multiplet. This is because the representation that appears in this gauge symmetry enhancement is a pseudo-real representation. In the cases of ADE gauge symmetries, if the matter fields locally exist at *all* intersection loci of the singularities as intersecting D-branes [134], the anomaly cancellation condition (4.3.5) is satisfied. On the other hand, in the cases of non-simply-laced gauge symmetries, it is difficult to assume that the matter fields are localized at *all* intersections. This is discussed in the next chapter and leads to the purpose of this thesis.

We can consider the following two different chains of the Higgs mechanism: (1) The unbroken E_7 case corresponds to instantons in $H=A_1$. (2) The unbroken D_6 case

corresponds to instantons in $H = A_1 \times A_1$. In this case, we obtain the Higgs chain

$$
\begin{array}{ccccccccc}
C_3 & & \leftarrow & A_5 & & \leftarrow & D_6 & & \\
\downarrow & & & \downarrow & & & \downarrow & & \\
\downarrow & & & \downarrow & & & B_5 & \leftarrow & E_7 \\
\downarrow & & & \downarrow & & & \downarrow & & \downarrow \\
\downarrow & & & A_4 & & \leftarrow & D_5 & \leftarrow & E_6 \\
\downarrow & & & \downarrow & & & \downarrow & & \downarrow \\
\downarrow & & & \downarrow & & & B_4 & \leftarrow & F_4 \\
\downarrow & & & \downarrow & & & \downarrow & & \\
\downarrow & & & \downarrow & & & D_4 & & \\
\downarrow & & & \downarrow & & & \downarrow & & \\
C_2 & \cong & B_2 & \leftarrow & A_3 & \cong & D_3 & \leftarrow & B_3 \\
\downarrow & & & & \downarrow & & & & \downarrow \\
\downarrow & & & & A_2 & & & \leftarrow & G_2 \\
\downarrow & & & & \downarrow & & & & \\
A_1 & \times & A_1 & \rightarrow & A_1 & & & &
\end{array}
\tag{4.4.3}
$$

In this section, we write only non-zero polynomials. Also, we do not write f_8 and g_12 since these polynomials are not associated with the E_8 with the instanton number $12+n$. Each setup is shown in Table 3.2.

(1) E_7 chain

(1-1) We obtain an unbroken E_7 case ($H = A_1$) when there remain f_{8+n} and g_{12+n}. Therefore, the dimension of the moduli spaces of compactification n_0 with "E_7" singularity in F-theory is

$$
\begin{aligned}
n_0 &= (9+n) + (13+n) - 1 \\
&= 2n + 21.
\end{aligned}
\tag{4.4.4}
$$

We also obtain the "E_7" discriminant locus (4.2.10)::

$$
\Delta(z, w) = (4f_{8+n}^3(w) + O(z))z^9.
\tag{4.4.5}
$$

At $f_{8+n} = 0$ locus, "E_7" is enhanced to "E_8"; thus, we obtain the half-hypermultiplets $\mathbf{56}\frac{1}{2}$ since $E_7 \times A_1 \subset E_8$. Therefore, the E_7 case has $(8 + n)$ half-hypermultiplets $\mathbf{56}\frac{1}{2}$ as charged matter fields.

(1-2) We obtain an unbroken E_6 case ($H = A_2$) when there remain f_{8+n}, g_{12+n} and g_{12+2n}. In addition, the "split" condition, discussed in the next chapter, requires

$$
g_{12+2n} = q_{6+n}^2.
\tag{4.4.6}
$$

Therefore, the dimension of the moduli spaces of compactification with "E_6" singularity in F-theory is

$$
\begin{aligned}
n_0 &= (9+n) + (13+n) + (7+n) - 1 \\
&= 3n + 28.
\end{aligned}
\tag{4.4.7}
$$

We also obtain the "E_6" discriminant locus (4.2.10):

$$
\Delta(z, w) = (27 q_{6+n}^4(w) + O(z)) z^8.
\tag{4.4.8}
$$

At $q_{6+n} = 0$ locus, "E_6" is enhanced to "E_7"; thus, we obtain the hypermultiplets **27** since $E_6 \times U(1) \subset E_7$. Therefore, the E_6 case has $(6+n)$ hypermultiplets **27** as charged matter fields.

(1-3) We obtain an unbroken F_4 case ($H = G_2$) when there remain f_{8+n}, g_{12+n} and g_{12+2n}. In addition, the "non-split" condition, discussed in the next chapter, requires

$$
g_{12+2n} \neq q_{6+n}^2.
\tag{4.4.9}
$$

Therefore, the dimension of the moduli spaces of compactification with "F_4" singularity in F-theory is

$$
\begin{aligned}
n_0 &= (9+n) + (13+n) + (13+2n) - 1 \\
&= 4n + 34.
\end{aligned}
\tag{4.4.10}
$$

We also obtain the "F_4" discriminant locus (4.2.10):

$$
\Delta(z, w) = (27 g_{12+2n}^2(w) + O(z)) z^8.
\tag{4.4.11}
$$

If we consider the matter representation **27** of E_6 is decomposed to **26** of F_4 at $g_{12+2n} = 0$ locus, $(12 + 2n)$ hypermultiplets **26** arise in the F_4 case since **26** is a real representation. However, since the expected number of **26**s from the anomaly cancellation condition (4.3.5) is $n + 5$ [87, 88], it is difficult that the matter fields are localized at *all* intersections in the F_4 case. This puzzle is not solved even if we consider the adjoint representation **78** of E_6 is decomposed to **52** + **26** of F_4. Since this puzzle generally arises in the case of non-simply-laced gauge symmetries, we are not discussing the matter representation of it in this chapter from now on.

(1-4) We obtain an unbroken B_5 case when there remain f_{8+n}, f_{8+2n}, g_{12+n}, g_{12+2n} and g_{12+3n}. In addition, the "non-split" condition requires

$$
\begin{aligned}
f_{8+2n} &\sim s_{4+n}^2, \\
g_{12+2n} &\sim f_{8+n} s_{4+n}, \\
g_{12+3n} &\sim s_{4+n}^3.
\end{aligned}
\tag{4.4.12}
$$

Therefore, the dimension of the moduli spaces of compactification with "B_5" singularity in F-theory is

$$
\begin{aligned}
n_0 &= (9+n) + (13+n) + (5+n) - 1 \\
&= 3n + 26.
\end{aligned}
\tag{4.4.13}
$$

(1-5) We obtain an unbroken D_5 case when there remain f_{8+n}, f_{8+2n}, g_{12+n}, g_{12+2n} and g_{12+3n}. In addition, the "split" condition requires

$$
\begin{aligned}
f_{8+2n} &\sim h_{4+n}^2, \\
g_{12+2n} &= q_{6+n}^2 - f_{8+n}h_{4+n}, \\
g_{12+3n} &\sim h_{4+n}^3.
\end{aligned}
\tag{4.4.14}
$$

Therefore, the dimension of the moduli spaces of compactification with "D_5" singularity in F-theory is

$$
\begin{aligned}
n_0 &= (9+n) + (13+n) + (5+n) + (7+n) - 1 \\
&= 4n + 33.
\end{aligned}
\tag{4.4.15}
$$

We also obtain the "D_5" discriminant locus (4.2.10):

$$
\Delta(z,w) = (h_{4+n}^3(w)q_{6+n}^2(w) + h_{4+n}^2(w)P_{16+2n}z + O(z^2))z^7, \tag{4.4.16}
$$

where P_{16+2n} is a non-factorizable polynomial constructed fs and gs. At $h_{4+n} = 0$ locus, "D_5" is enhanced to "E_6"; thus, we obtain the hypermultiplets **16** since $D_5 \times U(1) \subset E_6$. At $q_{6+n} = 0$ locus, "D_5" is also enhanced to "D_6"; thus, we obtain the hypermultiplets **10** since $D_5 \times U(1) \subset D_6$. Therefore, the D_5 case has $(4+n)$ hypermultiplets **16** and $(6+n)$ hypermultiplets **10** as charged matter fields.

(1-6) We obtain an unbroken B_4 case when there remain f_{8+n}, f_{8+2n}, g_{12+n}, g_{12+2n} and g_{12+3n}. In addition, the "non-split" condition requires

$$
\begin{aligned}
f_{8+2n} &\sim h_{4+n}^2, \\
g_{12+2n} &\neq q_{6+n}^2 - f_{8+n}h_{4+n}, \\
g_{12+3n} &\sim h_{4+n}^3.
\end{aligned}
\tag{4.4.17}
$$

Therefore, the dimension of the moduli spaces of compactification with "B_4" singularity in F-theory is

$$
\begin{aligned}
n_0 &= (9+n) + (13+n) + (5+n) + (13+2n) - 1 \\
&= 5n + 39.
\end{aligned}
\tag{4.4.18}
$$

(1-7) We obtain an unbroken D_4 case when there remain f_{8+n}, f_{8+2n}, g_{12+n}, g_{12+2n} and g_{12+3n}. In addition, the "split" condition requires

$$
\begin{aligned}
f_{8+2n} &\sim h_{4+n}^2, \\
g_{12+3n} &\sim r_{4+n}^3.
\end{aligned}
\tag{4.4.19}
$$

Therefore, the dimension of the moduli spaces of compactification with "D_4" singularity in F-theory is

$$
\begin{aligned}
n_0 &= (9+n)+(13+n)+(5+n)+(13+2n)+(5+n)-1 \\
&= 6n+44.
\end{aligned}
\tag{4.4.20}
$$

We also obtain the "D_4" discriminant locus (4.2.10):

$$
\begin{aligned}
\Delta(z,w) = &\; ((h_{4+n}^2(w)+r_{4+n}^2(w))(h_{4+n}^2(w)+\omega r_{4+n}^2(w)) \\
&\times (h_{4+n}^2(w)+\omega^2 r_{4+n}^2(w))+O(z))z^6,
\end{aligned}
\tag{4.4.21}
$$

where $\omega^3 = 1$. At $h_{4+n} = r_{4+n}$ locus, "D_4" is enhanced to "D_5"; thus, we obtain the hypermultiplets $\mathbf{8}$ since $D_4 \times U(1) \subset D_5$. In addition, since there is a Z_3 symmetry $q \to \omega q$ exchanging the various factors in the discriminant, we obtain the hypermultiplets $(\mathbf{8_v}+\mathbf{8_s}+\mathbf{8_c})$. Therefore, the D_4 case has $(4+n)$ hypermultiplets $(\mathbf{8_v}+\mathbf{8_s}+\mathbf{8_c})$ as charged matter fields.

(1-8) We obtain an unbroken B_3 case when there remain f_{8+n}, f_{8+2n}, g_{12+n}, g_{12+2n} and g_{12+3n}. In addition, the "semi-split" condition requires

$$
g_{12+3n} = f_{8+2n}r_{4+n}.
\tag{4.4.22}
$$

Therefore, the dimension of the moduli spaces of compactification with "B_3" singularity in F-theory is

$$
\begin{aligned}
n_0 &= (9+n)+(13+n)+(9+2n)+(13+2n)+(5+n)-1 \\
&= 7n+48.
\end{aligned}
\tag{4.4.23}
$$

(1-9) We obtain an unbroken G_2 case when there remain f_{8+n}, f_{8+2n}, g_{12+n}, g_{12+2n} and g_{12+3n}. In addition, the "non-split" condition requires

$$
g_{12+3n} \neq f_{8+2n}r_{4+n}.
\tag{4.4.24}
$$

Therefore, the dimension of the moduli spaces of compactification with "G_2" singularity in F-theory is

$$
\begin{aligned}
n_0 &= (9+n)+(13+n)+(9+2n)+(13+2n)+(13+3n)-1 \\
&= 9n+56.
\end{aligned}
\tag{4.4.25}
$$

(1-10) We obtain an unbroken A_4 case when there remain f_{8+n}, f_{8+2n}, f_{8+3n}, f_{8+4n}, g_{12+n}, g_{12+2n}, g_{12+3n}, g_{12+4n}, g_{12+5n} and g_{12+6n}. In addition, from the "split" condition, this singularity is given by the five polynomials as follows:

$$
f_{8+n}, \; g_{12+n}, \; H_{4+n}, \; q_{6+n}, \; k_{2+n}.
\tag{4.4.26}
$$

Therefore, the dimension of the moduli spaces of compactification with "A_4" singularity in F-theory is

$$
\begin{aligned}
n_0 &= (9+n)+(13+n)+(5+n)+(7+n)+(3+n)-1 \\
&= 5n+36.
\end{aligned} \tag{4.4.27}
$$

We also obtain the "A_4" discriminant locus (4.2.10):

$$
\Delta(z,w) = (k_{2+n}^4(w)P_{16+3n}^2(w)+O(z))z^5, \tag{4.4.28}
$$

where P_{16+3n} is a non-factorizable polynomial constructed fs and gs. At $k_{2+n}=0$ locus, "A_4" is enhanced to "D_5"; thus, we obtain the hypermultiplets **10** since $A_4 \times U(1) \subset D_5$. At $P_{16+3n}=0$ locus, "A_4" is also enhanced to "A_5"; thus, we obtain the hypermultiplets **5** since $A_4 \times U(1) \subset A_5$. Therefore, the A_3 case has $(2+n)$ hypermultiplets **10** and $(16+3n)$ hypermultiplets **5** as charged matter fields.

(1-11) We obtain an unbroken $A_3 \cong D_3$ case when there remain f_{8+n}, f_{8+2n}, f_{8+3n}, f_{8+4n}, g_{12+n}, g_{12+2n}, g_{12+3n}, g_{12+4n}, g_{12+5n} and g_{12+6n}. In addition, the "split" condition requires

$$
\begin{aligned}
&f_{8+3n} \sim k_{2+n}^2 H_{4+n}, \quad f_{8+4n} \sim k_{2+n}^4, \\
&g_{12+3n} = \frac{1}{216}H_{4+n}^3 + \frac{1}{6}f_{8+2n}H_{4+n} - f_{8+n}k_{2+n}^2, \\
&g_{12+4n} = -f_{8+2n}k_{2+n}^2 + \frac{1}{12}k_{2+n}^2 H_{4+n}^2, \\
&g_{12+5n} = -k_{2+n}^4 H_{4+n}, \quad g_{12+6n} = k_{2+n}^6.
\end{aligned} \tag{4.4.29}
$$

Therefore, the dimension of the moduli spaces of compactification with "A_3" singularity in F-theory is

$$
\begin{aligned}
n_0 &= (9+n)+(13+n)+(9+2n)+(13+2n)+(3+n)+(5+n)-1 \\
&= 8n+51.
\end{aligned} \tag{4.4.30}
$$

We also obtain the "A_3" discriminant locus (4.2.10):

$$
\Delta(z,w) = (k_{2+n}^2(w)P_{16+4n}^2(w)+O(z))z^4, \tag{4.4.31}
$$

where P_{16+4n} is a non-factorizable polynomial constructed fs and gs. At $k_{2+n}=0$ locus, "A_3" is enhanced to "D_4"; thus, we obtain the hypermultiplets **6** since $A_3 \times U(1) \subset D_4$. At $P_{16+4n}=0$ locus, "A_3" is also enhanced to "A_4"; thus, we obtain the hypermultiplets **4** since $A_3 \times U(1) \subset A_4$. Therefore, the A_3 case has $(2+n)$ hypermultiplets **6** and $(16+4n)$ hypermultiplets **4** as charged matter fields.

(1-12) We obtain an unbroken $C_2 \cong B_2$ case there remain when f_{8+n}, f_{8+2n}, f_{8+3n}, f_{8+4n}, g_{12+n}, g_{12+2n}, g_{12+3n}, g_{12+4n}, g_{12+5n} and g_{12+6n}. In addition, the "non-split" condition requires

$$
K_{4+2n} \neq k_{2+n}^2 \tag{4.4.32}
$$

in "A_3" condition (4.4.29). Therefore, the dimension of the moduli spaces of compactification with "A_3" singularity in F-theory is

$$
\begin{aligned}
n_0 &= (9+n) + (13+n) + (9+2n) + (13+2n) + (5+2n) + (5+n) - 1 \\
&= 9n + 53.
\end{aligned} \tag{4.4.33}
$$

(1-13) We obtain an unbroken $A_1 \times A_1 \cong D_2$ case when the discriminant locus has two irreducible divisors $D_u = D_v + nD_{u'}$ [87] with each A_1 singularity. Therefore, the dimension of the moduli spaces of compactification with "$A_1 \times A_1$" singularity in F-theory is $n_0 = (30n+112) - \{2(29+12n) - 4n\} = 10n + 54$. Since these two irreducible divisors intersect at $D_u^2 = n^5$ points, the $A_1 \times A_1$ case has n hypermultiplets $(\mathbf{2}, \mathbf{2})$ as charged matter fields.

(1-14) We obtain an unbroken A_2 case when there remain f_{8+n}, f_{8+2n}, f_{8+3n}, f_{8+4n}, g_{12+n}, g_{12+2n}, g_{12+3n}, g_{12+4n}, g_{12+5n} and g_{12+6n}. In addition, the "split" condition requires

$$
\begin{aligned}
&f_{8+3n} = k_{2+n}Q_{6+2n}, \quad f_{8+4n} \sim k_{2+n}^4, \\
&g_{12+4n} = -f_{8+2n}k_{2+n}^2 + \frac{1}{12}Q_{6+2n}^2, \\
&g_{12+5n} = -k_{2+n}^3 Q_{6+2n}, \quad g_{12+6n} \sim k_{2+n}^6.
\end{aligned} \tag{4.4.34}
$$

Therefore, the dimension of the moduli spaces of compactification with "A_2" singularity in F-theory is

$$
\begin{aligned}
n_0 &= (9+n) + (13+n) + (9+2n) + (13+2n) \\
&\quad +(3+n) + (13+3n) + (7+2n) - 1 \\
&= 12n + 66.
\end{aligned} \tag{4.4.35}
$$

We also obtain the "A_2" discriminant locus (4.2.10):

$$
\Delta(z, w) = (k_{2+n}^4(w)P_{16+5n}^2(w) + O(z))z^3, \tag{4.4.36}
$$

where P_{16+5n} is a non-factorizable polynomial constructed fs and gs. At $k_{2+n} = 0$ or $P_{16+5n} = 0$ locus, "A_2" is enhanced to "A_3"; thus, we obtain the hypermultiplets $\mathbf{3}$ since $A_2 \times U(1) \subset A_3$. Therefore, the A_2 case has $(18 + 6n)$ hypermultiplets $\mathbf{3}$ as charged matter fields.

(1-15) We obtain an unbroken A_1 ($\cong C_1$) case when there remain f_{8+n}, f_{8+2n}, f_{8+3n}, f_{8+4n}, g_{12+n}, g_{12+2n}, g_{12+3n}, g_{12+4n}, g_{12+5n} and g_{12+6n}. In addition, the ("non-split") condition requires

$$
\begin{aligned}
&f_{8+4n} \sim K_{4+2n}^2, \quad g_{12+6n} \sim K_{4+2n}^3 \\
&g_{12+5n} = -f_{8+3n}K_{4+2n}.
\end{aligned} \tag{4.4.37}
$$

---

[5]There are some relations in the case that the base space of F-theory compactification is the Hirzebruch surface $\mathbb{F}_n$: $D_{u'} \cdot D_{u'} = 0$, $D_{u'} \cdot D_v = 1$ and $D_v \cdot D_v = -n$.

Therefore, the dimension of the moduli spaces of compactification with "A_1" singularity in F-theory is

$$
\begin{aligned}
n_0 &= (9+n) + (13+n) + (9+2n) + (13+2n) \\
&\quad + (9+3n) + (13+3n) + (5+2n) + (13+4n) - 1 \\
&= 18n + 83.
\end{aligned}
\tag{4.4.38}
$$

We also obtain the "A_1" discriminant locus (4.2.10):

$$
\Delta(z,w) = (K_{4+2n}^2(w)P_{16+6n}^2(w) + O(z))z^2,
\tag{4.4.39}
$$

where P_{16+6n} is a non-factorizable polynomial constructed fs and gs. At $P_{16+6n} = 0$ locus, "A_1" is enhanced to "A_2"; thus, we obtain the hypermultiplets **2** since $A_1 \times U(1) \subset A_2$. $k_{2+n} = 0$ gives $(n+2)$ singlets (antisymmetric tensors) for A_1. Therefore, the A_1 case has $(16 + 6n)$ hypermultiplets **2** as charged matter fields.

(2) D_6 Chain

Following the previous section, we assume that $12 + n$ instantons are distributed among $(8 + n - r, 4 + r)$ in (A_1, A_1) in the D_6 chain. The range of r is determined by the fact that the subscripts of the polynomials appearing in the equation are non-negative.

(2-1) We obtain an unbroken D_6 case when there remain f_{8+n}, f_{8+2n}, g_{12+n}, g_{12+2n} and g_{12+3n}. In addition, the "split" condition from Tate form, discussed in the next chapter, requires

$$
\begin{aligned}
f_{8+n} &\sim t_r q_{8+n-r} + p_{4+n-r}u_{4+r}, \\
f_{8+2n} &\sim t_r^2 p_{4+n-r}^2, \quad g_{12+n} \sim q_{8+n-r}u_{4+r}, \\
g_{12+2n} &\sim -(t_r q_{8+n-r} + p_{4+n-r}u_{4+r})t_r p_{4+n-r}, \\
g_{12+3n} &\sim t_r^3 p_{4+n-r}^3.
\end{aligned}
\tag{4.4.40}
$$

where the condition for $(8 + n - r, 4 + r)$ instanton assignment is characterized by

$$
s_{4+n} \sim t_r p_{4+n-r}.
\tag{4.4.41}
$$

Therefore, the dimension of the moduli spaces of compactification with "D_6" singularity in F-theory is

$$
\begin{aligned}
n_0 &= (1+r) + (9+n-r) + (5+n-r) + (5+r) - 2 \\
&= 2n + 20.
\end{aligned}
\tag{4.4.42}
$$

We also obtain the "D_6" discriminant locus (4.2.10):

$$
\Delta(z,w) = (p_{4+n-r}^2(w)t_r^2(w)P_{8+n}z + O(z^2))z^8,
\tag{4.4.43}
$$

where P_{8+n} is a non-factorizable polynomial constructed fs and gs. At $t_r = 0$ or $p_{4+n-r} = 0$ locus, "D_6" is enhanced to "E_7"; thus, we obtain the half-hypermultiplets $\mathbf{32}\frac{1}{2}$ or $\mathbf{32'}\frac{1}{2}$, respectively, since $D_6 \times A_1 \subset E_7$. At $P_{8+n} = 0$ locus, "D_6" is also enhanced to "D_7"; thus, we obtain the hypermultiplets $\mathbf{12}$ since $D_6 \times U(1) \subset D_7$. Therefore, the D_5 case has r half-hypermultiplets $\mathbf{32}\frac{1}{2}$, $(4 + n - r)$ half-hypermultiplets $\mathbf{32'}\frac{1}{2}$ and $(8 + n)$ hypermultiplets $\mathbf{12}$ as charged matter fields.

(2-2) An unbroken A_5 case is discussed in more detail in the next chapter and is omitted here.

(2-3) An unbroken C_3 case is discussed in more detail in the next chapter and is omitted here.

Chapter 5

Half-hypermultiplets & Resolution in F-theory

In this chapter, we consider an F-theory on an elliptically fibred Calabi-Yau three-fold over $\mathbb{F}_n$, especially, in the case that conifold singularities play an essential role. In particular, we focus on the I_6 model, which has half-hypermultiplets and a distinction between the split and non-split fibre types [90, 91]. We first introduce the split and non-split fibre types. It is known that the expected gauge symmetry of a split and non-split fibre type would be a simply-laced and non-simply-laced one, respectively. Next, we demonstrate an explicit blow-up process [93, 98, 120] and investigated the matter contents [90] and the intersection diagrams of the exceptional curves [93, 98] in the split I_6 model. By the above, we provide a brief review of matter generation in F-theory in the case that conifold singularities are involved. We also investigate the non-split I_6 model, which has half-hypermultiplets, by the Heterotic index and the resolution. We then show the differences between the split models and the non-split models explicitly. Finally, we specifically discuss the puzzles associated with non-local matter generation in the split model near the codimension-two singularities where the codimension-one singularity is enhanced to D_6. This chapter is based on our paper [99].

5.1   "Split" and "non-split" singular fibre and resolution in six-dimensional F-theory

5.1.1   "Split" and "non-split" singular fibre in six-dimensional F-theory

In this chapter, we focus on six- or lower-dimensional F-theories, especially, an F-theory on an elliptically fibred Calabi-Yau threefold over a Hirzebruch surface $\mathbb{F}_n$. In other words, we consider the case that an elliptic Calabi-Yau threefold allows a fibration

of an elliptic surface over $\mathbb{P}^1$. Also, in this subsection, we introduce two types of singular fibre: "split" and "non-split" [90].

As shown in Section 3.2, Kodaira's classification of singular fibres of an elliptic surface is based on the intersection diagrams of exceptional curves that arise after the resolutions. In the case of $K3$ fibration over $(n-2)$-fold, the singularities of these fibred elliptic surfaces are aligned along the $(n-2)$-fold, forming a codimension-two locus in the total elliptic Calabi-Yau n-fold. In other words, a codimension-one locus in the base $(n-1)$-fold of the elliptic fibration, which is the projection of this codimension-two locus into the base, is the discriminant locus (3.1.19). This codimension-two locus is called the codimension-one singularity. We can blow up a codimension-one singularity to yield a collection of exceptional curves aligned along the codimension-one locus in the base. This is also called the resolution of codimension-one singularity. In the dual Type IIB superstring theory, a non-abelian gauge symmetry is realized on this codimension-one locus in the base, where 7-branes stack at a point.

In these six- or lower-dimensional F-theories, if the singular fibre type involves a condition that requires an exceptional curve to split into two irreducible components over a generic point on the codimension-one locus in the base, these two split curves generally meet on top of each other at some points along the codimension-one locus. In the next chapter, we will investigate the neighborhoods of these points by resolution. If the two split exceptional curves of each elliptic surface belong to different irreducible exceptional surfaces the total elliptic Calabi-Yau n-fold, the fibre type is called "split". In other words, this condition is that the exceptional curves can split globally. In the "split" case, their fibre types correspond to the expected ADE gauge symmetries G implied by Kodaira's classification like the eight-dimensional F-theory case [90]. On the other hand, if such exceptional curves constitute part of the same smooth irreducible locus in the total elliptic Calabi-Yau n-fold, the fibre type is called "non-split" [90]. In other words, this condition is that the exceptional curves can not split globally. In the "non-split" case, the two apparently distinct exceptional fibres are swapped with each other at these points when one goes along the $(n-2)$-fold and hence are considered to be identical. This phenomenon is known as a monodromy. The expected ADE gauge symmetry is then subject to a projection by a diagram automorphism, reduced to a corresponding non-simply-laced gauge symmetry G. The I_n ($n = 3, 4, \cdots$), I_n^* ($n = 0, 1, \cdots$), IV and IV^* singular fibre types can involve such identification of exceptional curves.

We summarize this discussion in Table 5.1, using the Tate form (3.1.4):

$$P = -(y^2 + a_1 xy + a_3 y) + x^3 + a_2 x^2 + a_4 x + a_6 = 0, \qquad (5.1.1)$$

where a_i is a holomorphic function of $z \in \mathbb{P}^1_{fibre}$ and $w \in \mathbb{P}^1_{base}$. Tate form is related to the

Weierstrass form, which is used in the previous chapter and in this chapter, as follows:

$$
\begin{aligned}
b_2 &= a_1^2 + 4a_2, \\
b_4 &= a_1 a_3 + 2a_4, \\
b_6 &= a_3^2 + 4a_6, \\
b_8 &= \frac{1}{4}(b_2 b_6 - b_4^2)
\end{aligned}
$$

(5.1.2)

and

$$
\begin{aligned}
f &= -\frac{1}{48}(b_2^2 - 24b_4), \\
g &= \frac{1}{864}\left(b_2^3 - 36b_2 b_4 + 216 b_6\right).
\end{aligned}
$$

(5.1.3)

More details on the Tate form are given in the next chapter.

Finally, we introduce the codimension-two singularity. The codimension-two singularity is associated with the codimension-two locus in the base $(n-1)$-fold of the elliptic fibration, on which codimension-one singularities intersect each other and their singularity is enhanced. In the dual Type IIB superstring theory, this codimension-two locus corresponds to the intersection of stacks of 7-branes, where the expected gauge symmetry G is enhanced to higher. Therefore, the codimension-two singularity is involved in matter generation. In particular, in the "split" case, after the resolution of a codimension-two singularity, we can obtain an intersection diagram of exceptional curves that is different from one on the codimension-one singularity; and then, we can explain the enhancement of the gauge symmetry by this diagram. In addition, at the points where the two exceptional curves meet on top of each other, there typically (but not always) arise conifold singularities [93,94]; and then, new two-cycles emerge by the small resolution. In the dual M-theory, a wrapped M2-brane around the new two-cycle accounts for the generation of the localized matter multiplet [96].

5.1.2 Resolution of codimension-one singularity in six-dimensional F-theory

In this subsection, we extend the blow-up method of codimension-one singularities from the eight-dimensional case, which was done in Section 3.2, to the six-dimensional case. We use inhomogeneous coordinates z and w as $\mathbb{P}^1_{fibre}$ and $\mathbb{P}^1_{base}$, respectively.

For simplicity, we start the local equation near a codimension-two singularity (Table 6.1):

$$
\Phi = -y^2 + x^3 + \frac{b_2}{4}x^2 + \frac{b_4}{2}x + \frac{b_6}{4} = 0. \tag{5.1.4}
$$

Here, we focus on a codimension-one singularity at $(x, y, z) = (0, 0, 0)$. We also assume that there is a codimension-two singularity at $(x, y, z, w) = (0, 0, 0, 0)$. Since singularity

Table 5.1: Tate forms in six or lower dimensions [90, 91]. Here, $k \in \mathbb{Z}$. Also, s, ns and ss mean split, non-split and semi-split fibre types, respectively [90]. The $\mathrm{ord}(a_i)$ and $\mathrm{ord}(\Delta)$ denote the order of z of (a_i) and (Δ), where z is a inhomogeneous coordinate of $\mathbb{P}^1_{fibre}$.

Fibre type	$\mathrm{ord}(a_1)$	$\mathrm{ord}(a_2)$	$\mathrm{ord}(a_3)$	$\mathrm{ord}(a_4)$	$\mathrm{ord}(a_6)$	$\mathrm{ord}(\Delta)$	Expected G
$smooth\ (I_0)$	0	0	0	0	0	0	$-$
I_1	0	0	1	1	1	1	$-$
I_2	0	0	1	1	2	2	A_1
I^s_{2k+1}	0	1	k	$k+1$	$2k+1$	$2k+1$	A_{2k}
I^{ns}_{2k+1}	0	0	$k+1$	$k+1$	$2k+1$	$2k+1$	C_k
I^s_{2k+2}	0	1	$k+1$	$k+1$	$2k+2$	$2k+2$	A_{2k+1}
I^{ns}_{2k+2}	0	0	$k+1$	$k+1$	$2k+2$	$2k+2$	C_{k+1}
II	1	1	1	1	1	2	$-$
III	1	1	1	1	2	3	A_1
IV^s	1	1	1	2	3	4	A_2
IV^{ns}	1	1	1	2	2	4	C_1
I^{*s}_0	1	1	2	2	4	6	D_4
I^{*ss}_0	1	1	2	2	4	6	B_3
I^{*ns}_0	1	1	2	2	3	6	G_2
$I^{*\ s}_{2k-1}$	1	1	$k+1$	$k+2$	$2k+3$	$2k+5$	D_{2k+3}
$I^{*\ ns}_{2k-1}$	1	1	$k+1$	$k+2$	$2k+2$	$2k+5$	B_{2k+2}
$I^{*\ s}_{2k}$	1	1	$k+2$	$k+2$	$2k+3$	$2k+6$	D_{2k+4}
$I^{*\ ns}_{2k}$	1	1	$k+2$	$k+2$	$2k+3$	$2k+6$	B_{2k+3}
I^*_n	0	0	0	0	0	0	D_{n+4}
I^*_n	0	0	0	0	0	0	D_{n+4}
II^*	1	2	3	4	5	10	E_8
III^*	1	2	3	3	5	9	E_7
IV^{*s}	1	2	2	3	5	8	E_6
IV^{*ns}	1	2	2	3	5	8	E_6
$non\text{-}minimal$	1	2	3	4	6	12	$-$

is enhanced at the codimension-two singularity, conifold singularities

$$\tilde{\Phi} \quad \sim \quad x^2 + y^2 + z^2 + w^2 = 0 \tag{5.1.5}$$

may appear. In this case, the blow-up of the codimension-one singularity is completed first, ignoring the existence of these conifold singularities.

Next, we consider the crepant resolution of a codimension-one singularity [93, 98, 120] of the local equation (5.1.4) along $(x, y, z, w) = (0, 0, 0, w)$ for arbitrary w. We then obtain $\mathcal{C}_i$'s at each point on $w \neq 0$ and δ_j's at $w = 0$. Here, the exceptional curve $\mathcal{C}_i$ is the intersection of $\mathbb{P}^2$ in Eq. (5.1.6) and the hypersurface after the blow-up of the

codimension-one singularity of fibred elliptic surfaces at each point on $w \neq 0$ (for example, $\Phi_z(x_1, y_1, z, w)$ in Eq. (5.1.7)). Also, δ_j's are the exceptional curves at $w = 0$ or the $\mathbb{P}^1$'s by small resolution of conifold singularities. Thus, $\mathcal{C}_i$'s and δ_j's are $\mathbb{P}^1$'s.

For the crepant resolution, we replace the point $(x, y, z) = (0, 0, 0)$ over a generic point of w with a $\mathbb{P}^2$ at each point of w, by replacing $\mathbb{C}^3$ with

$$\hat{\mathbb{C}}^3 = \{((x, y, z), (\xi : \eta : \zeta)) \in \mathbb{C}^4 \times \mathbb{P}^2 | (x : y : z) = (\xi : \eta : \zeta)\}. \tag{5.1.6}$$

We are blowing up the codimension-one singularity in inhomogeneous coordinates defined by the three different affine patches of $\mathbb{P}^2$, for example, $(x : y : z) = (\xi : \eta : \zeta) = (x_1 : y_1 : 1)$ ($\mathbf{1}_z$, $z \neq 0$). Thus, to replace $\mathbb{C}^3$ with $\hat{\mathbb{C}}^3$, we simply replace (x, y, z, w) with $(x_1 z, y_1 z, z, w)$ in the equation (5.1.4) in Chart $\mathbf{1}_z$. To not change the canonical class, the equation after the blow-ups is defined as follows:

$$z^{-2}\Phi(x_1 z, y_1 z, z, w) =: \Phi_z(x_1, y_1, z, w) = 0. \tag{5.1.7}$$

Similarly, we need to check the other patches: $\mathbf{1}_x$ ($x \neq 0$) and $\mathbf{1}_y$ ($y \neq 0$), by the same procedure.

If there remains the codimension-one singularity, which is the singularity along an arbitrary w, we repeat this process until there are no more codimension-one singularity. This is the resolution of the codimension-one singularity. We then obtain the exceptional curves $\mathcal{C}_i$'s and their intersection diagram at each point on $w \neq 0$. Finally, if there remain some conifold singularities after the resolution of the codimension-one singularity, we blow up the conifold singularities by the small resolution (Appendix A). We then obtain new two-cycles $\mathbb{P}^1$'s by small resolution of conifold singularities and intersection diagram of δ_j's which consists of the exceptional curves $\mathbb{P}^1$'s by the resolution of the codimension-one singularity at $w = 0$ and the new two-cycles $\mathbb{P}^1$'s by the small resolution. In addition, we can obtain the relations among $\mathcal{C}_i$'s and δ_j's, by examining whether each δ_j is "visible" from the standpoint of each $\mathcal{C}_i$ when each $\mathcal{C}_i$ is "lifted up" to the same subsequent blow-up step as each δ_j.

5.2 Magic square and half-hypermultiplets in F-theory

5.2.1 The Freudenthal-Tits magic square

A Freudenthal-Tits magic square is a four-by-four table whose entries are Lie algebras. They are determined by specifying a pair of composition algebras $(\mathbb{A}, \mathbb{B})$. When these composition algebras are the ones over the real number field $\mathbb{R}$, they are either one of the four division algebras $\mathbb{R}$, $\mathbb{C}$, $\mathbb{H}$ and $\mathbb{O}$, or they are one of the "split" algebras of

$\mathbb{C}$, $\mathbb{H}$ and $\mathbb{O}$, which are non-compact analogues of the corresponding division algebras. In this case, each entry of the magic square is some real form of a complex Lie algebra.

If $(\mathbb{A}, \mathbb{B})$ are a pair of either of the four division algebras $\mathbb{R}$, $\mathbb{C}$, $\mathbb{H}$ and $\mathbb{O}$, the magic square consists of compact Lie algebras with definite signatures (Table 5.2), while if $(\mathbb{A}, \mathbb{B})$ are chosen from the set of $\mathbb{R}$ and the three split algebras, the entries are all split real forms of the same complexifications as those of the compact Lie algebras in the corresponding cells. They typically arise (besides a few exceptions) as (Lie algebras of) duality groups or hidden symmetries of dimensionally reduced maximally symmetric supergravities, bosonic string or the NS-NS sector effective theory and pure gravities. Finally, if $\mathbb{A}$ is a division algebra and $\mathbb{B}$ is a split algebra, the magic square comprises a special set of real forms of exceptional Lie algebras arising as scalar manifolds of dimensional reductions of $D = 5$ "magical" supergravities [135–138].

The $(\mathbb{A}, \mathbb{B})$ entry of the magic square always has the following structure:

$$\mathfrak{der}\,\mathbb{A} \oplus \mathfrak{der}\,\mathfrak{J}^{\mathbb{B}} \oplus (\mathbb{A}_0 \otimes \mathfrak{J}_0^{\mathbb{B}}), \tag{5.2.1}$$

where $\mathfrak{der}\,\mathbb{A}$ and $\mathfrak{der}\,\mathfrak{J}^{\mathbb{B}}$ are the Lie algebras of the automorphism groups of $\mathbb{A}$ and $\mathfrak{J}^{\mathbb{B}}$, respectively, where $\mathfrak{J}^{\mathbb{B}}$ is the Jordan algebra associated with the composition algebra $\mathbb{B}$. $\mathbb{A}_0$ and $\mathfrak{J}_0^{\mathbb{B}}$ denote their traceless parts.

For example, for the compact case $\mathbb{A}, \mathbb{B} = \mathbb{R}, \mathbb{C}, \mathbb{H}, \mathbb{O}$ (Table 5.2)[1],

$$\mathfrak{der}\,\mathbb{A} = 0, 0, \mathfrak{su}(2), \mathfrak{g}_2, \tag{5.2.2}$$
$$\mathfrak{der}\,\mathfrak{J}^{\mathbb{B}} = \mathfrak{so}(3), \mathfrak{su}(3), \mathfrak{sp}(3), \mathfrak{f}_4, \tag{5.2.3}$$
$$\mathbb{A}_0 = 0, 0, \mathbf{3}, \mathbf{7} \quad \text{of } \mathfrak{der}\,\mathbb{A}, \tag{5.2.4}$$
$$\mathfrak{J}_0^{\mathbb{B}} = \mathbf{5}, \mathbf{8}, \mathbf{14}, \mathbf{26} \quad \text{of } \mathfrak{der}\,\mathfrak{J}^{\mathbb{B}}. \tag{5.2.5}$$

Then, for instance, $\mathfrak{e}_7$ allows a decomposition

$$E_7 \supset SU(2) \times F_4$$
$$\mathbf{133} = (\mathbf{3}, \mathbf{1}) \oplus (\mathbf{1}, \mathbf{52}) \oplus (\mathbf{3}, \mathbf{26}) \tag{5.2.6}$$

for $\mathbb{A} = \mathbb{H}, \mathbb{B} = \mathbb{O}$, and also

$$E_7 \supset G_2 \times Sp(3)$$
$$\mathbf{133} = (\mathbf{14}, \mathbf{1}) \oplus (\mathbf{1}, \mathbf{21}) \oplus (\mathbf{7}, \mathbf{14}) \tag{5.2.7}$$

for $\mathbb{A} = \mathbb{O}, \mathbb{B} = \mathbb{H}$. The other Lie algebras allow similar decompositions.

Remark. In this thesis the word "split" is used in three different meanings:

1. This word is used for a "split" composition algebra, which is a noncompact version of $\mathbb{C}$, $\mathbb{H}$ or $\mathbb{O}$ with an indefinite bilinear form.

---

[1]In this thesis, we use the notations $\mathfrak{sp}(n)$ and $Sp(n)$ to denote the Lie algebra and the Lie group of the C_n type Dynkin diagram.

Table 5.2: The Freudenthal-Tits magic square for $\mathbb{A}, \mathbb{B}$ being either of the four division algebras $\mathbb{R}, \mathbb{C}, \mathbb{H}, \mathbb{O}$. They are all compact Lie algebras with definite signatures. If the division algebras are replaced by split composition algebras, the entries become different real forms with the same complexifications.

$\mathbb{B}\backslash\mathbb{A}$	$\mathbb{R}$	$\mathbb{C}$	$\mathbb{H}$	$\mathbb{O}$
$\mathbb{R}$	$\mathfrak{so}(3)$	$\mathfrak{su}(3)$	$\mathfrak{sp}(3)$	$\mathfrak{f}_4$
$\mathbb{C}$	$\mathfrak{su}(3)$	$\mathfrak{su}(3) \oplus \mathfrak{su}(3)$	$\mathfrak{su}(6)$	$\mathfrak{e}_6$
$\mathbb{H}$	$\mathfrak{sp}(3)$	$\mathfrak{su}(6)$	$\mathfrak{so}(12)$	$\mathfrak{e}_7$
$\mathbb{O}$	$\mathfrak{f}_4$	$\mathfrak{e}_6$	$\mathfrak{e}_7$	$\mathfrak{e}_8$

2. "Split" is also used for a "split" real form of a complex Lie algebra, which has, besides the Cartan subalgebra, an equal number of positive and negative generators with respect to the invariant bilinear form.

3. Finally, the word "split" appears in the classification of singularities or the fibre types of exceptional curves [90]. Singularities of the "split" type are the ones in which relevant exceptional curves factor globally so that they yield simply-laced gauge symmetries.

The first two are closely related in that split real forms of item 2 arise in the magic square when the composition algebras are taken to be split ones in the sense of item 1. The third one is, however, a different notion from the two.

5.2.2 Summary of half-hypermultiplets in F-theory

In [90], a detailed analysis was carried out on the matter spectra of six-dimensional F-theory compactifications on an elliptically fibred Calabi-Yau threefold over a Hirzebruch surface [87, 88] for various patterns of unbroken gauge groups. In particular, it was revealed that there were (essentially) four cases of unbroken gauge groups[2] in which *half-hypermultiplets* (rather than normal hypermultiplets) appeared as massless matter. They are listed in Table 5.3 and 5.4. These spectra can be confirmed either by the heterotic index calculation [125][3] or by the generalized Green-Schwarz mechanism using the divisor data of the Hirzebruch surface [139, 140][4]. They satisfy the anomaly-free constraint for

---

[2]There is, in fact, one more example in [90] where half-hypermultiplets arise as massless matter: the **32** of $SO(11)$. This is also a non-split model (I_2^{*ns}), and this **32** is easily seen to arise at the E_7 point, where the corresponding split model (I_2^{*s}) with the $SO(12)$ gauge symmetry also yields **32**.

[3]For $Sp(3)$, the dual heterotic gauge bundle is $SU(2) \times G_2$ since the maximal embedding is $E_8 \supset SU(2) \times G_2 \times Sp(3)$ (see *e.g.* [133] for the branching rules). The spectrum in Table 5.4 is obtained by distributing the $12 + n$ instantons as $(4 + r, 8 + n - r)$ in $(SU(2), G_2)$.

[4]For $Sp(3)$, the relevant indices of a representation **R** for examining the generalized Green-Schwarz (GS) mechanism are given by $(\text{index}(\mathbf{R}), x_{\mathbf{R}}, y_{\mathbf{R}}) = (8, 14, 3), (1, 1, 0), (4, -2, 3)$ and $(5, -7, 6)$ for $\mathbf{R} =$

Table 5.3: Three cases in which half-hypermultiplets appear as massless matter in six-dimensional F-theory on an elliptic Calabi-Yau threefold over $\mathbb{F}_n$ / heterotic string theory on K3 (quoted from Table 3 of [90]).

gauge group H	fibre type	enhancement G	matter rep.	multiplicity	homogeneous space
E_7	III^{*s}	E_8	$\mathbf{56}\frac{1}{2}$	$n+8$	$\frac{E_8}{E_7 \times SU(2)}$
			$\mathbf{1}$	$2n+21$	$-$
D_6	I_2^{*s}	E_7	$\mathbf{32}\frac{1}{2}$	$n+4$	$\frac{E_7}{SO(12) \times SU(2)}$
		D_7	$\mathbf{12}$	$n+8$	$\frac{SO(14)}{SO(12) \times U(1)}$
			$\mathbf{1}$	$2n+18$	$-$
A_5	I_6^s	E_6	$\mathbf{20}\frac{1}{2}$	r	$\frac{E_6}{SU(6) \times SU(2)}$
		D_6	$\mathbf{15}$	$n+2-r$	$\frac{SO(12)}{SU(6) \times U(1)}$
		A_6	$\mathbf{6}$	$2n+16+r$	$\frac{SU(7)}{SU(6) \times U(1)}$
			$\mathbf{1}$	$3n+21-r$	$-$

Table 5.4: The massless matter spectrum of six-dimensional heterotic string theory on K3 with an unbroken $Sp(3)$ gauge symmetry. This is anomaly-free, and also contains half-hypermultiplets.

gauge group	representation	multiplicity
C_3	$\mathbf{14'}\frac{1}{2} + \mathbf{6}\frac{1}{2}$	r
	$\mathbf{14}$	$n+1-r$
	$\mathbf{6}$	$2n+16+r$
	$\mathbf{1}$	$4n+23-2r$

one of the E_8 factors with the instanton number $12 + n$ [90]

$$n_H - n_V = 30n + 112. \tag{5.2.8}$$

As we can see, the representations $\mathbf{56}$, $\mathbf{32}$, $\mathbf{20}$, together with $\mathbf{14'}$ and $\mathbf{6}$, to which the half-hypermultiplets belong, are precisely the ones of quaternionic Kähler manifolds (or "Wolf spaces" [141, 142]). All but the last $\mathbf{6}$ are obtained by taking the Lie groups of the extreme bottom and the third rows of the magic square as the groups of the numerator and denominator of the homogeneous space. The denominator groups also always come with an $SU(2)$ factor in contrast to the case of ordinary hypermultiplets, where the denominator group comprises not an $SU(2)$ but a $U(1)$ factor. In the latter case, the symmetric space

---

Adj, $\mathbf{6}$, $\mathbf{14}$ and $\mathbf{14'}$, respectively, where $\mathrm{tr}_{\mathbf{R}} F^2 = \mathrm{index}(\mathbf{R}) \mathrm{tr}_{\mathbf{6}} F^2$ and $\mathrm{tr}_{\mathbf{R}} F^4 = x_{\mathbf{R}} \mathrm{tr}_{\mathbf{6}} F^4 + y_{\mathbf{R}} (\mathrm{tr}_{\mathbf{6}} F^2)^2$. By using these data and assuming that the charged matter spectrum only contains $\mathbf{6}$, $\mathbf{14}$ and $\mathbf{14'}$, we can solve the equations of the generalized GS mechanism on $\mathbb{F}_n$ and obtain the unique solution given in Table 5.4.

is a homogeneous Kähler manifold [107]. In the M-theory Coulomb branch analysis of codimension-two or higher singularities [143], the Weyl-group invariant phases of this $SU(2)$ were shown to correspond to the resolutions yielding half-hypermultiplets.

Let us summarize what is known so far, for the three simply-laced split examples of Table 5.3, about the resolutions of the codimension-two singularities that yield half-hypermultiplets. The resolutions of the third example were studied in [93], and those of the first and second ones were worked out in [98]. The main relevant features are[5]:

(1) As in [87, 88], let z (w) be the affine coordinate of the $\mathbb{P}^1$ fibre ($\mathbb{P}^1$ base) of the Hirzebruch surface $\mathbb{F}_n$, respectively. Suppose that we have a codimension-one singularity along the line $z = 0$ with the fibre type specified in the second column of Table 5.3. The non-singlet matter arises where the singularity is "enhanced" from "H" to "G", in the sense that Kodaira's singular fibres read off at *right over that point* have intersections specified by the Dynkin diagram of G. However, where the half-hypermultiplets appear, the codimension-two singularity is already resolved by blowing up the nearby codimension-one singularities. No additional blow-up at the codimension-two point is required, even though the singularity is "enhanced" there in the sense explained above. Such a type of resolution is called an *incomplete resolution* [93].

(2) In an incomplete resolution, the relevant section that vanishes at codimension-two goes like $O(s)$, where s is a local coordinate holomorphic in w, and $s = 0$ is the codimension-two singularity. In this case, although the number of blow-ups required to resolve it is the same as that to resolve the nearby generic codimension-one singularities, the intersection matrix of the exceptional curves at $s = 0$ is not the same as the generic one determined by the Cartan matrix of H (nor that of G), but turns out to be a curious non-Dynkin diagram with some nodes having self-intersections $-\frac{3}{2}$.

(3) In the first three examples of Table 5.3 studied in [93] and [98], $\frac{3}{2}$ is the length square of the weight vector of the representations to which the half-hypermultiplets belong. It was confirmed that although the intersection matrix was not the (minus of the) Cartan matrix of G, the exceptional curves at $s = 0$ formed an extremal ray that could span all the weights of the relevant pseudo-real representation of the half-hypermultiplets.

(4) In the first two examples, there arise several codimension-one singularities during the intermediate stages of the blow-up process, and there are several options in which singularity we blow up first, and which we do afterwards. Depending on the ordering of the blow-ups, we obtain different intersection diagrams of the exceptional

---

[5]The local coordinate s parametrizing the base $\mathbb{P}^1$ of $\mathbb{F}_n$ will be denoted by w in Section 5.3 and 5.4 when we blow up the singularities.

curves at the codimension-two point $s = 0$ [98]. More specifically, the intersection diagram on every other row found in [143] can be obtained in this way, but not all of them.

(5) Instead, when the relevant section vanishes like $O(s^2)$ at the codimension-two point, the singularity becomes stronger than the case above so that there arises an additional conifold singularity. A small resolution generates an extra exceptional fibre at that point so that it completes the proper Dynkin diagram of group G. This type of resolution is called a *complete resolution* [93].

5.3   Six-dimensional A_5 global model

In this section, we consider a six-dimensional F-theory compactification on an elliptic fibration over a Hirzebruch surface $\mathbb{F}_n$ in which the unbroken gauge symmetry reduces to $A_5 = SU(6)$ with the half-hypermultiplets [90, 93][6]. We work in the dP_9 fibration so that we focus on the E_8 with $12 + n$ instantons of the heterotic dual.

5.3.1   The split I_6 equation on $\mathbb{F}_n$

As was shown in [90], the equation of this curve is the one that supports a Kodaira I_6 singular fibre of the split type at $z = 0$[7]. Specifically, we consider the equation describing the elliptic fibration using Tate form (3.1.4):

$$P \;\; = \;\; -(y^2 + a_1 xy + a_3 y) + x^3 + a_2 x^2 + a_4 x + a_6 = 0. \tag{5.3.1}$$

$z = 0$ is the divisor of self-intersection $+n$. The equation for the theory with the unbroken symmetry $H = SU(6)$ can be obtained by specializing the sections as

$$
\begin{aligned}
a_1 &= 2\sqrt{3}t_r h_{n-r+2}, \\
a_2 &= -3z t_r H_{n-r+4}, \\
a_3 &= 2\sqrt{3}z^2 u_{r+4} h_{n-r+2}, \\
a_4 &= z^3 \left(t_r f_{n-r+8} - 3u_{r+4} H_{n-r+4} \right) + f_8 z^4, \\
a_6 &= z^5 u_{r+4} f_{n-r+8} + g_{12} z^6,
\end{aligned}
\tag{5.3.2}
$$

where t_r, h_{n-r+2}, H_{n-r+4}, u_{r+4} and f_{n-r+8} (together with f_8 and g_{12}) are the sections of appropriate line bundles over the base $\mathbb{P}^1$ specified by their subscripts, which in this case denote nothing but the degrees of the polynomials in w. It can be verified that Eq. (5.3.1) with Eq. (5.3.2) correctly reproduces the anomaly-free heterotic massless spectrum for

---

[6]The other gauge symmetries with the half-hypermultiplets: E_7 and D_6 are in [98].

[7]z and w is the affine coordinate of the $\mathbb{P}^1$ fibre and $\mathbb{P}^1$ base of the Hirzebruch surface $\mathbb{F}_n$, respectively.

an unbroken $A_5 = SU(6)$ gauge symmetry with $A_2 \times A_1 = SU(3) \times SU(2)$ instanton numbers $(r, 12 + n - r)$ (see e.g. [144]).

Remark. While Eq. (5.3.1) and Eq. (5.3.2) successfully yield a consistent $A_5 = SU(6)$ model, the vanishing orders of $(a_1, a_2, a_3, a_4, a_6)$ in z are $(0, 1, 2, 3, 5)$, which are the same as those for the split I_5 fibre type I_5^s and differ from the "standard" Tate's orders $(0, 1, 3, 3, 6)$ for the split I_6 fibre type I_6^s classified in [90]. Indeed, it can be easily seen that the sections $(a_1, a_2, a_3, a_4, a_6)$ with orders $(0, 1, 3, 3, 6)$ only result in the Weierstrass model Eq. (5.3.3), Eq. (5.3.4) and Eq. (5.3.5) with constant t_r, that is, no instantons are distributed to the $SU(3)$ factor, and all the $12+n$ instantons are in the $SU(2)$ factor. In fact, we can redefine y and x so that the vanishing orders of $(a_1, a_2, a_3, a_4, a_6)$ may become $(0, 1, 3, 3, 6)$ only when $t_r \neq 0$, but cannot when $t_r = 0$ since the redefinitions of y and x contain shifts proportional to $\frac{1}{t_r}$, which diverge at $t_r = 0$. Thus, we use the Weierstrass equation in this chapter for the discussion about the half-hypermultiplets.

By redefining y and x, we obtain the Weierstrass form:

$$P_w = -y^2 + x^3 + f_{SU(6)}(z, w)x + g_{SU(6)}(z, w) = 0, \tag{5.3.3}$$

$$
\begin{aligned}
f_{A_5}(z, w) := \ & -3t_r^4 h_{n-r+2}^4 + 6zt_r^3 h_{n-r+2}^2 H_{n-r+4} \\
& + z^2 \left(6t_r u_{r+4} h_{n-r+2}^2 - 3t_r^2 H_{n-r+4}^2 \right) \\
& + z^3 \left(t_r f_{n-r+8} - 3u_{r+4} H_{n-r+4} \right) + f_8 z^4, \tag{5.3.4}
\end{aligned}
$$

$$
\begin{aligned}
g_{A_5}(z, w) := \ & 2t_r^6 h_{n-r+2}^6 - 6z \left(t_r^5 h_{n-r+2}^4 H_{n-r+4} \right) \\
& - 6z^2 \left(t_r^3 u_{r+4} h_{n-r+2}^4 - t_r^4 h_{n-r+2}^2 H_{n-r+4}^2 \right) \\
& + z^3 \left(-t_r^3 f_{n-r+8} h_{n-r+2}^2 + 9t_r^2 u_{r+4} h_{n-r+2}^2 H_{n-r+4} - 2t_r^3 H_{n-r+4}^3 \right) \\
& + z^4 \left(-f_8 t_r^2 h_{n-r+2}^2 + t_r^2 f_{n-r+8} H_{n-r+4} + 3u_{r+4}^2 h_{n-r+2}^2 - 3t_r u_{r+4} H_{n-r+4}^2 \right) \\
& + z^5 \left(f_8 t_r H_{n-r+4} + u_{r+4} f_{n-r+8} \right) + g_{12} z^6 \tag{5.3.5}
\end{aligned}
$$

with a discriminant

$$
\begin{aligned}
\Delta_{A_5}(z, w) &= 4f_{A_5}^3 + 27g_{A_5}^2 \\
&= z^6 t_r^3 h_{n-r+2}^4 P_{2n+r+16} + z^7 t_r^2 h_{n-r+2}^2 Q_{3n+20} + z^8 R_{4n+24} + O(z^9), \tag{5.3.6}
\end{aligned}
$$

where $P_{2n+r+16}$, Q_{3n+20} and R_{4n+24} are some non-factorizable polynomials in w of degrees specified by the subscripts. In generic cases, any two of t_r, h_{n-r+2} and $P_{2n+r+16}$ do not share a common zero locus, which we assume in this thesis. From Eq. (5.3.4), Eq. (5.3.5) and Eq. (5.3.6), we can see that Kodaira's singular fibre types over the zero loci of t_r, h_{n-r+2} and $P_{2n+r+16}$ are respectively the split types of IV^*, I_2^* and I_7, yielding the singularity enhancements from "$H = A_5 = SU(6)$" to "$G = E_6$", "D_6" and "A_6" as presented in the third column of Table 5.3.

5.3.2 The massless spectrum

In this subsection, we calculate on the F-theory side the number of charged and neutral matter fields that the $A_5 = SU(6)$ model has, according to Section 4.4. Following the previous section, we assume that $12 + n$ instantons are distributed among $(8 + n - r, 4 + r)$ $(0 \leq r \leq n + 2)$ in (A_1, A_1). We obtained an unbroken A_5 case in the previous subsection. This case consists of the five polynomials: t_r, h_{n-r+2}, H_{n-r+4}, u_{r+4} and f_{n-r+8}. In particular, the "split" condition requires [90]

$$I_{2n-2r+4} = h_{n-r+2}^2, \tag{5.3.7}$$

and the condition for $(8 + n - r, 4 + r)$ instanton assignment is characterized by

$$f_{4+2n} = k_{n+2}^2 = t_r^2 h_{n-r+2}^2. \tag{5.3.8}$$

Therefore, the dimension of the moduli spaces of compactification with "A_5" singularity in F-theory is

$$\begin{aligned} n_0 &= (1+r) + (3+n-r) + (5+n-r) + (5+r) + (9+n-r) - 2 \\ &= 3n - r + 21. \end{aligned} \tag{5.3.9}$$

We also obtain the "A_5" discriminant locus (5.3.6) a discriminant

$$\Delta(z,w) = z^6 t_r^3 h_{n-r+2}^4 P_{2n+r+16} + z^7 t_r^2 h_{n-r+2}^2 Q_{3n+20} + z^8 R_{4n+24} + O(z^9), \tag{5.3.10}$$

where $P_{2n+r+16}$, Q_{3n+20} and R_{4n+24} are some non-factorizable polynomials constructed fs and gs. At $t_r = 0$ locus, "A_5" is enhanced to "E_6"; thus, we obtain the half-hypermultiplets $\mathbf{20}\frac{1}{2}$ since $A_5 \times A_1 \subset E_6$. At $h_{n-r+2} = 0$ locus, "A_5" is enhanced to "D_6"; thus, we obtain the hypermultiplets $\mathbf{15}$ since $A_5 \times U(1) \subset D_6$. At $P_{2n+r+16} = 0$ locus, "A_5" is also enhanced to "A_6"; thus, we obtain the hypermultiplets $\mathbf{6}$ since $A_5 \times U(1) \subset A_6$. Therefore, the D_5 case has r half-hypermultiplets $\mathbf{20}\frac{1}{2}$, $(2 + n - r)$ half-hypermultiplets $\mathbf{15}$ and $(16 + n + r)$ hypermultiplets $\mathbf{12}$ as charged matter fields (Table 5.3).

5.3.3 The local equation near D_6 points and resolution of the singularities

The local equation near D_6 point

In this subsection, we carry out the process of blow-up of the codimension-two singularity at a zero locus of $h_{n-r+2} = 0$. To this aim, we consider a local equation in which the enhancement of "A_5" to "D_6" is achieved at the codimension-two singularity[8].

---

[8]They are quoted because they only imply the Lie algebras whose Dynkin diagrams specify the intersections of Kodaira's singular fibres right over those points with fixed w.

To obtain such an equation, we first complete the square with respect to y in Eq. (5.3.1) and substitute Eq. (5.3.2) into it. Writing $y + \frac{1}{2}(a_1 x + a_3) \equiv Y$, we have

$$
\begin{aligned}
-Y^2 + x^3 &+ x^2 \left(3t_r^2 h_{n-r+2}^2 - 3zt_r H_{n-r+4}\right) \\
&+ x \left(z^3 t_r f_{n-r+8} + f_8 z^4 + 6z^2 t_r u_{r+4} h_{n-r+2}^2 - 3z^3 u_{r+4} H_{n-r+4}\right) \\
&+ 3z^4 u_{r+4}^2 h_{n-r+2}^2 + z^5 u_{r+4} f_{n-r+8} + g_{12} z^6 \quad = \quad 0.
\end{aligned}
\tag{5.3.11}
$$

By setting[9]

$$
h_{n-r+2} = w,
$$
$$
t_r = H_{n-r+4} = u_{r+4} = \frac{1}{\sqrt{3}},
\tag{5.3.12}
$$
$$
f_{n-r+8} = f_8 = g_{12} = 0,
$$

we can obtain the desired equation, but it is more convenient to make a shift in the x coordinate $x + z^2 \equiv X$. In terms of X, the final equation is

$$
-Y^2 + X^3 + X^2 \left(w^2 - z(3z + 1)\right) + X(3z + 1)z^3 - z^6 = 0,
\tag{5.3.13}
$$

which we blow up in the following.

If we write Eq. (5.3.13) as

$$
-Y^2 + X^3 + \frac{b_2}{4} X^2 + \frac{b_4}{2} X + \frac{b_6}{4} = 0,
\tag{5.3.14}
$$

the vanishing orders of the sections b_2, b_4 and b_6 in z are 0, 3 and 6, respectively, which satisfy the criteria for the I_6 type Kodaira's singular fibre in Tate's algorithm. This is due to the shift $x + z^2 \equiv X$, as without it we would have instead the vanishing orders 0, 2, 4. Note that such a shift of the variable x to eliminate the order-2 term in z from b_4 is not possible globally, since near a zero locus of t_r, where a $\mathbf{20\frac{1}{2}}$ of $SU(6)$ appears, the necessary shift becomes divergent. This is why an equation with $\mathrm{ord}(b_2, b_4, b_6) = (0, 2, 4)$ was used in [93, 98].

Blowing up the singularity

Let us now consider the resolution of the singularity of the local equation (5.3.13):

$$
\Phi(x, y, z, w) := -y^2 + x^3 + x^2 \left(w^2 - z(3z + 1)\right) + x(3z + 1)z^3 - z^6 = 0,
\tag{5.3.15}
$$

where we have replaced X, Y with x, y. Eq. (5.3.15) has a codimension-one singularity[10] along $(x, y, z) = (0, 0, 0)$ for arbitrary w. In this case: $A_5 \to D_6$, we can confirm that

---

[9]In this thesis, the local coordinates of the base $\mathbb{P}^1$ of $\mathbb{F}_n$ (whose affine coordinate is w) will be denoted by w and not by s, in accordance with [95, 99].

[10]The condition for a singularity in six dimensions is that all of the following equations are satisfied:
$\Phi(x, y, z, w) = \partial_x \Phi(x, y, z, w) = \partial_y \Phi(x, y, z, w) = \partial_z \Phi(x, y, z, w) = \partial_w \Phi(x, y, z, w) = 0$.

there are some conifold singularities. In this subsection, only the conifold singularities that appear for the first time will be denoted. In other words, we do not denote any previous conifold singularities visible in the next blow-up.

1st blow-up

As Subsection 5.1.2, we replace the complex line $(x, y, z) = (0, 0, 0)$ with $\mathbb{P}^2 \times \mathbb{C}$ in $\mathbb{C}^4$ and examine the singularities of the local equations in three different charts corresponding to the affine patches of the $\mathbb{P}^2$ for some fixed w. We also give the explicit forms of the exceptional curves $\mathcal{C}_i$'s at $w \neq 0$ and δ_j's at $w = 0$.

Chart $\mathbf{1}_x$

$$\Phi(x, xy_1, xz_1, w) = x^2 \Phi_x(x, y_1, z_1, w),$$
$$\Phi_x(x, y_1, z_1, w) = w^2 - x^4 z_1^6 + 3x^3 z_1^4 + x^2(z_1 - 3)z_1^2 - xz_1 + x - y_1^2.$$
$$\mathcal{C}_{p_1}^{\pm} \text{ in } \mathbf{1}_x: \quad x = 0, \quad y_1 = \pm w. \tag{5.3.16}$$
$$\delta_{p_1} \text{ in } \mathbf{1}_x: \quad x = 0, \quad y_1 = 0.$$
$$\text{Singularities}: \quad (x, y_1, z_1, w) = (0, 0, 1, 0) \text{ (conifold sing. } \delta_{c_{1xz}}).$$

Chart $\mathbf{1}_y$

$$\Phi(x_1 y, y, yz_1, w) = y^2 \Phi_y(x_1, y, z_1, w),$$
$$\Phi_y(x_1, y, z_1, w) = w^2 x_1^2 + x_1^3 y - x_1^2 yz_1(3yz_1 + 1) + x_1 y^2 z_1^3(3yz_1 + 1) - y^4 z_1^6 - 1.$$
$$\mathcal{C}_{p_1}^{\pm} \text{ in } \mathbf{1}_y: \quad y = 0, \quad x_1 = \pm 1/w. \tag{5.3.17}$$
$$\delta_{p_1} \text{ in } \mathbf{1}_y: \quad \text{Invisible.}$$
$$\text{Singularities}: \quad \text{None.}$$

Chart $\mathbf{1}_z$

$$\Phi(x_1 z, y_1 z, z, w) = z^2 \Phi_z(x_1, y_1, z, w),$$
$$\Phi_z(x_1, y_1, z, w) = w^2 x_1^2 + z\left(x_1^3 - x_1^2(3z + 1) + x_1 z(3z + 1) - z^3\right) - y_1^2.$$
$$\mathcal{C}_{p_1}^{\pm} \text{ in } \mathbf{1}_z: \quad z = 0, \quad y_1 = \pm wx_1.$$
$$\delta_{p_1} \text{ in } \mathbf{1}_z: \quad z = 0, \quad y_1 = 0. \tag{5.3.18}$$
$$\text{Singularities}: \quad (x_1, y_1, z) = (0, 0, 0),$$
$$(x_1, y_1, z, w) = (1, 0, 0, 0) \text{ (conifold sing. } \delta_{c_{1xz}}).$$

Note that we have used the same "z" in $\mathbf{1}_x$ and $\mathbf{1}_y$ for different coordinate variables, and similarly for x_1 and y_1. There will be no confusion as we do not compare equations in different charts.

2nd blow-up

As we can see, the only codimension-one singularity after the first blow-up is $(x_1, y_1, z) = (0, 0, 0)$ on chart $\mathbf{1}_z$, which is not visible from the other charts. We also find the conifold singularity $\delta_{c_{1xz}}$ on chart $\mathbf{1}_x$ and $\mathbf{1}_z$, but here we ignore this conifold singularity until the resolution of the codimension-one singularity is completed. We blow up this singularity by similarly inserting a one-parameter $(= w)$ family of $\mathbb{P}^2$ along $(x_1, y_1, z, w) = (0, 0, 0, w)$. The computation is similar. We find a codimension-one singularity in chart $\mathbf{2}_{zz}$, while the blown-up equations are regular for chart $\mathbf{2}_{zy}$. We can also see two conifold singularities: $\delta_{c_{2xz}}$ on chart $\mathbf{2}_{zx}$ and $\mathbf{2}_{zz}$ and $\delta_{c_{2x}}$ on chart $\mathbf{2}_{zx}$, but here we ignore it too. Here we show the result for the relevant charts $\mathbf{2}_{zx}$ and $\mathbf{2}_{zz}$.

Chart $\mathbf{2}_{zx}$

$$
\begin{aligned}
\Phi_z(x_1, x_1 y_2, x_1 z_2, w) &= x_1^2 \Phi_{zx}(x_1, y_2, z_2, w), \\
\Phi_{zx}(x_1, y_2, z_2, w) &= x_1(z_2 - 1)z_2 - x_1^2(z_2 - 1)^3 + w^2 - y_2^2. \\
\mathcal{C}_{p_2}^{\pm} \text{ in } \mathbf{2}_{zx}: \quad & x_1 = 0, \quad y_2 = \pm w. \\
\delta_{p_2} \text{ in } \mathbf{2}_{zx}: \quad & x_1 = 0, \quad y_2 = 0. \\
\text{Singularities}: \quad & (x_1, y_2, z_2, w) = (0, 0, 1, 0) \text{ (conifold sing. } \delta_{c_{2xz}}), \\
& (x_1, y_2, z_2, w) = (0, 0, 0, 0) \text{ (conifold sing. } \delta_{c_{2x}}).
\end{aligned}
\tag{5.3.19}
$$

Chart $\mathbf{2}_{zz}$

$$
\begin{aligned}
\Phi_z(x_2 z, y_2 z, z, w) &= z^2 \Phi_{zz}(x_2, y_2, z, w), \\
\Phi_{zz}(x_2, y_2, z, w) &= w^2 x_2^2 + (x_2 - 1)z\left(x_2^2 z - 2x_2 z - x_2 + z\right) - y_2^2. \\
\mathcal{C}_{p_2}^{\pm} \text{ in } \mathbf{2}_{zz}: \quad & z = 0, \quad y_2 = \pm w x_2. \\
\delta_{p_2} \text{ in } \mathbf{2}_{zz}: \quad & z = 0, \quad y_2 = 0. \\
\text{Singularities}: \quad & (x_2, y_2, z) = (0, 0, 0), \\
& (x_2, y_2, z, w) = (1, 0, 0, 0) \text{ (conifold sing. } \delta_{c_{2xz}}).
\end{aligned}
\tag{5.3.20}
$$

3rd blow-up

We then blow up the codimension-one singularity $(x_2, y_2, z) = (0, 0, 0)$ in chart $\mathbf{2}_{zz}$. It turns out that the resolution process of the codimension-one singularity is finished with only some conifold singularities. The equations of the exceptional curve (with a definite w) in the relevant charts are:

Chart 3_{zzx}

$$\Phi_z z(x_2, x_2 y_3, x_2 z_3, w) = x_2^2 \Phi_{zzx}(x_2, y_3, z_3, w),$$
$$\Phi_{zzx}(x_2, y_3, z_3, w) = w^2 + (x_2 - 1)z_3 \left((x_2 - 1)^2 z_3 - 1\right) - y_3^2.$$
$$\mathcal{C}_{p_3} \text{ in } 3_{zzx} : \quad x_2 = 0, \quad y_3^2 = w^2 - (z_3 - 1)z_3. \qquad (5.3.21)$$
$$\delta_{p_3} \text{ in } 3_{zzx} : \quad x_2 = 0, \quad y_3^2 = -(z_3 - 1)z_3.$$
$$\text{Singularities}: \quad \text{None.}$$

Chart 3_{zzz}

$$\Phi_z z(x_3 z, y_3 z, z, w) = z_2^2 \Phi_{zzz}(x_3, y_3, z, w),$$
$$\Phi_{zzz}(x_3, y_3, z, w) = x_3^2(w^2 - z(3z + 1)) + x_3^3 z^3 + 3x_3 z + x_3 - y_3^2 - 1 = 0.$$
$$\mathcal{C}_{p_3} \text{ in } 3_{zzz} : \quad z_2 = 0, \quad y_3^2 = w^2 x_3^2 + x_3 - 1. \qquad (5.3.22)$$
$$\delta_{p_3} \text{ in } 3_{zzz} : \quad z_2 = 0, \quad y_3^2 = x_3 - 1.$$
$$\text{Singularities}: \quad \text{None.}$$

Finally, we blow up the conifold singularities by small resolution (Appendix A); then we obtain new two-cycles $\mathbb{P}^1$'s. After this, we complete all blowing-up process, and the total space is now smooth.

Intersections of the exceptional curves

At fixed $w \neq 0$, we have five exceptional curves $\mathcal{C}_{p_1}^{\pm}$'S, $\mathcal{C}_{p_2}^{\pm}$'s and $\mathcal{C}_{p_3}$. From the above explicit forms, we find that their intersection diagram (or matrix) is given by the A_5 Dynkin diagram (the top diagram of Fig. 5.1). In addition, at $w = 0$, we can obtain the relations among $\mathcal{C}_i$'s and δ_j's by lifting up the exceptional curves from the defining chart into subsequent charts:

$$\mathcal{C}_{p_1}^{\pm} = \delta_{p_1} + \delta_{c_{1xz}} + \delta_{c_{2x}},$$
$$\mathcal{C}_{p_2}^{\pm} = \delta_{p_2} + \delta_{c_{2xz}} + \delta_{c_{2x}}, \qquad (5.3.23)$$
$$\mathcal{C}_{p_3} = \delta_{p_3}.$$

Therefore, we can see the intersection diagram at $w = 0$ corresponding to the D_6 Dynkin diagram (the bottom diagram of Fig. 5.1).

5.3.4 Incomplete/complete resolution of the singularities near E_6 points

In this subsection, we consider the incomplete/complete resolution near the codimension-two singularity at a zero locus of $t_r = 0$. To this aim, we consider a local equation in which the enhancement of "A_5" to "E_6" at the codimension-two singularity.

$$C_{p_1}^+ \quad C_{p_2}^+ \quad C_{p_3} \quad C_{p_2}^- \quad C_{p_1}^-$$

$$\xrightarrow{C_i \rightarrow \delta_i} \qquad \delta_{c_{1xz}} \quad \delta_{p_1} \quad \delta_{c_{2x}} \quad \delta_{p_2} \qquad \delta_{p_3} \qquad \delta_{c_{2xz}}$$
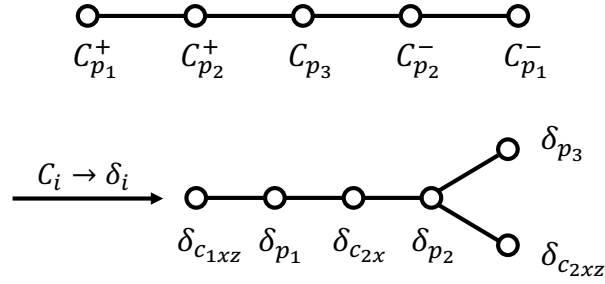
Figure 5.1: Intersection diagrams of the exceptional curves of the A_5 model at a D_6 point: (Top) $w \neq 0$; (Bottom) $w = 0$.

Incomplete resolutions and Half-hypermultiplets

We start from Eq. (5.3.11) and set

$$
\begin{aligned}
h_{n-r+2} &= \frac{1}{\sqrt{3}}, \\
H_{n-r+4} &= -u_{r+4} = -\frac{1}{2}, \\
f_{n-r+8} &= f_8 = g_{12} = 0,
\end{aligned}
\tag{5.3.24}
$$

and simply,

$$t_r = w. \tag{5.3.25}$$

In this case, we are led to the *incomplete* resolution. After performing the appropriate variable transformations, we can then obtain the local equation:

$$\Phi(x, y, z, w) := -y^2 + x^3 + x^2 \left(w + 3z\right) w + x \left(2w + 3z\right) z^2 + z^4 = 0, \tag{5.3.26}$$

where we have replaced Y with y. Eq. (5.3.26) has a codimension-one singularity along $(x, y, z) = (0, 0, 0)$ for arbitrary w. In this case, we can confirm that there are no conifold singularities.

We consider the same blow-up process in Subsection 5.3.3. In this case, there remain the codimension-one singularities during the blow-up process: $(x_1, y_1, z) = (0, 0, 0)$ in Chart $\mathbf{1}_z$ and $(x_1, y_2, z_2) = (0, 0, -w)$ in Chart $\mathbf{2}_{zx}$. Then, at fixed $w \neq 0$, we have five exceptional curves $\mathcal{C}_{p_1}^\pm$'s, $\mathcal{C}_{p_2}^\pm$'s and $\mathcal{C}_{p_3}$ and their intersection diagram which is given by the A_5 Dynkin diagram too (the top diagram of Fig. 5.2). At $w = 0$, in the first blow-up, two exceptional curves $\mathcal{C}_{p_1}^\pm$'s stack on top of each other to become a single curve δ_{p_1}. In the second blow-up, two exceptional curves $\mathcal{C}_{p_2}^\pm$ become two curves $\delta_{p_2}^\pm$, respectively. In

the third blow-up, one exceptional curve $\mathcal{C}_{p_3}$ splits into two curves $\delta_{p_3}^{\pm}$. Therefore, we can obtain the relations among $\mathcal{C}_i$'s and δ_j's by lifting up the exceptional curves from the defining chart into subsequent charts:

$$
\begin{aligned}
\mathcal{C}_{p_1}^{\pm} &= \delta_{p_1} + \delta_{p_3}^{\pm}, \\
\mathcal{C}_{p_2}^{\pm} &= \delta_{p_2}^{\pm}, \\
\mathcal{C}_{p_3} &= \delta_{p_3}^{+} + \delta_{p_3}^{-}.
\end{aligned}
\tag{5.3.27}
$$

In this case, the intersection diagram at $w = 0$ does not match the E_6 Dynkin diagram. However, although the number of δ_i is the same as the case of the nearby "A_5" codimension-one singularity, their intersection diagrams are different.

Since $\mathcal{C}_i$'s form an A_5 Dynkin diagram, we consider the intersection matrix:

$$
\begin{pmatrix} \mathcal{C}_{p_1}^{+} \\ \mathcal{C}_{p_2}^{+} \\ \mathcal{C}_{p_3} \\ \mathcal{C}_{p_2}^{-} \\ \mathcal{C}_{p_1}^{-} \end{pmatrix} \begin{pmatrix} \mathcal{C}_{p_1}^{+} & \mathcal{C}_{p_2}^{+} & \mathcal{C}_{p_3} & \mathcal{C}_{p_2}^{-} & \mathcal{C}_{p_1}^{-} \end{pmatrix} = \begin{pmatrix} -2 & 1 & 0 & 0 & 0 \\ 1 & -2 & 1 & 0 & 0 \\ 0 & 1 & -2 & 1 & 0 \\ 0 & 0 & 1 & -2 & 1 \\ 0 & 0 & 0 & 1 & -2 \end{pmatrix}.
\tag{5.3.28}
$$

This is the same as an A_5 Cartan matrix up to overall (-1). From Eq. (5.3.27), since we obtain the relation between $\mathcal{C}_i$'s and δ_j's:

$$
\begin{pmatrix} \mathcal{C}_{p_1}^{+} \\ \mathcal{C}_{p_2}^{+} \\ \mathcal{C}_{p_3} \\ \mathcal{C}_{p_2}^{-} \\ \mathcal{C}_{p_1}^{-} \end{pmatrix} = \begin{pmatrix} 0 & 1 & 1 & 0 & 0 \\ 1 & 0 & 0 & 0 & 0 \\ 0 & 1 & 0 & 1 & 0 \\ 0 & 0 & 0 & 0 & 1 \\ 0 & 0 & 1 & 1 & 0 \end{pmatrix} \begin{pmatrix} \delta_{p_2}^{+} \\ \delta_{p_3}^{+} \\ \delta_{p_1} \\ \delta_{p_3}^{-} \\ \delta_{p_2}^{-} \end{pmatrix},
\tag{5.3.29}
$$

the intersection matrix at the "E_6" codimension-two singularity is

$$
\begin{pmatrix} \delta_{p_2}^{+} \\ \delta_{p_3}^{+} \\ \delta_{p_1} \\ \delta_{p_3}^{-} \\ \delta_{p_2}^{-} \end{pmatrix} \begin{pmatrix} \delta_{p_2}^{+} & \delta_{p_3}^{+} & \delta_{p_1} & \delta_{p_3}^{-} & \delta_{p_2}^{-} \end{pmatrix} = \begin{pmatrix} -2 & 1 & 0 & 0 & 0 \\ 1 & -\frac{3}{2} & 1 & 1 & 0 \\ 0 & 1 & -\frac{3}{2} & 1 & 0 \\ 0 & 1 & 1 & -\frac{3}{2} & 1 \\ 0 & 0 & 0 & 1 & -2 \end{pmatrix}.
\tag{5.3.30}
$$

Therefore, we obtain the diagram of the intersection matrix in this case the bottom diagram of Fig. 5.2). This is called *incomplete* resolution. In this incomplete case [93,98], since $\frac{3}{2}$ is the length square of the weight vector of the pseudo-real representations, to which the half-hypermultiplets belong, we can confirm that δ_j's form an extremal ray that can span all the weights of the relevant pseudo-real representation.

Complete resolutions

Next, we consider the case in which only t_r is changed

$$
t_r = w \to t_r = w^2,
\tag{5.3.31}
$$
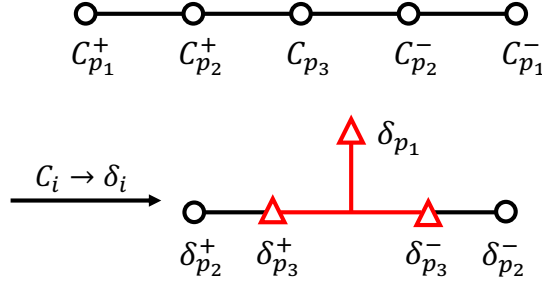
Figure 5.2: Intersection diagrams of the exceptional curves of the A_5 model at an E_6 point by the *incomplete* resolution: (Top) $w \neq 0$; (Bottom) $w = 0$. The triangle in the bottom figure represents the number of self-intersections is $-\frac{3}{2}$, not -2.

among the condition of the incomplete resolution (5.3.24) and (5.3.25). In this case, we are led to the *complete* resolution. After performing the appropriate variable transformations, we can then obtain the local equation:

$$\Phi(x, y, z, w) := -y^2 + x^3 + x^2 \left(w^2 + 3z \right) w^2 + x \left(2w^2 + 3z \right) z^2 + z^4 = 0. \quad (5.3.32)$$

Eq. (5.3.32) has a codimension-one singularity along $(x, y, z) = (0, 0, 0)$ for arbitrary w. In this case, we can confirm that there is one conifold singularity in the third blow-up.

The difference between this case and the *incomplete* one occurs only at $w = 0$. At $w = 0$, there arises a conifold singularity in the third blow-up. Thus, δ_{c3} is added because of the conifold singularity which is arising new. We can then obtain the relations among $\mathcal{C}_i$'s and δ_j's by lifting up the exceptional curves from the defining chart into subsequent charts:

$$\begin{aligned} \mathcal{C}_{p_1}^{\pm} &= \delta_{p_1} + \delta_{p_3}^{\pm} + \delta_{c3}, \\ \mathcal{C}_{p_2}^{\pm} &= \delta_{p_2}^{\pm}, \\ \mathcal{C}_{p_3} &= \delta_{p_3}^{+} + \delta_{p_3}^{-} + \delta_{c3}. \end{aligned} \quad (5.3.33)$$

Therefore, as in the previous results, we can obtain the intersection diagram at $w = 0$ corresponds to the E_6 Dynkin diagram (the bottom diagram of Fig. 5.3). Therefore, unlike in the incomplete case, we obtain not half-hypermultiplets but full-hypermultiplets in this case. This is called the *complete* resolution.

5.3.5 Resolution of the singularities near A_6 points

In this subsection, we consider the incomplete/complete resolution near the codimension-two singularity at a zero locus of $P_{2n+r+16} = 0$. To this aim, we consider a local equation
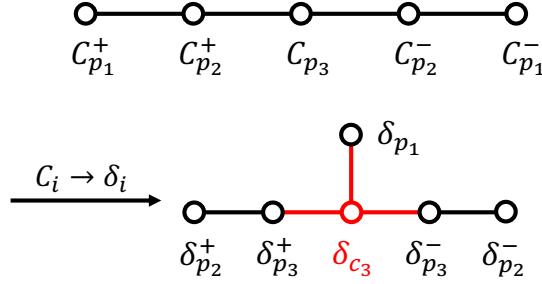
Figure 5.3: Intersection diagrams of the exceptional curves of the A_5 model at an E_6 point by the *complete* resolution: (Top) $w \neq 0$; (Bottom) $w = 0$.

in which the enhancement of "A_5" to "A_6" at the codimension-two singularity. In this case, we consider

$$P_{2n+r+16} = w \tag{5.3.34}$$

in Eq. (5.3.6), and we can confirm that there are no conifold singularities. Only in the third blow-up, there is a difference between the result of blow-ups at the "A_6" codimension-two singularity and the nearby generic "A_5" codimension-one singularity.

As in the past, we consider the same blow-up process in Subsection 5.3.3. at fixed $w \neq 0$, it is the same as in the previous results (the top diagram of Fig. 5.4). At $w = 0$, in the first and second blow-ups, four exceptional curves $\mathcal{C}_{p_1}^{\pm}$'s and $\mathcal{C}_{p_2}^{\pm}$ become four curves $\delta_{p_1}^{\pm}$ and $\delta_{p_2}^{\pm}$, respectively. In the third blow-up, one exceptional curve $\mathcal{C}_{p_3}$ splits into two curves $\delta_{p_3}^{\pm}$. This is the only difference between $\mathcal{C}_i$'s and δ_j's. Therefore, at $w = 0$, we can obtain the relations among $\mathcal{C}_i$'s and δ_j's by lifting up the exceptional curves from the defining chart into subsequent charts:

$$\begin{aligned}
\mathcal{C}_{p_1}^{\pm} &= \delta_{p_1}^{\pm}, \\
\mathcal{C}_{p_2}^{\pm} &= \delta_{p_2}^{\pm}, \\
\mathcal{C}_{p_3} &= \delta_{p_3}^{+} + \delta_{p_3}^{-}.
\end{aligned} \tag{5.3.35}$$

Therefore, we can see the intersection diagram at $w = 0$ corresponding to the A_6 Dynkin diagram (the bottom diagram of Fig. 5.4).

5.4 Six-dimensional C_3 global model

In this section, we consider a six-dimensional F-theory compactification on an elliptic fibration over a Hirzebruch surface $\mathbb{F}_n$ in which the unbroken gauge symmetry reduces
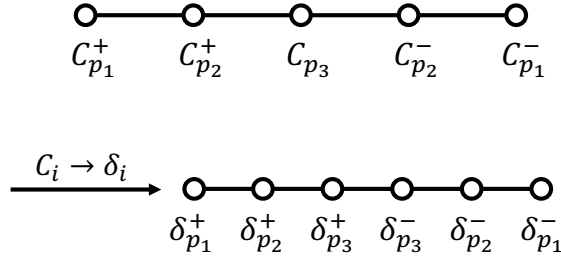
Figure 5.4: Intersection diagrams of the exceptional curves of the A_5 model at an A_6 point: (Top) $w \neq 0$; (Bottom) $w = 0$.

to $C_3 = Sp(3)$ with the half-hypermultiplets [90, 93][11]. We work in the dP_9 fibration so that we focus on the E_8 with $12 + n$ instantons of the heterotic dual. In particular, we consider the anomaly-free heterotic massless spectrum for an unbroken $Sp(3)$ gauge symmetry with $G_2 \times SU(2)$ instanton numbers $(4 + r, 8 + n - r)$.

5.4.1   The non-split I_6 equation on $\mathbb{F}_n$

As was shown in [90], the equation of this curve is the one that supports a Kodaira I_6 singular fibre of the non-split type at $z = 0$. A I_6 non-split curve may be obtained by replacing the relevant factorized section of a split I_6 curve with a non-factorized one. The equation for the theory with the unbroken symmetry $H = SU(6)$ can be obtained by Eq. (5.3.2). Thus, we obtain the Weierstrass form (5.3.3), (5.3.4) and (5.3.5) with a discriminant

$$
\begin{aligned}
\Delta_{A_5}(z, w) &= 4f_{A_5}^3 + 27g_{A_5}^2 \\
&= z^6 t_r^3 h_{n-r+2}^4 P_{2n+r+16} + z^7 t_r^2 h_{n-r+2}^2 Q_{3n+20} + z^8 R_{4n+24} + O(z^9). \quad (5.4.1)
\end{aligned}
$$

We can also see that the h_{n-r+2}-dependence of $f_{SU(6)}$ (5.3.4) or $g_{SU(6)}$ (5.3.5) is only through h_{n-r+2}^2, which allows us to replace every h_{n-r+2}^2 in $f_{SU(6)}$ and $g_{SU(6)}$ with a generic polynomial $I_{2n-2r+4}$. The resulting equation is the one for I_6^{ns} [90]. Therefore, we make a replacement $h_{n-r+2}^2 \to I_{2n-2r+4}$, and we obtain

$$
\begin{aligned}
f_{C_3}(z, w) := &-3t_r^4 I_{2n-2r+4}^2 + 6z t_r^3 I_{2n-2r+4} H_{n-r+4} \\
&+ z^2 \left(6t_r u_{r+4} I_{2n-2r+4} - 3t_r^2 H_{n-r+4}^2 \right) \\
&+ z^3 \left(t_r f_{n-r+8} - 3u_{r+4} H_{n-r+4} \right) + f_8 z^4, \quad (5.4.2)
\end{aligned}
$$

---

[11]The other gauge symmetries with the half-hypermultiplets: E_7 and D_6 are in [98].

$$
\begin{aligned}
g_{C_3}(z,w) \;:=\; & 2t_r^6 I_{2n-2r+4}^3 - 6z\left(t_r^5 I_{2n-2r+4}^2 H_{n-r+4}\right) \\
& -6z^2\left(t_r^3 u_{r+4} I_{2n-2r+4}^2 - t_r^4 I_{2n-2r+4} H_{n-r+4}^2\right) \\
& +z^3\left(-t_r^3 f_{n-r+8} I_{2n-2r+4} + 9t_r^2 u_{r+4} I_{2n-2r+4} H_{n-r+4} - 2t_r^3 H_{n-r+4}^3\right) \\
& +z^4\left(-f_8 t_r^2 I_{2n-2r+4} + t_r^2 f_{n-r+8} H_{n-r+4} + 3u_{r+4}^2 I_{2n-2r+4} - 3t_r u_{r+4} H_{n-r+4}^2\right) \\
& +z^5\left(f_8 t_r H_{n-r+4} + u_{r+4} f_{n-r+8}\right) + g_{12} z^6, \tag{5.4.3}
\end{aligned}
$$

$$
\Delta_{C_3}(z,w) \;=\; z^6 t_r^3 I_{2n-2r+4}^2 P_{2n+r+16} + z^7 t_r^2 I_{2n-2r+4} Q_{3n+20} + z^8 R_{4n+24} + O(z^9). \tag{5.4.4}
$$

As in a split I_6 case, any two of t_r, $I_{2n-2r+4}$ and $P_{2n+r+16}$ do not share a common zero locus, which we assume in this thesis. From Eq. (5.4.2), Eq. (5.4.3) and Eq. (5.4.4), we can see that Kodaira's singular fibre types over the zero loci of t_r, h_{n-r+2} and $P_{2n+r+16}$ are respectively the non-split types of IV^*, I_2^* and I_7. Since the difference from the split I_6 case is only $h_{n-r+2}^2 \to I_{2n-2r+4}$, we focus on near $I_{2n-2r+4} = 0$, at which $I_6^{ns} \to I_2^{*(ns)}$ is called a "D_6" point.

5.4.2 The massless spectrum

As we see explicitly in Section 4.4, the replacement of the section $h_{n-r+2}^2 \to I_{2n-2r+4}$ in the split I_6 equation results in the global non-factorization of the exceptional curves, which reduces the gauge symmetry from $SU(6)$ to $Sp(3)$. Let us examine what matter multiplets are expected to arise in this model.

In the transition $I_6^s \leftrightarrow I_6^{ns}$, nothing changes in the local singularity structure near the zero loci of t_r and $P_{2n+r+16}$, where $\mathbf{20}\frac{1}{2}$ and $\mathbf{6}$ of $SU(6)$ appear as massless matter in the split theory; the string junctions or the vanishing cycles there do not "know" whether the total equation is of the split type or of the non-split type. The only change they feel is that of the gauge symmetry, so they simply decompose into irreducible representations of $Sp(3)$, which is the gauge symmetry of the non-split theory. Thus, at a zero locus of t_r, a half-hypermultiplet in $\mathbf{20}$ of $SU(6)$, of which the quaternionic Kähler manifold $E_6/(SU(6)\times SU(2))$ is comprised, is decomposed into half-hypermultiplets in $\mathbf{14}'$ and $\mathbf{6}$ of $Sp(3)$, while at a zero locus of $P_{2n+r+16}$, a hypermultiplet in $\mathbf{6}$ of $SU(6)$ entirely becomes one in $\mathbf{6}$ of $Sp(3)$. Note that $\mathbf{6}$ is also a pseudo-real representation of $Sp(3)$, and the latter can be regarded as $2n+r+16$ pairs of half-hypermultiplets. The $\mathbf{14}'$ constitutes the quaternionic Kähler manifold $F_4/(Sp(3)\times SU(2))$, while the $\mathbf{6}$ does $Sp(4)/(Sp(3)\times SU(2))$. This will answer the original question of where the matter fields corresponding to the final magical coset arise; they arise at the E_6 points of the non-split I_6 model as an irreducible multiplet in the $Sp(3)$ decomposition of $\mathbf{20}$ of $SU(6)$.

5.4.3 A puzzle on matter fields near the D_6 points

On the other hand, there is a puzzle: With the replacement $h_{n-r+2}^2 \to I_{2n-2r+4}$, the $n-r+2$ double roots of the equation $h_{n-r+2}^2 = 0$ split into $n-r+2$ pairs of single roots

Table 5.5: Massless matter content in the I_6^s model of F-theory, if the matter fields locally exist at all codimension-two singularities. In I_6^{ns}, each representation of I_6^s simply decomposes into the irreducible representation of C_3 at each zero locus.

Enhancement in I_6^s	I_6^s (A_5)		I_6^{ns} (C_3)	
	Matter rep.	Multiplicity	Matter rep.	Multiplicity
IV^* (E_6)	$\mathbf{20}\frac{1}{2}$	r	$\mathbf{14'}\frac{1}{2} + \mathbf{6}\frac{1}{2}$	r
I_2^* (D_6)	$\mathbf{15}$	$n + 2 - r$	$\mathbf{14}$	$2n + 4 - 2r$
I_7 (A_6)	$\mathbf{6}$	$2n + 16 + r$	$\mathbf{6}$	$2n + 16 + r$
	$\mathbf{1}$	$3n + 21 - r$	$\mathbf{1}$	$4n + 23 - 2r$

of $I_{2n-2r+4} = 0$. Thus the number of loci where hypermultiplets in $\mathbf{15}$ of $SU(6)$ occur is doubled. A $\mathbf{15}$ of $SU(6)$ decomposes into $\mathbf{14} \oplus \mathbf{1}$ (and not $\mathbf{14'} \oplus \mathbf{1}$) of $Sp(3)$. Since the adjoint of $SU(6)$ decomposes as $\mathbf{35} = \mathbf{21} \oplus \mathbf{14}$, where $\mathbf{21}$ is the adjoint of $Sp(3)$, one $\mathbf{14}$ of $n - r + 2$ hypermultiplets can be thought of as eaten by the $SU(6)$ vector multiplet. Thus the anomaly-free massless matter spectrum shown in Table 5.4 can be reproduced if the $n - r + 2 - 1$ hypermultiplets in $\mathbf{14}$ are "distributed" at the $2n - 2r + 4$ zero loci of $I_{2n-2r+4}$ (Table 5.4.3). This, however, seems impossible, since the $\mathbf{14}$ of $Sp(3)$ is a real representation and does not allow half-hypermultiplets in this representation.

Of course, the original $SU(6)$ spectrum is already anomaly-free, so hypermultiplets in $\mathbf{14}$ can not be present equally at all the $2n - 2r + 4$ zeros of $I_{2n-2r+4} = 0$ as they are too many to be anomaly-free. If they were $\mathbf{14'}$ instead of $\mathbf{14}$, they could be split into pairs and equally be distributed (up to the eaten ones) at the $2n - 2r + 4$ zeros, but both the heterotic anomaly analysis and Sadov's generalized anomaly cancellation mechanism tell us that they must be $\mathbf{14}$, and not $\mathbf{14'}$.

This poses a question of how the $n - r + 1$ matter in $\mathbf{14}$ of $Sp(3)$ are generated and where they reside in the non-split I_6 model. In the next subsection, in order to explore what happens near a zero locus of $I_{2n-2r+4}$, we perform an explicit blow-up of the singularity.

5.4.4 The local equation near D_6 point and resolutions of the singularities

The local equation

In this subsection, we carry out the process of blow-up of the codimension-two singularity at a zero locus of $I_{2n-2r+4} = 0$. To this aim, we consider a local equation in which the enhancement of "A_5" to "D_6" is achieved at the codimension-two singularity.

To obtain such an equation, We start from Eq. (5.4.2) and Eq. (5.4.3). As Subsec-

tion 5.3.3, writing $y + \frac{1}{2}(a_1 x + a_3) \equiv Y$, we obtain

$$
\begin{aligned}
-Y^2 + x^3 + x^2 &\left(3t_r^2 I_{2n-2r+4} - 3zt_r H_{n-r+4}\right) \\
+x &\left(z^3 t_r f_{n-r+8} + f_8 z^4 + 6z^2 t_r u_{r+4} I_{2n-2r+4} - 3z^3 u_{r+4} H_{n-r+4}\right) \\
+3z^4 u_{r+4}^2 I_{2n-2r+4} &+ z^5 u_{r+4} f_{n-r+8} + g_{12} z^6 \quad = \quad 0.
\end{aligned}
\tag{5.4.5}
$$

By setting

$$
\begin{aligned}
h_{n-r+2}^2 \to I_{2n-2r+4} &= w, \\
t_r = H_{n-r+4} = u_{r+4} &= \frac{1}{\sqrt{3}}, \\
f_{n-r+8} = f_8 = g_{12} &= 0,
\end{aligned}
\tag{5.4.6}
$$

we can obtain the desired equation, but it is more convenient to make a shift in the x coordinate $x + z^2 \equiv X$ as in Subsection 5.3.3. In terms of X, the final equation is

$$
-Y^2 + X^3 + X^2\left(w - z(3z+1)\right) + X(3z+1)z^3 - z^6 = 0,
\tag{5.4.7}
$$

which we blow up in the following.

Blowing up the singularity

We start considering the resolution of the singularity of the local equation (5.4.7):

$$
\Phi(x, y, z, w) \equiv -y^2 + x^3 + x^2\left(w - z(3z+1)\right) + x(3z+1)z^3 - z^6 = 0, \tag{5.4.8}
$$

where we have replaced X, Y with x, y. Eq. (5.4.8) has a codimension-one singularity along $(x, y, z) = (0, 0, 0)$ for arbitrary w.

1st blow-up

As Subsection 5.1.2, we replace the complex line $(x, y, z) = (0, 0, 0)$ with $\mathbb{P}^2 \times \mathbb{C}$ in $\mathbb{C}^4$ and examine the singularities of the local equations in three different charts corresponding to the affine patches of the $\mathbb{P}^2$ for some fixed w. We also give the explicit forms of the exceptional curves $\mathcal{C}_i$'s at $w \neq 0$ and δ_j's at $w = 0$.

Chart $\mathbf{1}_x$

$$
\begin{aligned}
\Phi(x, xy_1, xz_1, w) &= x^2 \Phi_x(x, y_1, z_1, w), \\
\Phi_x(x, y_1, z_1, w) &= w - x^4 z_1^6 + 3x^3 z_1^4 + x^2(z_1 - 3)z_1^2 - xz_1 + x - y_1^2. \\
\mathcal{C}_{p_1}^{\pm} \text{ in } \mathbf{1}_x : \quad &x = 0, \quad y_1 = \pm\sqrt{w}. \\
\delta_{p_1} \text{ in } \mathbf{1}_x : \quad &x = 0, \quad y_1 = 0. \\
\text{Singularities}: \quad &\text{None.}
\end{aligned}
\tag{5.4.9}
$$

Chart $\mathbf{1}_y$

$$\Phi(x_1y, y, yz_1, w) = y^2 \Phi_y(x_1, y, z_1, w),$$
$$\Phi_y(x_1, y, z_1, w) = wx_1^2 + x_1^3 y - x_1^2 yz_1(3yz_1 + 1) + x_1 y^2 z_1^3(3yz_1 + 1) - y^4 z_1^6 - 1.$$
$$\mathcal{C}_{p_1}^{\pm} \text{ in } \mathbf{1}_y: \quad y = 0, \quad x_1 = \pm 1/\sqrt{w}. \tag{5.4.10}$$
$$\delta_{p_1} \text{ in } \mathbf{1}_y: \quad \text{Invisible.}$$
$$\text{Singularities}: \quad \text{None.}$$

Chart $\mathbf{1}_z$

$$\Phi(x_1z, y_1z, z, w) = z^2 \Phi_z(x_1, y_1, z, w),$$
$$\Phi_z(x_1, y_1, z, w) = wx_1^2 + z\left(x_1^3 - x_1^2(3z + 1) + x_1 z(3z + 1) - z^3\right) - y_1^2.$$
$$\mathcal{C}_{p_1}^{\pm} \text{ in } \mathbf{1}_z: \quad z = 0, \quad y_1 = \pm\sqrt{w}x_1. \tag{5.4.11}$$
$$\delta_{p_1} \text{ in } \mathbf{1}_z: \quad z = 0, \quad y_1 = 0.$$
$$\text{Singularities}: \quad (x_1, y_1, z) = (0, 0, 0).$$

Here, chart $\mathbf{1}_x$ is the affine patch of $\mathbb{P}^2 \ni (x : y : z)$ for $x \neq 0$ in which $(x : y : z) = (1 : y_1 : z_1)$. The other charts are also similar[12].

2nd blow-up

As we can see, the only singularity after the first blow-up is $(x_1, y_1, z) = (0, 0, 0)$ on chart $\mathbf{1}_z$, which is not visible from the other charts. This is codimension-one, and we blow up this singularity by similarly inserting a one-parameter $(= w)$ family of $\mathbb{P}^2$ along $(x_1, y_1, z, w) = (0, 0, 0, w)$. The computation is similar. We find a singularity in chart $\mathbf{2}_{zz}$, while the blown-up equations are regular for charts $\mathbf{2}_{zx}$ and $\mathbf{2}_{zy}$. Here we show the result for the relevant charts $\mathbf{2}_{zx}$ and $\mathbf{2}_{zz}$.

Chart $\mathbf{2}_{zx}$

$$\Phi_z(x_1, x_1y_2, x_1z_2, w) = x_1^2 \Phi_{zx}(x_1, y_2, z_2, w),$$
$$\Phi_{zx}(x_1, y_2, z_2, w) = x_1(z_2 - 1)z_2 - x_1^2(z_2 - 1)^3 + w - y_2^2.$$
$$\mathcal{C}_{p_2}^{\pm} \text{ in } \mathbf{2}_{zx}: \quad x_1 = 0, \quad y_2 = \pm\sqrt{w}. \tag{5.4.12}$$
$$\delta_{p_2} \text{ in } \mathbf{2}_{zx}: \quad x_1 = 0, \quad y_2 = 0.$$
$$\text{Singularities}: \quad \text{None.}$$

---

[12]Note that we have used the same "z_1" in $\mathbf{1}_x$ and $\mathbf{1}_y$ for different coordinate variables, and similarly for x_1 and y_1. There will be no confusion as we do not compare equations in different charts.

Chart $\mathbf{2}_{zz}$

$$\Phi_z(x_2z, y_2z, z, w) = z^2 \Phi_{zz}(x_2, y_2, z, w),$$
$$\Phi_{zz}(x_2, y_2, z, w) = wx_2^2 + (x_2 - 1)z\left(x_2^2z - 2x_2z - x_2 + z\right) - y_2^2.$$
$$\mathcal{C}_{p_2}^{\pm} \text{ in } \mathbf{2}_{zz}: \quad z = 0, \quad y_2 = \pm\sqrt{w}x_2. \tag{5.4.13}$$
$$\delta_{p_2} \text{ in } \mathbf{2}_{zz}: \quad z = 0, \quad y_2 = 0.$$
$$\text{Singularities}: \quad (x_2, y_2, z) = (0, 0, 0).$$

3rd blow-up

We finally blow up the codimension-one singularity $(x_2, y_2, z) = (0, 0, 0)$ in chart $\mathbf{2}_{zz}$. It turns out that this completes the resolution process completely without leaving any singularities. The equations of the exceptional curve (with a definite w) in the relevant charts are:

Chart $\mathbf{3}_{zzx}$

$$\Phi_z z(x_2, x_2y_3, x_2z_3, w) = x_2^2 \Phi_{zzx}(x_2, y_3, z_3, w),$$
$$\Phi_{zzx}(x_2, y_3, z_3, w) = w + (x_2 - 1)z_3\left((x_2 - 1)^2z_3 - 1\right) - y_3^2.$$
$$\mathcal{C}_{p_3} \text{ in } \mathbf{3}_{zzx}: \quad x_2 = 0, \quad y_3^2 = w - (z_3 - 1)z_3. \tag{5.4.14}$$
$$\delta_{p_3} \text{ in } \mathbf{3}_{zzx}: \quad x_2 = 0, \quad y_3^2 = -(z_3 - 1)z_3.$$
$$\text{Singularities}: \quad \text{None.}$$

Chart $\mathbf{3}_{zzz}$

$$\Phi_z z(x_3z, y_3z, z, w) = z_2^2 \Phi_{zzz}(x_3, y_3, z, w),$$
$$\Phi_{zzz}(x_3, y_3, z, w) = x_3^2(w - z(3z + 1)) + x_3^3z^3 + 3x_3z + x_3 - y_3^2 - 1 = 0.$$
$$\mathcal{C}_{p_3} \text{ in } \mathbf{3}_{zzz}: \quad z_2 = 0, \quad y_3^2 = wx_3^2 + x_3 - 1. \tag{5.4.15}$$
$$\delta_{p_3} \text{ in } \mathbf{3}_{zzz}: \quad z_2 = 0, \quad y_3^2 = x_3 - 1.$$
$$\text{Singularities}: \quad \text{None.}$$

This completes the blowing-up process, and the space is now smooth. We have seen that conifold singularities do not appear at any stage of the blow-up at the D_6 points. This is similar to the case of the incomplete resolution at the E_6 point in the split I_6 model. However, unlike that case, the intersection of the exceptional curves does not change at all at the D_6 points.

Intersections of the exceptional curves

At fixed $w \neq 0$, we obtain five exceptional curves $\mathcal{C}_{p_1}^{\pm}$, $\mathcal{C}_{p_2}^{\pm}$ and $\mathcal{C}_{p_3}$. From the above explicit forms, we can see that their intersection matrix is given by the A_5 Dynkin diagram

(the top diagram of Fig. 5.5). Although $\mathcal{C}_{p_1}^{\pm}$ and $\mathcal{C}_{p_2}^{\pm}$ are respectively factorized into two lines on this fixed $w \neq 0$ plane, they do not factor in the polynomial ring of w. The two lines at some fixed $w \neq 0$ are interchanged with each other at $w = 0$, meaning that this is a non-split type of singularity. Thus the two lines for $\mathcal{C}_{p_1}^{\pm}$ or $\mathcal{C}_{p_2}^{\pm}$ at fixed $w \neq 0$ comprising the Kodaira fibres of type I_6 are identified. Hence we define

$$\mathcal{C}_{p_i} \equiv \frac{1}{2}(\mathcal{C}_{p_i}^{+} + \mathcal{C}_{p_i}^{-}) \quad (i = 1, 2), \tag{5.4.16}$$

which are the projections onto the components invariant under the diagram automorphism of the A_5 Dynkin diagram. Then we can show that the three exceptional curves $\mathcal{C}_{p_1}$, $\mathcal{C}_{p_2}$ and $\mathcal{C}_{p_3}$ form a non-simply-laced Dynkin diagram of C_3 (the middle diagram of Fig. 5.5).

At $w = 0$, we again encounter another difference between the present non-split case and the previous examples of singularities associated with the magic square. In the incomplete resolutions for the previous examples $(G, H) = (E_6, SU(6))$, $(E_7, SO(12))$ and (E_8, E_7), while the number of the exceptional fibres at $w = 0$ is the same as that at $w \neq 0$, some of the exceptional fibres at $w = 0$ turn out to be linear combinations of those at $w \neq 0$. Therefore, the intersection diagram of the exceptional fibres at $w = 0$ becomes different from that at $w \neq 0$ as we summarized in Section 5.2. Here, we see something different. As in the previous section, by lifting up the exceptional curves from the defining chart into subsequent charts and seeing their relations, one finds that

$$\mathcal{C}_{p_1}^{\pm} \to \delta_{p_1}, \quad \mathcal{C}_{p_2}^{\pm} \to \delta_{p_2}, \quad \mathcal{C}_{p_3} \to \delta_{p_3}. \tag{5.4.17}$$

Substituting them into (5.4.16), we obtain

$$\mathcal{C}_{p_1} \to \delta_{p_1}, \quad \mathcal{C}_{p_2} \to \delta_{p_2}, \quad \mathcal{C}_{p_3} \to \delta_{p_3}. \tag{5.4.18}$$

Thus, the intersection matrix remains identical even at the codimension-two point (see the bottom diagram of Fig. 5.5). This is a sharp contrast to the previous examples, where the intersection matrices at $w = 0$ did not coincide with any of (the minus of) the Lie algebra Cartan matrices.
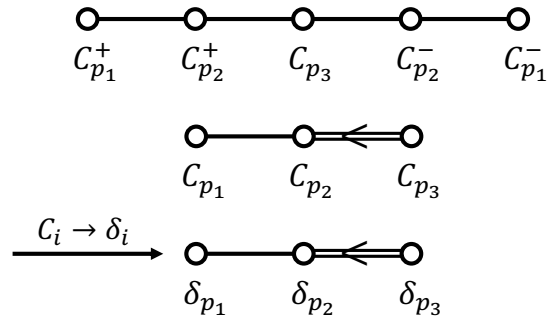
Figure 5.5: Intersection diagrams of the exceptional curves of C_3 model at a D_6 point: (Top) $w \neq 0$ before the projection (5.4.16); (Middle) $w \neq 0$ after the projection (5.4.16); (Bottom) $w = 0$.

Chapter 6

Split/Non-split Transitions as Conifold Transitions

In this chapter, toward understanding the puzzles associated with non-local matter generation discussed in the previous chapter, we investigate the relationship between the split models and the non-split models for all cases that we can distinguish between the split and non-split fibre types: I_n ($n \geq 3$), I_n^* ($n \geq 0$), IV and IV^* [95]. We focus on the conifold singularities which arise at certain codimension-two singularities and which characterize the difference between the split models and the non-split models. We then show that the split/non-split transition is a conifold transition except for a special class of models. This chapter is based on our paper [95].

6.1 "Deligne form"

In this section, we introduce the "Deligne form" from the Tate form (5.3.1) for the resolution analysis in this chapter. Let us consider six-dimensional F-theory compactified on an elliptic Calabi-Yau threefold Y_3 with section fibred over a Hirzebruch surface $\mathbb{F}_n$ ($n \geq 0$) [87, 88]. We define Y_3 as a hypersurface

$$P = -(y^2 + a_1 xy + a_3 y) + x^3 + a_2 x^2 + a_4 x + a_6 = 0 \qquad (6.1.1)$$

in a complex four-dimensional ambient space X_4, which itself is a $\mathbb{P}^2$ fibration over $\mathbb{F}_n$. (x, y) are the affine coordinates in a coordinate patch of $\mathbb{P}^2$ where one of the homogeneous coordinates does not vanish and hence is set to 1. Let $\mathcal{K}$ be the canonical bundle of $\mathbb{F}_n$, then x and y are sections of $\mathcal{K}^{-2}$ and $\mathcal{K}^{-3}$, whereas a_j ($j = 1, 2, 3, 4, 6$) are ones of $\mathcal{K}^{-j}$, respectively, so that the hypersurface (6.1.1) defines a Calabi-Yau threefold.

A Hirzebruch surface $\mathbb{F}_n$ is a $\mathbb{P}^1$ fibration over $\mathbb{P}^1$, defined as a toric variety with the

following toric charges (4.2.2)

	u'	v'	u	v
$Q^{(\lambda)}$	1	1	n	0
$Q^{(\mu)}$	0	0	1	1.

$(6.1.2)$

$(u' : v')$ are the homogeneous coordinates of the base $\mathbb{P}^1$, while $(u : v)$ are the ones of the fibre $\mathbb{P}^1$. The anti-canonical bundle corresponds to the divisor $(n+2)D_{u'}+2D_v$, where we denote, for a given coordinate X, by D_X a divisor defined by the zero locus $X = 0$. Thus, if we define affine coordinates $z \equiv \frac{u}{v}$, $w \equiv \frac{u'}{v'}$ in a patch $v \neq 0$ and $v' \neq 0$, the section a_j is given as a $2j$th degree polynomial in z and a $j(n+2)$th degree polynomial in w.

The hypersurface so defined is also a $K3$ fibration, the base of which is the base $\mathbb{P}^1$ of $\mathbb{F}_n$. We next consider the stable degeneration limit of this $K3$. Schematically, this is regarded as a limit of splitting into a pair of rational elliptic surfaces dP_9 glued together along the torus fibre over the "infinite points" of the respective bases. See [88, 145] for a more rigorous definition.

It is convenient to move on to a dP_9 fibration over the same $\mathbb{P}^1$ with u', v' being its coordinates. To do this, we have only to change the divisor class of a_j from $j((n+2)D_{u'} + 2D_v)$ $(=$ the divisor of $\mathcal{K}^{-j})$ to

$$j((n+2)D_{u'} + D_v). \tag{6.1.3}$$

With this change, a_j is still a $j(n+2)$th degree polynomial in w but becomes jth degree in z. Likewise, the divisor classes of x and y are modified from $2((n+2)D_{u'} + 2D_v)$, $3((n+2)D_{u'} + 2D_v)$ to

$$2((n+2)D_{u'} + D_v), \quad 3((n+2)D_{u'} + D_v), \tag{6.1.4}$$

respectively. This dP_9 fibre describes one E_8 of the $E_8 \times E_8$ gauge symmetry. The terms of degrees from $j+1$ to $2j$ appearing in a_j for the $K3$ fibration correspond to the other dP_9 residing "beyond the infinity". For generic dP_9 fibrations, a_j is expanded as

$$a_j = a_{j,0} + a_{j,1}z + \cdots + a_{j,j-1}z^{j-1} + a_{j,j}z^j \quad (j = 1, 2, 3, 4, 6), \tag{6.1.5}$$

then the section $a_{j,k}$ of each coefficient becomes a $((j-k)n + 2j)$th degree polynomial in w due to the nonzero Q^1 charge carried by u.

As an equation of an elliptic fibre, Eq. (6.1.1) is commonly referred to as Tate form. We can complete the square with respect to y in Eq. (6.1.1) to obtain (with a redefinition of y)

$$-y^2 + x^3 + \frac{b_2}{4}x^2 + \frac{b_4}{2}x + \frac{b_6}{4} = 0, \tag{6.1.6}$$

$$
\begin{aligned}
b_2 &= a_1^2 + 4a_2, \\
b_4 &= a_1a_3 + 2a_4, \\
b_6 &= a_3^2 + 4a_6,
\end{aligned}
\tag{6.1.7}
$$

which, though less common, we call the "Deligne form" in this thesis [146]. b_j is a section of the same line bundle as a_j and similarly expanded as

$$b_j = b_{j,0} + b_{j,1}z + \cdots + b_{j,j-1}z^{j-1} + b_{j,j}z^j \quad (j = 2, 4, 6), \tag{6.1.8}$$

where $b_{j,k}$ is also a $((j - k)n + 2j)$th degree polynomial in w. It is also convenient to define [90]

$$b_8 = \frac{1}{4}(b_2 b_6 - b_4^2), \tag{6.1.9}$$

which is the (minus of the) discriminant of the quadratic equation

$$\frac{b_2}{4}x^2 + \frac{b_4}{2}x + \frac{b_6}{4} = 0 \tag{6.1.10}$$

of x.

Finally, we can "complete the cube" with respect to x in Eq. (6.1.6) and find (with a redefinition of x)

$$-y^2 + x^3 + fx + g = 0, \tag{6.1.11}$$

$$\begin{aligned}
f &= -\frac{1}{48}(b_2^2 - 24b_4), \\
g &= \frac{1}{864}\left(b_2^3 - 36b_2 b_4 + 216b_6\right),
\end{aligned} \tag{6.1.12}$$

which is called the "Weierstrass form". f and g are sections of the same line bundle as a_4 and a_6, respectively, and in the dP_9 fibration they are expanded as

$$\begin{aligned}
f &= f_{4,0} + f_{4,1}z + \cdots + f_{4,4}z^4, \\
g &= g_{6,0} + g_{6,1}z + \cdots + g_{6,6}z^6,
\end{aligned} \tag{6.1.13}$$

where $f_{4,k}$, $g_{6,k}$ are written as $f_{(4-k)n+8}$, $g_{(6-k)n+12}$ in [87], whose degrees in w are specified by their subscripts. The discriminant Δ of Eq. (6.1.11) is

$$\begin{aligned}
\Delta &= 4f^3 + 27g^2 \\
&= \frac{1}{16}\left(b_2^2 b_8 - 9b_2 b_4 b_6 + 8b_4^3 + 27b_6^2\right).
\end{aligned} \tag{6.1.14}$$

Consider the case where the elliptic fibre over $z = 0$ of the base $\mathbb{P}^1$ of this dP_9 (i.e. the fibre $\mathbb{P}^1$ of the $\mathbb{F}_n$) has a singularity, and the exceptional fibres after the resolution fall into one of Kodaira's fibre types. It is well-known that the fibre type of a given singularity is determined in terms of the vanishing orders of the sections f, g of the Weierstrass form as well as the discriminant Δ (Table 6.1).

Note that, in Kodaira's classification, there is no upper limit on the vanishing orders of f, g or Δ (since any large value of n is allowed for the fibre type I_n or I_n^* as a fibre

type)[1], but there *is* when we try to realize singular fibres in a dP_9 fibration. Since the relationship between the split/non-split transition and the conifold transition discussed below is also a local one in the sense that it does not depend on another singularity located far away, we will also need to consider a high vanishing order that cannot be realized in a dP_9 fibration. So in this thesis, we will first start from a dP_9 fibration and consider the heterotic duality when it makes sense, while discussing the relationship between the two transitions locally in the same set-up even when the fibre cannot be realized in a dP_9 fibration.

As we already described in Subsection 5.1.1, if the type of a singular fibre is either I_n ($n = 3, 4, \ldots$), I_n^* ($n = 0, 1, \ldots$), IV or IV^* at a generic point w on the divisor $z = 0$ in $\mathbb{F}_n$, it is further classified as a split type or a non-split type, depending on whether or not the split condition is satisfied globally[2]. We have listed them in Table 6.1 together with the required constraints for the fibres to be classified into the respective types[3]. In the following, we will study these individual cases.

6.2 Split/non-split transitions as conifold transitions (I): the I_{2k} models

6.2.1 Generalities of the I_n models

Let us first summarize the generalities of the I_n models common to both cases when n is even and when n is odd[4]. As displayed in Table 6.1, the vanishing orders of the sections b_2, b_4 and b_6 of Eq. (6.1.6) are $(0, k, 2k)$ for both I_{2k} and I_{2k+1}. The only difference is that the order of b_8 (6.1.9) is the generic value $2k$ in the I_{2k} type, while in the I_{2k+1} type b_2, b_4 and b_6 take special values so that the order of b_8 goes up to $2k + 1$. Explicitly, the equation of these models is given by

---

[1]Of course, as is well known, if the orders of f and g increase simultaneously to 4 and 6, the resulting singularities will have bad properties.

[2]$k = 1$ (I_0^*) is a special case because there are three different types (split, non-split and semi-split) in this case; see [147] for details.

[3]Note that the vanishing orders for b_i's ($i = 2, 4, 6, 8$) presented here are, unlike the conventional orders in Tate form [1,90,91], the ones which are such that a given fibre type can be described by *generic* b_i's with these orders. For example, the orders of the sections a_i's determining Tate form ($i = 1, 2, 3, 4, 6$) for the non-split I_{2k+1} model are known to be $(0, 0, k + 1, k + 1, 2k + 1)$, which imply the orders of b_4 and b_6 calculated using these data are $k + 1$ and $2k + 1$ instead of k and $2k$. These Tate's orders are the ones that are maximally raised within what a given fibre type can achieve, and only the specially tuned sections with appropriate redefinitions of x and y can satisfy the condition. Indeed, as we show explicitly below, the orders of the generic b_4 and b_6 that can achieve a non-split I_{2k+1} model are k and $2k$.

[4]The resolutions of the split I_n and I_n^* models for even and odd n were already computed in detail in [120].

Table 6.1: Singularities of the split and non-split fibre types. I_{2k+1}^{os} denotes the "over-split" type which is explained in the text [95]. The $\text{ord}(b_i)$ and $\text{ord}(\Delta)$ denote the order of z of (b_i) and (Δ), where z is a inhomogeneous coordinate of $\mathbb{P}^1_{fibre}$.

Kodaira's fibre type	$\text{ord}(b_2)$	$\text{ord}(b_4)$	$\text{ord}(b_6)$	$\text{ord}(b_8)$	$\text{ord}(\Delta)$	Additional constraint(s)	Split/non-split fibre type
$I_{2k}(k \geq 2)$	0	k	$2k$	$2k$	$2k$	$b_{2,0} = c_{1,0}^2$	I_{2k}^s
						$b_{2,0}$ generic	I_{2k}^{ns}
$I_{2k+1}(k \geq 1)$	0	k	$2k$	$2k+1$	$2k+1$	$\begin{cases} b_{2,0} = c_{1,0}^2 \\ b_{4,k} = c_{1,0}c_{3,k} \\ b_{6,2k} = c_{3,k}^2 \end{cases}$	I_{2k+1}^s
						$\begin{cases} b_{2,0}\ \text{generic} \\ b_{4,k} = b_{2,0}c_{2,k} \\ b_{6,2k} = b_{2,0}c_{2,k}^2 \end{cases}$	I_{2k+1}^{ns}
						$\begin{cases} b_{2,0} = c_{1,0}^2 \\ b_{4,k} = c_{1,0}^2 c_{2,k} \\ b_{6,2k} = c_{1,0}^2 c_{2,k}^2 \end{cases}$	I_{2k+1}^{os}
I_0^*	1	2	3	4	6	$\begin{cases} b_{2,1} = 4(p_{2,1} + q_{2,1} + r_{2,1}) \\ b_{4,2} = 2(p_{2,1}q_{2,1} + q_{2,1}r_{2,1} + r_{2,1}p_{2,1}) \\ b_{6,3} = 4p_{2,1}q_{2,1}r_{2,1} \end{cases}$	I_0^{*s}
						$\begin{cases} b_{2,1} = 4(p_{2,1} + q_{2,1}) \\ b_{4,2} = 2(p_{2,1}q_{2,1} + r_{4,2}) \\ b_{6,3} = 4p_{2,1}r_{4,2} \end{cases}$	I_0^{*ss}
						$b_{2,1}, b_{4,2}, b_{6,3}$ generic	I_0^{*ns}
$I_{2k-3}^*(k \geq 2)$	1	$k+1$	$2k$	$2k+1$	$2k+3$	$b_{6,2k} = c_{3,k}^2$	I_{2k-3}^{*s}
						$b_{6,2k}$ generic	I_{2k-3}^{*ns}
$I_{2k-2}^*(k \geq 2)$	1	$k+1$	$2k+1$	$2k+2$	$2k+4$	$b_{8,2k+2} = c_{4,k+1}^2$	I_{2k-2}^{*s}
						$b_{8,2k+2}$ generic	I_{2k-2}^{*ns}
IV	1	2	2	3	4	$b_{6,2} = c_{3,1}^2$	IV^s
						$b_{6,2}$ generic	IV^{ns}
IV^*	2	3	4	6	8	$b_{6,4} = c_{3,2}^2$	IV^{*s}
						$b_{6,4}$ generic	IV^{*ns}

$$\Phi(x, y, z, w) \equiv -y^2 + x^3 + \tfrac{1}{4}(b_{2,0} + b_{2,1}z + \cdots)x^2$$
$$+ \tfrac{1}{2}(b_{4,k}z^k + b_{4,k+1}z^{k+1} + \cdots)x$$
$$+ \tfrac{1}{4}(b_{6,2k}z^{2k} + b_{6,2k+1}z^{2k+1} + \cdots) = 0. \qquad (6.2.1)$$

As mentioned at the end of the previous section, this equation is not well defined as a dP_9 fibration when k is large (e.g., $k \geq 4$), but even in that case we will use it to analyze the

local structure near the conifold singularities associated with the split/non-split transition.

Eq. (6.2.1) has a singularity at $(x, y, z) = (0, 0, 0)$ for arbitrary w in both cases. We will blow up this singularity, as well as the ones we will subsequently encounter, by taking the usual steps. Let us explain the general procedure of how this is done by taking the present case as an example. Our notation is similar to the one used in our paper [98].

We first replace the point $(x, y, z) = (0, 0, 0)$ in the complex three-dimensional (x, y, z) space, which is a local patch of the three-dimensional ambient space defining the dP_9, by a $\mathbb{P}^2$ by replacing $\mathbf{C}^3 \ni (x, y, z)$ with

$$\hat{\mathbf{C}}^3 = \{((x, y, z), (\xi : \eta : \zeta)) \in \mathbf{C}^3 \times \mathbb{P}^2 \mid (x : y : z) = (\xi : \eta : \zeta)\}. \qquad (6.2.2)$$

We work in inhomogeneous coordinates defined in three different patches of this $\mathbb{P}^2$

$$\begin{aligned}
(x : y : z) = (\xi : \eta : \zeta) &= (1 : y_1 : z_1) & (\mathbf{1}_x, \, x \neq 0), \\
&= (x_1 : 1 : z_1) & (\mathbf{1}_y, \, y \neq 0), \\
&= (x_1 : y_1 : 1) & (\mathbf{1}_z, \, z \neq 0),
\end{aligned} \qquad (6.2.3)$$

where $\mathbf{1}_x$, $\mathbf{1}_y$ and $\mathbf{1}_z$ are the names of the coordinate patches[5]. Then replacing $\mathbf{C}^3$ with $\hat{\mathbf{C}}^3$ (6.2.2) is simply achieved by replacing (x, y, z) with (x, xy_1, xz_1) in $\mathbf{1}_x$, (x_1y, y, yz_1) in $\mathbf{1}_y$ and (x_1z, y_1z, z) in $\mathbf{1}_z$ in Eq. (6.2.1), respectively, followed by dividing by the square of the scale factor

$$\begin{aligned}
x^{-2}\Phi(x, xy_1, xz_1, w) &\equiv \Phi_x(x, y_1, z_1, w) = 0 & (\mathbf{1}_x), \\
y^{-2}\Phi(x_1y, y, yz_1, w) &\equiv \Phi_y(x_1, y, z_1, w) = 0 & (\mathbf{1}_y), \\
z^{-2}\Phi(x_1z, y_1z, z, w) &\equiv \Phi_z(x_1, y_1, z, w) = 0 & (\mathbf{1}_z)
\end{aligned} \qquad (6.2.4)$$

so as not to change the canonical class.

Then we see that, unless $k = 1$ (I_2 and I_3), another singularity appears in the patch $\mathbf{1}_z$ at $(x_1, y_1, z) = (0, 0, 0)$, then we do a similar replacement and factorization

$$\begin{aligned}
x_1^{-2}\Phi_z(x_1, x_1y_2, x_1z_2, w) &\equiv \Phi_{zx}(x_1, y_2, z_2, w) = 0 & (\mathbf{2}_{zx}), \\
y_1^{-2}\Phi_z(x_2y_1, y_1, y_1z_2, w) &\equiv \Phi_{zy}(x_2, y_1, z_2, w) = 0 & (\mathbf{2}_{zy}), \\
z^{-2}\Phi_z(x_2z, y_2z, z, w) &\equiv \Phi_{zz}(x_2, y_2, z, w) = 0 & (\mathbf{2}_{zz}).
\end{aligned} \qquad (6.2.5)$$

for each patch of another $\mathbb{P}^2$ put at $(x_1, y_1, z) = (0, 0, 0)$. Again, if k is larger than two, we find a singularity in the patch $\mathbf{2}_{zz}$, which we blow up to obtain $\Phi_{zzz}(x_3, y_3, z, w)$. Repeating these steps k times yields $\Phi_{\underbrace{z \cdots z}_{k}}(x_k, y_k, z, w)$, the properties of which differ between the types I_{2k} and I_{2k+1}.

---

[5] In Eq. (6.2.3), one and the same symbol represents two different variables in different equations (y_1 in $\mathbf{1}_x$ and $\mathbf{1}_z$, for instance). There will be no confusion, however, since these two patches will not be considered at the same time.

In the following, we will use the following j-times blown-up equations recursively defined by

$$z^{-2}\Phi_{\underbrace{z\ldots z}_{j-1}}(x_j z, y_j z, z, w) \equiv \Phi_{\underbrace{z\ldots z}_{j}}(x_j, y_j, z, w) = 0 \quad (\boldsymbol{j}_{\underbrace{z\ldots z}_{j}}), \qquad (6.2.6)$$

$$x_{j-1}^{-2}\Phi_{\underbrace{z\ldots z}_{j-1}}(x_{j-1}, x_{j-1}y_j, x_{j-1}z_j, w) \equiv \Phi_{\underbrace{z\ldots z}_{j-1}x}(x_{j-1}, y_j, z_j, w) = 0 \quad (\boldsymbol{j}_{\underbrace{z\ldots z}_{j-1}x})(6.2.7)$$

from the $(j-1)$-times blown-up equation $\Phi_{\underbrace{z\ldots z}_{j-1}}(x_{j-1}, y_{j-1}, z, w) = 0$ defined in the coordinate patch $(\boldsymbol{j-1})_{\underbrace{z\ldots z}_{j-1}}$. (Again, y_j's in Eq. (6.2.6) and Eq. (6.2.7) are different.)

6.2.2 Codimension-one singularities of the I_n models

We have seen in the previous subsection that there appears a singularity in $\mathbf{1}_z$ at $(x_1, y_1, z) = (0,0,0)$ for arbitrary w, and after the blow-up there is, if $k \geq 3$, another at $(x_2, y_2, z) = (0,0,0)$ in $\mathbf{2}_{zz}$ for arbitrary w. These singular "points" in the sense of Kodaira are aligned along the base $\mathbb{P}^1$ of $\mathbb{F}_n$, and hence form complex one-dimensional curves. If, though not considered in this thesis, our set-up is generalized to a 4D F-theory compactification where the dP_9 is fibred on some complex two-dimensional base, these singularities are aligned to form complex surfaces. Thus, in this thesis, we will call such a singularity in the sense of Kodaira, that forms a codimension-one locus when projected onto the base of the elliptic fibration, a codimension-one singularity.

Using this terminology, we can say that, in the process of blowing up, both the I_{2k} and I_{2k+1} models yield a codimension-one singularity p_j at $(x_j, y_j, z, w) = (0,0,0,w)$ for every $j = 0, \ldots, k-1$ in $\boldsymbol{j}_{\underbrace{z\ldots z}_{j}}$, where we define $(x_0, y_0, z, w) \equiv (x, y, z, w)$. The explicit form of $\Phi_{\underbrace{z\ldots z}_{j}}(x_j, y_j, z, w)$ representing the model in this patch is given by

$$\begin{aligned}
\Phi_{\underbrace{z\ldots z}_{j}}(x_j, y_j, z, w) &= -y_j^2 + x_j^3 z^j + \tfrac{1}{4}(b_{2,0} + b_{2,1}z + \cdots)x_j^2 \\
&\quad + \tfrac{1}{2}(b_{4,k}z^{k-j} + b_{4,k+1}z^{k-j+1} + \cdots)x_j \\
&\quad + \tfrac{1}{4}(b_{6,2k}z^{2(k-j)} + b_{6,2k+1}z^{2(k-j)+1} + \cdots) \\
&\xrightarrow{z\to 0} -y_j^2 + \tfrac{1}{4}b_{2,0}x_j^2, \qquad\qquad (6.2.8)
\end{aligned}$$

where the exceptional "curve" (in the $\mathbb{P}^2$ blown up over some point of the base with fixed (generic) w) splits into two lines in the sense of Kodaira. Thus, for each generic w, p_j is located at the intersection point of these exceptional curves that have arisen from blowing up p_{j-1} $(j = 1, \ldots, k-1)$. Blowing up the final singularity p_{k-1} yields a single irreducible exceptional curve for the I_{2k} case, and a pair of split lines for the I_{2k+1} case (see Fig 6.1 and 6.2). Putting them all together, they constitute the A_{2k-1} and A_{2k} Dynkin diagrams as their intersection diagrams, as is well known.

6.2.3 Conifold singularities associated with the split/non-split transition in the I_{2k} models

Now let us explain what "conifold singularities associated with the split/non-split transition" are, by taking I_{2k} models as an example. Since there is no distinction between split and non-split fibre types in the fibre type I_2, let us consider I_{2k} for $k \geq 2$.

The equation of the *split* I_{2k} model for $k \geq 2$ is given by Eq. (6.2.1) with

$$b_{2,0} = c_{1,0}^2 \tag{6.2.9}$$

for some section $c_{1,0}$. A split I_{2k} model exhibits, in addition to these codimension-one singularities, conifold singularities on singular fibres over some special loci on the base of the elliptic fibration, where the generic A_{n-1} singularity is enhanced to some higher-rank one.

The discriminant of Eq. (6.2.1) with Eq. (6.2.9) reads

$$\Delta \;\; = \;\; \frac{1}{16} c_{1,0}^4 b_{8,2k} z^{2k} + \cdots . \tag{6.2.10}$$

f and g (6.1.12) derived from Eq. (6.2.1) are

$$\begin{aligned} f &= -\frac{1}{48} c_{1,0}^4 + \cdots , \\ g &= \frac{1}{864} c_{1,0}^6 + \cdots . \end{aligned} \tag{6.2.11}$$

Eq. (6.2.10) shows that at the zero loci of $c_{1,0}$ and $b_{8,2k}$, the singularity is enhanced from A_{2k-1}. Since Eq. (6.2.11) implies that the vanishing orders of f and g are unchanged at the zero loci of $b_{8,2k}$, they are "A_{2k} points", which means that they are the places on the base over which the singularities of the fibres are enhanced to A_{2k}. On the other hand, at the zero loci of $c_{1,0}$, it turns out that the vanishing orders of f , g and Δ go up to two, three and $2k + 2$, so the zero loci of $c_{1,0}$ are "D_{2k} points", which similarly means that the singularities are enhanced to D_{2k} there. In fact, they are singularities of the type of the "complete resolution" [93], meaning that they develop the necessary amount of conifold singularities to yield the degrees of freedom of matter hypermultiplets arising there. Thus, according to the general rule [96], the zero loci of $b_{8,2k}$ are the places (on the base) where a hypermultiplet transforming in $\mathbf{2k}$ of A_{2k-1} arises, and those of $c_{1,0}$ are where a hypermultiplet in $\mathbf{k(2k-1)}$ appears. In general, a section $c_{i,j}$ or $b_{i,j}$ or whatever with a subscript (i,j) is expressed as a polynomial of degree $(i-j)n + 2i$ in w [148], so we have $(8 - 2k)n + 16$ hypermultiplets in the $\mathbf{2k}$ representation, and $n + 2$ hypermultiplets in the $\mathbf{k(2k-1)}$ representation.

We will focus on the singularity enhancement to D_{2k} at the zero loci of $c_{1,0}$ since it is this singularity enhancement that its associated conifold singularities and their transitions are closely related to the split/non-split transitions in F-theory. Indeed, if we do *not*

impose the condition (6.2.9) to Eq. (6.2.1), we have an equation of the *non-split* I_{2k} model, for which the corresponding f, g and Δ are the ones obtained by simply replacing every $c_{1,0}^2$ with $b_{2,0}$ in Eq. (6.2.11) and Eq. (6.2.10). Even then, the vanishing orders of f, g and Δ at the zero loci of $b_{2,0}$ remain the same as those at the loci of $c_{1,0}$, which means that the number of D_{2k} points is doubled ($b_{2,0}$ is represented as a polynomial of degree $2n + 4$ in w).

Of course, in this process of the transition from the split model to the non-split one, the D_{2k} points, which have doubled in number, cannot continue to produce **k(2k − 1)**'s after the transition to the non-split side; they are too many to satisfy the anomaly cancellation condition. Therefore, the structure of the conifold singularities that existed before the transition to the non-split model must change after the transition. They are what we call the conifold singularities associated with the split/non-split transition. In contrast, singularity structures of the fibres over the A_{2k} points at which $b_{8,2k}$ vanishes do not change by the replacement $c_{1,0}^2 \leftrightarrow b_{2,0}$[6].

6.2.4 Conifold singularities in the split I_{2k} models for $k \geq 3$

To show how these conifold singularities arise at the D_{2k} points in the blowing-up process of the split I_{2k} models, let us consider the j-times blown-up equation $\Phi_{\underbrace{z \cdots z}_{j-1} x}(x_{j-1},$
$y_j, z_j, w) = 0$ in the patch $\boldsymbol{j}_{\underbrace{z \cdots z}_{j-1} x}$ for $j = 2, \ldots, k - 1$ with $k \geq 3$ which is recursively defined in Eq. (6.2.7) in Subsection 6.2.1. $k = 2$ (I_4) is a special case, so we will consider it separately in the next subsection.

The left-hand side of this equation is explicitly given by

$$
\begin{aligned}
\Phi_{\underbrace{z \cdots z}_{j-1} x}(x_{j-1}, y_j, z_j, w) \;=\;& -y_j^2 + x_{j-1}^j z_j^{j-1} \\[4pt]
& + \tfrac{1}{4}\big(c_{1,0}^2 + b_{2,1} x_{j-1} z_j + \cdots\big) \\
& + \tfrac{1}{2} x_{j-1}^{k-j} z_j^{k-j+1}\big(b_{4,k} + b_{4,k+1} x_{j-1} z_j + \cdots\big) \\
& + \tfrac{1}{4} x_{j-1}^{2(k-j)} z_j^{2(k-j+1)}\big(b_{6,2k} + b_{6,2k+1} x_{j-1} z_j + \cdots\big) \\[4pt]
=\;& -y_j^2 + \tfrac{1}{4} c_{1,0}^2 + x_{j-1} z_j \Big(x_{j-1}^{j-1} z_j^{j-2} + \tfrac{1}{4} b_{2,1} \\
& + \tfrac{1}{2} b_{4,k} x_{j-1}^{k-j-1} z_j^{k-j} + \tfrac{1}{4} b_{6,2k} x_{j-1}^{2(k-j)-1} z_j^{2(k-j)+1} + O(x_{j-1} z_j) \Big).
\end{aligned}
$$
$$(6.2.12)$$

---

[6]The six-dimensional F-theory models with an unbroken A_5 or A_7 gauge symmetry also allow E_6 or E_8 points, but it is known [91, 149] that they cannot be realized in Tate or Deligne forms with maximal Tate's orders, but require to be formulated in a Weierstrass form or Tate form with lower Tate's orders. In any case, however, these singularities also do not change by the replacement $c_{1,0}^2 \leftrightarrow b_{2,0}$ and hence have nothing to do with the split/non-split transition.

In general, a conifold is defined in $\mathbf{C}^4 \ni (z_1, z_2, z_3, z_4)$ by the equation

$$z_1 z_4 + z_2 z_3 = 0, \tag{6.2.13}$$

where $(z_1, z_2, z_3, z_4) = (0,0,0,0)$ is the conifold singularity. Thus Eq. (6.2.12) shows that the geometry near $y_j = c_{1,0} = x_{j-1} = z_j = 0$ is locally approximated by that of a conifold, and the point itself is the conifold singularity for each $j = 2, \ldots, k - 1$ $(k \geq 3)$.

Since these $k - 2$ conifold singularities arise in the blowing-up process of a split I_{2k} model at each zero locus of $c_{1,0}$, the number of which is $n + 2$ in total in the present $\mathbb{F}_n$ case (because $c_{1,0}$ is a polynomial of degree $n + 2$; see Subsection 6.2.3.). Let us pay attention to a particular zero of this $c_{1,0}$, and we can take it to $w = 0$ without loss of generality. That is,

$$c_{1,0} = w + O(w^2) \tag{6.2.14}$$

near $w = 0$. Then we see from Eq. (6.2.12) that the equation $\Phi_{\underbrace{z \cdots z}_{j-1} x}(x_{j-1}, y_j, z_j, w) = 0$ near $(x_{j-1}, y_j, z_j, w) = (0,0,0,0)$ is

$$-y_j^2 + \tfrac{1}{4}w^2 + (\text{const.} \times) x_{j-1} z_j \quad = \quad 0 \tag{6.2.15}$$

up to higher-order terms. The first two terms are factorized to yield the standard conifold equation (6.2.13).

Eq. (6.2.15) tells us that it is precisely the fact that the section $b_{2,0}$ is in the form of a square $c_{1,0}^2$ that the blown-up equations $\Phi_{\underbrace{z \cdots z}_{j-1} x}(x_{j-1}, y_j, z_j, w) = 0$ give rise to conifold singularities. If $b_{2,0}$ were not in square form $c_{1,0}^2$, which implies that the model is non-split, Eq. (6.2.12) would be

$$\Phi_{\underbrace{z \cdots z}_{j-1} x}(x_{j-1}, y_j, z_j, w) \quad = \quad -y_j^2 + \tfrac{1}{4}b_{2,0} + x_{j-1} z_j (\cdots), \tag{6.2.16}$$

in which $b_{2,0}$ generically vanishes like w near $w = 0$, and the corresponding local equation would be

$$-y_j^2 + \tfrac{1}{4}w + (\text{const.} \times) x_{j-1} z_j \quad = \quad 0 \tag{6.2.17}$$

up to higher-order terms, which is not a conifold equation.

In the following, we will refer to the $k - 2$ conifold singularities arising at each zero locus of $c_{1,0}$ as[7]

---

[7] At first glance, this way of naming the conifold singularities may seem strange, but as we will see later, its subscript q_j denotes the corresponding codimension-one D_{2k} singularity. We will use "v" to denote that it is a conifold singularity.
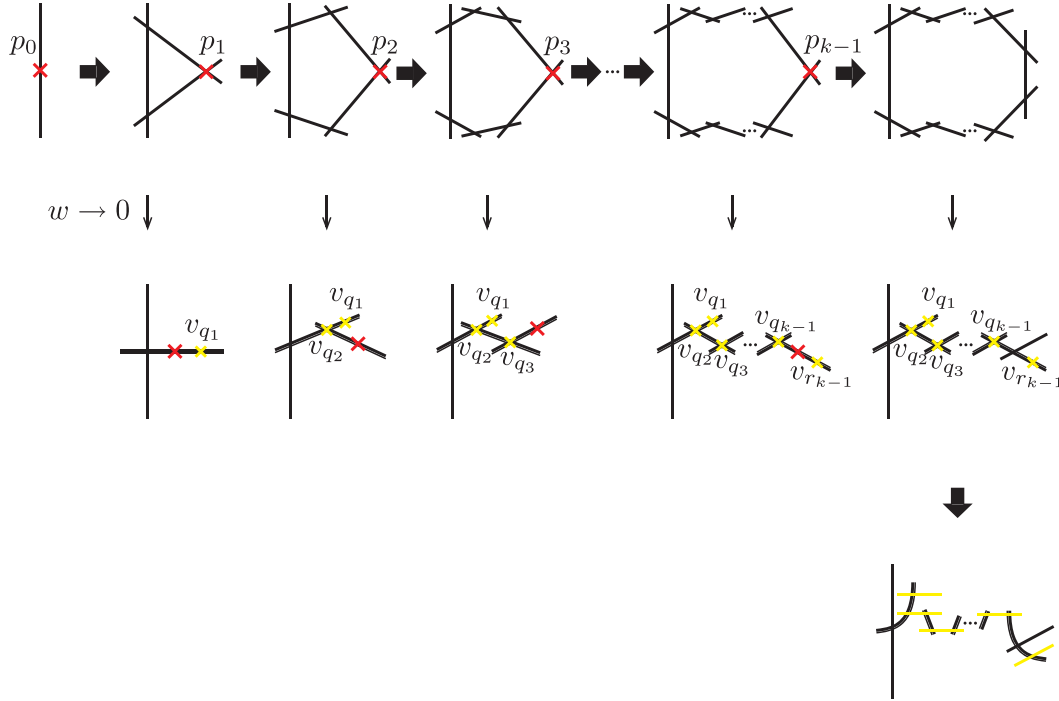
Figure 6.1: Singularities and exceptional curves arising in the blow-up of a split I_{2k} model near a D_{2k} point $w = 0$. codimension-one singularities and conifold singularities are depicted with red and yellow x's, respectively. Each bold horizontal arrow indicates a blow-up at a codimension-one singularity, and the final thick downward arrow means small resolutions of all the conifold singularities. The thin downward arrows denote the $w \to 0$ limit. The left-most vertical line in each figure represents the original singular fibre.

$$v_{q_2}: \quad (x_1, y_2, z_2, w) = (0, 0, 0, 0) \quad (\mathbf{2}_{zx}),$$

$$\vdots$$

$$v_{q_j}: \quad (x_{j-1}, y_j, z_j, w) = (0, 0, 0, 0) \quad (\boldsymbol{j}_{\underbrace{z \cdots z}_{j-1} x}), \tag{6.2.18}$$

$$\vdots$$

$$v_{q_{k-1}}: \quad (x_{k-2}, y_{k-1}, z_{k-1}, w) = (0, 0, 0, 0) \quad ((\boldsymbol{k-1})_{\underbrace{z \cdots z}_{k-2} x}).$$

They are depicted with a yellow x in Fig. 6.1.

In addition to the $k - 2$ conifold singularities $v_{q_2}, \ldots, v_{q_{k-1}}$, there are two more conifold singularities. One is the one on the locus of the one-time blown-up equation $\Phi_z(x_1, y_1, z, w) = 0$ given by Eq. (6.2.8) with $j = 1$, where $b_{2,0}$ satisfies the split condition $b_{2,0} = c_{1,0}^2$. If $k \geq 3$, $\Phi_z(x_1, y_1, z, w)$ can be written as

$$\Phi_z(x_1, y_1, z, w) = -y_1^2 + \tfrac{1}{4}c_{1,0}^2 x_1^2 + z\left(x_1^3 + \tfrac{1}{4}b_{2,1}x_1^2 + O(z)\right), \tag{6.2.19}$$

so focusing on a particular zero of $c_{1,0}$ and set $c_{1,0} = w$, the equation becomes

$$-y_1^2 + \tfrac{1}{4}w^2 x_1^2 + z\left(x_1^3 + \tfrac{1}{4}b_{2,1}x_1^2\right) = 0 \tag{6.2.20}$$

near $z = w = 0$. $y_1 = w = z = x_1 = 0$ is a special case of p_1, so assuming $x_1 \neq 0$, we find

$$v_{q_1}: \quad (x_1, y_1, z, w) = (-\tfrac{1}{4}b_{2,1}, 0, 0, 0) \quad (\mathbf{1}_z) \tag{6.2.21}$$

is a conifold singularity that arises besides $v_{q_2}, \ldots, v_{q_{k-1}}$.

The other conifold singularity can be found on the locus of $\underbrace{\Phi_{z \cdots z}}_{k-1}(x_{k-1}, y_{k-1}, z, w)$, which is given by Eq. (6.2.8) with setting $j = k - 1$. We have already discussed that it has a codimension-one singularity p_{k-1} at $(x_{k-1}, y_{k-1}, z, w) = (0, 0, 0, w)$. We can show that it also has a conifold singularity if $b_{2,0} = c_{1,0}^2$ for some $c_{1,0}$ by writing, for $k \geq 3$,

$$\underbrace{\Phi_{z \cdots z}}_{k-1}(x_{k-1}, y_{k-1}, z, w) = -y_{k-1}^2 + \tfrac{1}{4}c_{1,0}^2 x_{k-1}^2$$

$$+z\left(x_{k-1}^3 z^{k-2} + \tfrac{1}{4}b_{2,1}x_{k-1}^2 + \tfrac{1}{2}b_{4,k}x_{k-1} + O(z)\right). \tag{6.2.22}$$

Thus, by setting $c_{1,0} = w$, the blown-up equation is reduced near $z = 0$ to

$$-y_{k-1}^2 + \tfrac{1}{4}w^2 x_{k-1}^2 + z\left(\tfrac{1}{4}b_{2,1}x_{k-1}^2 + \tfrac{1}{2}b_{4,k}x_{k-1}\right) = 0, \tag{6.2.23}$$

which shows that

$$v_{r_{k-1}}: \quad (x_{k-1}, y_{k-1}, z, w) = \left(-\frac{2b_{4,k}}{b_{2,1}}, 0, 0, 0\right) \quad (\underbrace{(\mathbf{k-1})_{z \cdots z}}_{k-1}). \tag{6.2.24}$$

is another conifold singularity.

Thus, the split I_{2k} model gives rise to a total of $k - 2 + 2 = k$ conifold singularities at each zero locus of $c_{1,0}$. They are resolved by small resolutions to give k exceptional curves, and comprise, together with the k exceptional curves coming from the codimension-one singularities, the D_{2k} Dynkin diagram (Fig. 6.1).

6.2.5 Conifold singularities in the split I_4 model (the $k = 2$ case)

Although similar, the split I_4 model, which is the lowest $k(= 2)$ case, is slightly different from the models for $k \geq 3$ in the way the conifold singularities appear, so we will briefly comment on this special case for completeness.

We have seen that in a split I_{2k} model with $k \geq 3$, two special conifold singularities v_{q_1} and $v_{r_{k-1}}$ appear in the patches $\mathbf{1}_z$ and $\underbrace{(\mathbf{k-1})_{z \cdots z}}_{k-1}$, respectively. If $k = 2$, they are the same patches. Therefore, in the $k = 2$ case, there appear both conifold singularities on the zero locus of $\Phi_z(x_1, y_1, z, w)$ defined in $(\mathbf{1}_z)$, in addition to the codimension-one singularity p_1. After the resolutions, they yield the D_4 Dynkin diagram as their intersection diagram.

6.2.6 Split/non-split transitions as conifold transitions in the I_{2k} models

Now, we can discuss the relationship between the split/non-split transition and the conifold transition. To summarize what we have learned so far about the I_{2k} model:

- If $b_{2,0}$ is a square of some $c_{1,0}$, the model is split, otherwise non-split.

- In the split models, D_{2k} points are $n+2$ double roots of the $(2n+4)$th order equation $b_{2,0} = c_{1,0}^2 = 0$ of w, while in the non-split models, they are generically $2n+4$ single roots.

- In the split case, there arise k conifold singularities at each zero locus of $c_{1,0}$, while in the non-split case, no conifold singularities appear at the loci of $b_{2,0}$.

So let us consider a deformation of the complex structure (of the total elliptic fibration) in which a particular double root, say $w = 0$, "splits" into two single roots $w = \pm\epsilon$ that are minutely separated $|\epsilon| \ll 1$. By deforming just one of the $n + 2$ double roots into a pair of single roots, $b_{2,0}$ can no longer be written in the form of a square of anything, so this deformation turns the split model into a non-split model. This deformation is achieved by replacing w^2 with $w^2 - \epsilon^2$, and turns the conifold

$$-y^2 + w^2 + xz = 0 \tag{6.2.25}$$

into

$$-y^2 + w^2 + xz = \epsilon^2, \tag{6.2.26}$$

which is the *deformed conifold*!

We can easily verify that all the conifold singularities $v_{q_1}, \ldots, v_{q_{k-1}}, v_{r_{k-1}}$ are deformed into local deformed conifolds[8] by the replacement $w^2 \to w^2 - \epsilon^2$. This means that the special deformation of the complex structure of the total elliptic fibration that makes a double zero of w split into a pair is exactly the deformation of the complex structure of the local conifolds.

Suppose that we start from a singular split I_{2k} model given by Eq. (6.2.1), where $b_{2,0} = c_{1,0}^2$, and $b_{2k,8}$ does not vanish. By blowing up all the codimension-one singularities of it, we end up with a geometry whose only singularities are conifold singularities. There are two ways to smooth these singularities. One is to resolve them by small resolutions; this just yields a smooth split I_{2k} model. The other is to deform the conifold singularities; this is achieved by replacing $b_{2,0} = c_{1,0}^2$ with $b_{2,0} = c_{1,0}^2 - \epsilon_{1,0}^2$ for some section $\epsilon_{1,0}$, then

---

[8]By a "local conifold" we mean the geometry near the conifold singularity described by an equation $(z_1 z_4 + z_2 z_3)(1 + O(z_i)) = 0$. Similarly, by a "local deformed conifold" we mean the one described by $(z_1 z_4 + z_2 z_3 - \epsilon^2)(1 + O(z_i)) = 0$.

the model is a smooth *non-split* I_{2k} model. In other words, the split/non-split transition in a I_{2k} model is nothing but a conifold transition.

As we have seen above, there is not just one conifold singularity that appears at each zero locus of $c_{1,0}$ and is involved in the transition. There are k such conifold singularities at each locus, and they are simultaneously deformed to give a non-split model.

6.2.7 The mechanism proposed by [1] for non-local matter generation

The origin of non-local matter was proposed [1] as due to the adjoint hypermultiplets associated with a certain genus-g curve in the elliptically fibred Calabi-Yau threefold. In this subsection, let's see how their proposal can be actually implemented in the blowing-up process we have discussed so far.

In general, fibre degeneration occurs at a codimension-one discriminant locus on the base, which is a curve on the two-dimensional base ($\mathbb{F}_n$ in our case) of the Calabi-Yau threefold. Thus, together with the degenerate $\mathbb{P}^1$ fibre, with a possible singularity before blowing up, it forms a ruled (=$\mathbb{P}^1$-fibred) surface in the Calabi-Yau threefold. We are interested in the gauge divisor, over which there is a distinction between the split or the non-split fibre type.

Since we take the gauge divisor to be a divisor of the *fibre* $\mathbb{P}^1$ of the Hirzebruch surface $\mathbb{F}_n$ (that is, $z = 0$), we may naturally take the base of the ruled surface to be the *base* $\mathbb{P}^1$ of the $\mathbb{F}_n$ (parametrized by w), which was called M_1 in [1]. Its genus is 0; this agrees with [139], in which, by an anomaly analysis, the number of the adjoint hypers was shown to coincide with the genus of the gauge divisor, and the fact that there is no massless adjoint hypermultiplet in the spectrum [90].

The proposal of [1] was as follows: Taking a non-split I_{2k} model as an example, if the singularity of the $\mathbb{P}^1$ fibre of the ruled surface is blown up, the singular point at each fixed w is replaced by a collection of $\mathbb{P}^1$'s, which form (over the whole base) a smooth surface consisting of multiple components corresponding to different nodes of the A_{2k-1} Dynkin diagram. In the non-split case, these $\mathbb{P}^1$'s (exceptional fibres) are merged in pairs smoothly, except for the one corresponding to the middle node. This is precisely why the gauge algebra is reduced to a non-simply-laced one by the identification under the diagram automorphism, but in [1] they further note that a component of the surface swept by a particular pair of such exceptional fibres is also a ruled surface, whose base is a 2-sheeted Riemann surface of genus g. This genus-g base, called M_2 in [1], is a double cover of M_1 and has $2g + 2$ branch points over which the pair of exceptional fibres meet and join smoothly in the non-split model. [1] argued that, according to [150,151], g hypermultiplets arise from the harmonic 1-forms of the genus-g Riemann surface and are assigned to one of the short simple roots of the C_k Dynkin diagram.

Let us consider how this genus-g Riemann surface can be seen in our set-up. We could consider the general equation for I_{2k} given in Subsection 6.2.4, but to simplify the notation and clarify the issue, we will instead repeat the blow-up procedure with the *homogeneous* coordinates in the I_6 model, the simplest case where there are more than one pair of exceptional curves identified by monodromy.

Again, starting from Eq. (6.2.1), let $k = 3$. This time, instead of Eq. (6.2.3), we change the coordinates as

$$(x, y, z) = (\alpha x_1, \alpha y_1, \alpha z_1), \tag{6.2.27}$$

where $(x_1 : y_1 : z_1)$ are homogeneous coordinates of $\mathbb{P}^2$ and $\alpha \in \mathbf{C}$. Plugging Eq. (6.2.27) into $\Phi(x, y, z, w)$, we define

$$
\begin{aligned}
\alpha^{-2}\Phi(\alpha x_1, \alpha y_1, \alpha z_1, w) &\equiv \Phi_\alpha(x_1, y_1, z_1, \alpha, w) \\
&= -y_1^2 + x_1^3\alpha + \tfrac{1}{4}(b_{2,0} + b_{2,1}z_1\alpha + \cdots)x_1^2 \\
&\quad + \tfrac{1}{2}(b_{4,3}z_1^3\alpha^2 + \cdots)x_1 \\
&\quad + \tfrac{1}{4}(b_{6,6}z_1^6\alpha^4 + \cdots),
\end{aligned}
\tag{6.2.28}
$$

similarly to Eq. (6.2.4). Of course, if $z_1 = 1$ and α is renamed z, $\Phi_\alpha(x_1, y_1, z_1 = 1, \alpha = z, w)$ becomes $\Phi_z(x_1, y_1, z, w)$ (6.2.8) with $j = 1$, $k = 3$. As we discussed in the previous subsection, if the section $b_{2,0}$ is a deformation of a square $c_{1,0}^2$, the equation $\Phi_\alpha(x_1, y_1, z_1, \alpha, w) = 0$ describes a three-manifold with $n + 2$ deformed conifold "singularities" near the zero loci of $c_{1,0}$. The exceptional curves can be found at the intersection with the divisor $\alpha = 0$:

$$\Phi_\alpha(x_1, y_1, z_1, \alpha = 0, w) = -y_1^2 + \tfrac{1}{4}b_{2,0}(w)x_1^2 = 0, \tag{6.2.29}$$

where we have recovered the argument of $b_{2,0}$ to remember that it is a polynomial of degree $2n + 4$ in w. With fixed w, Eq. (6.2.29) represents a pair of $\mathbb{P}^1$'s in $\mathbb{P}^2 \ni (x_1 : y_1 : z_1)$ if $b_{2,0}(w) \neq 0$ intersecting at $(x_1 : y_1 : z_1) = (0 : 0 : 1)$, which is a singularity to be blown up in the next step, thereby it is to be separated into two distinct points on the respective two $\mathbb{P}^1$'s. Thus if the value of w is varied, the two $\mathbb{P}^1$'s as a whole yield a surface, which comprises S_2 in [1].

On the other hand, Eq. (6.2.29) can also be viewed as a 2-sheeted Riemann surface, and, by "forgetting" z_1, any point on this (component of the) surface S_2 has a unique projection onto this Riemann surface. Therefore, it is a ruled surface whose base is a 2-sheeted Riemann surface given by Eq. (6.2.29) (provided that $(x_1 : y_1 : z_1) = (0 : 0 : 1)$ is blown up), which may be called M_2 in the notation of [1].

However, another similar Riemann surface arises in the next step of the blow-up. Since $\Phi_\alpha(x_1, y_1, z_1, \alpha, w) = 0$ is singular at $(x_1 : y_1 : z_1) = (0 : 0 : 1)$, we blow up there by defining

$$(x_1, y_1, \alpha) = (\beta x_2, \beta y_2, \beta \alpha_2), \tag{6.2.30}$$

where $(x_2 : y_2 : \alpha_2)$ are also homogeneous coordinates of $\mathbb{P}^2$ and $\beta \in \mathbf{C}$. Plugging Eq. (6.2.30) into $\Phi_\alpha(x_1, y_1, z_1, \alpha, w)$, we similarly obtain

$$
\begin{aligned}
\beta^{-2}\Phi_\alpha(\beta x_2, \beta y_2, z_1, \beta\alpha_2, w) &\equiv \Phi_{\alpha\beta}(x_2, y_2, z_1, \alpha_2, \beta, w) \\
&= -y_2^2 + x_2^3\alpha_2\beta^2 + \tfrac{1}{4}(b_{2,0} + b_{2,1}z_1\alpha_2\beta + \cdots)x_2^2 \\
&\quad + \tfrac{1}{2}(b_{4,3}z_1^3\alpha_2^2\beta + \cdots)x_2 \\
&\quad + \tfrac{1}{4}(b_{6,6}z_1^6\alpha_2^4\beta^2 + \cdots).
\end{aligned} \tag{6.2.31}
$$

The exceptional curves are at the intersection with the divisor $\beta = 0$:

$$
\Phi_{\alpha\beta}(x_2, y_2, z_1, \alpha_2, \beta = 0, w) = -y_2^2 + \tfrac{1}{4}b_{2,0}(w)x_2^2 = 0. \tag{6.2.32}
$$

This is again a ruled surface (without any further blowing up), whose base is also a Riemann surface given by the same equation (6.2.32) with α_2 forgotten.

Clearly, Eq. (6.2.29) and Eq. (6.2.32) are different components of the ruled surface S_2, residing on different divisors $\alpha = 0$ and $\beta = 0$, respectively. The important point, however, is that they represent the *same* Riemann surface as the base space. Indeed, for a given w, Eq. (6.2.29) and Eq. (6.2.32) respectively determine the ratios $x_1 : y_1$ and $x_2 : y_2$, but they are the same by definition and are consistent. Thus we may successfully say that S_2 is a ruled surface over *a genus-g ($= n + 1$ here) Riemann surface M_2, as [1] claimed.

It is also straightforward to check that, for general I_{2k} ($k \geq 3$) models defined by Eq. (6.2.1), all the genus-g bases that appear at each blow-up are the same (except at the final blow-up where such a genus-g curve does not arise). Similar holds for the I_{2k+1} non-split models[9]. In the non-split I_n^* and IV models, since there is only one pair of exceptional curves identified by monodromy, the problem described above does not arise. Finally, it can be verified that the two genus-g bases appearing in the non-split IV^* model are also the same.

Thus we have seen that, even when there are multiple pairs of exceptional curves and S_2 consists of multiple components, the genus-g Riemann surface M_2 is well-defined and serves the mechanism proposed by [1].

6.3 Split/non-split transitions as conifold transitions (II): the I_{2k+1} models

Although the defining equations of the I_{2k} and I_{2k+1} models are common (6.2.1), the relationship between the split/non-split transition and the conifold transition in the I_{2k+1} models is quite different from that in the I_{2k} models.

---

[9]In this case, the exceptional curve arising at the final blow-up splits into two lines, but still the genus-g Riemann surfaces arising before the final blow-up are all identical.
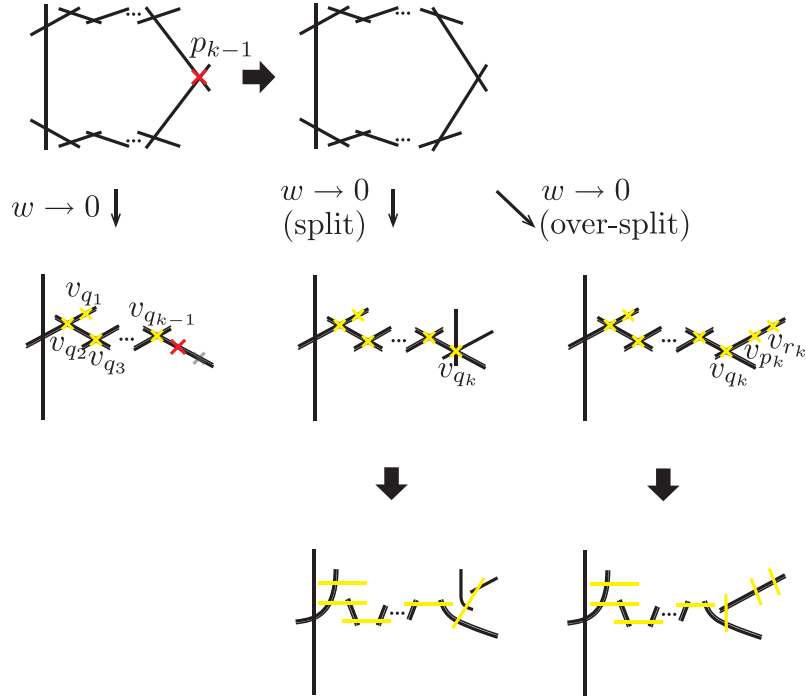
Figure 6.2: Singularities and exceptional curves in a split and an over-split I_{2k+1} model for $k \geq 2$ near a double root of $c_{1,0}^2 = 0$.

The most significant difference is that in the split I_{2k+1} model, the singularity (in the sense of Kodaira's singular fibre) is enhanced from A_{2k} to D_{2k+1} at the zero loci of $b_{2,0}$ (which is in the form of a square $c_{1,0}^2$ for some $c_{1,0}$), whereas in the non-split model, the singularity at the generic zero loci of $b_{2,0}$ is enhanced to D_{2k+2} instead of to D_{2k+1}. Consequently, a generic split I_{2k+1} model does not directly transition to a non-split I_{2k+1} model. Rather, we will show that there is a certain special interface model that connects the split and non-split I_{2k+1} models via a conifold transition.

6.3.1 The split, non-split and "over-split" I_{2k+1} models

The vanishing orders of the sections b_2, b_4, b_6 for a I_{2k+1} model are 0, k, $2k$, respectively, which are the same as those for a I_{2k} model. The difference from the I_{2k} model is that the vanishing order of b_8 is $2k + 1$ instead of $2k$, which means that

$$0 = 4b_{8,2k} = b_{4,k}^2 - b_{2,0}b_{6,2k}. \qquad (6.3.1)$$

In the split models, $b_{2,0}$ is given by a square $c_{1,0}^2$ for some $c_{1,0}$, so we have

$$b_{6,2k} = \left(\frac{b_{4,k}}{c_{1,0}}\right)^2. \qquad (6.3.2)$$

Thus $b_{4,k}$ must be divisible by $c_{1,0}$. We can then write

$$
\begin{aligned}
b_{2,0} &= c_{1,0}^2, \\
b_{4,k} &= c_{1,0}c_{3,k}, \\
b_{6,2k} &= c_{3,k}^2
\end{aligned}
\tag{6.3.3}
$$

for some $c_{3,k}$, which is a section of the line bundle specified by its subscripts. Again, $k = 1$ is a special case so will be discussed later. For $k \geq 2$, we find

$$
\begin{aligned}
f &= -\frac{1}{48}c_{1,0}^4 + \cdots \\
&\xrightarrow{c_{1,0} \to 0} -\frac{1}{48}b_{2,1}^2 z^2 + \cdots,
\end{aligned}
\tag{6.3.4}
$$

$$
\begin{aligned}
g &= \frac{1}{864}c_{1,0}^6 + \cdots \\
&\xrightarrow{c_{1,0} \to 0} \frac{1}{864}b_{2,1}^3 z^3 + \cdots
\end{aligned}
\tag{6.3.5}
$$

and

$$
\begin{aligned}
\Delta &= \frac{1}{16}c_{1,0}^4 b_{8,2k+1} z^{2k+1} + \cdots \\
&\xrightarrow{c_{1,0} \to 0} \frac{1}{64}b_{2,1}^3 c_{3,k}^2 z^{2k+3} + \cdots.
\end{aligned}
\tag{6.3.6}
$$

Therefore, the zero loci of $c_{1,0}$ are where the apparent fibre type changes to I_{2k-3}^*, or from A_{2k} to D_{2k+1} in terms of the singularity[10].

In the non-split I_{2k+1} models, Eq. (6.3.1) is assumed to be satisfied, but $b_{2,0}$ is not assumed to be in the form of a square. So suppose that $b_{2,0}$ is not a complete square but takes the product form

$$
b_{2,0} = c_{r,0}^2 \tilde{b}_{2-2r,0}
\tag{6.3.7}
$$

for some $c_{r,0}$ and $\tilde{b}_{2-2r,0}$. In this case, $b_{4,k}$ must be divisible by $c_{r,0}$. Then the same discussion as we did in the split I_{2k+1} model can apply to show that at the zero loci of $c_{r,0}$ the fibre type changes there to I_{2k-3}^* and the singularity is enhanced to D_{2k+1}.

Thus let us assume that $b_{2,0}$ is completely generic and has no square factor, that is, the equation $b_{2,0} = 0$ has no double root. In this case, the constraint (6.3.1) requires that $b_{4,k}$ is divisible by $b_{2,0}$:

$$
\begin{aligned}
b_{2,0} &: \quad \text{generic}, \\
b_{4,k} &= b_{2,0}c_{2,k}, \\
b_{6,2k} &= b_{2,0}c_{2,k}^2
\end{aligned}
\tag{6.3.8}
$$

---

[10]Again, as we noted in Subsection 6.2.3, an enhancement to E_7 is possible in the F-theory model with an unbroken A_6 gauge symmetry, but it also cannot be realized in our Deligne form [144, 149]. It is also irrelevant for the split/non-split transition.

for some section $c_{2,k}$ of the line bundle implied by the subscripts. For $k \geq 2$, we can see that the z-expansions of f and g are similar to Eq. (6.3.4) and (6.3.5), but the discriminant in the present case is

$$
\Delta \quad = \quad \frac{1}{16} b_{2,0}^2 b_{8,2k+1} z^{2k+1} + \cdots
$$
$$
\overset{b_{2,0} \to 0}{\longrightarrow} \quad \frac{1}{64} b_{2,1}^2 (b_{2,1} b_{6,2k+1} - b_{4,k+1}^2) z^{2k+4} + \cdots , \tag{6.3.9}
$$

in which the order of z at the zero loci of $b_{2,0}$ is one order higher than that in the split case. This shows that, in a non-split I_{2k+1} model, the fibre type in the sense of Kodaira changes to I^*_{2k-2} instead of I^*_{2k-3}, and the apparent singularity there is enhanced from A_{2k} to D_{2k+2} instead of D_{2k+1}.

Therefore, a generic split I_{2k+1} model cannot directly transition to a non-split I_{2k+1} model. The interface model that connects the split and non-split models can be obtained by tuning the complex structure of a split model so that it can yield the D_{2k+2} points which are originally absent in generic split I_{2k+1} models. The existence of such models was already pointed out in [85]. More specifically, we consider a special class of split I_{2k+1} models in which the relevant sections $b_{2,0}$, $b_{4,k}$ and $b_{6,2k}$ are given by

$$
b_{2,0} = c_{1,0}^2
$$
$$
b_{4,k} = c_{1,0}^2 c_{2,k}, \tag{6.3.10}
$$
$$
b_{6,2k} = c_{1,0}^2 c_{2,k}^2,
$$

which we call an "over-split I_{2k+1} model". Eq. (6.3.10) can be obtained by specializing $c_{3,k}$ to the factorized form $c_{1,0} c_{2,k}$ for some $c_{2,k}$. This in particular implies that $c_{3,k}$ in Eq. (6.3.6) vanishes as $c_{1,0} \to 0$. The next non-vanishing order is $2k + 4$, yielding the desired enhancement to D_{2k+2}. It is also clear that replacing $c_{1,0}^2$ with $b_{2,0}$ in Eq. (6.3.10) yields the specifications of the sections in the non-split models (6.3.8).

6.3.2 Conifold singularities in the I_{2k+1} models for $k \geq 2$

We will now blow up the codimension-one singularities of the split and over-split I_{2k+1} models. Since the only difference between the I_{2k} and the I_{2k+1} models (in their definitions) is the vanishing order of b_8, the way the singularities are blown up is very similar between the two. When we blow up the codimension-one singularities of a split I_{2k+1} model, the first difference from the I_{2k} models we encounter is the absence of the conifold singularity $v_{r_{k-1}}$ in the coordinate patch $(\boldsymbol{k-1})_{\underbrace{z \cdots z}_{k-1}}$ (6.2.24), which appeared in the I_{2k} models when $w \equiv c_{1,0} \to 0$. Instead, if we blow up the codimension-one singularity p_{k-1}, we get a pair of exceptional curves, at the intersection of which there is a conifold singularity v_{q_k} (Fig. 6.2). If we resolve all the conifold singularities by small resolutions, we obtain the D_{2k+1} Dynkin diagram as the intersection diagram of the resulting exceptional curves.

On the other hand, if we blow up the singularity p_{k-1} in the over-split I_{2k+1} model, the pair of exceptional lines come on top of each other to form a single irreducible line, on which three conifold singularities v_{p_k}, v_{q_k} and v_{r_k} appear. Resolving all the conifold singularities gives the D_{2k+2} Dynkin diagram in this case.

How these conifold singularities arise in the blowing-up process of the split and over-split I_{2k+1} models near a double root of $c_{1,0}^2 = 0$ is summarized in Fig. 6.2.

6.3.3 The split/non-split transitions and conifold transitions in the I_{2k+1} models for $k \geq 2$

Again, let us focus on a particular double root of $c_{1,0}^2 = 0$, and let it be $w = 0$. Then the local equations yielding the conifold singularities $v_{q_1}, \ldots, v_{q_{k-1}}$ are the same as those in the split I_{2k} models. To see how the conifold singularities $v_{p_k}, v_{q_k}, v_{r_k}$ arise, let us consider the k-times blown-up equation $\Phi_{\underbrace{z \cdots z}_{k-1} x}(x_{k-1}, y_k, z_k, w) = 0$ in the patch $\boldsymbol{k}_{\underbrace{z \cdots z}_{k-1} x}$,

where

$$
\begin{aligned}
\Phi_{\underbrace{z \cdots z}_{k-1} x}(x_{k-1}, y_k, z_k, w) \quad &\equiv \quad x_{k-1}^{-2} \Phi_{\underbrace{z \cdots z}_{k-1}}(x_{k-1}, x_{k-1} y_k, x_{k-1} z_k, w) \\
&= \quad -y_k^2 + x_{k-1}^k z_k^{k-1} \\
&\quad + \tfrac{1}{4}(c_{1,0}^2 + b_{2,1} x_{k-1} z_k + \cdots) \\
&\quad + \tfrac{1}{2}(c_{1,0} c_{3,k} z_k + b_{4,k+1} x_{k-1} z_k^2 + \cdots) \\
&\quad + \tfrac{1}{4}(c_{3,k}^2 z_k^2 + b_{6,2k+1} x_{k-1} z_k^3 + \cdots) \\
&\overset{x_{k-1} \to 0}{\longrightarrow} \quad -y_k^2 + \tfrac{1}{4}(c_{1,0} + c_{3,k} z_k)^2 \quad (6.3.11)
\end{aligned}
$$

in the split case. The last line shows that the exceptional curve splits into two lines, which intersect at

$$
x_{k-1} = y_k = c_{1,0} + c_{3,k} z_k = 0. \quad (6.3.12)
$$

If $c_{1,0} = 0$, z_k also vanishes for generic $c_{3,k}$; this is a conifold singularity. Indeed, we can write $\Phi_{\underbrace{z \cdots z}_{k-1} x}(x_{k-1}, y_k, z_k, w)$ as, setting $c_{1,0} = w$,

$$
\begin{aligned}
\Phi_{\underbrace{z \cdots z}_{k-1} x}(x_{k-1}, y_k, z_k, w) \quad = \quad &-y_k^2 + \tfrac{1}{4}(w + c_{3,k} z_k)^2 + x_{k-1} z_k \left(x_{k-1}^{k-1} z_k^{k-2} \right. \\
&\left. + \tfrac{1}{4} b_{2,1} + \tfrac{1}{2} b_{4,k+1} z_k + \tfrac{1}{4} b_{6,2k+1} z_k^2 + O(x_{k-1} z_k) \right). (6.3.13)
\end{aligned}
$$

This shows that

$$
v_{q_k} : \quad (x_{k-1}, y_k, z_k, w) = (0, 0, 0, 0) \quad (\boldsymbol{k}_{\underbrace{z \cdots z}_{k-1} x}) \quad (6.3.14)
$$

is a conifold singularity. This is the only conifold singularity in this patch in the split case. Note that the w-dependence of Eq. (6.3.13) is not only through w^2.

In the over-split case, Eq. (6.3.11) becomes

$$\Phi_{\underbrace{z\cdots z}_{k-1}x}(x_{k-1}, y_k, z_k, w) = -y_k^2 + x_{k-1}^k z_k^{k-1}$$

$$+\tfrac{1}{4}(c_{1,0}^2 + b_{2,1}x_{k-1}z_k + \cdots)$$
$$+\tfrac{1}{2}(c_{1,0}^2 c_{2,k}z_k + b_{4,k+1}x_{k-1}z_k^2 + \cdots)$$
$$+\tfrac{1}{4}(c_{1,0}^2 c_{2,k}^2 z_k^2 + b_{6,2k+1}x_{k-1}z_k^3 + \cdots)$$
$$\overset{x_{k-1}\to 0}{\to} -y_k^2 + \tfrac{1}{4}c_{1,0}^2(1 + c_{2,k}z_k)^2. \tag{6.3.15}$$

Thus, the exceptional curves that are split into two lines at $c_{1,0} \neq 0$ overlap into a single line at $c_{1,0} = 0$. In this case, by setting $c_{1,0} \equiv w$, Eq. (6.3.15) can be written as

$$\Phi_{\underbrace{z\cdots z}_{k-1}x}(x_{k-1}, y_k, z_k, w) = -y_k^2 + \tfrac{1}{4}w^2(1 + c_{2,k}z_k)^2 + x_{k-1}z_k\left(x_{k-1}^{k-1}z_k^{k-2}\right.$$

$$\left. +\tfrac{1}{4}b_{2,1} + \tfrac{1}{2}b_{4,k+1}z_k + \tfrac{1}{4}b_{6,2k+1}z_k^2 + O(x_{k-1}z_k)\right), \tag{6.3.16}$$

which shows that there are three conifold singularities at $x_{k-1} = y_k = w = 0$ and

$$z_k\left(\tfrac{1}{4}b_{2,1} + \tfrac{1}{2}b_{4,k+1}z_k + \tfrac{1}{4}b_{6,2k+1}z_k^2\right) = 0. \tag{6.3.17}$$

They are shown in Fig. 6.2 as v_{q_k} (when $z_k = 0$), v_{p_k} and v_{r_k} (when z_k is one of the roots of $\tfrac{1}{4}b_{2,1} + \tfrac{1}{2}b_{4,k+1}z_k + \tfrac{1}{4}b_{6,2k+1}z_k^2 = 0$). In the split case, the two points where z_k is a non-zero root of the latter equation are not conifold singularities since the second term in Eq. (6.3.13) is $O(w^0)$ near these points, whereas in the non-split case, the second term in Eq. (6.3.16) is $O(w^2)$ there.

We can see that, unlike the (ordinary) split I_{2k+1} case, Eq. (6.3.16) is a function of w^2, so we can do the same unfolding $w^2 \to w^2 - \epsilon^2$ as we did in the I_{2k} models. Again, on one hand, this replacement amounts to deforming all the conifold singularities occurring at $w = 0$, and on the other hand, one of the square factors of $b_{2,0}$ becomes generic, which turns the over-split I_{2k+1} model into a non-split I_{2k+1} model.

6.3.4 The split/non-split transitions and conifold transitions in the I_3 models

Finally, to make the discussion complete, let us briefly describe the split/non-split transitions in the I_{2k+1} models for $k = 1$, i.e. the I_3 model. This lowest k case is rather special and exhibits slightly different intersection patterns of the exceptional curves.

We have shown in Fig. 6.3 the singularities and exceptional curves in a split and an over-split I_3 model near a double root of $c_{1,0}^2 = 0$. In an ordinary split I_3 model,
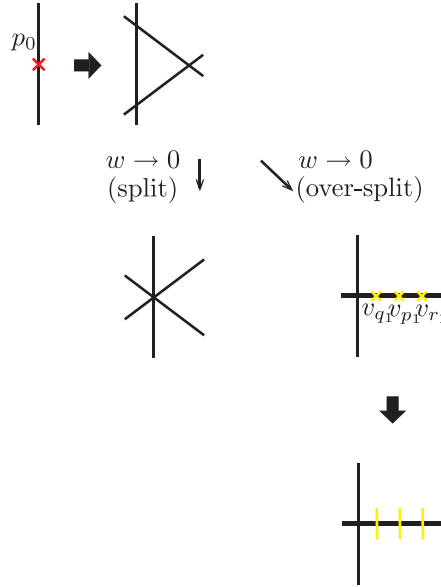
Figure 6.3: Singularities and exceptional curves in a split and an over-split I_3 model.

no conifold singularity appears once the codimension-one singularity is blown up, even when $c_{1,0} \equiv w$ is taken to zero, where the fibre type changes from I_3 to IV. No matter hypermultiplet arises at the zero loci of $c_{1,0}$. In the over-split I_3 model, where we take

$$
\begin{aligned}
b_{2,0} &= c_{1,0}^2 \\
b_{4,1} &= c_{1,0}^2 c_{2,1}, \\
b_{6,2} &= c_{1,0}^2 c_{2,1}^2,
\end{aligned}
\tag{6.3.18}
$$

three conifold singularities appear at each zero locus of $c_{1,0}$, whose small resolutions yield exceptional curves of the I_0^* type, and the singularity is enhanced from A_2 to D_4.

Although the way the conifold singularities appear is slightly different from the cases for $k \geq 2$, the over-split I_3 model is also turned into the non-split I_3 model by the replacement $w^2 \to w^2 - \epsilon^2$, which is a deformation of a conifold singularity.

6.4 Split/non-split transitions as conifold transitions (III): IV

Let us next consider the IV model. The IV model is defined in the Deligne form (6.1.6) for b_2, b_4, b_6 with vanishing orders 1, 2, 2, respectively. The sections f, g characterizing the Weierstrass equation read

$$
\begin{aligned}
f &= -\frac{1}{48}(b_{2,1}^2 - 24 b_{4,2}) z^2 + \cdots, \\
g &= \frac{1}{4} b_{6,2} z^2 + \cdots,
\end{aligned}
\tag{6.4.1}
$$

and the discriminant is

$$\Delta = \frac{27}{16}b_{6,2}^2 z^4 + \cdots, \tag{6.4.2}$$

so $\text{ord}(f, g, \Delta) = (2, 2, 4)$ and the generic fibre type at $z = 0$ is IV. At the zero loci of $b_{6,2}$, they are enhanced to $(2, 3, 6)$, showing that the Kodaira fibre type there is I_0^*. If the section $b_{6,2}$ can be written in the form of a square $c_{3,1}^2$ for some $c_{3,1}$, the model is said a split IV model, while if $b_{6,2}$ cannot be written that way, it is said a non-split IV model [90].

In this case, the only codimension-one singularity at a generic point on $z = 0$ is $p_0 : (x, y, z, w) = (0, 0, 0, w)$, which can be resolved by just a one-time blow-up. The resulting exceptional curves split into two, which intersect the original fibre at a single point; they come on top of each other at $b_{6,2} = 0$.

In the split case, they are all double roots, and three new conifold singularities appear on the overlapping exceptional lines. To see this, consider the equation blown up once $\Phi_z(x_1, y_1, z, w) = 0$ with

$$\begin{aligned}
\Phi_z(x_1, y_1, z, w) &= -y_1^2 + x_1^3 z \\
&\quad + \tfrac{1}{4}(b_{2,1}z + \cdots)x_1^2 + \tfrac{1}{2}(b_{4,2}z + \cdots)x_1 + \tfrac{1}{4}(w^2 + b_{6,3}z + \cdots) \\
&\xrightarrow{z \to 0} -y_1^2 + \tfrac{1}{4}w^2,
\end{aligned} \tag{6.4.3}$$

in $\mathbf{1}_z$, where we have set $b_{6,2} = w^2$ to focus on a particular double root of $b_{6,2} = 0$. Eq. (6.4.3) indeed shows that the generic exceptional curve splits into two lines, and they coincide with each other at $w = 0$. Conifold singularities can be seen by rewriting Eq. (6.4.3) as

$$\Phi_z(x_1, y_1, z, w) = -y_1^2 + \tfrac{1}{4}w^2 + z(x_1^3 + \tfrac{1}{4}b_{2,1}x_1^2 + \tfrac{1}{2}b_{4,2}x_1 + \tfrac{1}{4}b_{6,3} + O(z)). \tag{6.4.4}$$

For generic $b_{2,1}$, $b_{4,2}$, $b_{6,3}$, the cubic equation of x_1 has three distinct roots, giving rise to three conifold singularities at $y_1 = w = z = 0$. Again, the replacement $w^2 \to w^2 - \epsilon^2$ amounts to the transition from the split to non-split IV model, at the same time it unfolds the conifold singularity to yield a local deformed conifold. Singularities and exceptional curves in the split IV model near $w = 0$ are depicted in Fig. 6.4.

6.5 Split/non-split transitions as conifold transitions (IV): IV^*

In the IV^* model, the vanishing orders of b_2, b_4, b_6 are $2, 3, 4$, respectively. f and g (6.1.12) are

$$\begin{aligned}
f &= \frac{1}{2}b_{4,3}z^3 + \cdots, \\
g &= \frac{1}{4}b_{6,4}z^4 + \cdots.
\end{aligned} \tag{6.5.1}$$
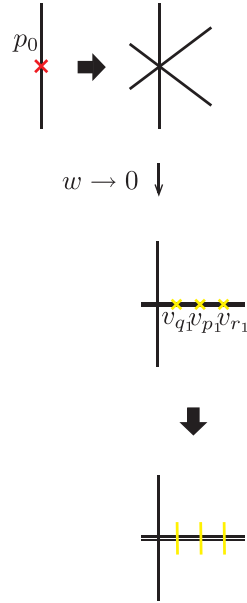
Figure 6.4: Singularities and exceptional curves in a split IV model.

The discriminant is

$$\Delta \;=\; \frac{27}{16} b_{6,4}^2 z^8 + \cdots . \tag{6.5.2}$$

These imply that the fibre type is IV^* at a generic point of $z = 0$. The split IV^* model has $b_{6,4}$ in the form of a square $c_{3,2}^2$ for some $c_{3,2}$. The non-split IV^* model has generic $b_{6,4}$ [90]. In both the split and non-split models, the vanishing orders of (f, g, Δ) at the zero locus of $b_{6,4}$ changes from $(3, 4, 8)$ to $(3, 5, 9)$, implying that the apparent fibre type there is III^*, that is, the zero locus of $b_{6,4}$ is an E_7 point.

We have illustrated in Fig. 6.5 how the singularities appear and exceptional curves intersect in the split IV^* model near $w = 0$, which is one of the double roots of $c_{3,2}^2 = 0$. At the stage where the three codimension-one singularities are blown up, there remain three conifold singularities at each double root of $b_{6,4} = c_{3,2}^2 = 0$. We will show that, if all these conifold singularities are resolved by small resolutions, we obtain a smooth, fully resolved split IV^* model, while if all the conifold singularities are simultaneously deformed, we are led to a smooth non-split IV^* model.

We start with a split IV^* model. The defining equation is[11]

$$
\begin{aligned}
\Phi(x, y, z, w) \equiv \;\; &-y^2 + x^3 \;\; + \tfrac{1}{4} b_{2,2} z^2 x^2 \\
&+ \tfrac{1}{2}(b_{4,3} z^3 + b_{4,4} z^4) x \\
&+ \tfrac{1}{4}(c_{3,2}^2 z^4 + b_{6,5} z^5 + \cdots) = 0.
\end{aligned}
\tag{6.5.3}
$$

---

[11]Although we are interested in the local structure of the singularity, the IV^* models are well-defined as a dP_9 fibration to consider the heterotic dual, so we have kept in Eq. (6.5.3) only terms with coefficients $b_{k,j}$ up to $j \leq k$. In any case, it doesn't really matter whether we do so or not.
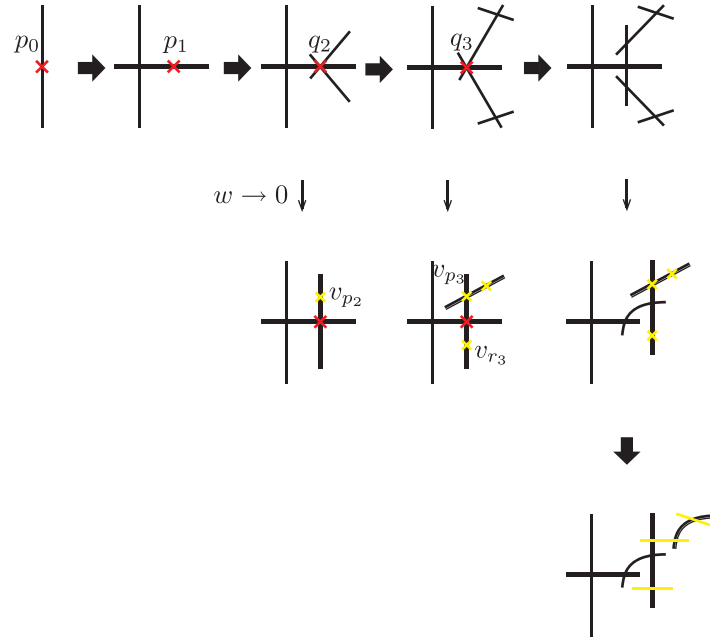
Figure 6.5: Singularities and exceptional curves in the split IV^* model near a double root of $c_{3,2}^2 = 0$.

The first codimension-one singularity (next to the original singularity p_0) can be found on $\Phi_z(x_1, y_1, z, w) = 0$ defined in Eq. (6.2.4) with $\Phi(x, y, z, w)$ given by Eq. (6.5.3). This is

$$p_1 : \quad (x_1, y_1, z, w) = (0, 0, 0, 0) \quad (\mathbf{1}_z). \tag{6.5.4}$$

Blowing up $\Phi_z(x_1, y_1, z, w) = 0$ at p_1, we have

$$
\begin{aligned}
\Phi_{zx}(x_1, y_2, z_2, w) = \quad & -y_2^2 + x_1^2 z_2 \quad + \tfrac{1}{4} b_{2,2} x_1^2 z_2^2 \\
& + \tfrac{1}{2}(b_{4,3} x_1 z_2^2 + b_{4,4} x_1^2 z_2^3) \\
& + \tfrac{1}{4}(c_{3,2}^2 z_2^2 + b_{6,5} x_1 z_2^3 + \cdots) = 0,
\end{aligned}
\tag{6.5.5}
$$

where $\Phi_{zx}(x_1, y_2, z_2, w)$ is defined similarly to Eq. (6.2.5). In the $x_1 \to 0$ limit, this equation reduces to $y_2^2 = 0$, which is a double line. It has a codimension-one singularity

$$q_2 : \quad (x_1, y_2, z_2, w) = (0, 0, 0, w) \quad (\mathbf{2}_{zx}) \tag{6.5.6}$$

as well as a conifold singularity

$$v_{p_2} : \quad (x_1, y_2, z_2, w) = \left(0, 0, -\frac{2b_{4,3}}{b_{6,5}}, 0\right) \quad (\mathbf{2}_{zx}). \tag{6.5.7}$$

The latter can be seen by writing Eq. (6.5.5) as

$$-y_2^2 + \tfrac{1}{4} w^2 z_2^2 + x_1\left(\tfrac{1}{2} b_{4,3} z_2^2 + \tfrac{1}{4} b_{6,5} z_2^3 + O(x_1)\right) = 0, \tag{6.5.8}$$

where we again set $c_{3,2}^2 = w^2$ to focus on a particular double root of $b_{6,4} = c_{3,2}^2 = 0$.

Blowing up $\Phi_{zx}(x_1, y_2, z_2, w) = 0$ at q_2, we have

$$
\begin{aligned}
\Phi_{zxx}(x_1, y_3, z_3, w) = \quad &-y_3^2 + x_1 z_3 \quad +\tfrac{1}{4}b_{2,2}x_1^2 z_3^2 \\
&+\tfrac{1}{2}(b_{4,3}x_1 z_3^2 + b_{4,4}x_1^3 z_3^3) \\
&+\tfrac{1}{4}(c_{3,2}^2 z_3^2 + b_{6,5}x_1^2 z_3^3 + \cdots) = 0 \qquad (6.5.9)
\end{aligned}
$$

in the patch $\mathbf{3}_{zxx}$, where we have defined

$$
\Phi_{zxx}(x_1, y_3, z_3, w) \quad \equiv \quad x_1^{-2}\Phi_{zx}(x_1, x_1 y_3, x_1 z_3, w). \qquad (6.5.10)
$$

Eq. (6.5.9) still has a codimension-one singularity

$$
q_3: \qquad (x_1, y_3, z_3, w) = (0, 0, 0, w) \quad (\mathbf{3}_{zxx}). \qquad (6.5.11)
$$

Eq. (6.5.9) has also a conifold equation, but in fact, there arise two conifold singularities after blowing up at q_2 as we displayed in Fig. 6.5, and it is only the one of two that can be seen in the patch $\mathbf{3}_{zxx}$.

To see both conifold singularities we consider

$$
\begin{aligned}
\Phi_{zxz}(x_3, y_3, z_2, w) = \quad &-y_3^2 + x_3^2 z_2 \quad +\tfrac{1}{4}b_{2,2}x_3^2 z_2^2 \\
&+\tfrac{1}{2}(b_{4,3}x_3 z_2 + b_{4,4}x_3^2 z_2^3) \\
&+\tfrac{1}{4}(c_{3,2}^2 + b_{6,5}x_3 z_2^2 + \cdots) = 0 \qquad (6.5.12)
\end{aligned}
$$

in the patch $\mathbf{3}_{zxz}$, where

$$
\Phi_{zxz}(x_3, y_3, z_2, w) \quad \equiv \quad z_2^{-2}\Phi_{zx}(x_3 z_2, y_3 z_2, z_2, w). \qquad (6.5.13)
$$

Eq. (6.5.12) can also be transformed into the form of a conifold equation

$$
-y_3^2 + \tfrac{1}{4}w^2 + z_2\left(x_3^2 + \tfrac{1}{2}b_{4,3}x_3 + O(z_2)\right) = 0, \qquad (6.5.14)
$$

which indicates the existence of two conifold singularities

$$
\begin{aligned}
v_{p3}: \quad &(x_3, y_3, z_2, w) = (0, 0, 0, 0), \\
v_{r3}: \quad &(x_3, y_3, z_2, w) = (-\tfrac{1}{2}b_{4,3}, 0, 0, 0) \quad (\mathbf{3}_{zxz}).
\end{aligned} \qquad (6.5.15)
$$

By looking at the form of the conifold equations (6.5.8) and (6.5.14) and following the discussion we have presented in the previous sections, it is now clear that the transition from the split IV^* model to the non-split IV^* model is the conifold transition from the resolved side to the deformed side. Note that this is the only example in which the transition occurs at an E_7 point; as we saw in the previous sections, as well as we will see in the next section, the transition always occurs at a D_{2k} point in all the other examples.
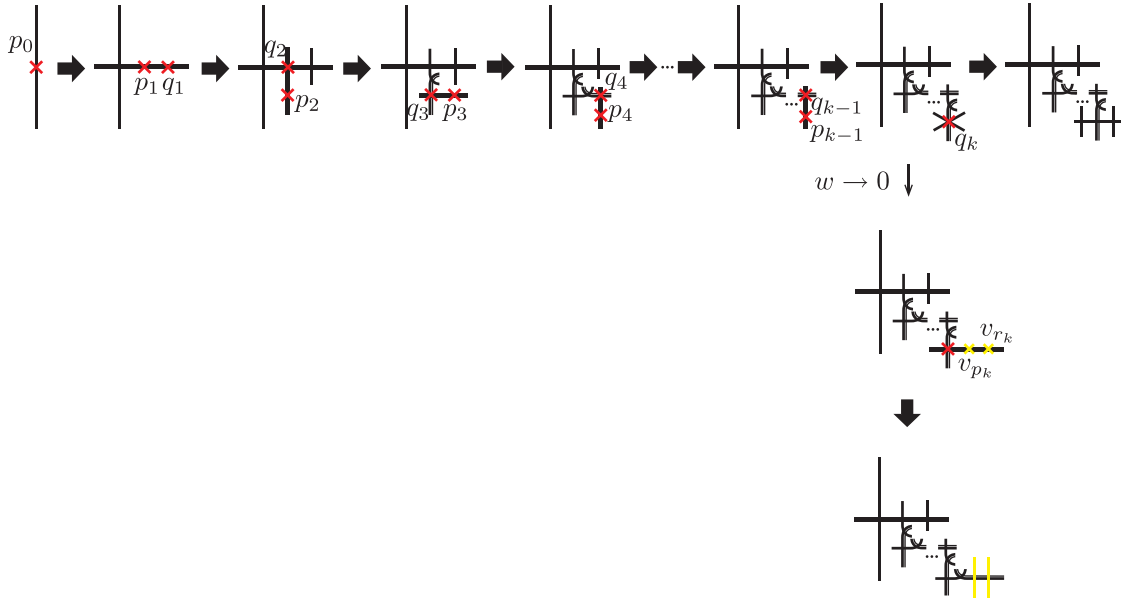
Figure 6.6: Singularities and exceptional curves in the split I^*_{2k-3} model.

6.6 The I^*_n models

Finally, we will deal with the I^*_n cases. The situation is quite different when n is even and when n is odd. We will consider the odd case first.

6.6.1 The I^*_{2k-3} models

The I^*_{2k-3} models ($k \geq 2$) have a D_{2k+1} singularity. In the split I^*_{2k-3} models ($k \geq 2$), conifold singularities appear as in the previous examples, and the deformation at the D_{2k+2} points turns a split I^*_{2k-3} model into a non-split one and can be regarded as a deformation of the conifold singularities.

The model is defined by Eq. (6.1.6) with vanishing orders $\mathrm{ord}(b_2, b_4, b_6) = (1, k + 1, 2k)$ ($k \geq 2$). Whether the model is split or non-split depends on whether or not the section $b_{6,2k}$ takes the form of a square $c^2_{3,k}$ for some $c_{3,k}$ [90]. In the split case, the Lie algebra of the unbroken gauge symmetry is $D_{2k+1} = SO(4k + 2)$. Whether split or non-split, the zero loci of $b_{6,2k}$ are $D_{2k+2} = SO(4k+4)$ points. Besides them, E_6 and E_8 points may occur for $k = 2$ and 3, but they are not important here.

As we have shown in Fig. 6.6, one of the differences in the split I^*_n model is that the conifold singularities appear only at the final step of blowing up. We can see the conifold singularities in the equation $\Phi_{\underbrace{z \ldots z}_{k}}(x_k, y_k, z, w) = 0$, where, setting $c^2_{3,k} \equiv w^2$,

$$
\begin{aligned}
\Phi_{\underbrace{z\cdots z}_{k}}(x_k, y_k, z, w) = \ & -y_k^2 + x_k^3 z^k && +\tfrac{1}{4}(b_{2,1}z + \cdots)x_k^2 \\
& && +\tfrac{1}{2}(b_{4,k+1}z + \cdots)x_k \\
& && +\tfrac{1}{4}(w^2 + b_{6,2k+1}z + \cdots) \\
= \ & -y_k^2 + \tfrac{1}{4}w^2 && +z\left(\tfrac{1}{4}b_{2,1}x_k^2 + \tfrac{1}{2}b_{4,k+1}x_k + \tfrac{1}{4}b_{6,2k+1} + O(z)\right).
\end{aligned}
\tag{6.6.1}
$$

The discriminant of the quadratic equation $\tfrac{1}{4}b_{2,1}x_k^2 + \tfrac{1}{2}b_{4,k+1}x_k + \tfrac{1}{4}b_{6,2k+1} = 0$ is proportional to $b_{8,2k+2}$, which does not vanish generically. Therefore it has two distinct roots, yielding the two conifold singularities. Eq. (6.6.1) again depends on w through w^2 near the singularities, and unfolding the conifold singularity is exactly what turns a split model into a non-split one.

6.6.2 The I^*_{2k-2} models

So far we have seen various examples in which the split/non-split transition is precisely the conifold transition associated with the conifold singularities occurring at the D_{2k} points, or the E_7 points in the IV^* case. In fact, in the I^*_{2k-2} model, the situation is quite different. The crucial difference is that, in that case, no conifold singularity arises at the zero locus of the section relevant to the split/non-split transition.

In this class of models, the orders of b_2, b_4, b_6 are 1, $k+1$, $2k+1$, instead of 1, $k+1$, $2k$ in the previous I^*_{2k-3} models. $k = 1$ is a special case and has already been discussed in detail in [147][12], so we will consider $k \geq 2$. f and g (6.1.12) read

$$
\begin{aligned}
f &= -\frac{1}{48}b_{2,1}^2 z^2 + \cdots, \\
g &= +\frac{1}{864}b_{2,1}^3 z^3 + \cdots,
\end{aligned}
\tag{6.6.2}
$$

which are the same as those in the I^*_{2k-3} models. The discriminant is

$$
\Delta = \frac{1}{16}b_{2,1}^2 b_{8,2k+2}z^{2k+4} + \cdots,
\tag{6.6.3}
$$

so, for a generic $b_{2,1}$, the singularity is enhanced from D_{2k+2} to D_{2k+3} at the zero locus of $b_{8,2k+2}$, where

$$
b_{8,2k+2} = \frac{1}{4}(b_{2,1}b_{6,2k+1} - b_{4,k+1}^2).
\tag{6.6.4}
$$

---

[12]For the I_0^* models, we have, again, presented in Table 6.1 the *generic* orders of b_2, b_4, b_6 (= 1, 2, 3) that can achieve these fibre types with the additional constraints shown there. For the split and semi-split I_0^* models, $p_{2,1}$ can be eliminated by a redefinition of x, so that the orders of b_2, b_4, b_6 become 1, 2, 4, which are the values derived from the standard Tate's orders for the split and semi-split I_0^* models.
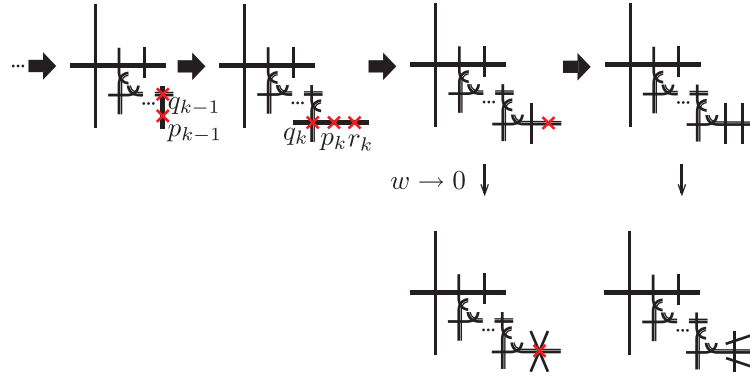
Figure 6.7: Singularities and exceptional curves in the split I^*_{2k-2} model.

If this $b_{8,2k+2}$ is written as $c^2_{4,k+1}$ for some $c_{4,k+1}$, this I^*_{2k-2} model is called split, otherwise non-split [90].

The blowing-up procedure proceeds similarly to the I^*_{2k-3} models. In the split case, a difference arises when p_{k-1} is blown up, where the exceptional curves overlap to one line instead of splitting into two lines, and three codimension-one singularities arise on the line. This is precisely what was seen in the $w \to 0$ limit after p_{k-1} was blown up in the I^*_{2k-3} models, where the two conifold singularities found there are now replaced by two codimension-one singularities (Fig. 6.7). Concretely,

$$\Phi_{\underbrace{z \cdots z}_{k}}(x_k, y_k, z, w) = \quad -y_k^2 + x_k^3 z^k \quad + \tfrac{1}{4}(b_{2,1}z + \cdots)x_k^2$$
$$+ \tfrac{1}{2}(b_{4,k+1}z + \cdots)x_k$$
$$+ \tfrac{1}{4}(b_{6,2k+1}z + \cdots). \tag{6.6.5}$$

Since $b_{8,2k+2}$ is proportional to the discriminant of the quadratic equation of $\tfrac{1}{4}b_{2,1}x_k^2 + \tfrac{1}{2}b_{4,k+1}x_k + \tfrac{1}{4}b_{6,2k+1} = 0$, we can further write, by assuming $b_{8,2k+2} = c^2_{4,k+1}$, as

$$\Phi_{\underbrace{z \cdots z}_{k}}(x_k, y_k, z, w) = -y_k^2 + z\left(\tfrac{1}{4}b_{2,1}x_k^2 + \tfrac{1}{2}b_{4,k+1}x_k + \tfrac{1}{4}b_{6,2k+1} + O(z)\right)$$
$$= -y_k^2 + \frac{z}{b_{2,1}}\left(\left(\frac{b_{2,1}}{2}x_k + b_{4,k+1}\right)^2 + c^2_{4,k+1} + O(z)\right). \tag{6.6.6}$$

Thus, the codimension-one singular loci of $\Phi_{\underbrace{z \cdots z}_{k}}(x_k, y_k, z, w) = 0$ split into two irreducible components

$$y_k = 0, \quad z = 0, \quad \frac{b_{2,1}}{2}x_k + b_{4,k+1} \pm ic_{4,k+1} = 0. \tag{6.6.7}$$

Their intersection is where $c_{4,k+1}$ vanishes, or equivalently, $b_{8,2k+2} = 0$ vanishes, so it is a D_{2k+3} point. The codimension-one singularities can be blown up along either of the two irreducible components (6.6.7) first. We can verify that the exceptional curve obtained in such a way splits into two lines precisely at the intersection D_{2k+3} point. Blowing up

along the remaining irreducible component thus yields the D_{2k+3} intersection diagram only there. This is how the higher-rank intersection diagram emerges without conifold singularities in the I^*_{2k-2} models.

On the other hand, the equation of the non-split I^*_{2k-2} model can be obtained by replacing $c^2_{4,k+1}$ with a generic $b_{8,2k+2}$ in Eq. (6.6.6). In this case, the codimension-one singular loci consist of only one irreducible component, along which we can blow up the singularities only once. No conifold singularity is found. Therefore, only the I^*_{2k-2} models (including the I^*_0 model [147]) cannot interpret the split/non-split transition there as a conifold transition.

Chapter 7

Conclusion

In this chapter, we conclude this thesis. We have considered F-theory compactifications. F-theory describes non-perturbative compactifications of Type IIB superstring theory with general 7-branes geometrically. In F-theory, singularities play a particularly essential role in geometrically realizing various aspects of string theory: gauge symmetries and matter generation, and so on. In particular, the codimension-two singularities are associated with matter generation [87, 88, 90, 96]. Thus, for considering mater generation in F-theory, we have focused on the codimension-two singularities in a six-dimensional F-theory, especially, an F-theory on an elliptically fibred Calabi-Yau threefold over $\mathbb{F}_n$ in the stable degeneration limit.

In six- or lower-dimensional F-theories, if a fibre type has the condition that an exceptional curve splits into two irreducible ones, we can distinguish the singular fibre type into two types. In the case that the exceptional curve can split globally, these fibre types are called the split fibre types. On the other hand, in the case that it can *not* split globally, these fibre types are called call it the non-split fibre types. Models with the split singular fibre correspond to the *ADE* gauge symmetries implied by Kodaira's classification [62, 113, 114]. On the other hand, in models with the non-split singular fibre, the two split irreducible exceptional curves are identified by monodromy around a certain codimension-two singularity. Therefore, the expected gauge symmetries in the non-split models are reduced to the non-simply-laced ones. However, the non-split models have puzzles associated with non-local matter generation; thus, we have focused on the non-split models whose expected gauge symmetries are the non-simply-laced ones.

We have briefly reviewed the basics of F-theory and the dualities between F-theory and other superstring theories. First, we have introduced the $[p, q]$7-brane and their monodromies. We have then discussed the classification of the 7-brane configurations and the expected gauge symmetries by analyzing the monodromies in Type IIB superstring theory [63–65]. Next, we construct F-theory and see that the singularities of F-theory compact space have the information associated with gauge symmetries implied by Kodaira's classification [62, 113, 114]. We then discuss the dualities between F-theory and other

theories: M-theory [52, 59, 111] and Heterotic superstring theory [52, 53, 87–89, 123, 124]. Finally, we introduce the anomaly cancellation condition [90, 125] and see that matter content in a model with ADE codimension-one singularity matches this condition if the charged matter fields are localized at all codimension-two singularities [90].

Moreover, we have considered models in which not full-hypermultiplets but half-hypermultiplets appear as matter multiplets. In these cases, the singularity enhancement is characterized by $G'/(G \times A_1)$. We have mentioned these gauge symmetries correspond to particular Wolf spaces and are related to the Freudenthal-Tits magic square. In the first half of Chapter 5, we consider the split I_6 model in which half-hypermultiplets arise and whose expected gauge symmetry is A_5. We have demonstrated explicit blow-up processes and investigated the intersection diagrams of the exceptional curves. In particular, we have shown that the conifold singularities play an essential role in several aspects of this example.

In the last half of Chapter 5, as a final magical example, we have studied an F-theory on an elliptic fibration over a Hirzebruch surface $\mathbb{F}_n$ with a codimension-one singularity of the *non-split* I_6 singular fibre type whose expected gauge symmetry is C_3. We have then found significant qualitative differences between the F-theory models of the split types with half-hypermultiplets and the present model [99]. First, we have shown that the massless half-hypermultiplets of C_3: $\mathbf{14'}\frac{1}{2}$ and $\mathbf{6}\frac{1}{2}$, which are related to $F_4/(Sp(3) \times SU(2))$ and $Sp(4)/(Sp(3) \times SU(2)))$, arise at the codimension-two singularities where the gauge symmetry is enhanced to E_6 and the half-hypermultiplets $\mathbf{20}\frac{1}{2}$ of A_5 appear in the split I_6 model. We have then considered the puzzles associated with non-local matter generation in the base space near the codimension-two singularities where the codimension-one singularity is enhanced to D_6. Not only the non-split I_6 model but also other non-split models have these puzzles [1, 90, 95, 100–104]. In terms of the anomaly cancellation condition and the resolution of the singularities, we have stated what the puzzles are as follows:

(1) In split models, if the charged matter fields are localized at all codimension-two singularities, the number of the matter fields is consistent with the anomaly cancellation condition. This is one of the reasons why the massless charged matter fields are localized at all codimension-two singularities, which correspond to intersections of 7-branes in Type IIB superstring theory, in six-dimensional F-theory models with ADE gauge symmetries. On the other hand, in non-split models, there is a puzzle in which the anomaly cancellation condition and the naive counting of the number of the matter fields under the same condition for split models do not match.

(2) At a D_{2k+2} $(k \geq 1)$ or an E_7 codimension-two singularity, some conifold singularities remain in the split models even after blowing up all codimension-one singularities, but not in the non-split models. In the split models, since we can yield new two-cycles by small resolutions of the conifold singularities, we can obtain an intersection

diagram of exceptional curves that is different from one on a codimension-one singularity; therefore, the enhancement of the gauge symmetry can be explained. In the M-theory dual, an M2-brane wrapped around the new two-cycle generates local matter fields. On the other hand, in the non-split models, no additional blow-up at these singularities is required since they are simultaneously resolved together by the resolution of codimension-one singularity; then, the intersection diagrams remain the same and there is no new two-cycle around which an $M2$-brane can be wrapped. Therefore, there is no sign of localized matter fields, although the anomaly cancellation condition requires charged matter fields to arise.

In the last half of this thesis, toward understanding these puzzles, we have examined the relationship between the split and the non-split models [95]. We have then shown that the transition from the split model after the blow-ups to the corresponding non-split model, except for a special class of models, is a conifold transition from the resolved to the deformed side. This transition is related to the conifold singularities remaining at the codimension-two singularities where the codimension-one singularity is enhanced to D_{2k+2} ($k \geq 1$) or E_7 after the blow-ups of the codimension-one singularity.

In Chapter 6, we have investigated this fact separately for all cases in that we can distinguish between the split and non-split fibre types: I_n ($n \geq 3$), I_n^* ($n \geq 0$), IV and IV^*. The results, respectively, have been as follows:

(1) I_{2k} ($k \geq 2$), IV and I_{2k-3}^* ($k \geq 2$) models (A_{2k-1}, H_2 and D_{2k+1} models)

The I_{2k}, IV and I_{2k-3}^* split models have the D_{2k}, D_4 and D_{2k+2} codimension-two singularities in general. After the resolution of the codimension-one singularities, we have found that there have remained some conifold singularities there. If these conifold singularities have been resolved by small resolutions, we have obtained a smooth split model for each case. This is the resolved side of the conifold transition. On the other hand, we can resolve these conifold singularities by the deformation. We have found that a certain deformation has caused the transition from the split models to the corresponding non-split model. In this case, since all conifold singularities have been simultaneously resolved by this deformation, we have obtained a smooth non-split model for each case. This is the deformed side of the conifold transition.

(2) IV^* model (E_6 model)

This model is similar to the models belonging to (1), but only in this case, the codimension-two singularity where the conifold transition occurs is an E_7 codimension-two singularity instead of a D_{2k} one.

(3) I_{2k-1} ($k \geq 2$) models (A_{2k-2} models)

These models do not have the D_{2k} codimension-two singularities but have the D_{2k-1} and A_{2k-1} codimension-two singularities in general. However, by adjusting the complex structure as if a D_{2k-1} and an A_{2k-1} codimension-two singularity superimpose each other, we have obtained a D_{2k} codimension-two singularity. We called such a split I_{2k-1} model with this special complex structure an "over-split" model [99]. In "over-split" models, we have found that there have remained some conifold singularities at the D_{2k} codimension-two singularities after the resolution of their codimension-one singularities. We have then obtained the non-split I_{2k-1} model by the deformation of the conifold singularities in the corresponding "over-split" models similarly.

(4) I_{2k-2}^* ($k \geq 1$) models (D_{2k+2} models)

In these models, no conifold singularities appear after the resolution of the codimension-one singularity. Therefore, these models are a special class in which the split/non-split transition cannot be regarded as a conifold transition.

These results have clarified, in cases except (4), that the deformations of conifold singularities that remain after the resolution of the codimension-one singularities correspond to diagram automorphisms of the expected simply-laced Dynkin diagrams in the corresponding split models. And these also have shown that "local deformed conifolds", which are nontrivial three-cycles S^3, appear in non-split models where matter fields exist in compact space *without* any special parameter tuning and that the puzzle in resolution analysis [99] is because of conifold singularities becoming deformed. These are non-local in the base space and thus it implies non-local matter generation.

[1] has proposed a mechanism for non-local matter generation in the non-split model that requires no additional exceptional curves and due to the adjoint hypermultiplets associated with a genus-g Riemann surface. We have investigated how this proposal can be realized in our resolution analysis. We have then shown that the genus-g Riemann surface can be obtained as an intersection of the blown-up threefold and a certain divisor by "forgetting" the fibre $\mathbb{P}^1$. We have found that even when there are multiple split pairs of exceptional curves, similar results are obtained.

It would be very interesting to consider this transition from the standpoint of deformation theory [152,153] since the non-split model includes having a deformation condition in its definition. Moreover, as emphasized above, without any special parameter tuning of the moduli, the conifold singularities associated with our discussion appear where the matter fields arise. The conifold transition has been a key concept when discussing AdS/CFT [154,155], topological string theory [156,157], and string cosmology, for example, in [2,158]. Also, the "local deformed conifolds" have been utilized in models of early cosmology such as the construction of de Sitter Vacua in superstring theory [2,155]. From these facts, we hope to consider new applications of the facts revealed in this thesis to string phenomenology and cosmology. In particular, it would be significant to investigate

this transition from the standpoint of dual M-theory (e.g., the box graph [143, 159–162]), since on the F-theory side this conifold singularity involves virtual space, while on the dual M-theory side, it is all physical space.

Acknowledgement

Appendix A

Conifold singularity

A.1 Conifold singularity

In this Appendix, we consider the deformation and resolution of a conifold singularity (see [163]). A (singular) conifold is a cone-like complex Calabi-Yau threefold with a singularity at the cone's tip. And this manifold has the base of $S^2 \times S^3$ in the neighborhood of the singularity (Fig. A.1). This singularity is called a conifold singularity. A conifold
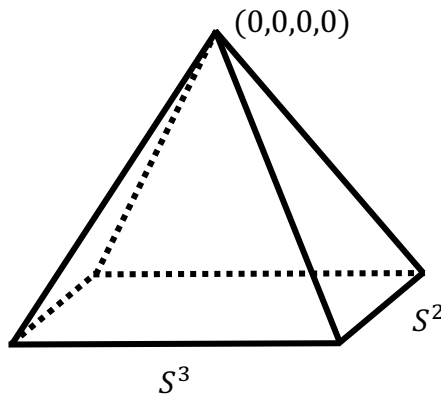
Figure A.1: The neighborhood of conifold singularity.

is defined as by

$$P_c = x^2 + y^2 + z^2 + w^2 = 0, \tag{A.1.1}$$

where $(x, y, z, w) \in \mathbb{C}$. In this case, there is a conifold singularity at $(x, y, z, w) = (0, 0, 0, 0)$. There are two ways to resolve the conifold singularity: Deformation and small resolution.

A.2 Deformed conifold

In this section, we consider the deformation of a conifold singularity. By deforming the right-hand side of Eq. (A.1.1) from 0 to ϵ^2, it can be deformed as in

$$x^2 + y^2 + z^2 + w^2 = \epsilon^2, \tag{A.2.1}$$

where $\epsilon(\neq 0) \in \mathbb{R}$ (or $\mathbb{C}$). When a conifold singularity is resolved in this way, we obtain a manifold called a "deformed conifold". In other words, We obtain the deformed conifold as the singularity at the tip of Fig. A.1 is resolved by blowing up S^3 (Fig. A.2). From Fig. A.2, $S^2 \times \mathbb{R} \simeq \mathbb{R}^3 \simeq T_x^* S^3$ ($x \in S^3$) can be regarded as a fiber at each point x of S^3, so the total manifold is $T^* S^3$. This can be shown as follows. By variable transformation
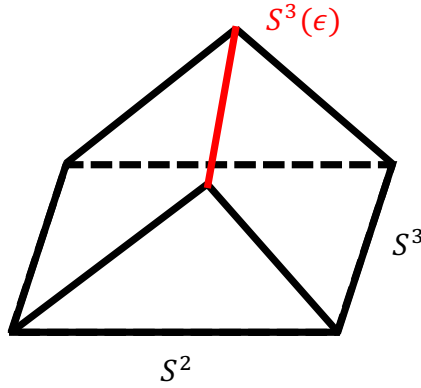
Figure A.2: Deformed conifold.

as

$$\begin{aligned} x &= Y_1 + iZ_1, \quad y = Y_2 + iZ_2, \\ z &= Y_3 + iZ_3, \quad w = Y_4 + iZ_4, \end{aligned} \tag{A.2.2}$$

from Eq. (A.2.1), we obtain

$$Y_1^2 + Y_2^2 + Y_3^2 + Y_4^2 - Z_1^2 - Z_2^2 - Z_3^2 - Z_4^2 = \epsilon^2, \tag{A.2.3}$$

$$Y_1 Z_1 - Y_2 Z_2 - Y_3 Z_3 - Y_3 Z_3 = 0, \tag{A.2.4}$$

where Y_i, $Z_i \in \mathbb{R}$ and Z_i are the coordinates of the cotangent space of $(x \in)S^3$. The base $(Z_i = 0)$ is given by

$$Y_1^2 + Y_2^2 + Y_3^2 + Y_4^2 = \epsilon^2 \tag{A.2.5}$$

and is S^3 whose radius is ϵ. If we consider $\epsilon \to 0$, the deformed conifold becomes singular again.

A.3 Resolved conifold

In this section, we consider the small resolution of a conifold singularity. We can resolve a singularity on a hypersurface in the ambient space $\mathbb{C}_4$ by inserting $\mathbb{P}^3$ in $\mathbb{C}_4$ in general. If the singularity is a conifold singularity, this operation is equivalent to inserting $\mathbb{P}^1 \times \mathbb{P}^1$. However, it is sufficient to insert only one of the two $\mathbb{P}^1$s to resolve the conifold singularity. Thus, This resolution is called the *small* resolution. When a conifold singularity is resolved by the small resolution, we obtain a manifold called a "resolved conifold". In other words, We obtain the resolved conifold as the singularity at the tip of Fig. A.1 is resolved by blowing up S^2 (Fig. A.3). This can be shown as follows. By
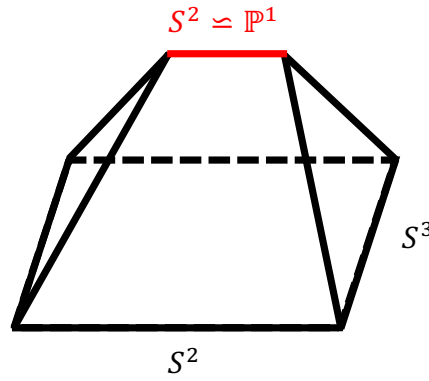
Figure A.3: Resolved conifold.

variable transformation as

$$
\begin{aligned}
X_1 &= x + iy, & X_2 &= z + iw, \\
X_3 &= -z + iw, & X_4 &= x - iy,
\end{aligned}
\tag{A.3.1}
$$

from Eq. (A.2.1), we obtain

$$
P_c = X_1 X_4 - X_2 X_3 = 0.
\tag{A.3.2}
$$

In this case, there is a conifold singularity at $(X_1, X_2, X_3, X_4) = (0, 0, 0, 0)$. Inserting one $\mathbb{P}^1$ at the conifold singularity in C is given by

$$
\hat{C} = \left\{ ((x, y, z, w) \times (\xi : \eta)) \in \mathbb{C}^4 \times \mathbb{P}^1 \, \middle| \, \begin{pmatrix} X_1 & X_2 \\ X_3 & X_4 \end{pmatrix} \begin{pmatrix} \xi \\ \eta \end{pmatrix} = \begin{pmatrix} 0 \\ 0 \end{pmatrix} \right\},
\tag{A.3.3}
$$

where $\det \begin{pmatrix} X_1 & X_2 \\ X_3 & X_4 \end{pmatrix} = 0$. Since $\operatorname{rank} \begin{pmatrix} X_1 & X_2 \\ X_3 & X_4 \end{pmatrix} = 0$ at only $(X_1, X_2, X_3, X_4) = (0, 0, 0, 0)$, $(\xi : \eta)(\in \mathbb{P}^1)$ is undetermined. On the other hand, at $(X_1, X_2, X_3, X_4) \neq (0, 0, 0, 0)$, $(\xi : \eta)$ is determined at a single point. Therefore, considering $\hat{C}$ means that $\mathbb{P}^1$ is *only* inserted at the conifold singularity $(X_1, X_2, X_3, X_4) = (0, 0, 0, 0)$. We also confirm that the conifold singularity is resolved by this operation.

$$\partial_{X_1}(X_1 \xi + X_2 \eta) = \xi = 0 \tag{A.3.4}$$

and

$$\partial_{X_2}(X_1 \xi + X_2 \eta) = \eta = 0 \tag{A.3.5}$$

give $(\xi, \eta) = (0, 0)$. However, since $(\xi : \eta) \in \mathbb{P}^1$, $\hat{C}$ is regular.

From Eq. (A.3.3), we obtain

$$\xi X_1 = -\eta X_2, \quad \xi X_3 = -\eta X_4. \tag{A.3.6}$$

And $\hat{C}$ is covered by two local patches: $\xi \neq 0$ and $\eta \neq 0$. In the local patch $\xi \neq 0$, Eq. (A.3.6) is

$$X_1 = -\lambda X_2, \quad X_3 = -\lambda X_4, \tag{A.3.7}$$

where $\lambda := \eta/\xi$. Hence, (X_2, X_4, λ) are the local coordinates of this patch. In this patch, inserted $\mathbb{P}^1$ is

$$(X_2, X_4, \lambda) = (0, 0, \lambda). \tag{A.3.8}$$

On the other hand, in the local patch $\eta \neq 0$, Eq. (A.3.6) is

$$X_2 = -\mu X_1, \quad X_4 = -\mu X_3, \tag{A.3.9}$$

where $\mu := \xi/\eta$. Hence, (X_1, X_3, μ) are the local coordinates of this patch. In this patch, inserted $\mathbb{P}^1$ is

$$(X_1, X_3, \mu) = (0, 0, \mu). \tag{A.3.10}$$

A.4 Conifold transition

Finally, we consider introducing a conifold transition based on the fact in the previous section. The size of S^3 in the deformed conifold is reduced to zero ($\epsilon \to 0$) to give the singular conifold, from which blowing up $S^2 \simeq \mathbb{P}^1$ gives the resolved conifold. This transition is called a conifold transition from the deformed to the resolved side (Fig. A.4).
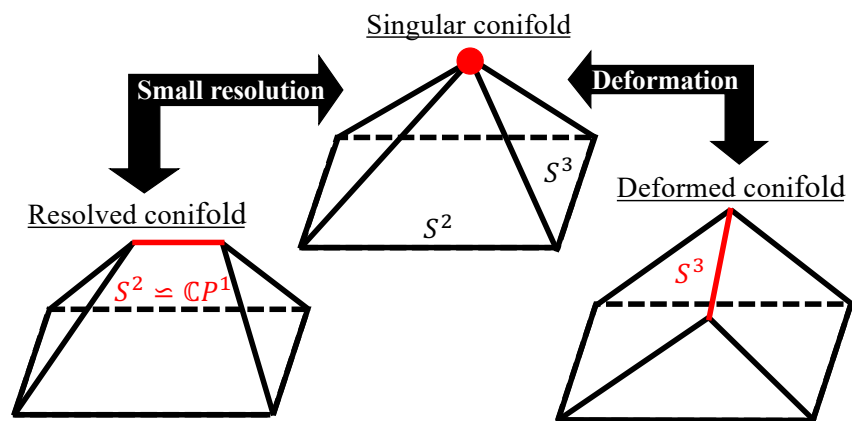
Figure A.4: Conifold transition.

References

[1] P. S. Aspinwall, S. H. Katz, and D. R. Morrison, *Lie groups, Calabi-Yau threefolds, and F theory*, Adv. Theor. Math. Phys. **4** (2000) 95–126 [arXiv:hep-th/0002012].

[2] S. Kachru, R. Kallosh, A. D. Linde, and S. P. Trivedi, *De Sitter vacua in string theory*, Phys. Rev. D **68** (2003) 046005 [arXiv:hep-th/0301240].

[3] S. Kachru, R. Kallosh, A. D. Linde, J. M. Maldacena, L. P. McAllister, and S. P. Trivedi, *Towards inflation in string theory*, JCAP **10** (2003) 013 [arXiv:hep-th/0308055].

[4] E. Witten, *Strong coupling expansion of Calabi-Yau compactification*, Nucl. Phys. B **471** (1996) 135–158 [arXiv:hep-th/9602070].

[5] A. Giveon and D. Kutasov, *Brane Dynamics and Gauge Theory*, Rev. Mod. Phys. **71** (1999) 983–1084 [arXiv:hep-th/9802067].

[6] R. Blumenhagen, B. Kors, D. Lust, and T. Ott, *The standard model from stable intersecting brane world orbifolds*, Nucl. Phys. B **616** (2001) 3–33 [arXiv:hep-th/0107138].

[7] R. Tatar and T. Watari, *Proton decay, Yukawa couplings and underlying gauge symmetry in string theory*, Nucl. Phys. B **747** (2006) 212–265 [arXiv:hep-th/0602238].

[8] H. Hayashi, R. Tatar, Y. Toda, T. Watari, and M. Yamazaki, *New Aspects of Heterotic–F Theory Duality*, Nucl. Phys. B **806** (2009) 224–299 [arXiv:0805.1057 [hep-th]].

[9] B. Andreas and G. Curio, *From Local to Global in F-Theory Model Building*, J. Geom. Phys. **60** (2010) 1089–1102 [arXiv:0902.4143 [hep-th]].

[10] J. Marsano, N. Saulina, and S. Schafer-Nameki, *F-theory Compactifications for Supersymmetric GUTs*, JHEP **08** (2009) 030 [arXiv:0904.3932 [hep-th]].

[11] A. Collinucci, *New F-theory lifts. II. Permutation orientifolds and enhanced singularities*, JHEP **04** (2010) 076 [arXiv:0906.0003 [hep-th]].

[12] R. Blumenhagen, T. W. Grimm, B. Jurke, and T. Weigand, *F-theory uplifts and GUTs*, JHEP **09** (2009) 053 [arXiv:0906.0013 [hep-th]].

[13] J. Marsano, N. Saulina, and S. Schafer-Nameki, *Monodromies, Fluxes, and Compact Three-Generation F-theory GUTs*, JHEP **08** (2009) 046 [arXiv:0906.4672 [hep-th]].

[14] R. Blumenhagen, T. W. Grimm, B. Jurke, and T. Weigand, *Global F-theory GUTs*, Nucl. Phys. B **829** (2010) 325–369 [arXiv:0908.1784 [hep-th]].

[15] J. Marsano, N. Saulina, and S. Schafer-Nameki, *Compact F-theory GUTs with U(1) (PQ)*, JHEP **04** (2010) 095 [arXiv:0912.0272 [hep-th]].

[16] T. W. Grimm, S. Krause, and T. Weigand, *F-Theory GUT Vacua on Compact Calabi-Yau Fourfolds*, JHEP **07** (2010) 037 [arXiv:0912.3524 [hep-th]].

[17] M. Cvetic, I. Garcia-Etxebarria, and J. Halverson, *Global F-theory Models: Instantons and Gauge Dynamics*, JHEP **01** (2011) 073 [arXiv:1003.5337 [hep-th]].

[18] C.-M. Chen, J. Knapp, M. Kreuzer, and C. Mayrhofer, *Global SO(10) F-theory GUTs*, JHEP **10** (2010) 057 [arXiv:1005.5735 [hep-th]].

[19] C.-M. Chen and Y.-C. Chung, *Flipped SU(5) GUTs from E_8 Singularities in F-theory*, JHEP **03** (2011) 049 [arXiv:1005.5728 [hep-th]].

[20] T. W. Grimm and T. Weigand, *On Abelian Gauge Symmetries and Proton Decay in Global F-theory GUTs*, Phys. Rev. D **82** (2010) 086009 [arXiv:1006.0226 [hep-th]].

[21] J. Knapp, M. Kreuzer, C. Mayrhofer, and N.-O. Walliser, *Toric Construction of Global F-Theory GUTs*, JHEP **03** (2011) 138 [arXiv:1101.4908 [hep-th]].

[22] M. J. Dolan, J. Marsano, N. Saulina, and S. Schafer-Nameki, *F-theory GUTs with U(1) Symmetries: Generalities and Survey*, Phys. Rev. D **84** (2011) 066008 [arXiv:1102.0290 [hep-th]].

[23] J. Marsano and S. Schafer-Nameki, *Yukawas, G-flux, and Spectral Covers from Resolved Calabi-Yau's*, JHEP **11** (2011) 098 [arXiv:1108.1794 [hep-th]].

[24] T. W. Grimm, M. Kerstan, E. Palti, and T. Weigand, *Massive Abelian Gauge Symmetries and Fluxes in F-theory*, JHEP **12** (2011) 004 [arXiv:1107.3842 [hep-th]].

[25] D. R. Morrison and D. S. Park, *F-Theory and the Mordell-Weil Group of Elliptically-Fibered Calabi-Yau Threefolds*, JHEP **10** (2012) 128 [arXiv:1208.2695 [hep-th]].

[26] C. Mayrhofer, E. Palti, and T. Weigand, *U(1) symmetries in F-theory GUTs with multiple sections*, JHEP **03** (2013) 098 [arXiv:1211.6742 [hep-th]].

[27] V. Braun, T. W. Grimm, and J. Keitel, *New Global F-theory GUTs with U(1) symmetries*, JHEP **09** (2013) 154 [arXiv:1302.1854 [hep-th]].

[28] J. Borchmann, C. Mayrhofer, E. Palti, and T. Weigand, *Elliptic fibrations for SU(5) × U(1) × U(1) F-theory vacua*, Phys. Rev. D **88** no. 4, (2013) 046005 [arXiv:1303.5054 [hep-th]].

[29] M. Cvetic, D. Klevers, and H. Piragua, *F-Theory Compactifications with Multiple U(1)-Factors: Constructing Elliptic Fibrations with Rational Sections*, JHEP **06** (2013) 067 [arXiv:1303.6970 [hep-th]].

[30] V. Braun, T. W. Grimm, and J. Keitel, *Geometric Engineering in Toric F-Theory and GUTs with U(1) Gauge Factors*, JHEP **12** (2013) 069 [arXiv:1306.0577 [hep-th]].

[31] M. Cvetič, A. Grassi, D. Klevers, and H. Piragua, *Chiral Four-Dimensional F-Theory Compactifications With SU(5) and Multiple U(1)-Factors*, JHEP **04** (2014) 010 [arXiv:1306.3987 [hep-th]].

[32] M. Cvetič, D. Klevers, and H. Piragua, *F-Theory Compactifications with Multiple U(1)-Factors: Addendum*, JHEP **12** (2013) 056 [arXiv:1307.6425 [hep-th]].

[33] J. Borchmann, C. Mayrhofer, E. Palti, and T. Weigand, *SU(5) Tops with Multiple U(1)s in F-theory*, Nucl. Phys. B **882** (2014) 1–69 [arXiv:1307.2902 [hep-th]].

[34] M. Cvetic, D. Klevers, H. Piragua, and P. Song, *Elliptic fibrations with rank three Mordell-Weil group: F-theory with U(1) x U(1) x U(1) gauge symmetry*, JHEP **03** (2014) 021 [arXiv:1310.0463 [hep-th]].

[35] I. Antoniadis and G. K. Leontaris, *F-GUTs with Mordell–Weil U(1) 's*, Phys. Lett. B **735** (2014) 226–230 [arXiv:1404.6720 [hep-th]].

[36] C. Lawrie, S. Schafer-Nameki, and J.-M. Wong, *F-theory and All Things Rational: Surveying U(1) Symmetries with Rational Sections*, JHEP **09** (2015) 144 [arXiv:1504.05593 [hep-th]].

[37] M. Cvetič, D. Klevers, H. Piragua, and W. Taylor, *General U(1)×U(1) F-theory compactifications and beyond: geometry of unHiggsings and novel matter structure*, JHEP **11** (2015) 204 [arXiv:1507.05954 [hep-th]].

[38] M. Cvetic, A. Grassi, D. Klevers, M. Poretschkin, and P. Song, *Origin of Abelian Gauge Symmetries in Heterotic/F-theory Duality*, JHEP **04** (2016) 041 [arXiv:1511.08208 [hep-th]].

[39] Y. Kimura and S. Mizoguchi, *Enhancements in F-theory models on moduli spaces of K3 surfaces with ADE rank 17*, PTEP **2018** no. 4, (2018) 043B05 [arXiv:1712.08539 [hep-th]].

[40] Y. Kimura, *F-theory models on K3 surfaces with various Mordell-Weil ranks — constructions that use quadratic base change of rational elliptic surfaces*, JHEP **05** (2018) 048 [arXiv:1802.05195 [hep-th]].

[41] C. Beasley, J. J. Heckman, and C. Vafa, *GUTs and Exceptional Branes in F-theory - I*, JHEP **01** (2009) 058 [arXiv:0802.3391 [hep-th]].

[42] C. Beasley, J. J. Heckman, and C. Vafa, *GUTs and Exceptional Branes in F-theory - II: Experimental Predictions*, JHEP **01** (2009) 059 [arXiv:0806.0102 [hep-th]].

[43] R. Donagi and M. Wijnholt, *Model Building with F-Theory*, Adv. Theor. Math. Phys. **15** no. 5, (2011) 1237–1317 [arXiv:0802.2969 [hep-th]].

[44] H. Hayashi, T. Kawano, R. Tatar, and T. Watari, *Codimension-3 Singularities and Yukawa Couplings in F-theory*, Nucl. Phys. B **823** (2009) 47–115 [arXiv:0901.4941 [hep-th]].

[45] R. Donagi and M. Wijnholt, *Breaking GUT Groups in F-Theory*, Adv. Theor. Math. Phys. **15** no. 6, (2011) 1523–1603 [arXiv:0808.2223 [hep-th]].

[46] R. Donagi and M. Wijnholt, *Higgs Bundles and UV Completion in F-Theory*, Commun. Math. Phys. **326** (2014) 287–327 [arXiv:0904.1218 [hep-th]].

[47] J. J. Heckman, J. Marsano, N. Saulina, S. Schafer-Nameki, and C. Vafa, *Instantons and SUSY breaking in F-theory*, arXiv:0808.1286 [hep-th].

[48] J. Marsano, N. Saulina, and S. Schafer-Nameki, *Gauge Mediation in F-Theory GUT Models*, Phys. Rev. D **80** (2009) 046006 [arXiv:0808.1571 [hep-th]].

[49] J. J. Heckman and C. Vafa, *F-theory, GUTs, and the Weak Scale*, JHEP **09** (2009) 079 [arXiv:0809.1098 [hep-th]].

[50] A. Font and L. E. Ibanez, *Yukawa Structure from U(1) Fluxes in F-theory Grand Unification*, JHEP **02** (2009) 016 [arXiv:0811.2157 [hep-th]].

[51] A. Sen, *An Introduction to nonperturbative string theory*, in A Newton Institute Euroconference on Duality and Supersymmetric Theories, pp. 297–413. 2, 1998. arXiv:hep-th/9802051.

[52] C. Vafa, *Evidence for F theory*, Nucl. Phys. B **469** (1996) 403–418 [arXiv:hep-th/9602022].

[53] W. Lerche, *On the heterotic / F theory duality in eight-dimensions*, in NATO Advanced Study Institute: TMR Summer School on Progress in String Theory and M-Theory, pp. 15–46. 5, 1999. arXiv:hep-th/9910207.

[54] F. Denef, *Les Houches Lectures on Constructing String Vacua*, Les Houches **87** (2008) 483–610 [arXiv:0803.1194 [hep-th]].

[55] T. Weigand, *Lectures on F-theory compactifications and model building*, Class. Quant. Grav. **27** (2010) 214004 [arXiv:1009.3497 [hep-th]].

[56] W. Taylor, *TASI Lectures on Supergravity and String Vacua in Various Dimensions*, arXiv:1104.2051 [hep-th].

[57] T. Weigand, *F-theory*, PoS **TASI2017** (2018) 016 [arXiv:1806.01854 [hep-th]].

[58] M. Cvetič and L. Lin, *TASI Lectures on Abelian and Discrete Symmetries in F-theory*, PoS **TASI2017** (2018) 020 [arXiv:1809.00012 [hep-th]].

[59] E. Witten, *Nonperturbative superpotentials in string theory*, Nucl. Phys. B **474** (1996) 343–360 [arXiv:hep-th/9604030].

[60] A. Sen, *Orientifold limit of F theory vacua*, Phys. Rev. D **55** (1997) R7345–R7349 [arXiv:hep-th/9702165].

[61] M. Bianchi, A. Collinucci, and L. Martucci, *Magnetized E3-brane instantons in F-theory*, JHEP **12** (2011) 045 [arXiv:1107.3732 [hep-th]].

[62] K. Kodaira, *On Compact Analytic Sureface II*, Annals of Math. **77** (1963) 563.

[63] M. R. Gaberdiel and B. Zwiebach, *Exceptional groups from open strings*, Nucl. Phys. B **518** (1998) 151–172 [arXiv:hep-th/9709013].

[64] O. DeWolfe and B. Zwiebach, *String junctions for arbitrary Lie algebra representations*, Nucl. Phys. B **541** (1999) 509–565 [arXiv:hep-th/9804210].

[65] O. DeWolfe, T. Hauer, A. Iqbal, and B. Zwiebach, *Uncovering the symmetries on [p,q] seven-branes: Beyond the Kodaira classification*, Adv. Theor. Math. Phys. **3** (1999) 1785–1833 [arXiv:hep-th/9812028].

[66] K. Hashimoto, H. Hata, and N. Sasakura, *Three - string junction and BPS saturated solutions in SU(3) supersymmetric Yang-Mills theory*, Phys. Lett. B **431** (1998) 303–310 [arXiv:hep-th/9803127].

[67] K. Hashimoto, H. Hata, and N. Sasakura, *Multipronged strings and BPS saturated solutions in SU(N) supersymmetric Yang-Mills theory*, Nucl. Phys. B **535** (1998) 83–115 [arXiv:hep-th/9804164].

[68] K. Hashimoto, *String junction from world sheet gauge theory*, Prog. Theor. Phys. **101** (1999) 1353–1370 [arXiv:hep-th/9808185].

[69] Y. Imamura, *E(8) flavor multiplets*, Phys. Rev. D **58** (1998) 106005 [arXiv:hep-th/9802189].

[70] Y. Imamura, *String junctions and their duals in heterotic string theory*, Prog. Theor. Phys. **101** (1999) 1155–1164 [arXiv:hep-th/9901001].

[71] K. Dasgupta and S. Mukhi, *BPS nature of three string junctions*, Phys. Lett. B **423** (1998) 261–264 [arXiv:hep-th/9711094].

[72] M. Krogh and S. Lee, *String network from M theory*, Nucl. Phys. B **516** (1998) 241–254 [arXiv:hep-th/9712050].

[73] Y. Matsuo and K. Okuyama, *BPS condition of string junction from M theory*, Phys. Lett. B **426** (1998) 294–296 [arXiv:hep-th/9712070].

[74] J. J. Heckman, C. Lawrie, T. B. Rochais, H. Y. Zhang, and G. Zoccarato, *S-folds, string junctions, and $\mathcal{N} = 2$ SCFTs*, Phys. Rev. D **103** no. 8, (2021) 086013 [arXiv:2009.10090 [hep-th]].

[75] F. Hassler, J. J. Heckman, T. B. Rochais, T. Rudelius, and H. Y. Zhang, *T-Branes, String Junctions, and 6D SCFTs*, Phys. Rev. D **101** no. 8, (2020) 086018 [arXiv:1907.11230 [hep-th]].

[76] M. Cvetič, M. Dierigl, L. Lin, and H. Y. Zhang, *All eight- and nine-dimensional string vacua from junctions*, Phys. Rev. D **106** no. 2, (2022) 026007 [arXiv:2203.03644 [hep-th]].

[77] A. Sen, *String network*, JHEP **03** (1998) 005 [arXiv:hep-th/9711130].

[78] M. R. Gaberdiel, T. Hauer, and B. Zwiebach, *Open string-string junction transitions*, Nucl. Phys. B **525** (1998) 117–145 [arXiv:hep-th/9801205].

[79] O. Bergman, *Three pronged strings and 1/4 BPS states in N=4 super Yang-Mills theory*, Nucl. Phys. B **525** (1998) 104–116 [arXiv:hep-th/9712211].

[80] O. Bergman and A. Fayyazuddin, *String junctions and BPS states in Seiberg-Witten theory*, Nucl. Phys. B **531** (1998) 108–124 [arXiv:hep-th/9802033].

[81] J. H. Schwarz, *Lectures on superstring and M theory dualities: Given at ICTP Spring School and at TASI Summer School*, Nucl. Phys. B Proc. Suppl. **55** (1997) 1–32 [arXiv:hep-th/9607201].

[82] O. Aharony, J. Sonnenschein, and S. Yankielowicz, *Interactions of strings and D-branes from M theory*, Nucl. Phys. B **474** (1996) 309–322 [arXiv:hep-th/9603009].

[83] E. Witten, *Bound states of strings and p-branes*, Nucl. Phys. B **460** (1996) 335–350 [arXiv:hep-th/9510135].

[84] O. Bergman and A. Fayyazuddin, *String junction transitions in the moduli space of N=2 SYM*, Nucl. Phys. B **535** (1998) 139–151 [arXiv:hep-th/9806011].

[85] T. Tani, *Matter from string junction*, Nucl. Phys. B **602** (2001) 434–452.

[86] L. Bonora and R. Savelli, *Non-simply-laced Lie algebras via F theory strings*, JHEP **11** (2010) 025 [arXiv:1007.4668 [hep-th]].

[87] D. R. Morrison and C. Vafa, *Compactifications of F theory on Calabi-Yau threefolds. 1*, Nucl. Phys. B **473** (1996) 74–92 [arXiv:hep-th/9602114].

[88] D. R. Morrison and C. Vafa, *Compactifications of F theory on Calabi-Yau threefolds. 2.*, Nucl. Phys. B **476** (1996) 437–469 [arXiv:hep-th/9603161].

[89] R. Friedman, J. Morgan, and E. Witten, *Vector bundles and F theory*, Commun. Math. Phys. **187** (1997) 679–743 [arXiv:hep-th/9701162].

[90] M. Bershadsky, K. A. Intriligator, S. Kachru, D. R. Morrison, V. Sadov, and C. Vafa, *Geometric singularities and enhanced gauge symmetries*, Nucl. Phys. B **481** (1996) 215–252 [arXiv:hep-th/9605200].

[91] S. Katz, D. R. Morrison, S. Schafer-Nameki, and J. Sully, *Tate's algorithm and F-theory*, JHEP **08** (2011) 094 [arXiv:1106.3854 [hep-th]].

[92] J. J. Heckman and C. Vafa, *Flavor Hierarchy From F-theory*, Nucl. Phys. B **837** (2010) 137–151 [arXiv:0811.2417 [hep-th]].

[93] D. R. Morrison and W. Taylor, *Matter and singularities*, JHEP **01** (2012) 022 [arXiv:1106.3563 [hep-th]].

[94] M. Esole and S.-T. Yau, *Small resolutions of SU(5)-models in F-theory*, Adv. Theor. Math. Phys. **17** no. 6, (2013) 1195–1253 [arXiv:1107.0733 [hep-th]].

[95] R. Kuramochi, S. Mizoguchi, and T. Tani, *Non-split singularities and conifold transitions in F-theory*, JHEP **10** (2022) 070 [arXiv:2108.10136 [hep-th]].

[96] S. H. Katz and C. Vafa, *Matter from geometry*, Nucl. Phys. B **497** (1997) 146–154 [arXiv:hep-th/9606086].

[97] D. R. Morrison and W. Taylor, *Classifying bases for 6D F-theory models*, Central Eur. J. Phys. **10** (2012) 1072–1088 [arXiv:1201.1943 [hep-th]].

[98] N. Kan, S. Mizoguchi, and T. Tani, *Half-hypermultiplets and incomplete/complete resolutions in F-theory*, JHEP **08** (2020) 063 [arXiv:2003.05563 [hep-th]].

[99] R. Kuramochi, S. Mizoguchi, and T. Tani, *The magic square and half-hypermultiplets in F-theory*, PTEP **2022** no. 3, (2022) 033B09 [arXiv:2008.09272 [hep-th]].

[100] A. Grassi, J. Halverson, C. Long, J. L. Shaneson, and J. Tian, *Non-simply-laced Symmetry Algebras in F-theory on Singular Spaces*, JHEP **09** (2018) 129 [arXiv:1805.06949 [hep-th]].

[101] P. Arras, A. Grassi, and T. Weigand, *Terminal Singularities, Milnor Numbers, and Matter in F-theory*, J. Geom. Phys. **123** (2018) 71–97 [arXiv:1612.05646 [hep-th]].

[102] M. Esole, P. Jefferson, and M. J. Kang, *The Geometry of F_4-Models*, arXiv:1704.08251 [hep-th].

[103] M. Esole and M. J. Kang, *The Geometry of the SU(2)× G_2-model*, JHEP **02** (2019) 091 [arXiv:1805.03214 [hep-th]].

[104] M. Esole and P. Jefferson, *USp(4)-models*, arXiv:1910.09536 [hep-th].

[105] J. Polchinski, S. Chaudhuri, and C. V. Johnson, *Notes on D-branes*, arXiv:hep-th/9602052.

[106] B. R. Greene, A. D. Shapere, C. Vafa, and S.-T. Yau, *Stringy Cosmic Strings and Noncompact Calabi-Yau Manifolds*, Nucl. Phys. B **337** (1990) 1–36.

[107] S. Mizoguchi, *F-theory Family Unification*, JHEP **07** (2014) 018 [arXiv:1403.7066 [hep-th]].

[108] J. H. Schwarz, *Covariant Field Equations of Chiral N=2 D=10 Supergravity*, Nucl. Phys. B **226** (1983) 269.

[109] P. S. Howe and P. C. West, *The Complete N=2, D=10 Supergravity*, Nucl. Phys. B **238** (1984) 181–220.

[110] M. R. Douglas and M. Li, *D-brane realization of N=2 superYang-Mills theory in four-dimensions*, arXiv:hep-th/9604041.

[111] J. H. Schwarz, *An SL(2,Z) multiplet of type IIB superstrings*, Phys. Lett. B **360** (1995) 13–18 [arXiv:hep-th/9508143]. [Erratum: Phys.Lett.B 364, 252 (1995)].

[112] A. Hanany and E. Witten, *Type IIB superstrings, BPS monopoles, and three-dimensional gauge dynamics*, Nucl. Phys. B **492** (1997) 152–190 [arXiv:hep-th/9611230].

[113] K. Kodaira, *On Compact Analytic Sureface I*, Annals of Math. **71** (1960) 111.

[114] K. Kodaira, *On Compact Analytic Sureface III*, Annals of Math. **78** (1963) 1.

[115] S. Fukuchi, N. Kan, S. Mizoguchi, and H. Tashiro, *Dessin d'enfant and a description of mutually nonlocal 7-branes without using branch cuts*, Phys. Rev. D **100** no. 12, (2019) 126025 [arXiv:1808.04135 [hep-th]].

[116] S. Fukuchi, N. Kan, R. Kuramochi, S. Mizoguchi, and H. Tashiro, *More on a dessin on the base: Kodaira exceptional fibers and mutually (non-)local branes*, Phys. Lett. B **803** (2020) 135333 [arXiv:1912.02974 [hep-th]].

[117] A. Grothendieck, *Esquisse d'un Programme*, Published in Schneps and Lochak (1997, I), pp.5-48; English transl. **ibid.** (MR1483107) pp. 243–283.

[118] A. K. Zvonkin and S. K. Lando, *Graphs on Surfaces and Their Applications, Encyclopaedia of Mathematical Sciences: Lower-Dimensional Topology II*, Berlin, New York: Springer-Verlag, ISBN 978-3-540-00203-1, Zbl 1040.05001 (2004) 141.

[119] G. V. Belyi, *Galois extensions of a maximal cyclotomic field*, F Izv. Akad. Nauk SSSR Ser. Mat. **43** (1979) 267–276, 479.

[120] C. Lawrie and S. Schäfer-Nameki, *The Tate Form on Steroids: Resolution and Higher Codimension Fibers*, JHEP **04** (2013) 061 [arXiv:1212.2949 [hep-th]].

[121] M. J. Duff, J. T. Liu, and R. Minasian, *Eleven-dimensional origin of string-string duality: A One loop test*, Nucl. Phys. B **452** (1995) 261–282 [arXiv:hep-th/9506126].

[122] E. Witten, *String theory dynamics in various dimensions*, Nucl. Phys. B **443** (1995) 85–126 [arXiv:hep-th/9503124].

[123] A. Clingher and J. W. Morgan, *Mathematics underlying the F theory / Heterotic string duality in eight-dimensions*, Commun. Math. Phys. **254** (2005) 513–563 [arXiv:math/0308106].

[124] G. Lopes Cardoso, G. Curio, D. Lust, and T. Mohaupt, *On the duality between the heterotic string and F theory in eight-dimensions*, Phys. Lett. B **389** (1996) 479–484 [arXiv:hep-th/9609111].

[125] M. B. Green, J. H. Schwarz, and P. C. West, *Anomaly Free Chiral Theories in Six-Dimensions*, Nucl. Phys. B **254** (1985) 327–348.

[126] L. B. Anderson and W. Taylor, *Geometric constraints in dual F-theory and heterotic string compactifications*, JHEP **08** (2014) 025 [arXiv:1405.2074 [hep-th]].

[127] O. J. Ganor, D. R. Morrison, and N. Seiberg, *Branes, Calabi-Yau spaces, and toroidal compactification of the N=1 six-dimensional E(8) theory*, Nucl. Phys. B **487** (1997) 93–127 [arXiv:hep-th/9610251].

[128] N. Seiberg and E. Witten, *Comments on string dynamics in six-dimensions*, Nucl. Phys. B **471** (1996) 121–134 [arXiv:hep-th/9603003].

[129] M. Reid, *Chapters on algebraic surfaces*, Complex algebraic geometry (Park City, UT, 1993), IAS/Park City Math. Ser. 3 (1997), 3–159 [arXiv:alg-geom/9602006]. https://arxiv.org/abs/alg-geom/9602006.

[130] V. Kumar, D. R. Morrison, and W. Taylor, *Global aspects of the space of 6D N = 1 supergravities*, JHEP **11** (2010) 118 [arXiv:1008.1062 [hep-th]].

[131] S. B. Johnson and W. Taylor, *Enhanced gauge symmetry in 6D F-theory models and tuned elliptic Calabi-Yau threefolds*, Fortsch. Phys. **64** (2016) 581–644 [arXiv:1605.08052 [hep-th]].

[132] W. Taylor and A. P. Turner, *Generic matter representations in 6D supergravity theories*, JHEP **05** (2019) 081 [arXiv:1901.02012 [hep-th]].

[133] N. Yamatsu, *Finite-Dimensional Lie Algebras and Their Representations for Unified Model Building*, arXiv:1511.08771 [hep-ph].

[134] M. Bershadsky, C. Vafa, and V. Sadov, *D strings on D manifolds*, Nucl. Phys. B **463** (1996) 398–414 [arXiv:hep-th/9510225].

[135] M. Gunaydin, G. Sierra, and P. K. Townsend, *Exceptional Supergravity Theories and the MAGIC Square*, Phys. Lett. B **133** (1983) 72–76.

[136] M. Gunaydin, G. Sierra, and P. K. Townsend, *The Geometry of N=2 Maxwell-Einstein Supergravity and Jordan Algebras*, Nucl. Phys. B **242** (1984) 244–268.

[137] N. Kan and S. Mizoguchi, *On Dimensional Reduction of Magical Supergravity Theories*, Phys. Lett. B **762** (2016) 177–183 [arXiv:1605.01904 [hep-th]].

[138] S. Fukuchi and S. Mizoguchi, *On an Algebraic Structure of Dimensionally Reduced Magical Supergravity Theories*, Phys. Lett. B **781** (2018) 77–82 [arXiv:1802.06555 [hep-th]].

[139] V. Sadov, *Generalized Green-Schwarz mechanism in F theory*, Phys. Lett. B **388** (1996) 45–50 [arXiv:hep-th/9606008].

[140] S. Mizoguchi and T. Tani, *Anomaly-free multiple singularity enhancement in F-theory*, PTEP **2016** no. 7, (2016) 073B05 [arXiv:1508.07423 [hep-th]].

[141] J. A. Wolf, J. of Math. Mech. **14** (1965) 1033.

[142] D. Alekseevskii, Funct. Anal. Appl. 2 (1968), 97; Funct. Anal. Appl. 2 (1968), 106; Math. USSR Izv. 9 (1975) 297.

[143] H. Hayashi, C. Lawrie, D. R. Morrison, and S. Schafer-Nameki, *Box Graphs and Singular Fibers*, JHEP **05** (2014) 048 [arXiv:1402.2653 [hep-th]].

[144] S. Mizoguchi and T. Tani, *Non-Cartan Mordell-Weil lattices of rational elliptic surfaces and heterotic/F-theory compactifications*, JHEP **03** (2019) 121 [arXiv:1808.08001 [hep-th]].

[145] P. S. Aspinwall, *M theory versus F theory pictures of the heterotic string*, Adv. Theor. Math. Phys. **1** (1998) 127–147 [arXiv:hep-th/9707014].

[146] P. Deligne, Lecture Notes in Math. **Vol. 476** (1975) Springer, Berlin.

[147] M. Esole, R. Jagadeesan, and M. J. Kang, *The Geometry of G_2, Spin(7), and Spin(8)-models*, arXiv:1709.04913 [hep-th].

[148] S. Mizoguchi and T. Tani, *Looijenga's weighted projective space, Tate's algorithm and Mordell-Weil Lattice in F-theory and heterotic string theory*, JHEP **11** (2016) 053 [arXiv:1607.07280 [hep-th]].

[149] L. B. Anderson, J. Gray, N. Raghuram, and W. Taylor, *Matter in transition*, JHEP **04** (2016) 080 [arXiv:1512.05791 [hep-th]].

[150] E. Witten, *Phase transitions in M theory and F theory*, Nucl. Phys. B **471** (1996) 195–216 [arXiv:hep-th/9603150].

[151] S. H. Katz, D. R. Morrison, and M. R. Plesser, *Enhanced gauge symmetry in type II string theory*, Nucl. Phys. B **477** (1996) 105–140 [arXiv:hep-th/9601108].

[152] A. Grassi, J. Halverson, and J. L. Shaneson, *Matter From Geometry Without Resolution*, JHEP **10** (2013) 205 [arXiv:1306.1832 [hep-th]].

[153] A. Grassi, J. Halverson, and J. L. Shaneson, *Non-Abelian Gauge Symmetry and the Higgs Mechanism in F-theory*, Commun. Math. Phys. **336** no. 3, (2015) 1231–1257 [arXiv:1402.5962 [hep-th]].

[154] I. R. Klebanov and E. Witten, *Superconformal field theory on three-branes at a Calabi-Yau singularity*, Nucl. Phys. B **536** (1998) 199–218 [arXiv:hep-th/9807080].

[155] I. R. Klebanov and M. J. Strassler, *Supergravity and a confining gauge theory: Duality cascades and chi SB resolution of naked singularities*, JHEP **08** (2000) 052 [arXiv:hep-th/0007191].

[156] R. Gopakumar and C. Vafa, *On the gauge theory / geometry correspondence*, Adv. Theor. Math. Phys. **3** (1999) 1415–1443 [arXiv:hep-th/9811131].

[157] C. Vafa, *Superstrings and topological strings at large N*, J. Math. Phys. **42** (2001) 2798–2817 [arXiv:hep-th/0008142].

[158] S. B. Giddings, S. Kachru, and J. Polchinski, *Hierarchies from fluxes in string compactifications*, Phys. Rev. D **66** (2002) 106006 [arXiv:hep-th/0105097].

[159] A. P. Braun and S. Schafer-Nameki, *Box Graphs and Resolutions II: From Coulomb Phases to Fiber Faces*, Nucl. Phys. B **905** (2016) 480–530 [arXiv:1511.01801 [hep-th]].

[160] A. P. Braun and S. Schafer-Nameki, *Box Graphs and Resolutions I*, Nucl. Phys. B **905** (2016) 447–479 [arXiv:1407.3520 [hep-th]].

[161] M. Esole, S.-H. Shao, and S.-T. Yau, *Singularities and Gauge Theory Phases*, Adv. Theor. Math. Phys. **19** (2015) 1183–1247 [arXiv:1402.6331 [hep-th]].

[162] M. Esole, S.-H. Shao, and S.-T. Yau, *Singularities and Gauge Theory Phases II*, Adv. Theor. Math. Phys. **20** (2016) 683–749 [arXiv:1407.1867 [hep-th]].

[163] P. Candelas and X. C. de la Ossa, *Comments on Conifolds*, Nucl. Phys. B **342** (1990) 246–268.